

Identification of the sphingolipid desaturase *DEGS1* as
a novel gene for a leukodystrophy with therapeutic hope

Devesh Chandra Pant

TESI DOCTORAL UPF / 2018

DIRECTOR DE LA TESI

Dr. Aurora Pujol Onofre and Dr. Stéphane Fourcade

DEPARTAMENTO DE CIENCIAS EXPERIMENTALES

Y DE LA SALUD

UNIVERSIDAD POMPEU FABRA



Dedicated to my parents...

Acknowledgement

I wish to express my sincere gratitude to my supervisors, Professor Aurora Pujol and Dr. Stéphane Fourcade for their support, critical thinking and guidance throughout my PhD.

I am deeply indebted to the patients and their families for their participation in the study. I would also like to thank the current and past members of Neurometabolic disease group, IDIBELL, the members of Developmental Biology group, UPF and ZeClinics, PRBB for their help, advice, valuable suggestions during my PhD. I also thank all our collaborators for their essential contribution to my research. I would also like to acknowledge the grants that supported this work.

A special thanks to my precious family members, for encouraging my curiosity and instilling determination and perseverance in me. Thank you for giving me confidence and believing in me. I am forever grateful to all of you, and I could not have completed this PhD without you. I also thank all my friends who provided moral support and motivation during my stay in Barcelona.

I thank you all...

*“All that we are is the result of what we have thought.
The mind is everything.
What we think we become.”*

(Gautama Buddha, 563-483 B.C.)

Abstract

In spite of recent advances in understanding the genetic bases of leukodystrophies, a large number of clinical cases remain unexplained, suggesting that many leukodystrophy-associated genes have yet to be identified. Here we report 18 patients from 12 families with biallelic deleterious variants in the *DEGS1* gene identified *via* WES. *DEGS1* encodes an enzyme which catalyzes the conversion of dihydroceramide to ceramide. Common features among the patients include severe cerebellum atrophy, thinning of the corpus callosum and hypomyelination suggesting a critical role of DEGS1 in the central nervous system.

Using patient's fibroblasts, we evidenced abnormal biochemical profiles. Knockdown of *degs1* in zebrafish recapitulated the biochemical imbalance, showed impaired locomotor abilities and weak myelination. Moreover, a widely used drug for neurological disorders, fingolimod, able to normalized the toxic effects associated due to impaired DEGS1. These results pave the way to clinical translation, illustrating the transformative impact of genomics in patient care.

Resum

El hecho de que un gran número de casos clínicos de leucodistrofias sigan sin explicar sugiere que muchos de los genes asociados a esta enfermedad estarían aún por identificar. Secuenciando el exoma completo de 18 pacientes de 12 familias hemos encontrado variantes deletéreas bialélicas en el gen *DEGS1*, un gen que codifica para una enzima que cataliza la conversión de dihidroceramida a ceramida. Las características comunes entre estos pacientes incluyen atrofia grave del cerebelo, delgadez del cuerpo calloso e hipomielinización, sugiriendo un papel crítico de la proteína DEGS1 en el SNC. Sus fibroblastos evidencian un perfil bioquímico anormal.

Hemos comprobado que un modelo de knockdown del gen *degs1* en pez cebra muestra capacidades locomotoras alteradas, desequilibrio bioquímico y una mielinización débil. Hemos conseguido normalizar sus efectos tóxicos con fingolimod, un fármaco ampliamente usado para trastornos neurológicos. Son resultados que ilustran el impacto transformador de la genómica en la atención al paciente, abriendo un nuevo camino en la clínica traslacional.

Preface

Leukodystrophies are heritable myelin disorders affecting white matter of the central nervous system (CNS). All leukodystrophies result in destruction (demyelination) or failed development (dysmyelination) of myelin leads to a large clinical spectrum from rapidly fatal early infantile to slow late adult forms. There are about 80 genes responsible for leukodystrophies so far suggesting that novel forms still need to be characterized. Genetic research is evolving rapidly, with technologies like Next Generation Sequencing (NGS) generating vast amounts of genetic data.

Part I of the thesis focusses on the genetic diagnosis of patients with leukodystrophy. Genome-wide association studies (GWAS) have been instrumental to link genes and pathways to the etiology of leukodystrophy. The identification of the novel disease gene, *DEGS1*, associated with early-onset hypomyelinating leukodystrophy was more than routine and required a collaborative effort of neurologists and medical geneticists from Spain, France, Canada and the United States we collected 18 patients from 12 families with a *DEGS1* variant. Standardized phenotypic data were collected by review of the clinical histories and follow-up investigations. Affected individuals were examined by experienced neurologists at their primary care centers, and all available clinical and magnetic resonance image (MRI) data were collected and jointly reviewed. *DEGS1* was previously not known to be associated with neurological disorders. However, understanding the effects of the variants identified remains a major problem in diseases. Bringing this research “from bench to bedside” requires intensive effort in translational research studies.

In Part II, by taking advantage of human patient fibroblasts, we performed functional validation of a candidate gene *DEGS1*. To confirm the genetic analyses, we found abnormal biochemical measurements in patients fibroblasts which were explained by the altered lipidomics profile characterized by high dihydroceramide (DhCer) and low ceramide (Cer) in four affected individuals. Additionally, altered mRNA levels in patient fibroblasts further confirmed this. These results indicate loss of *DEGS1* activity in the patients. We also found an increase in intracellular ROS levels in patients' fibroblasts, which was rescued upon treatment with fingolimod, ceramide synthase

inhibitor. However, we found exogenous long-chain DhCer increases the ROS levels in control fibroblasts suggesting the toxic effects of DhCer. Moreover, we found low mitochondria membrane potential in one patient fibroblasts and impaired autophagy in two patients fibroblasts. Determination of the pathogenicity of variants identified through screening of mutation has allowed clinicians to define *DEGS1* related pathogenicity.

In part III, a *degs1* knockdown (KD) zebrafish model for the neurological disorder associated with *DEGS1* was generated. A systemic knockout of *DeGS1* in mice ultimately failed to thrive, dying within 8 to 10 weeks of birth and fruitfly is believed to be embryonic lethal. In order to generate the *degs1* KD zebrafish, antisense morpholino was used. Morpholino-mediated knockdown in a zebrafish model demonstrates that loss of the evolutionarily highly conserved *DEGS1* alters lipidomics profiles, causes movement abnormalities and reduced number of mature oligodendrocytes. They developed signs of neuropathology at 4.5 days of age making this model suitable for therapeutic studies. Preliminary data suggests this gene is highly expressed in CNS. Intensive characterization of the *degs1* zebrafish model found a resemblance to the human phenotype in several facets. The defects observed in the zebrafish model were rescued upon treatment with FTY720. Thus, the overlapping phenotype of *degs1* knockdown zebrafish increases the potential impact of therapeutic studies.

Collectively, the findings of this doctoral thesis show the utility of implementing genomic diagnosis in the clinic, with respect to providing simple and effective treatments in a timely manner to improve outcomes for patients with rare inborn errors of metabolism.

Table of Contents

Abbreviations	xvii
1 INTRODUCTION	3
1.2 Leukodystrophies.....	3
1.1.1 Overview	3
1.1.2 MRI Pattern Recognition and Leukodystrophies	5
1.1.3 Genetics and Leukodystrophies	6
1.2 Technologies for Gene Identification.....	7
1.2.1 Next Generation Sequencing	7
1.2.2 Whole Exome Sequencing.....	9
1.2.3 Whole Genome sequencing	12
1.2.4 Human Gene Variant Databases and Interpretation	13
1.3 Sphingolipids	18
1.3.1 Introduction	18
1.3.2 Metabolism	21
1.4 Bioactive Sphingolipids	23
1.4.1 Ceramides	23
1.4.2 Dihydroceramides.....	25
1.5 Dihydroceramide desaturase (DEGS1)	27
1.6 Sphingolipids Mediating Axon-Glia Architecture.....	29
1.7 Spingolipids in Neurological Disorders	30
1.8 Therapeutic Interventions targeting spingolipids	39
1.8.1 Fingolimod and Sphingolipid Metabolism	40
1.9 The Zebrafish as a Model System	42
1.9.1 Advantages of Zebrafish Model	43
1.9.2 Zebrafish Genetic Toolkit.....	45
1.9.3 Transient Genetic Approaches.....	46
1.9.4 Stable Genetic Approaches.....	47
1.9.5 Modelling Human Neurological Disorders Using Zebrafish	51
1.9.6 Zebrafish in Drug Discovery	53
2 AIMS & OBJECTIVES	60
3 MATERIALS AND METHODS.....	64
3.1 MATERIALS	64
3.1.1 Reagents, Probes and Antibodies	64
3.1.2 Human Samples	64
3.1.2.1 Clinical Recruitment.....	64
3.1.2.2 Post-Mortem CNS Samples.....	65
3.1.2.3 Primary Human Fibroblasts.....	65
3.1.2.4 Treatments	65
3.1.2.5 Extraction of Genomic DNA	66
3.1.3 Mouse Strain	66
3.1.4 Zebrafish Strain.....	66

3.14.1 Production of Zebrafish Embryos.....	67
3.14.2 Generation of <i>Tg(mbp:egfp)</i>	67
3.14.3 PTU Treatment to Prevent Pigmentation.....	68
3.15 Synthesis of DIG Labelled Antisense RNA Probe	68
3.15.1 Cloning of <i>degs1</i>	68
3.15.2 Ligation.....	68
3.15.3 Heat Shock Transformation.....	68
3.15.4 Screening	69
3.15.5 Riboprobe Synthesis	69
3.15.6 Cryosectioning.....	69
3.16 FTY720 Treatment in <i>Danio rerio</i>	70
3.2 METHODS.....	70
3.2 Whole Exome Sequencing (WES)	70
3.3 Candidate Variant Filtering and Selection	71
3.4 Sanger Confirmation.....	72
3.6 Lipidomics	72
3.7 Evaluation of Reactive Oxygen Species	73
3.8 Inner Mitochondrial Membrane Potential Quantification.....	73
3.9 Mitochondria Network.....	74
3.10 Quantitative Reverse Transcription Polymerase Chain Reaction (qRT-PCR).....	75
3.11 Western Blotting	75
3.12 Immunofluorescence	76
3.13 <i>In situ</i> Hybridization (ISH).....	76
3.14 Morpholinos	78
3.14.1 Microinjection	78
3.14.2 PCR Screening.....	78
3.15 Locomotor Assay	79
3.16 Immunofluorescence Studies in Zebrafish Larvae.....	80
3.17 Imaging.....	80
3.18 Statistical Analysis	80
4 RESULTS	86
4.1 Chapter 1.....	86
4.1.1 Identification of Novel Genetic Variants.....	86
4.1.2 Novel Variants in <i>DEGSI</i>	91
4.1.3 Evaluation of The Effect of <i>DEGSI</i> Variants	95
4.1.4 Clinical Manifestations of <i>DEGSI</i> Variants.....	100
4.2 Chapter 2	107
4.2.1 <i>Degs1</i> is Highly Expressed in Mice Central Nervous System (CNS).....	107
4.2.2 <i>DEGSI</i> Transcript Level is Altered in Patient Fibroblasts.....	108
4.2.3 <i>DEGSI</i> Activity is Inhibited in Patients.....	109

4.2.4 Impaired Function of DEGS1 Induces Intracellular ROS Production	112
4.2.5 Exogenous Long Chain DhCer Increases ROS Levels in Control Fibroblasts	114
4.2.6 Lack of DEGS1 Activity Results in Low MMP and Mitochondrial Fragmentation in Patient 9.....	115
4.2.7 Lack of DEGS1 Activity Results in Impaired Autophagy Patient 4,9	117
4.2.8 FTY720 Attenuates ROS Levels in Patient’s Fibroblasts	118
4.3 Chapter 3	121
4.3.1 Localization of <i>degs1</i> in Oligodendrocytes	121
4.3.2 Morphogenetic and Functional Defects Induced by Downregulation of Zebrafish <i>degs1</i> During Early Development	123
4.3.3 Loss of <i>degs1</i> in Zebrafish Causes Locomotor Impairment and Reduced Number of Mature oligodendrocytes.....	126
4.3.5 FTY720 Ameliorates Locomotor Deficits in MO-DEGS1 larvae	127
4.3.6 FTY720 Prevents The Imbalance of Dihydroceramide and Ceramide Imbalance in <i>degs1</i> Knockdown Zebrafish Larvae.....	128
4.3.7 Knockdown of <i>degs1</i> Mediated Loss of Oligodendrocytes is Normalised by FTY720.....	130
5 DISCUSSION.....	135
5.1 Expression of DEGS1 in CNS.....	136
5.2 Dihydroceramides/Ceramides as Regulators of Lipid Homeostasis.....	137
5.3 Role of DhCer and Oxidative Stress	139
5.4 DhCer Accumulation and Autophagy Impairment.....	142
5.5 Knockdown Of <i>degs1</i> in Zebrafish Larvae Reproduces Patient’s Main Phenotypes.....	143
5.6 FTY720: A Potential Therapeutic Target Against Neurological Disorders	144
5.7 Global Discussion.....	147
6 CONCLUSIONS	153
APPENDIX I.....	156
7 REFERENCES	160

Abbreviations

AD	Autosomal dominant
ANOVA	Analysis of variance
AR	Autosomal recessive
ATP	Adenosine 5'-triphosphate
bp	Base pair
BSA	Bovine serum albumin
c.	Coding DNA
C18:0	N-(octadecanoyl)-sphinganine
cDNA	Complementary deoxyribonucleic acid
Cer	Ceramide
CerS	Ceramide synthase
Chr	Chromosome
CMT	Charcot-Marie-Tooth disease
CNS	Central nervous system
CSF	Cerebrospinal fluid
C _t	Threshold cycle
dbSNP	Single nucleotide polymorphism database
dNTP	Deoxyribonucleotide triphosphate
dH ₂ O	Deionised water
DEGS1	Dihydroceramide desaturase
DhCer	Dihydroceramide
dpf	Days post fertilization
DMEM	Dulbecco's modified eagle medium
DMSO	Dimethyl sulfoxide
DNA	Deoxyribonucleic acid
ECL	Electrochemiluminescence
EDTA	Ethylenediaminetetraacetic acid
ER	Endoplasmic reticulum
EVS	Exome Variant Server
FBS	Foetal bovine serum
FTY720	Fingolimod or 2-(4-octylphenethyl)-2-aminopropane-1,3-diol hydrochloride
GATK	Genome Analysis Tool Kit
gDNA	Genomic DNA
EGFP	Enhanced green fluorescent protein
GWAS	Genome-wide association study
HGVS	Human genome variation society
hpf	Hours post fertilization
hr	Hour
Indel	Insertion/deletion
ISH	In situ hybridization

IF	Immunofluorescence
Kb	Kilobase
KO	Knockout
KD	Knockdown
LB	Luria Bertani (broth)
MAF	Minor allele frequency
Mb	Megabase
Mbp	Myelin basic protein
MEF	Mouse embryonic fibroblast
MO	Morpholino
MRI	Magnetic resonance imaging
MS	Multiple Sclerosis
mRNA	Messenger ribonucleic acid
NCBI	National Centre for Biotechnology Information
NGS	Next generation sequencing
nl	Normal
nt	Nucleotide
ORF	Open reading frame
p.	Protein
PBS	Phosphate buffered saline
PCR	Polymerase chain reaction
PFA	Paraformaldehyde
PNS	Peripheral nervous system
PTU	Phenylthiourea
qPCR	Quantitative polymerase chain reaction
RNA	Ribonucleic acid
ROS	Reactive oxygen species
rpm	Revolutions per minute
RT	Reverse transcription
SAT	Saturated
SEM	Standard error of the mean
sec	Seconds
SD	Standard deviation
SIFT	Sorting Intolerant From Tolerant
SNP	Single nucleotide polymorphism
SNV	Single nucleotide variant
UNSAT	Unsaturated
URL	Uniform Resource Locator
UTR	Untranslated region
WES	Whole exome sequencing
WM	White matter
WT	Wild type
$\Delta\Psi_m$	Mitochondrial membrane potential

This list only includes abbreviations used more than once in the text.

INTRODUCTION

1 INTRODUCTION

1.2 Leukodystrophies

1.1.1 Overview

The term ‘leukodystrophy’ is derived from Greek roots leuko = white, dys = lack of, and trophy = growth. Leukodystrophies are a group of white matter disorders with a diverse genetic basis and phenotypic variability (P. Morell, 1984; Vanderver et al., 2015). Leukodystrophies are a heterogeneous group of inherited disorders primarily affecting the white matter development and maintenance. A large clinical spectrum from rapidly fatal early infantile to slow late adult forms exists. Cells that are specifically affected in this pathology are involved in the axon-glia units, such as oligodendrocytes, astrocytes, ependymal cells and microglia (Marjo S. van der Knaap & Bugiani, 2017). The underlying pathological mechanisms of leukodystrophies differ widely, involving inborn errors of metabolism, disrupted protein biosynthesis, oxidative stress. In many cases, pathological assessment is not beneficial, so clinicians rely on the molecular diagnosis of the disorder and, importantly, on the appearance of the white matter on neuroimaging to define and classify the disorder (Schiffmann & Van Der Knaap, 2009). In principle, leukodystrophies can be subdivided into hypomyelinating leukodystrophies, which are characterized by primary deficits in white color sheath i.e. myelin, and demyelinating leukodystrophies, where myelin develops normally but undergoes progressive disruption.

The occurrence of leukodystrophies can present over the lifespan. It is important to know that leukodystrophies rarely show precisely a genotype-phenotype correlation, as observed in case of in X-linked adrenoleukodystrophy (X-ALD), the same gene defect may cause both childhood and adulthood phenotypes in the same family (Moser, 1997). Leukoencephalopathies is a more general term and can be defined as all conditions in which the white matter of the central nervous system (CNS) is predominantly or exclusively affected (M.S. van der Knaap & Valk, 2006). The causes of leukoencephalopathies are various and include acquired conditions, such as inflammatory, autoimmune, vascular, neurotoxic, or infectious disorders, and genetic conditions. Genetic leukoencephalopathies are referred to as leukodystrophies. Leukodystrophies are common in children and a rare to ultra-rare form can exist, estimation is that the overall incidence is higher and a live birth incidence of 1: 7,663 is reported (Bonkowsky et al., 2010).

To shed light on the clinical symptoms of leukodystrophies, they are clinically heterogeneous and can present with a large variety of neurological signs and symptoms, ranging from a mild developmental delay to severe combined cognitive and motor impairment. Although epilepsy is seen in almost half of the cases (Bonkowsky et al., 2010), it rarely dominates the clinical phenotype, whereas it is more frequent and characteristic for neuronal disorders. Onset can be as early as *in utero* affecting fetal brain development or later in infancy, childhood, adolescence, adulthood or even senescence. Initially, leukodystrophies were thought to be invariably progressive (Lyon, Fattal-Valevski, & Kolodny, 2006). However, in recent years it has become clear that it is not true for all disorders, as illustrated by patients with leukoencephalopathy and thalamus and brainstem involvement and high lactate (LTBL), who typically have an early infantile presentation and initial magnetic resonance imaging (MRI) abnormalities with subsequent clinical amelioration and dramatic improvement of MRI abnormalities over time (Steenweg, Vanderver, et al., 2012). The death rate over life time is high and mortality of 34% with a median age at death of 8.2 years in a cohort of 122 children with a leukodystrophy in a 9 year period is reported (Bonkowsky et al., 2010), and another study reported a mortality of 22% in a cohort of 78 children with a genetic white matter disorder in a 5 year period, which was strikingly higher than in patients with an acquired leukoencephalopathy, of whom none died (Vanderver et al., 2015).

Over the years, different techniques have been applied to address white matter disorders depending on technological developments, with limited success. With the help of generating of cellular and transgenic animal models has allowed major advances in leukodystrophies pathophysiological mechanisms but also in comprehension of myelin development and maintenance. Tightly regulated interactions exist between the different cell compartments of the white matter (Micu, Plemel, Caprariello, Nave, & Stys, 2017). Axonopathy but not demyelination is frequently observed in genetically engineered mice demonstrating that myelin maintenance is more sensitive and regulated in the human brain (Pujol et al., 2002). Since a few years, an exponential increase in numbers of ultra-rare cases with novel genetic anomalies was seen. The path to reach a definitive diagnosis is often very long for white matter disorders. It comprises numerous specialist visits, tests, and sometimes invasive diagnostic procedures, which are a burden for patients and families and also very expensive. And even after this long diagnostic excursion, a diagnosis cannot be established in many cases. In 2010 it was found that despite the use

of brain MRI and extensive biochemical and metabolic investigations, no diagnosis could be established in more than 50% of the patients with a leukodystrophy (Bonkowsky et al., 2010). Lastly, a genetic diagnosis can only be realized when the gene associated with the disease is known, whereas this information lacks for several defined leukodystrophies and for all the unclassified leukodystrophies.

1.1.2 MRI Pattern Recognition and Leukodystrophies

With the onset of MRI technology in the 1980s had a major impact on the studies of leukodystrophies, because for the first time white matter abnormalities could be visualized in detail *in vivo* (I. R. Young et al., 1981). MRI creates high-resolution anatomic images and is highly sensitive in the detection of white matter abnormalities (Miller et al., 1990). The unmyelinated white matter has a very long T₁ and T₂, resulting in a lower signal than gray matter structures on T₁-weighted images and a higher signal on T₂-weighted images (Barkovich, Kjos, Jackson, & Norman, 1988). The development in the field of MRI pattern recognition came in the early 1990s and was a major step forward in the diagnostic of white matter disorders and it became the most important tool in the diagnostic process (M. S. van der Knaap, Valk, de Neeling, & Nauta, 1991). Different pulse sequences can be used that each result in different contrast between tissues and the T₁- and T₂-weighted sequences are best known. During birth, the brain is still largely unmyelinated and the increasing deposition of myelin in the first two years of life results in shortening of first the T₁ and then the T₂, leading to a reversal of the gray-white matter contrast on T₁- and T₂-weighted images (Barkovich, 2000). Fully myelinated white matter structures have a higher signal on T₁-weighted images than gray matter structures and a lower signal on T₂-weighted images than gray matter structures (M.S. van der Knaap & Valk, 2006). Lack of myelin deposition leads to a mildly elevated signal on T₂-weighted images and a variable signal on T₁-weighted images, depending on the amount of myelin deposited (Schiffmann & Van Der Knaap, 2009; Steenweg et al., 2010). Abnormalities of the white matter other than lack of myelin deposition result in a much lower T₁ signal and a much higher T₂ signal than gray matter structures, allowing distinction between hypomyelination and other pathologies *in vivo*.

The starting point to reach a definitive molecular diagnosis begins with the identification and classification of patients. MRI pattern recognition has not only proven to be highly

successful for the recognition of known leukodystrophies, but also for the identification and classification of novel white matter disorders.

1.1.3 Genetics and Leukodystrophies

In the last two decades several novel leukodystrophies have been defined using MRI pattern recognition analysis often combined with clinical and laboratory data (e.g. vanishing white matter (VWM), megalencephalic leukoencephalopathy (MLC), hypomyelination and congenital cataract (HCC, OMIM 603532), Leukoencephalopathy with brainstem and spinal cord involvement and lactate elevation (LBSL) and 4H syndrome is a leukodystrophy (4H) (OMIM 607694) typically characterized by the triad of hypomyelination, hypodontia, and hypogonadotropic hypogonadism (Marjo S van der Knaap et al., 2002). The validity of this approach has been shown by the identification of the associated genes (in 2001 and 2002 *EIF2B1-5* mutations in patients with VWM (P. A. J. Leegwater et al., 2001), and mutations in *MLC1* in patients with MLC (P. A. Leegwater et al., 2001), in 2007 mutations in the gene *FAM126A* in patients with HCC syndrome (Zara et al., 2006), in 2007 *DARS2* mutations in patients with LBSL (Scheper et al., 2007), and in 2011 mutations in the genes *POLR3A* and *POLR3B* in patients with 4H syndrome (Bernard et al., 2011). The identification of the molecular cause of these disorders was accomplished after time-consuming, laborious and costly efforts that included linkage by positional cloning to pinpoint the chromosomal location of the candidate gene and subsequent narrowing the candidate region, followed by reconstructing which genes were located in the candidate region and sequential analysis of candidate genes in the region by Sanger sequencing. This approach required the presence of multiple, preferably large and/or consanguineous families to identify a small enough candidate region with a significant logarithm of odds (LOD) score. Although this approach was indeed successful for the disorders mentioned above, for substantial numbers of patients with an unclassified or undetermined leukodystrophy this technique was not applicable. The rarity of these disorders and the presence of only a few families hampered the success of this approach and made it impossible to successfully apply the traditional gene-discovery approaches. In addition, *de novo* germline mutations could not be identified using this technique.

The introduction of Next-Generation-Sequencing (NGS) technologies could overcome these problems and create opportunities to perform unbiased gene search approaches to

identify the candidate gene in patients with extremely rare Mendelian disorders, including most leukodystrophies.

1.2 Technologies for Gene Identification

The discovery of the DNA structure in 1953 by Watson and Crick launched the era of molecular genetics, which was followed by the development of various important molecular biology techniques, such as cloning (Cohen et al., 2010), Sanger sequencing (Sanger, Nicklen, & Coulson, 1977) and PCR (Saiki et al., 1985). The decade of the 2000s offered two major achievements: first, the draft of the human genome by the International Human Genome Sequencing Consortium, led in the United States by the National Human Genome Research Institute (NHGRI) and the Department of Energy (DOE); and second, the development of new high-throughput genotyping technologies.

1.2.1 Next Generation Sequencing

A whole new genetic explorative era has emerged since the release of the first draft of the human genome sequence. NGS is referred to as massively parallel sequencing, which means that millions or even billions of small fragments of DNA are sequenced simultaneously, creating a massive amount of data. Depending on the application, the starting DNA material is obtained by different means. In applications such as Whole Genome Sequencing (WGS) or total RNA sequencing (RNA-seq), the starting material is gDNA/RNA directly obtained from cells. In the case of RNA, a reverse transcription step is needed to convert RNA into cDNA. In WES, it involves the capture of fragmented gDNA by oligonucleotide probes that collectively cover all exonic regions and in Targeted-enrichment strategies, only a selective region of the genome is sequenced, and for this reason, an enrichment of DNA from the candidate regions is performed by various methods. A wide variety of protocols exist, but all of them have in common that the starting DNA/cDNA material is fragmented and ligated to sequencing adaptors to produce a final NGS library (Mamanova et al., 2010; van Dijk, Auger, Jaszczyszyn, & Thermes, 2014).

The first NGS platform to be released in 2005 was the pyrosequencing method (Margulies et al., 2005). One year later, Illumina sequencing platform was commercialized. The third technology to be released was the Sequencing by Oligo Ligation Detection (SOLiD) by Applied Biosystems in 2007 (Valouev et al., 2008). Other commercialized NGS platforms

include Ion Torrent (semi-conductor technology) and PacBio by Pacifica Biosciences. Illumina platform is currently the leader in the NGS industry and most library preparation protocols are compatible with the Illumina system. In addition, Illumina offers the highest throughput of all platforms and the lowest per-base cost (L. Liu et al., 2012). Read lengths of up to 300 bp, compatible with almost all types of application. However, it has some limitations such as sample loading is technically challenging.

Illumina NGS workflows include four basic steps (from www.illumina.com):

- i. **Library Preparation:** The sequencing library is prepared by random fragmentation of the starting (DNA or cDNA) sample and followed by 5' and 3' adapter ligation to enable hybridization of the sequencing primer.
- ii. **Cluster Generation:** For cluster generation, the library is loaded into a flow cell where fragments are captured on a lawn of surface-bound oligos complementary to the library adapters. Each fragment is amplified into distinct, clonal clusters through bridge amplification which generated millions of clusters containing identical templates.
- iii. **Sequencing:** In this step incorporation of nucleotides to a nascent DNA strand by a terminal transferase enzyme generate fluorescent signals. Illumina technology uses a proprietary reversible terminator-based method that detects single bases as they are incorporated into DNA template strands. After nucleotide incorporation, fluorescence image acquisition, washing, and sequencing step starts over again.
- iv. **Data Analysis:** During data analysis and alignment, the newly identified sequence reads are aligned to a reference genome. Following alignment, many variations of analysis are possible, such as single nucleotide polymorphism (SNP) or insertion-deletion (indel) identification, read counting for RNA methods, phylogenetic or metagenomic analysis, and more. Finally, FastQ files are generated which contain information about all reads sequenced during the experiment.

Modern high throughput sequencers can generate tens of millions of sequences in a single run. Before analyzing this sequence to draw biological conclusions one should always perform some simple quality control (QC) checks to ensure that the raw data looks good and there are no problems or biases in the data which may affect how a bioinformatic person can usefully use it. FastQC program is to filter low quality bases (www.bioinformatics.babraham.ac.uk/projects/fastqc/), Burrows-Wheeler Alignment tool to align reads to the reference, and sequence alignment/map (SAM) tools (H. Li & Durbin, 2009) or GATK (Genome Analysis Toolkit) to detect variants (McKenna et al., 2010). Picard (<http://broadinstitute.github.io/picard/>) is a tool to remove duplicate reads generated as a result of PCR steps in most protocols. Finally, programs such as ANNOVAR (K. Wang, Li, & Hakonarson, 2010) can be used to annotate variants.

1.2.2 Whole Exome Sequencing

Whole-exome sequencing (WES) refers to the massive parallel sequencing of the protein-coding part of the genome comprising 1% (30 Mb) of the total human genome (Ng et al., 2009; Shendure & Ji, 2008). The main steps of WES (Weiss et al., 2013) includes: 1) genomic DNA extraction and purification; 2) exome enrichment (exome capture kits are offered by different companies), which is accomplished by using oligonucleotide probes to hybridize fragment of interests; 3) aqueous-phase hybridization of DNA to biotinylated probes targeting coding regions of the genome; 4) pull-down of hybridised fragments by biotin-streptavidin method and washing of non-hybridized fragments; 5) high throughput parallel sequencing which can be executed using different available platforms; 6) the last step is bioinformatics processing of the reads including quality assessment, mapping and alignment to the human reference genome and variant calling and annotation (**Fig. 1**) (Bamshad et al., 2011).

The utility of WES in disease gene discovery came in 2009 with the demonstration that the causative gene for a known Mendelian disorder, Freeman-Sheldon syndrome (MIM 193700), could be identified directly by WES (Ng et al., 2009). In 2010, the first discovery of the genetic cause for a rare Mendelian disorder of unknown cause, Miller syndrome (MIM 274200), was established (Ng et al., 2010). At the time of the start of my PhD project, an increasing number of novel genes and new clinical phenotypes linked to a known gene using WES were published within a time period of roughly two years (Boycott, Vanstone, Bulman, & MacKenzie, 2013). In addition, the first mutations in a

novel gene associated with a leukodystrophy were identified with WES was *CSF1R* mutations in patients with ‘Hereditary Diffuse Leukoencephalopathy with Spheroids’, MIM 221820, (Rademakers et al., 2012) and soon thereafter research groups identified *EARS2* mutations in patients with LTBL using WES (Steenweg, Ghezzi, et al., 2012). The exponential increase of the identification of novel genes associated with a broad variety of rare Mendelian disorders illustrates the high potential of this technique for candidate gene finding (Boycott et al., 2013).

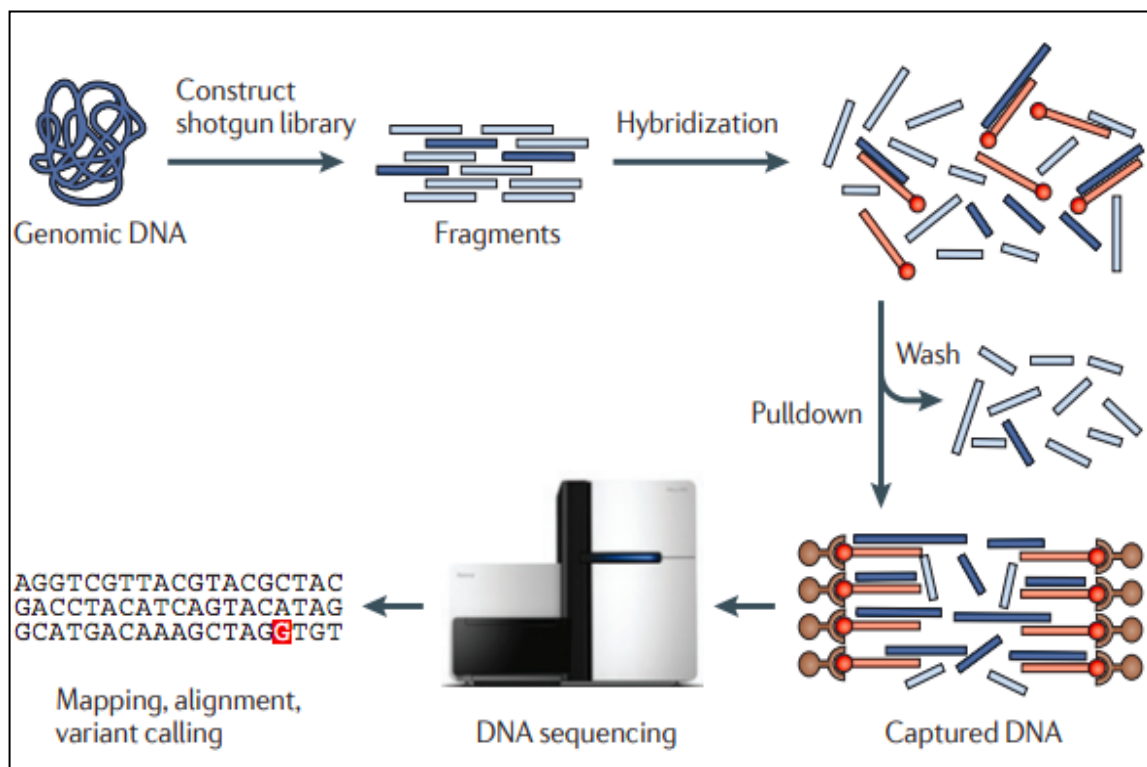


Figure 1. Workflow for Whole Exome Sequencing. From (Bamshad et al., 2011).

Successful WES depends firstly on the variant being detected in the captured portion of the genome and secondly on our ability to identify the variant of interest. Thorough prioritization of variants is therefore crucial to the gene finding process. After sequencing and bioinformatics processing, approximately 20,000 to 25,000 variants can be identified in each individual exome (Gilissen, Hoischen, Brunner, & Veltman, 2012). The challenge is to pinpoint the variant of interest within this large pool of insignificant variants. Filtering strategies to identify mutations usually rely on certain assumptions. For most Mendelian disorders prioritization assumes that the mutation has a potentially large effect and is therefore unique or extremely rare (i.e. only present in patients), located within the protein-coding part of the genome and is predicted to have a direct effect on the function

of the protein (e.g. non-synonymous single nucleotide variants (SNVs), insertions/deletions (indels) or splice-site mutations). The initial filtering approach commonly used is the exclusion of common variants (e.g. SNVs present in public databases such as dbSNP, 1000Genomes, and the NHBI Exome Variant Server (EVS) genome database), which can reduce the number of potential candidate variants substantially by 90 - 95 % (Gilissen et al., 2012). After that, a total of 150-500 rare non-synonymous SNVs, indels or splice-site mutations will remain for further prioritizing.

Different approaches can be applied to achieve the most efficient reduction of candidate variants for a certain supposed inheritance pattern. De novo mutations can be identified using a trio-based approach. WES is performed in both unaffected parents and the affected child, and the data are subsequently filtered for de novo variants. Theoretically, this would be extremely efficient because the average exome only contains 0-3 true de novo mutations (Gilissen et al., 2012). In the case of an autosomal recessively inherited disorder with reported consanguinity, additional genetic techniques like a single nucleotide polymorphism (SNP) microarray can reduce the number of candidate variants by selection of an overlapping homozygous region between affected patients. In large families with an autosomal dominant disorder conventional genetic linkage analyses preceding WES could be helpful by narrowing down the candidate search area (J. L. Wang et al., 2010). Although the combination of these filtering strategies will ultimately reduce the number of candidate variants significantly, comparison of identified variants among unrelated patients with (presumably) the same disorder is often required to pinpoint the candidate gene, especially in disorders caused by a novel gene. Importantly, effective intra-group comparison depends on precise phenotyping of the patients and the absence of genetic heterogeneity.

It is important to realize that every filtering step used can discard the pathogenic variant. Furthermore, in addition to SNVs, patients can carry copy number variations (CNVs), inversions and deletions, which can be missed by WES due to limitations of this technique (Ng et al., 2010; Norton et al., 2011). Also, insufficient exome coverage, which is most often caused by the presence of extreme GC rich regions hampering good exome capture and sequencing, may result in negative results. Furthermore, it is estimated that 85% of the disease-causing mutations are located in functional and coding regions of the genome (Botstein & Risch, 2003; Majewski, Schwartzentruber, Lalonde, Montpetit, & Jabado,

2011), the remaining part (non-coding causal mutations) is refractory to WES analysis and requires whole-genome sequencing (WGS).

For the studies described in this thesis, we use WES as the main approach to identify the variants of not yet associated with leukodystrophies. We consider intra-group comparison an effective additional filtering approach because this strategy will not only reduce the number of candidate variants substantially, it will also provide evidence of the causality of the identified variant when (different) variants in the same gene are found in multiple unrelated patients with the same phenotype. By using MRI pattern recognition for the classification of patients we aim at creating phenotypically homogeneous groups of patients that represent a reliable discovery cohort for the application WES. However, researchers have found that DNA variations outside the exons would be miss and can affect gene activity and protein production and lead to genetic disorders. Another method, called whole genome sequencing, described in the following section determines the order of all the nucleotides in an individual's DNA.

1.2.3 Whole Genome sequencing

Whole-genome sequencing (WGS) is a method for analyzing the whole genome and has been helpful in identifying various genetic disorders. It aids in characterizing the mutations that drive disease progression. WGS refers to the sequencing of all genomic DNA regions from an individual. The recent development of NGS technologies has rapidly dropped the sequencing costs and the ability to produce large volumes of data with today's sequencers make WGS a powerful tool for genomics research. For example, the first draft of the human genome complete sequence obtained by the Human Genome Project (2004), which was performed by Sanger sequencing, cost \$3 billion and needed the collaboration of 97 research groups around the world. Nowadays, it is already possible to sequence a whole human genome by only \$1000. This means a 10,000 fold reduction in price relative to the cost of a human genome in 2004 (<http://www.genome.gov/sequencingcosts>). Nonetheless, this level of optimization and bioinformatics resources needed to analyze WGS are not available in most research laboratories (Schloss, 2008; van Dijk et al., 2014).

WGS has more reliable sequence coverage. The sequencing coverage is described by the mean of reads that align to, or cover, known reference bases. Sequencing of genome

generates a much higher amount of data than WES which generates computational storage and variant interpretation problems. WGS was initially used for *de novo* genome sequencing of different species, or to generate data on human polymorphisms for public databases. In the context of Mendelian diseases research, WGS was first used to unravel the genetic cause of Mendelian disease in 2010 (Lupski et al., 2010) and has been later used for clinical diagnostics. Nowadays, it is starting to be used in cases where WES strategies have failed to identify genetic defect underlying a hereditary disease. Indeed, causal mutations may be located in genome regions which are not screened by WES, such as promoters, introns, or UTR regions. If prices continue to fall, it is probable that WGS will become the method of choice for all kind of human genetic studies, as it will contain all data which was previously interrogated by other genotyping methods (microarrays, candidate gene Sanger sequencing, other NGS resequencing approaches) at a very attractive price and speed.

1.2.4 Human Gene Variant Databases and Interpretation

After the completion of human genome project in 2004 and implementation of NGS technologies, the next goal was to create a detailed information of both common and rare human variants. As a result, several initiatives were taken in this direction and it resulted in the creation of human gene variant databases as listed (**Table 1**). All of these databases are freely available online. Many Clinical laboratories around the globe are increasingly detecting novel sequence variants in the course of testing patient specimens for a rapidly increasing number of genes associated with genetic disorders.

In order to enable effective sharing of novel variants, a uniform nomenclature was introduced, by a set of standardized criteria, to ensure the designation of a variant. A standard gene variant nomenclature (<http://www.hgvs.org/mutnomen>) is maintained by the Human Genome Variation Society (HGVS), e.g., “g.” for genomic sequence, “c.” for coding DNA sequence. Genomic coordinates should be used and defined according to a standard genome build (e.g., hg19). In the report standards and guidelines for the interpretation of sequence variants: a joint consensus of the American College of Medical Genetics and Genomics (ACMG) made the recommendation for changes with respect to human disorders by classifying a mutation as a permanent change in the nucleotide sequence, whereas a polymorphism is defined as a variant with a frequency above 1%. Variants should be sub-classified under one of five sections: (i) pathogenic, (ii) likely

pathogenic, (iii) uncertain significance, (iv) likely benign, or (v) benign (Richards et al., 2015).

The use of NGS has multiplied the number of variants to be assessed. To study the deleteriousness of each variant by experimental approaches is costly and time-consuming. Therefore, researchers have to rely on several approaches to assess variant pathogenicity and prioritize variants before undertaking functional experiments. Variants selection should consider three main parameters: i) it should affect the coding regions, ii) cosegregate with the phenotype and iii) not frequent in population. Nevertheless, the number of variants after filtering is very high, and for this reason, new computational tools have received continuous attention. For this reason, a large number of *in silico* prediction tools have been developed as listed (**Table 2**). Each of these algorithms is based on different principles. *In silico* tools are further divided into two main categories: i) those that predict whether a missense change is damaging to the resultant protein function and ii) those that predict whether there is an effect on splicing (Richards et al., 2015). In addition, the Exome Aggregation Consortium (ExAC) has computed a score called pLI, which indicates the probability that a gene is intolerant to a Loss of Function (LoF) mutation. With the launch of GeneMatcher in 2013, submitters are encouraged to enter only strong candidate genes with validated candidate causative variants; it is best used for candidate genes that are not yet known to have an associated human phenotype. Submitters have access to the details of the matches and can follow up on own matches by personal communication (Sobreira, Schiettecatte, Valle, & Hamosh, 2015).

Table 1. Human population and disease databases URLs. From (Richards et al., 2015).

Database	Website	Type
Exome Aggregation Consortium	http://exac.broadinstitute.org/	Population
Exome Variant Server	http://evs.gs.washington.edu/	Population
1000 Genomes Project	http://browser.1000genomes.org	Population
dbSNP	http://www.ncbi.nlm.nih.gov/snp	Population
dbVar	http://www.ncbi.nlm.nih.gov/dbvar	Population
gnomAD	http://gnomad.broadinstitute.org/	Population
ClinVar	http://www.ncbi.nlm.nih.gov/	Disease
OMIM	http://www.omim.org	Disease
Human Gene Mutation Database	http://www.hgmd.org	Disease
Human Genome Variation Society	http://www.hgvs.org/dblist/dblist.html	Disease
Leiden Open Variation Database	http://www.lovd.nl	Disease
DECIPHER	http://decipher.sanger.ac.uk	Disease
GeneMatcher	http://www.genematcher.org	Disease

Table 2. *In silico* predictive algorithms URLs. From (Richards et al. 2015).

Name	Website	Basis
Missense prediction		
ConSurf	http://consurf.tau.ac.il	Evolutionary conservation
FATHMM	http://fathmm.biocompute.org.uk	Evolutionary conservation
MutationAssessor	http://mutationassessor.org	Evolutionary conservation
PANTHER	http://www.pantherdb.org/tools/csnpScoreForm.jsp	Evolutionary conservation
PhD-SNP	http://snps.biofold.org/phd-snp/phd-snp.html	Evolutionary conservation
SIFT	http://sift.jcvi.org	Evolutionary conservation
SNPs&GO	http://snps-and-go.biocomp.unibo.it/snps-and-go	Protein structure/function
Align GVD	http://agvgd.iarc.fr/agvgd_input.php	Protein structure/function and evolutionary conservation
MAPP	http://mendel.stanford.edu/SidowLab/downloads/MAPP/index.html	Protein structure/function and evolutionary conservation
Mutation Taster	http://www.mutationtaster.org	Protein structure/function and evolutionary conservation
MutPred	http://mutpred.mutdb.org	Protein structure/function and evolutionary conservation
PolyPhen-2	http://genetics.bwh.harvard.edu/pph2	Protein structure/function and evolutionary conservation
PROVEAN	http://provean.jcvi.org/index.php	Alignment and measurement of similarity between variant sequence and protein sequence homology
nsSNPAnalyzer	http://snpanalyzer.uthsc.edu	Multiple sequence alignment and protein structure analysis
Condel	http://bg.upf.edu/fannssdb/	Combines SIFT, PolyPhen-2, and Mutation Assessor
CADD	http://cadd.gs.washington.edu	Contrasts annotations of fixed/nearly fixed derived alleles in humans with simulated variants
Splice site prediction		
GeneSplicer	http://www.cbcb.umd.edu/software/GeneSplicer/gene_spl.shtml	Markov models
Human Splicing Finder	http://www.umd.be/HSF/	Position-dependent logic
MaxEntScan	http://genes.mit.edu/burgelab/maxent/Xmaxentscan_scoreseq.html	Maximum entropy principle
NetGene2	http://www.cbs.dtu.dk/services/NetGene2	Neural networks
NNSplice	http://www.fruitfly.org/seq_tools/splice.html	Neural networks
FSPLICE	http://www.softberry.com/berry.phtml?topic=fsplICE&group=programs&subgroup=gfind	Species-specific predictor for splice sites based on weight matrices model

Nucleotide conservation prediction		
GERP	http://mendel.stanford.edu/sidowlab/downloads/gerp/index.html	Genomic evolutionary rate profiling
PhastCons	http://compgen.bscb.cornell.edu/phast/	Conservation scoring and identification of conserved elements
PhyloP	http://compgen.bscb.cornell.edu/phast/help-pages/phyloP.txt	Alignment and phylogenetic trees, computation of p-values

1.3 Sphingolipids

1.3.1 Introduction

In eukaryotic cells, sphingolipids represent one of the major classes of lipids. Historically, the first sphingolipids were isolated from brain in the late 19th century by Johan L. W. Thudichum, who introduced the term ‘sphingosin’ after the Greek mythical creature, the Sphinx, in deference to “the many enigmas which it presented to the inquirer” (Thudichum, 1962). The name sphingolipid was introduced by Herbert Carter and co-workers in 1947. In the 20th century different biochemical approaches were used to elucidate the chemical structure of sphingosine, one of the major sphingoid bases (1,3-dihydroxy-2-aminoalkane and its derivatives) as the structural backbone, which are the building blocks of all sphingolipids. The discovery of sphingosine led the biochemist’s explication of the classes of complex sphingolipids (sphingomyelins and glycosphingolipids), which were the most important components of the cell membrane and act as modulators of cell-cell interactions and cell recognition. Accordingly, the defects in the metabolism of sphingolipids were collectively known as sphingolipidoses and were further classified as lysosomal storage disorders (LSDs) in humans. Sphingolipids have a hydrophobic nonpolar tail consisting of a fatty acid, a sphingoid base, and a polar hydrophilic head. There are three major chemical types of sphingoid bases as shown (Fig. 2).

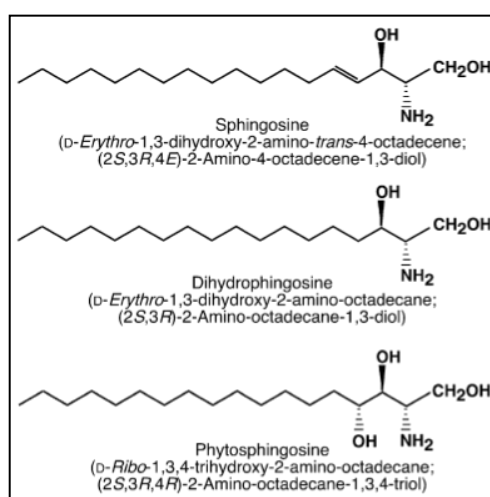


Figure 2. Structure of sphingoid bases.

Systematic names of the major sphingoid bases are also indicated in the bracket. From (Hanada, 2003).

Sphingosine is the principal sphingoid base of sphingolipids in mammalian cells, and dihydrosphingosine (commonly known as “sphinganine”) is the second most abundant type. Phytosphingosine (4-hydroxydihydrosphingosine) is the principal sphingoid base in plants and fungi, although some tissues including the kidney and stomach in mammals also have considerable amounts of phytosphingosine containing sphingolipids. Sphingolipids are a very diverse group of lipids and can be classified according to the structural combination of long-chain sphingoid bases, by the length of the fatty acids, and by the various polar head groups. Depending on the type of polar head group, there are two major classes of sphingolipids: phosphosphingolipids (PSLs), including sphingomyelin (SM), and glycosphingolipids (GSLs), including cerebrosides, gangliosides, and globosides. Based on the nature of the sphingoid base backbone, we can distinguish three main subgroups in the ceramide family: the compound named ceramide contains sphingosine, which has a trans-double bond at the C4–5 position in the sphingoid base backbone; dihydroceramide, the inactive precursor of ceramide, contains sphinganine, which presents a saturated sphingoid backbone devoid of the 4, 5-trans-double bond (**Fig. 3**).

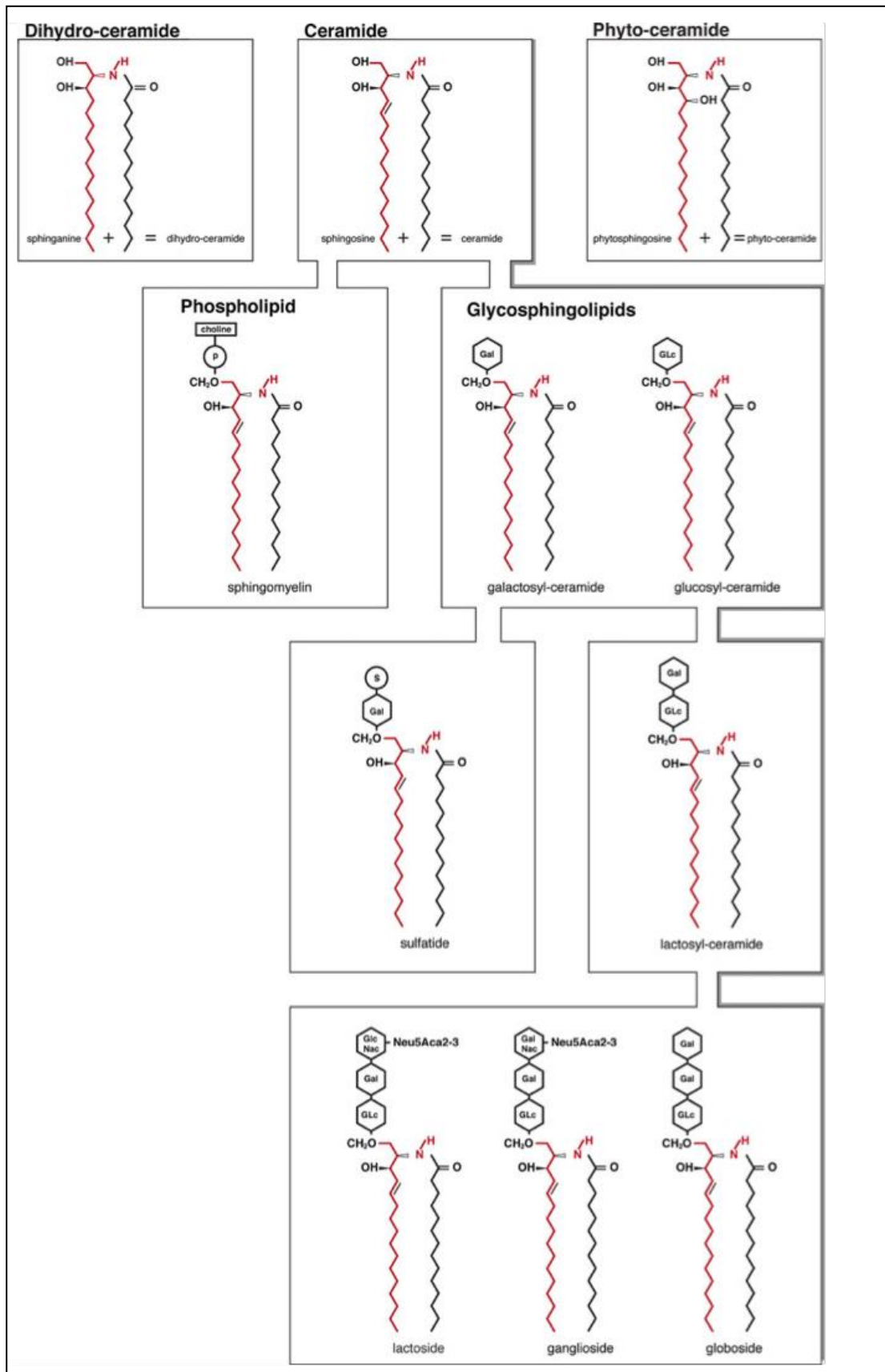


Figure 3. Overview of sphingolipid structures.

Structure of ceramide, the central intermediate in the sphingolipid network. Attachment of phosphocholine, glucose, or galactose to ceramide at the C1 position generates the more complex sphingolipids sphingomyelin, glucosylceramide, and galactosylceramide, respectively. From (Mencarelli, Martinez-Martinez, & Martinez-Martinez, 2013).

1.3.2 Metabolism

The sphingolipids metabolism have been studied enormously by many groups including most of the biochemical pathways of synthesis and degradation (Hannun & Luberto, 2004). The sphingolipid metabolism is a highly coordinated system and its importance lies in connecting various cellular pathway together, where Ceramide occupies a key position in both biosynthesis and catabolism, thereby forming a sphingolipid network. In eukaryotes, there are three main pathways of sphingolipid biosynthesis which are described below:

1. The ***de novo* pathway** takes place in ER where serine palmitoyltransferase (SPT) catalyses the condensation of serine with a fatty acyl-CoA to yield 3-ketosphinganine (3-ketodihydrosphingosine). In turn, 3-ketodihydrosphingosine is reduced to dihydrosphingosine, which is then followed by acylation by the dihydroceramide synthase to produce dihydroceramide (DhCer). The final step is the desaturase reaction is the addition of a double bound by dihydroceramide desaturase (DEGS1) to form Ceramide. Ceramide generated needs to be transported to the Golgi complex, where it serves as a substrate for production of complex sphingolipids like sphingomyelin and glycosphingolipids. After synthesis, Ceramide can be transported by vesicular and non-vesicular transport mechanisms. In mammals, the non-vesicular transport is mediated by the ceramide transfer protein (CERT), in an ATP-dependent manner (Hanada, 2003). Once successfully traffic to the Golgi complex, several different functional head groups can be added to Ceramide to form different classes of complex sphingolipids. These complex sphingolipids span different cellular locations mainly through vesicular transport.
2. The **sphingomyelinase pathway** takes place in the plasma membrane, Golgi and mitochondria and converts sphingomyelin into Ceramide, bidirectionally. Ceramide can be generated in the cell through the hydrolysis of complex

sphingolipids. For example, from glycosphingolipids (GSLs) and sphingomyelin through the action of specific hydrolases and phosphodiesterase (Clarke & Hannun, 2006). The process takes place in the outer layer of the plasma membrane and the formation of Ceramide from sphingomyelin occurs. At the same time, conversion of sphingosine to Ceramide takes place in the inner layer. The synthesis of Ceramide from sphingomyelin is carried out by the plasma membrane bound enzyme sphingomyelin phosphodiesterase (SMPD).

3. The **salvage pathway** allows reformation of Ceramide. It occurs in the late endosomes and the lysosomes and converts long-chain sphingoid bases into Ceramide through the action of ceramide synthase (CerS). Ceramide synthesis from complex GSLs can be regulated by either lysosomal or non-lysosomal degradation. In lysosomal degradation, catabolism of GSLs occurs by cleavage of sugar residues which leads to the formation of glucosylceramide and galactosylceramide. Thereafter, specific β -glucosidases and galactosidases hydrolyze these lipids to produce ceramide that can later be deacylated by an acid ceramidase to form sphingosine (Hannun & Obeid, 2018). The sphingosine thus produced can further be salvaged to form Ceramide.

The common lipophilic moiety of all sphingolipids is Ceramide, in which a long-chain sphingoid base is attached by an amide linkage to a long-chain fatty acid (**Fig. 3**). Sphingolipids are regulated by various enzymes and different metabolites as depicted (**Fig. 4**), with around 40 enzymes in mammals involved in their metabolism (Hannun & Obeid, 2018). These enzymes are the products of distinct genes, can occur as splice variants and can feature a plethora of post-translational modifications, which affect their enzymatic activity and function. Mammals have six ceramide synthases (CerS1-CerS6), each using specific substrates and producing dihydroceramides (DhCers) with different fatty acid moieties to generate a large array of Ceramide (Tidhar & Futerman, 2013). Ceramide are made in many cellular compartments, not just the ER, and they perform a wide range of functions. Critically, all key enzymes in sphingolipid metabolism have now been molecularly identified, which has revealed the vast complexity of these metabolic pathways and their precise subcellular compartmentalization. Defects in the function of these enzymes lead to a variety of LSDs. In this thesis, we will focus on two bioactive

sphingolipids i.e. Ceramide and precursor of Ceramide in the *de novo* pathway, the DhCers.

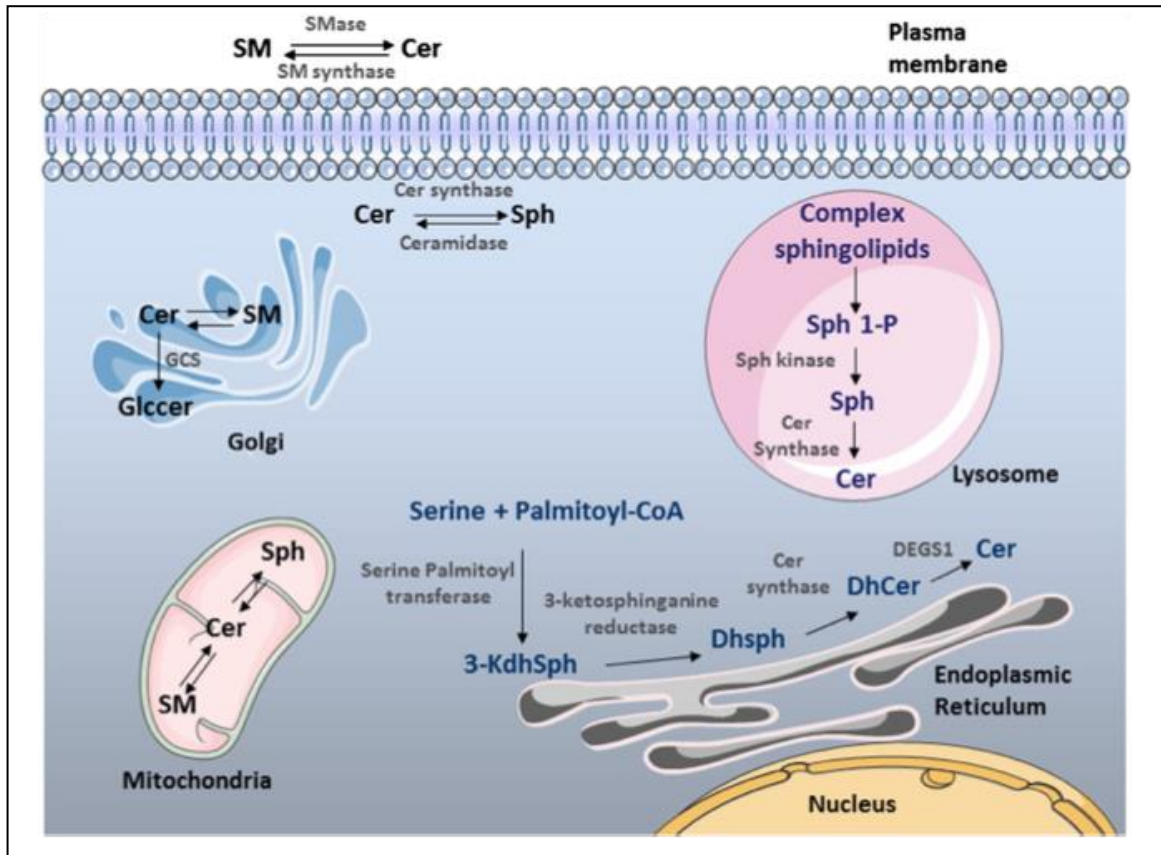


Figure 4. Overview of sphingolipid metabolism.

The three main pathways of sphingolipid metabolism. The *de novo* biosynthetic pathway is initiated in the ER by the action of serine palmitoyltransferase (SPT). Sequential reactions lead to the generation of ceramides. The sphingomyelinase pathway takes place in the plasma membrane, Golgi, and mitochondria and converts sphingomyelin into Ceramide. The salvage pathway occurs in the late endosomes and the lysosomes and converts long-chain sphingoid bases into Ceramide through the action of CerS (purple letters). SM: Sphingomyelin, Cer: Ceramide, SMase: Sphingomyelinase, Sph: Sphingosine, GlcCer: Glucosylceramide, GCS: Glucosylceramide synthase, 3-kdhSph: 3-ketodihydrosphingosine, DhSph: Dihydrosphingosine, DhCer: Dihydroceramide. From (Rodriguez-Cuenca, Barbarroja, & Vidal-Puig, 2015).

1.4 Bioactive Sphingolipids

1.4.1 Ceramides

The term ceramide (Cer) is used specifically for N-acylsphingosines. Most mammalian sphingolipids comprised mainly of the 18-carbon alkyl chain. Ceramide contains sphingosine, which has a trans-double bond at the C4–5 position in the sphingoid base backbone. The shorthand nomenclature suggested by Lipid MAPS (Metabolites and Pathways Strategy) consortium for Ceramide is d18:1 backbone and the amide-linked fatty acids can also be designated by this nomenclature (e.g. N-stearoyl-D-erythro-

sphingosine would be d18:1/18:0). The fatty acids are typically 16 to 26 carbon atoms in length (short and long chains). As per the LIPID MAPS consortium, this sphingolipid family includes over 4000 distinct species (www.lipidmaps.org) that are integral components of cell membranes (Fahy et al., 2009).

Ceramide is an important bioactive molecule and plays important roles in many cellular processes. For example, Ceramide has emerged as an important effector in development and stress responses, regulation of autophagy, mediating the crosstalk with apoptosis. A rise in Ceramide formation in many types of cells, including nerve cells, results in toxicity expressed as pro-apoptotic actions. The consequence of this process is tissue injury. On the other hand, Ceramide low levels have trophic effects. Thus, Ceramide exerts a positive effect on early growth and differentiation of cells. Ceramide in the plasma membrane has a structural role as it creates lipid rafts and microdomains in the lipid bilayer that cluster of receptors and other signaling molecules (Schenck, Carpinteiro, Grassmé, Lang, & Gulbins, 2007).

The ceramide synthases (CerSs) plays an important role in the sphingolipid metabolism and in the generation of the Ceramide. As discussed before, the CerSs are responsible for the acylation of sphinganine to produce DhCer which is subsequently desaturated, yielding Ceramide. The importance of these CerSs could be deduced from the fact that they there are six different CerSs (CerS1 to 6) compare to other enzymes involved in sphingolipids metabolism which exist in only one or two isoforms (Pewzner-Jung, Bendor, & Futerman, 2006). One of the more notable characteristics of the CerSs is the ability of the individual isoforms to produce Ceramide of particular fatty acyl-chain lengths. For example, CerS1 specifically generates C18 ceramide and is highly expressed in the brain (Jiang, Kirchman, Zagulski, Hunt, & Jazwinski, 1998). The preference of the different CerSs for producing specific acyl-chain length Ceramide has been characterized by several studies. Each CerS regulates the *de novo* synthesis of endogenous Ceramide with a high degree of fatty acid specificity (Binks & Wattenberg, 2018). In line with the presence of multiple CerSs, ceramides occur with a broad fatty acids length distribution inside the cell. Although some CerSs are ubiquitously expressed, other isoforms present a very specific distribution among tissues, according to the need of each tissue for specific ceramide species (Pewzner-Jung et al., 2006; Riebeling, Allegood, Wang, Merrill, & Futerman, 2003). Recently, the role of ceramide synthase during phagocytosis in

mammalian macrophages has been described (Pathak, Mehendale, Singh, Mallik, & Kamat, 2018).

1.4.2 Dihydroceramides

Dihydroceramides (DhCers) are precursors of Ceramide as seen in the *de novo* pathway. They are synthesized from sphinganine by the enzyme CerS and desaturated by a desaturase (DEGS1) to produce Ceramide. Historically, DhCers were considered to be biologically inactive due to the *in vitro* studies resulting from the exogenous addition of mainly C2-ceramide and C2-DhCer, as long-chain ceramide was not easily membrane permeable. These results showed that C2-DhCer did not show biological activity on the basis that it could not mimic ceramide targets in these studies (Bielawska, Crane, Liotta, Obeid, & Hannun, 1993). Unfortunately, most of these *in vitro* studies used permeable short chain Cer/DhCer and no endogenous long-chain DhCer. This raises some concerns about the physiological relevance of such findings. As a result, DhCer species were overlooked for several years. In addition, the classical thin-layer chromatography (TLC) methods cannot distinguish DhCer from ceramide; this guided several research groups to conclude that DhCer is a biological inactive biochemical precursor of the bioactive lipid ceramide (Bielawska et al., 1993).

The turning point in the field of sphingolipid biology came after the introduction of mass spectrometry. These are more accurate methods in lipidomics analysis. Studies conducted by Cabot group treated cells with N-(4-hydroxy-phenyl) retinamide (4HPR, also called fenretinide), an agent that has been thought to increase ceramide to induce apoptosis, as a part of the mechanism of action of this cancer chemotherapeutic agent (Keshelava, Seeger, Groshen, & Reynolds, 1998; H. Wang, Charles, Frankel, & Cabot, 2003). In 2006, Merrill group treated human prostate cancer cell line (DU145) with fenretinide (10 μ M) and sphingolipidome was profiled using liquid chromatography-tandem MS (Zheng et al., 2006). They found that treated cells did not display increased in ceramide and in some cases, ceramide species (mainly C24) decreased, but rather large increases in DhCer species (C16, C18, C22, C24, C26). The possibility that 4HPR thought to elevate ceramide might instead cause increased in DhCer. This critical breakthrough inspired a large number of groups to evaluate the role of DhCer in cellular responses. This raises the question that DhCer can also serve as bioactive species. Altogether, these *in vitro* data suggested that the bioactivity of the DhCer may strongly depend on the cellular

environment, the molecular target, and the chemical nature of the DhCer (length and fatty acid moiety).

Coming to the biophysical properties of DhCer, they might perform different cellular functions than ceramide as they have a higher dipole potential compared to ceramide, which could decrease the packing density (Brockman et al., 2004); they have a lesser tendency than ceramide to promote flip-flop bilayer movement (Contreras, Sot, Alonso, & Goñi, 2006); and are less prone to form membrane channels (Stiban, Fistere, & Colombini, 2006). On the other hand, the uncovered roles of DhCer in autophagy, hypoxia, and cellular proliferation and its implication in the etiology, treatment, or diagnosis of diabetes, cancer, ischemia/reperfusion injury, and neurodegenerative diseases have been summarized (Monowarul Mobin Siddique, Li, Chaurasia, Kaddai, & Summers, 2015).

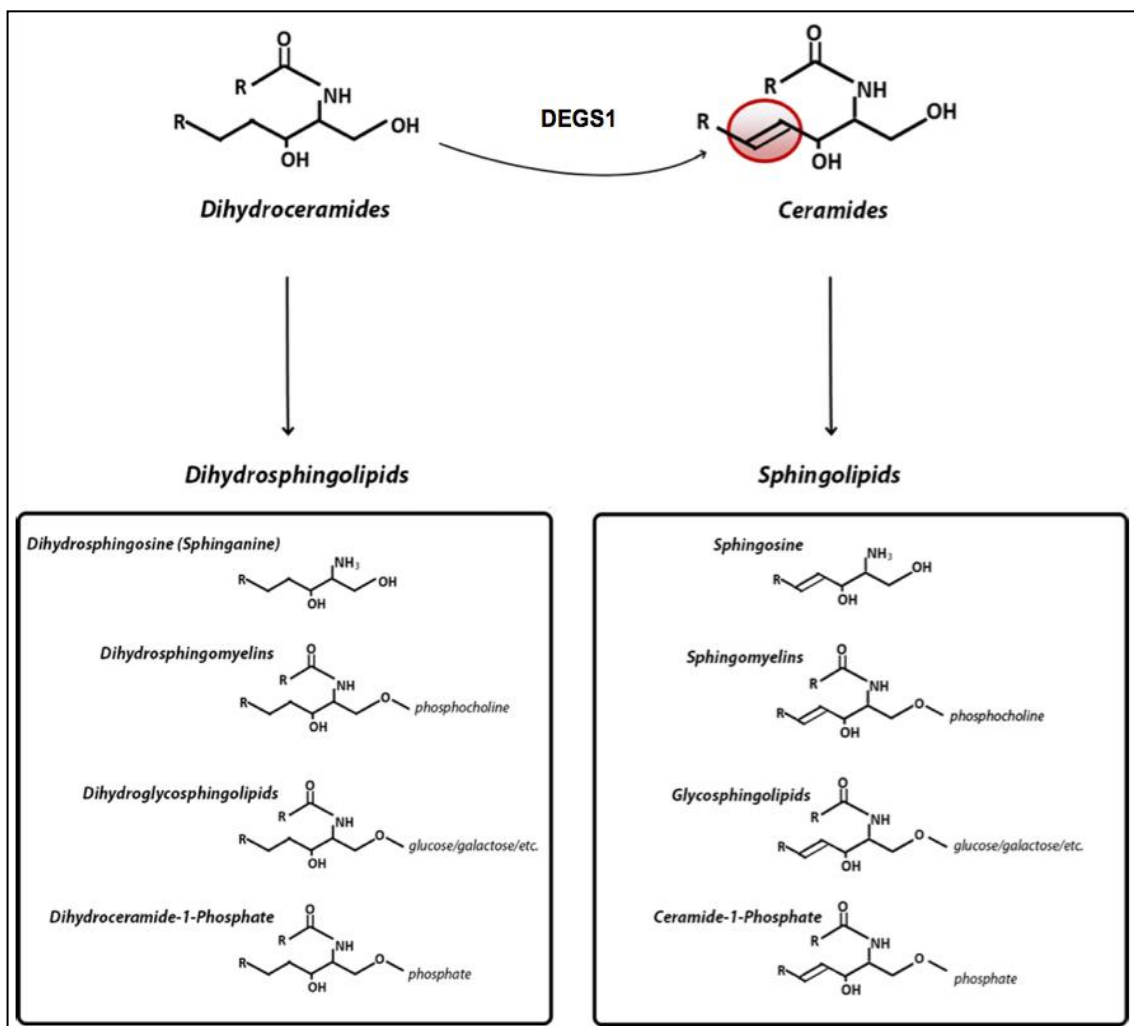


Figure 5. Scheme depicting the importance of DhCer and Ceramide in sphingolipid metabolism pathway. From (Monowarul Mobin Siddique et al., 2015).

1.5 Dihydroceramide desaturase (DEGS1)

The levels of DhCer are controlled by desaturase enzyme – DEGS1. DEGS1 catalyzes the insertion of a double bond into DhCer to convert them to ceramide, both of which are further metabolized to more complex sphingolipids (**Fig. 5**). In 1996, Okada group cloned this gene from *Drosophila melanogaster* and named it “*drosophila degenerative spermatocyte 1*” (Endo, Akiyama, Kobayashi, & Okada, 1996). One year later, Gordon Gill group cloned a membrane fatty acid desaturase gene and named it membrane lipid desaturase (MLD) (Cadena, Kurten, & Gill, 1997). MLD was predicted to be a multiple membrane-spanning protein, highly-conserved histidine motif HX₍₃₋₄₎H, HX₍₂₋₃₎HH, and H/QX₍₂₋₃₎HH and is found to be localized in the cytosolic surface of ER. Currently, the dihydroceramide desaturase gene is known as either *DES1* or *DEGS1*. Ternes et al. (Ternes, Franke, Zähringer, Sperling, & Heinz, 2002) identified a *Degs1* homolog, namely *Degs2*, as a bifunctional enzyme with dihydro-ceramide C4-desaturase and C-4-hydroxylase activities. Suzuki group explored desaturase and hydroxylase activity of mouse *Degs1* and *Degs2*. They transfected *Degs1* and *Degs2* clone in COS7 cell line. They postulate that *Degs1* exhibits high dihydroceramide C4-desaturase and very low C-4 hydroxylase activities whereas *Degs2* exhibits high C-4 hydroxylase and low C-4-desaturase activities (Omae, Miyazaki, Enomoto, & Suzuki, 2004). The desaturase and hydroxylase activity of these enzymes are cell dependent. For example, when mouse *Degs2* expressed in yeast, it exhibits both desaturase and hydroxylase activity. However, no desaturase activity was detected when human DEGS2 was transfected in HEK293 cell line (Mizutani, Kihara, & Igarashi, 2004). It is not clear whether, in mammalian cells, DEGS2 possesses only hydroxylase activity or whether the desaturase activity is masked by a high background activity. In addition, data from different mice tissues suggests tissue distribution profile of both enzymes is considerably different. *mDegs1* is ubiquitously distributed, whereas *mDegs2* is preferentially expressed in small intestine, skin and kidney (Omae et al., 2004), where the production of phytoceramides is essential.

The importance of DEGS1 can be evidenced by studies in different animal models supporting an essential role of this gene in development (**Fig. 6**). In 2007, the group of

Scott Summers generated mouse model of *Degs1*. The homozygous *Degs1*^{-/-} mice die within the first 8 weeks of age, and are small in size with a complex phenotype, including scaly skin and sparse hair and tremors, although no in-depth characterization of neural phenotypes was undertaken. Lipidomics analysis showed that *Degs1* heterozygous mice exhibit high DhCer and low ceramide levels in multiple organs (Holland et al., 2007). In another study by the same group, studies using *Degs1*^{-/-} mice embryonic fibroblasts (MEF) exhibits high autophagy, low ATP levels, high mitochondria membrane potential, decreased mitochondria respiration, reduced mitochondria complex IV activity and elongated mitochondria (M. M. Siddique et al., 2013). Recently, in *Drosophila melanogaster*, KO of the infertile crescent (*ifc*, the closest *DEGS1* orthologue) gene, results in larval lethality with increased DhCer, decreased ceramide levels, degeneration of photoreceptors, increased ROS levels and increased lipophagy (Jung et al., 2017). These results suggest the broad spectrum of metabolic effects associated with DEGS1 depletion. To date, only a single mutation in the *DEGS1* gene (L175Q) has been reported in humans and is associated with increased DhCer, decreased cholesterol esters and decreased waist to hip ratio (Curran et al 2013, ASHG Meeting Abstract, Boston).

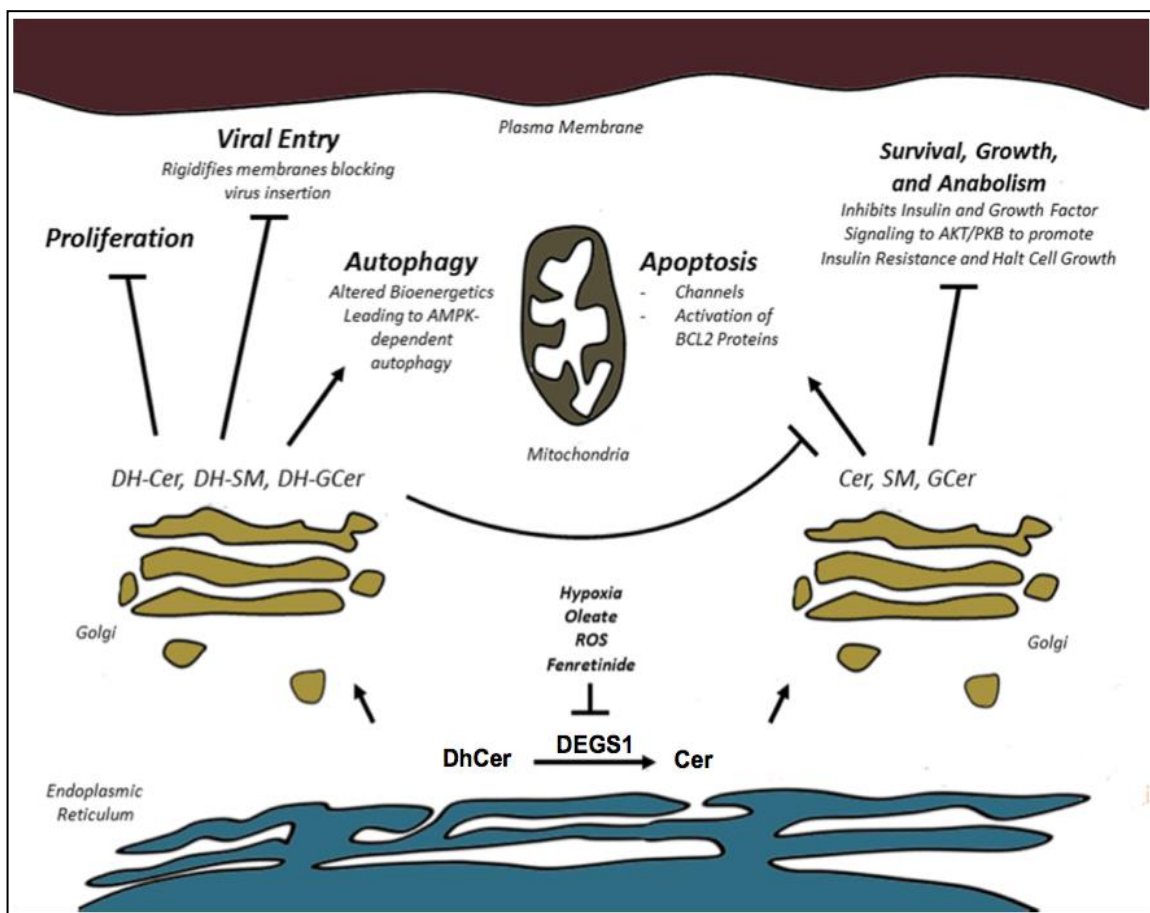


Figure 6. Schematic depicting the non-overlapping biological responses triggered by dihydroceramides versus ceramides.

AMPK, AMP-activated protein kinase; DhCer, dihydroceramide; DH-SM, dihydrosphingomyelin; DH-GCer, dihydroglucosylceramide. From (Monowarul Mobin Siddique et al., 2015).

1.6 Sphingolipids Mediating Axon-Glia Architecture

Myelin is formed by oligodendrocytes and Schwann cells as a lipid-rich and multi-lamellar structure that encloses segments of axons in the central (CNS) and peripheral nervous systems (PNS) of vertebrates. Myelin is formed in the CNS and PNS by the innermost sheet-like glial process in contact with the axon spiraling around it and spinning out multiple layers of overlapping membrane. The sole purpose of myelin and its sheet is to increase the speed of an impulse that travels along the axon. To understand demyelinating diseases such as leukodystrophies, it is important to look at myelin as a functional unit. In humans, myelination occurs around the 14th week of fetal development, and it continues all the way through infancy, childhood, and adolescence. Myelin sheet consists mostly of lipids and proteins; those parts are synthesized in different organelles and must be sorted and transported to the target molecules (Gielen et al., 2006). A major function of lipids in myelin is to pack the membrane into a stable, long-lived insulating sheath (Schmitt, Cantuti Castelvetri, & Simons, 2015). The importance of lipids in myelin can be seen from the difference between myelin sheet and other cell membranes in the percentage of lipids and proteins. In the most of common membranes, proteins prevail in numbers, in myelin sheet numbers are quite the opposite; lipids can occupy up to 70% of the content, while protein numbers can go only 30%. It is important to mention that there are no lipids that are exclusive for myelin sheet (Velić, 2015). The most significant lipids in myelin are ethanolamine, galactosylceramide and cholesterol. The molar ratio of phospholipids, and glycosphingolipids and cholesterol, is in most membranes in the order of 65%:10%:25%, the molar ratios in myelin are in the range of 40%:20%:40% (O'BRIEN, 1965).

The formation and stability of the myelin sheath depend on protein-lipid interaction between the sheath and axon, but it also depends on lipid-lipid interactions between myelin sheath layers. Gangliosides GD1a and GT1b localized in microdomains in the axonal membrane interact and regulate the myelin protein MAG (myelin-associated glycoprotein) (Pan et al., 2005; Schnaar & Lopez, 2009), which itself is located in

galactosylceramide (GalCer) enriched microdomains in mature myelin (DeBruin et al., 2005). Nevertheless, cerebroside is the most common of all myelin lipids and its concentration in the tissue is directly dependant on the quantity of myelin. Cerebrosides are in fact a group of glycosphingolipids; they consist of ceramide (sphingosine and a fatty acid) and a single sugar, which can be either glucose or galactose. It is precisely galactocerebrosides that are usually found in nervous tissue, while glucocerebrosides are found in the membranes of the muscles. It is important to note that in myelin sheets, one-fifth of all galactolipids is sulfatide, known as sulfated galactocerebrosides or 3-O-sulfogalactosylceramide, which are essentially glycolipids that contain a sulfate group. In addition, the myelin composition is different in the CNS and PNS; in the peripheral nervous system, there is an apparent increase in sphingomyelin, while cerebroside and sulfatide are present in lesser extent (Pierre Morell & Quarles, 1999).

The importance of sphingolipids metabolism in the maintenance of myelin could be seen from the myelin defects associated with *CerS2*^{-/-} (ceramide synthase 2), *CST*^{-/-} (galactosylceramide sulfotransferase), and *CGT*^{-/-} (ceramide galactosyltransferase) mouse models. The level of ceramide, SM, and in particular GalCeramide were significantly changed in the *CeramideS2*^{-/-} mice. As a result, mice were not able to compensate for the loss of C22 and C24 GalCeramide, these mice develop unstable myelin including degeneration and detachment (Ben-David et al., 2011). Disturbances of the nodes of Ranvier have been observed in *Cst*^{-/-} (Ishibashi et al., 2002) and *Cgt*^{-/-} (Dupree, Coetzee, Blight, Suzuki, & Popko, 1998) mice lacking the ability to synthesize both GalCeramide as well as sulfatide. Myelin degeneration after the age of 1.5 months was seen in *Cgt*^{-/-} mice. Therefore, the composition and structural properties of myelin lipids are clearly important to impose stability for the long-term maintenance of myelin, they may also be relevant for our understanding of neurodegenerative diseases.

1.7 Spingolipids in Neurological Disorders

Early evidence had shown that genetic defects of enzymes involved in the metabolism of sphingolipids (SLs) have been highly associated with several neurological disorders. The importance of SLs in health and disease had actually been appreciated by early converging studies using both mouse knockouts and genetic tracing of human diseases (Grassi, Chiricozzi, Mauri, Sonnino, & Prinetti, 2018). The physiological functions of

ceramideamides can be approached by analyzing the role of two groups of enzymes: the ones which generate ceramide from more complex SLs and the second which catabolize ceramide or use it as a precursor using mice models and *in-vitro* models from human patients.

The obstruction in sphingolipid catabolism (lipid hydrolases) form the basis of a wide variety of human diseases, collectively known as sphingolipidoses. These catabolic enzymes associated diseases are characterized by inherited defects of SL degradation within the endosomal-lysosomal system (Futerman & van Meer, 2004) resulting in accumulation of undegraded SLs often manifests as lysosomal storage disorders (LSDs), severe neurodegenerative diseases (**Fig. 7**). LSDs are a family of clinically heterogeneous inherited diseases arising from defects in lysosomal hydrolases or their activators, lysosomal membrane proteins or transporters that causes chronic and progressive deterioration of cells, tissues and organs due to lack of function of lysosomes (Neufeld, 1991). Given that lipids are important components of the brain, it can reasonably be expected that excess storage of these compounds will impact neurodevelopment. However, neurodegeneration occurs in the majority of LSD, not just in those with a defect in lipid metabolism, manifesting a contiguous spectrum from slowly progressing loss of neurocognitive function to aggressive, precipitous perinatal death. Many LSDs have a progressive neurodegenerative clinical course and often present in infancy or childhood (Rapola, 1994; Sedel, 2007). Such LSDs includes Gaucher disease, arises due to the accumulation of glycosphingolipids, glucosylceramide (GlcCer) and inability to degrade into glucose and ceramide. Consequently, very high levels of GlcCer have been found in postmortem brain tissue in the cerebral and cerebellar cortices of Gaucher disease patients (Nilsson & Svennerholm, 1982). Moreover, the levels of more complex glycosphingolipids, such as the gangliosides or more simple sphingolipids such as ceramide found to be significantly normal in the brain in Gaucher disease, suggesting that pathology is directly related to levels of GlcCer, along with its deacetylated derivative glucosylsphingosine (GlcSph) (Farfel-Becker et al., 2014). Niemann-Pick Type C (NPC) is also considered a secondary disorder of lipid metabolism which includes accumulation of cholesterol, glycosphingolipids, sphingomyelin and sphingosine. The manifestations of this disease, range from a very severe, neuronopathic form to a non-neuronopathic form with hepatosplenomegaly and diffuse parenchymal lung involvement. Recently, cholesterol accumulation was postulated to inhibit a key enzyme necessary for GM2

degradation using iPSC-derived neurons from NPC patients fibroblasts (Trilck et al., 2017), supporting earlier reports of secondary ganglioside accumulation in NPC. Gangliosides are the most complex glycosphingolipids, residing primarily in the plasmalemma where they are involved in neurodevelopment. GM1 gangliosidosis results from deficiency of lysosomal GM1-galactosidase that cleaves ganglioside GM1. GM1 gangliosidosis mice show severe neurological defects which resemble to the human disease (Hahn et al., 1997). GM2 gangliosidoses are unified by the excessive accumulation of GM2 ganglioside mainly in neuronal cells. The alpha and beta subunits of this enzyme is encoded by the genes *HEXA* and *HEXB* respectively, where *HEXA* showed to be involved in the development of Tay-Sachs disease, results from the deficiency of the subunit that produces the specific loss of HEXA whereas *HEXB* is involved in Sandhoff disease (SRIVASTAVA & BEUTLER, 1973). Unlike Tay-Sachs patients who stored mainly GM2-ganglioside, Sandhoff patients accumulate additional N-acetyl. In mice there are two proposed pathways: GM2 hydrolysis to GM3 mainly by *HexA* and GM2 hydrolysis by sialidase first to GA2 and then to LacCer by *HexB* (Greenfield, Love, Louis, & Ellison, 2008) In an attempt to create mouse model for Tay-Sachs disease, knockout of *HexA* mice was generated. These animals showed milder phenotype with no detectable neurological impairment compared to human due to the differences in the catabolism pathway of GM2 (Sango et al., 1995). Unlike *HexA*^{-/-} mice, *Hex B*^{-/-} (Sandhoff mice) animals were severely affected. The lack of Hex A and B activities in Sandhoff mice provides an authentic model of acute human Sandhoff disease (Sango et al., 1995). Elevations in GM2 and GM3 in the brains of mice with acid sphingomyelinase deficiency have also been reported secondary to elevations in the enzyme's primary substrate, sphingomyelin, demarcating Niemann-Pick A (NPA) as another secondary disorder of ganglioside metabolism (Scandroglio et al., 2008). There are many other related and associated genetic diseases that includes; Metachromatic Leukodystrophy caused by a deficiency of arylsulfatase A, Krabbe disease or globoid cell leukodystrophy caused by a deficiency of galactosylceramide-β-galactosidase and Farber disease caused by a deficiency of lysosomal acid ceramidase causing storage of excess ceramide in the lysosomes as depicted (**Table 3**).

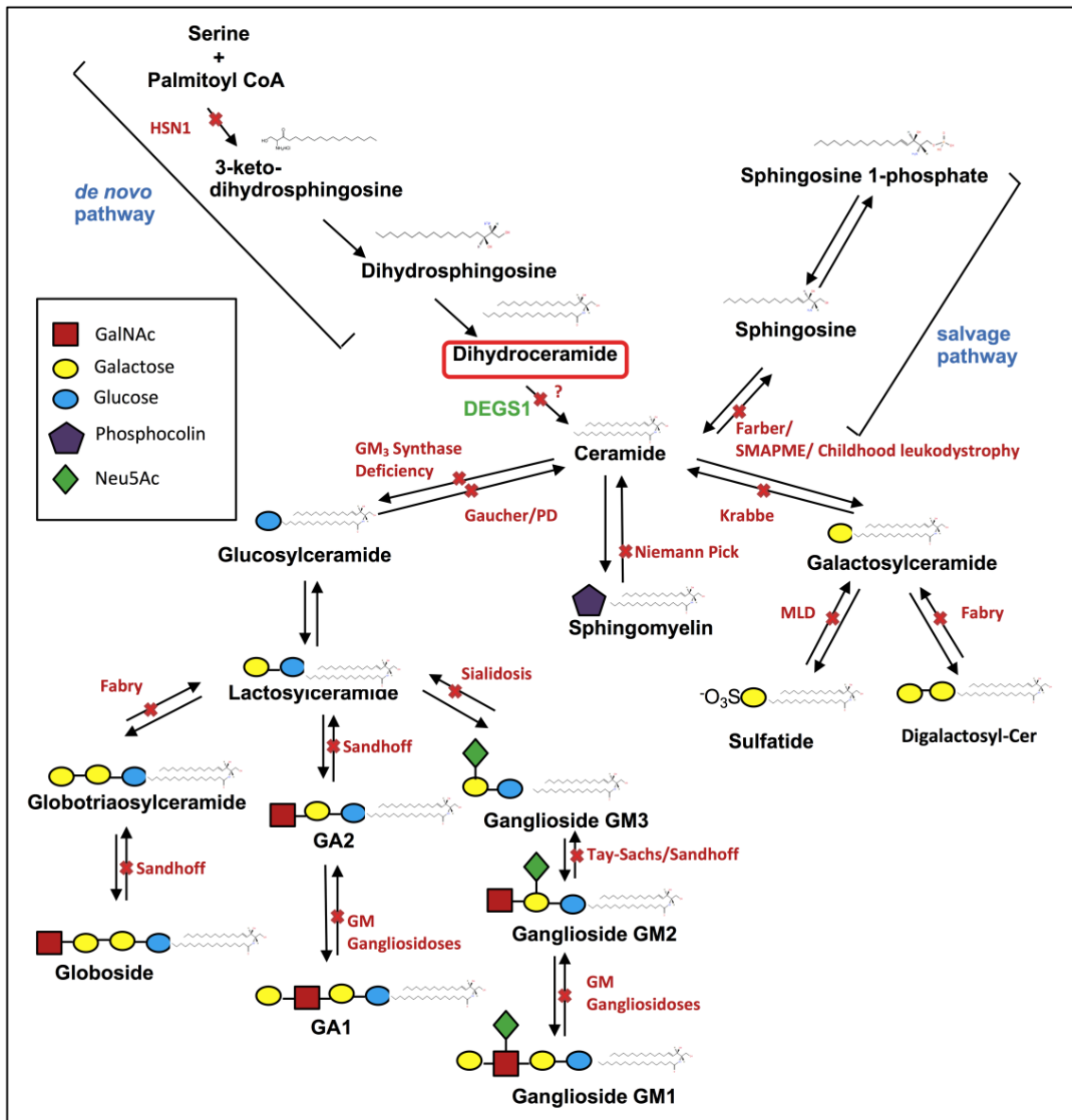


Figure 7. Scheme depicting enzyme defects involved in sphingolipid metabolism pathway associated with neurological symptoms.

Reactions are indicated by arrows; defects are indicated by red cross and associated diseases indicated in red. DEGS1, dihydroceramide desaturase; GA1, asialo - GM1; GA2, asialo - GM2; GM1, monosialotetrahexosylganglioside; GM2, disialotetrahexosylganglioside; GM3, trisialotetrahexosylganglioside; GalNAc, N-acetylgalactosamine; HSN1, Hereditary sensory neuropathy type I; PD, Parkinson disease; MLD, metachromatic leukodystrophy; Neu5Ac, N-acetylneuraminic acid; SMAPME, spinal muscular atrophy and progressive myoclonus epilepsy. Adapted from (Vanni et al., 2014).

Further, recent studies have emerged showing the development of monogenic disorders caused by mutations in the genes encoding enzymes of SL biosynthesis. Few of them have been linked to the development of neurological disorders. Among them, the most common SL synthesis disorder is a rare inherited sensory and autonomic neuropathy (HSAN), which is characterized by a defect in the very first step of SL metabolism.

HSANs are a group of clinically and genetically heterogeneous peripheral neuropathies. They can be subdivided into five clinical entities, which are all characterized by the progressive loss of pain and temperature sensation spreading from the distal limbs. (Rotthier, Baets, Timmerman, & Janssens, 2012). SPT catalyzes the condensation of palmitoyl-CoA and L-serine which is the initial and rate-limiting step in the de novo synthesis of SLs (Hanada, 2003). The condensation of palmitoyl-CoA with L-alanine and glycine results in the formation of 1-deoxy-sphinganine (deoxySa) and 1-desoxymethylsphinganine (deoxymetSa), respectively. Exogenous addition of these deoxy ceramides to primary neurons showed a dose-dependent neurite retraction and disruption of cytoskeletal structures indicating the neurotoxic role of these ceramides (Penno et al., 2010). Also, there was a correlation between disease severity and increased levels of deoxyCer levels were observed in the plasma of HSAN1 patients (Murphy et al., 2012). Mutations in *SPTLC1* could be conclusively linked to HSAN1 (Bejaoui et al., 2001; Dawkins, Hulme, Brahmabhatt, Auer-Grumbach, & Nicholson, 2001), and genetic screenings of HSAN patients in the UK confirmed that mutations in *SPTLC1* are also the most frequent cause for HSAN1 (Davidson et al 2012). A common feature of all HSAN1 mutants is a shift in the substrate specificity of SPT. Another important candidate of this panel, *FA2H* encodes for an enzyme that introduces a hydroxyl group at the C2-position of fatty acids. Homozygous *FA2H* mutations are associated with a rapidly progressive neurological disorder characterized by white matter degeneration that may present with spastic paraplegia (SPG35), leukodystrophy or neurodegeneration (Hama, 2010). The deficient function of two enzymes of SL synthesis, GM3 synthase, and ceramide synthase results in epilepsy (Harlalka et al., 2013). HSAN1 was also associated with mutations in genes encoding the enzymes involved in the synthesis of GM2 and GD2 gangliosides. Mice lacking GM2/GD2 synthase activity showed (Chiavegatto, Sun, Nelson, & Schnaar, 2000; Sheikh et al., 1999) no major histological or behavioral abnormalities; nonetheless, gait disturbance and tremor have been reported. Moreover, the higher brain levels of GM3 and GD3 were observed which might compensate for the lack of complex gangliosides in these animals. These findings point to the critical role of complex gangliosides in central nervous system functions. A comprehensive description of SLs metabolic enzymes and their related neurological disorders have been summarized (**Table 3**).

Table 3. Human neurological disorders linked to metabolic enzymes of sphingolipid pathway.

Gene	Effects	Disease and symptoms	References
<i>SPTLC1/ SPTLC2 SPT</i>	Increased de novo GluCer Accumulation of neurotoxic deoxySa	Inherited sensory and autonomic neuropathy (HSAN). first symptoms are already observed in early childhood and comprise considerable motor involvement, global hypotrophy, developmental retardation, vocal cord paresis, significant loss of myelinated fibers in several afferent peripheral nerves.	(Bejaoui et al., 2001) (Rotthier et al., 2012)
<i>ST3GAL5</i>	Increased level of lactosylceramide as well as intermediates ganglioside series	Amish epilepsy syndrome seizures with developmental stagnation and intellectual disability. Variability in phenotypes ranging from reduced or absent upper limb reflexes and deterioration of visual function with some optic atrophy in children to occipital white matter abnormalities and significant cortical atrophy, mainly in the occipital visual cortex in some patients Autosomal recessive neurocutaneous syndrome combining hyper and hypopigmented skin maculae called 'salt-and-pepper' syndrome Facial dysmorphism, scoliosis associated with severe intellectual disability, seizures, spasticity and an abnormal electrocardiogram with non specific conduction changes.	(Boccutto et al., 2014; Fragaki et al., 2013; Simpson et al., 2004)
<i>CERS2</i>	Reduced levels of C24:0 and C26:0 ceramides	Progressive myoclonic epilepsy generalized tonic-clonic seizures, dysarthria, photosensitivity, tremor and developmental delay	(Mosbech et al., 2014)

(Continued on next page)

<i>CERS1</i>	Reduced levels of C18-ceramide	Myoclonus epilepsy generalized tonic-clonic seizures, and moderate to severe cognitive impairment	(Vanni et al., 2014)
<i>GBA2</i>		Autosomal recessive cerebellar ataxia spasticity of the lower limbs, severe axonal sensory or sensory-motor neuropathy. In most cases, cerebral and spinal MRI is normal except for one case with a global atrophy. Hereditary spastic paraplegia cerebellar ataxia, cataract, and mild mental impairment. Some patients showed hearing loss, axonal neuropathy, and bilateral testicular hypotrophy associated with severe spermatozoid head abnormalities.	(Hammer et al., 2013; Martin et al., 2013)
<i>B4GALNT1</i>	GM3 accumulation	Hereditary spastic paraplegia progressive weakness and spasticity, brain MRI remains normal, cortical atrophy, subcortical atrophy and/or white matter hyperintensities	(Boukhris et al., 2013; Harlalka et al., 2013)
<i>FA2H</i>	-	Spastic paraplegia (SPG35) spastic paraparesis, gait disturbance, dystonia, and late mental deterioration. Some patients exhibit dysarthria, ataxia, dysmetria, and seizures.	(Edvardson et al., 2008)
<i>ACER3</i>	Increased levels of C18:1, C20:1 and long-chain ceramides and dihydroceramides	Childhood leukodystrophy movement problems and language developmental problems	(Edvardson et al., 2016)

(Continued on next page)

<i>SMPD1</i>	Accumulation of cholesterol, sphingolipids, GluCer, LacCer, GM2 and GM3	Niemann-Pick Disease type A infantile-onset of severe neurodegeneration with progressive psychomotor deterioration, neuronal cell loss in cerebral and cerebellar cortices, gliosis, demyelination, and infiltration of foam cells	(da Veiga Pereira, Desnick, Adler, Distèche, & Schuchman, 1991; Schuchman, 2010)
<i>GALC</i>	Accumulation of galactosylceramides and galactosylsphingosine	Krabbe disease progressive CNS and PNS involvement, stiffness, seizures, feeding difficulty, slowing of mental and motor development, and growth retardation, hypertonicity/hyperactive reflexes, progressive flaccidity, peripheral neuropathy, severe developmental delay, blindness, loss of vision, infiltration of characteristic “globoid cells”	(Lissens et al., 2007; Won, Singh, & Singh, 2016)
<i>GBA1</i>	Accumulation of glucosylceramides, GM1, GM2, GM3, GD3, glucosylsphingosine GluCer	Gaucher disease type 2 progressive CNS and lung involvement, neural death/drop-out Gaucher disease type 3 variable seizures, normal intelligence, short stature with splenomegaly, abnormal eye movements	(Bendikov-Bar & Horowitz, 2012; Stirnemann et al., 2017)
<i>ASAH1</i>	Accumulation of ceramides and hydroxyl ceramides	Farber disease granulomas, lipid-laden macrophages in the CNS, mild or no neurological involvement, subcutaneous skin nodules near or over joints	(C. M. Li et al., 1999)
<i>HEXB</i>	Accumulation of, GD1aGalNac, globoside, oligosaccharides, lyso-GM2	Sandhoff disease facial dysmorphism, skeletal dysplasia, hepatosplenomegaly	(Hendriksz et al., 2004)

(Continued on next page)

HEXA	Accumulation of GM2, lyso-GM2, GA2	Tay-Sachs disease progressive motor, mental and visual deficiencies, startled response to noise, hypotonia and paralysis, to a chronic form with no alteration in intelligence	(Okada & O'Brien, 1969)
ASRA	Accumulation of sulfatide	Metachromatic leukodystrophy difficulties walking, progressive peripheral neuropathies, muscle wasting/weakness, developmental delay, seizures, dementia	(R. Wang et al., 2016)

1.8 Therapeutic Interventions targeting spingolipids

Development of therapeutic treatments for sphingolipids related neurological disorders rely on two main approaches. Firstly, by reducing the excess of accumulated lipids by decreasing the activity of synthesis enzymes. Secondly, by targeting the increased activity of degrading enzymes. Several drugs have already been successful in pre-clinical studies and some of them are under the phase of clinical trials. The presence of the blood-brain barrier (BBB), physiologically shielding the penetrance of these drugs that lacks treatment of such neurological disorders. To overcome this problem, there are currently few specific types of treatment have been applied: 1) gene therapy includes delivery of target enzyme by using different viral vectors; 2) Enzyme replacement therapy (ERT): supplementation recombinant forms of wild-type enzymes delivered through frequent intravenous infusions. The most useful strategy proposed shown to be effective in treating systemic symptoms and slowing down the disease progression in the LSDs (Brady, 2006); 3) Enzyme enhancement therapy (EET): use of small molecules that interact directly with the specific mutant enzyme in cells to increase its activity *in situ* by improving trafficking to the lysosome, enhancing its stability, improving its catalytic rate constant, re-establishing proteostasis by diminishing the unfolded protein response (UPR) that a mutant enzyme creates, or a combination of all these mechanisms (Sawkar et al., 2002). Moreover, with the developed knowledge of dysregulated pathways in the pathogenesis of LSDs, effective and cheap treatment using drugs that able to cross BBB targeting the mutant gene could be applicable. For example, studies conducted in some animal models have shown that non-steroidal anti-inflammatory drugs (NSAIDs) have modest, but significant protective effects (Smith, Wallom, Williams, Jeyakumar, & Platt, 2009). However, effective CNS gene therapy coupled with systemic treatment (anti-inflammatory drugs) might possibly ameliorate the quality of life for patients with these disorders (Jeyakumar et al., 2001); 4) Substrate reduction therapy (SRT) aims to reduce the excess lipids by decreasing its synthesis. An example is Miglustat, which reduces the production of GSL and this drug is approved for the treatment of type 1 Gaucher disease, as well as for NPC disease (Cox et al., 2015; Lachmann, 2006). Another substrate inhibitor, eliglustat was authorized in 2015, it is GlcCer synthase inhibitor but is more specific and more potent than miglustat, because it is an analogue of the ceramide part. It was evaluated in phase-1, -2 and -3 clinical studies comprising nearly 400 patients overall whose follow-up results were published after four years (Cox et al., 2015; Lukina et al.,

2010). There are certain limitations to these therapies. As gene therapy is not yet in routine clinical use for these diseases and ERT cannot target the brain because of the inability of the therapeutic enzyme to cross the BBB (Beck, 2009). Specific therapies developed for treating LSDs (for example ERT and SRT) are also extremely expensive, so combination therapy that uses multiple high cost drugs would be unrealistic. Thus, development of efficient therapeutic treatments will be needed to halt these devastating diseases.

1.8.1 Fingolimod and Sphingolipid Metabolism

Pathways of sphingolipid metabolism have become important targets for the development of therapeutics. Initially, a compound known as myriocin was isolated from the supernatant of *Isaria sinclairii* (fungus) culture and was shown to retain the immunosuppressive properties (Fujita et al., 1994). Myriocin was then chemically modified to make fingolimod (FTY720) and was shown to induce immunosuppression and prevent allograft rejection in animal models (Suzuki, Li, Enosawa, & Shinomiya, 1996). As shown (**Fig. 8**) FTY720 is phosphorylated by sphingosine kinases (SphKs) in the cell to form FTY720 phosphate or FTY720-P (Billich et al., 2003). FTY720 deserves special recognition since it is the first drug to be approved by the US FDA (food and drug administration) whose primary mechanism of action is the modulation of S1P (sphingosine-1-phosphate) signalling (Chiba, Kataoka, Seki, Maeda, & Sugahara, 2011). FTY720 (also known as Gilenya[®], Novartis AG) is a potent immunosuppressant which was approved as a first-line therapy for relapsing forms of multiple sclerosis (MS) in 2010 (Chun J, 2011).

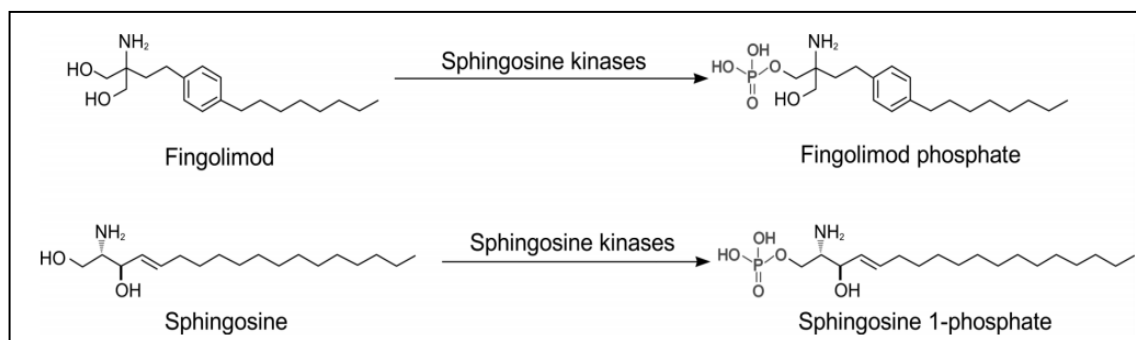


Figure 8. Fingolimod is a structural analog of naturally occurring sphingosine.

Fingolimod (molecular weight, 307.47 g/mol), like sphingosine (molecular weight, 299.49 g/mol) is phosphorylated by sphingosine kinases, in particular sphingosine kinase 2, to produce fingolimod phosphate (molecular weight, 387.47 g/mol) while sphingosine undergoes phosphorylation to sphingosine 1-phosphate (molecular weight, 379.47 g/mol). From (Chun & Hartung, 2010).

As a structural analog of natural sphingosine (**Fig. 8**), FTY720 can undergo rapid phosphorylation *in vivo* by sphingosine kinase 2 to produce FTY720-P (modulates immune cell kinetics) which binds to four of the five S1P receptors i.e. S1P₁ and S1P₃₋₅ (Brinkmann, 2007). FTY720 exerts its therapeutic effects through modulation of S1P receptors by FTY720-P. FTY720 is multiple targets in sphingolipid metabolism pathway. FTY720 has the ability to inhibit both S1P synthesizing as well as degrading enzymes such as SphK1 (Lim et al., 2011), S1P lyase (Bandhuvula, Tam, Oskouian, & Saba, 2005), the ceramide synthases (Lahiri et al., 2009) and the acid sphingomyelinase (Dawson & Qin, 2011). A number of studies demonstrating FTY720 interaction with sphingolipid metabolism has been reviewed (Brunkhorst, Vutukuri, & Pfeilschifter, 2014a). FTY720 demonstrated a proven efficacy in multiple *in vitro* and *in vivo* cancer models by inhibiting sphingosine kinase 1 (White, Alshaker, Cooper, Winkler, & Pchejetski, 2016). Many of the enzymes of sphingolipid metabolism have themselves become targets for therapeutics (detailed in discussion section). Analogs of bioactive sphingolipids are proving to be of use in the treatment of immune and metabolic disorders, as well as cancer. Inhibitors of acid ceramidase are the subject of intensive development (Realini et al., 2013). In the case of sphingosine-1-phosphate (S1P) and its G protein-coupled receptors are receiving increasing attention as therapeutic targets.

Furthermore, evidence is now emerging that alterations in sphingolipid metabolism, leading to enhanced pro-inflammatory ceramide production, occur in several neurological disorders, such as hereditary sensory neuropathy type I (Dawkins et al., 2001), Batten's syndrome (Puranam et al., 1997) and Wilson's disease (Lang et al., 2007). Notably, inflammatory mediators, including tumor necrosis factor, TNF- α (Schütze et al., 1992), reactive oxygen species (ROS) (Sanvicens & Cotter, 2006), and interleukin-1, IL-1 β (Hofmeister et al., 1997) induces the production of ceramide through activation of sphingomyelinases, which in turn amplifies the inflammatory cascade either by direct activation of downstream targets or by affecting membrane organization. The group of De Varies had shown that FTY720-P decreases acid sphingomyelinase enzyme expression and reduces ceramide production in human MS reactive astrocytes, thereby attenuating inflammatory events at the neurovascular unit (van Doorn et al., 2012). More studies are needed to determine which specific receptor and downstream pathways are involved in altering ceramide levels or their dihydro counterparts and whether FTY720 may also have direct intracellular effects.

The safety profile of FTY720 therapy has been carefully examined, particularly in the light of its anticipated long-term use. The cumulative datasets from clinical trials and their extensions, plus post-marketing studies, have well delineated the safety profile of FTY720 in MS patients (Kappos et al., 2014). However, the common adverse effects seen in some patients were cardiovascular events, including bradycardia and first-degree or second-degree atrioventricular block, after administration of the first dose (Laroni et al., 2014). Very recently (May 11, 2018), Novartis has announced that US FDA has approved FTY720 for the treatment of children and adolescents 10 to less than 18 years of age with relapsing forms of MS, making it the first disease-modifying therapy indicated for these patients (www.novartis.com). Therefore, observational studies that have larger patient recruitment and longer follow up durations are needed in order to corroborate the FTY720 benefits observed in clinical trials.

1.9 The Zebrafish as a Model System

The zebrafish, *Danio rerio*, is a small teleost fish commonly found in slow-running waters originating from the rivers of the Indian subcontinent (Arunachalam, Raja, Vijayakumar, Malaiammal, & Mayden, 2013). The use of zebrafish as an animal model began in the 1960s with the work of George Streisinger due to their embryo transparency and rapid organogenesis features (David Jonah Grunwald & Eisen, 2002). The group of Streisinger developed a number of techniques to manipulate the ploidy of zebrafish eggs and zygotes (Streisinger, Walker, Dower, Knauber, & Singer, 1981). Streisinger and his co-workers also established techniques for forwarding genetic screening in zebrafish (David J. Grunwald, Kimmel, Westerfield, Walker, & Streisinger, 1988; Walker & Streisinger, 1983). Currently, it is one of the leading models for studying development and human diseases (Rubinstein, 2003).

The animal model zebrafish has received a lot of attraction from the scientific communities worldwide which result in underpinning its anatomy, behavior, and physiology. The critical breakthrough came from two publications showing first three-dimensional (3D) digital atlas of the zebrafish brain from T_2^* -weighted magnetic resonance histology (MRH) images of the zebrafish brain (Ullmann, Cowin, Kurniawan, & Collin, 2010) and an atlas of anatomy and histology of adult zebrafish (Menke,

Spitsbergen, Wolterbeek, & Woutersen, 2011). There are several reasons which made researchers using zebrafish as an animal model, the most fascinating characteristics of all was the embryo transparency during early life stages which made the observation process of the whole body and organ formation possible by light microscopy. Zebrafish is becoming popular and useful for the biomedical field, as a high degree of conservation exists between the human and zebrafish genomes. This was revealed by Wellcome Trust Sanger Institute, UK, developed a high quality annotated sequence of zebrafish genome (started in 2001) and compared it with the human genome reference sequence. The study highlighted that 70 % of human protein-coding genes were related to zebrafish genes and 82 % of genes known to be associated with human disease have a zebrafish orthologue. The study highlights the importance of zebrafish as an ideal model organism for human disease research (Howe et al., 2013).

1.9.1 Advantages of Zebrafish Model

The use of animal models in research can be dated long back to the history of biomedical sciences. The current and growing popularity of using zebrafish for research is attributed to its favorable physical characteristics, easy experimental manipulation and the extensive knowledge based on this organism that now exists. The characteristics that make them desirable tools for research are discussed below:

- a) **Ease of use:** Zebrafish is a vertebrate organism, while maintaining the ease of use of a lower organism. Embryos or larvae can be raised in laboratory with water and temperature (28.5 °C) Adult zebrafish are small in size (1.6 in) and they require much less space and are cheaper to maintain than mice.
- b) **Large offspring:** Zebrafish have high fecundity rate. A pair of adult zebrafish can breed rapidly (approximately every 7 days) and can produce as many as 100 to 200 eggs at a time (**Fig. 9**). This is helpful where large number of animals is needed for phenotypic screening to produce more accurate and reproducible results.
- c) **Optical transparency:** Zebrafish embryos are transparent and this can be extended to up to 5 dpf (days post fertilization) or more with the addition of the melanocyte inhibitor phenylthiourea (PTU). Moreover, this transparency of

zebrafish larvae can be exploited in several ways, utilization of fluorescence proteins (e.g. GFP, for “Green Fluorescent Protein”) to label proteins or cellular entities, allows for powerful imaging of biological and disease processes.

- d) **Rapid development:** Zebrafish embryos developed quickly from a single cell in a fertilized egg into larvae in few hours, makes them easy for genetic manipulation (**Fig. 9**).

- e) **Genetic manipulations:** Using microinjection techniques at one-cell stage of the embryo, zebrafish mutants can be generated by application of antisense morpholino (MO) oligonucleotide mediated transient gene knockdown (KD). Knockout (KO) and Knockin (KI) using Transcription Activator-Like Effector Nucleases (TALENs) and Clustered Regularly Interspaced Short Palindromic Repeats (CRISPRs) to generate stable lines. Exploiting UAS-Gal4 system, Tol2-mediated UAS-Gal4, Cre/Lox system and tamoxifen-inducible Cre/lox mediated transgenesis methods are becoming successful in defining the functional roles of target genes in cell or tissue-specific regions.

- f) **Drug Screening:** To take full advantage of high fecundity, optical transparency and rapid development of zebrafish embryos, it is possible to monitor drug efficacy in embryo or larvae in a 96 well plate. The parameters of screening might be simple as survival, or direct visual assessment of the severity of a specific phenotype. This approach can be greatly facilitated by using strain expressing GFP in a tissue that is affected by the pathogenic process. Thus, *in vivo* analysis of the effects of compounds can be undertaken in early stages of drug discovery process.

- g) **Zebrafish database:** Finally, the researchers are benefited from an up-to-date database of genetic strains, expression data, and other useful resources at Zebrafish Model Organism Database (ZFIN, <http://zfin.org/>). This helps researchers to collaborate with others and it also provides training lessons for the beginners in the field of zebrafish.

In spite of a large number of advantages, the model has certain limitations which need to be considered while project designing. For example, genome duplication, long generation time and low efficiency of homologous recombination (HR).

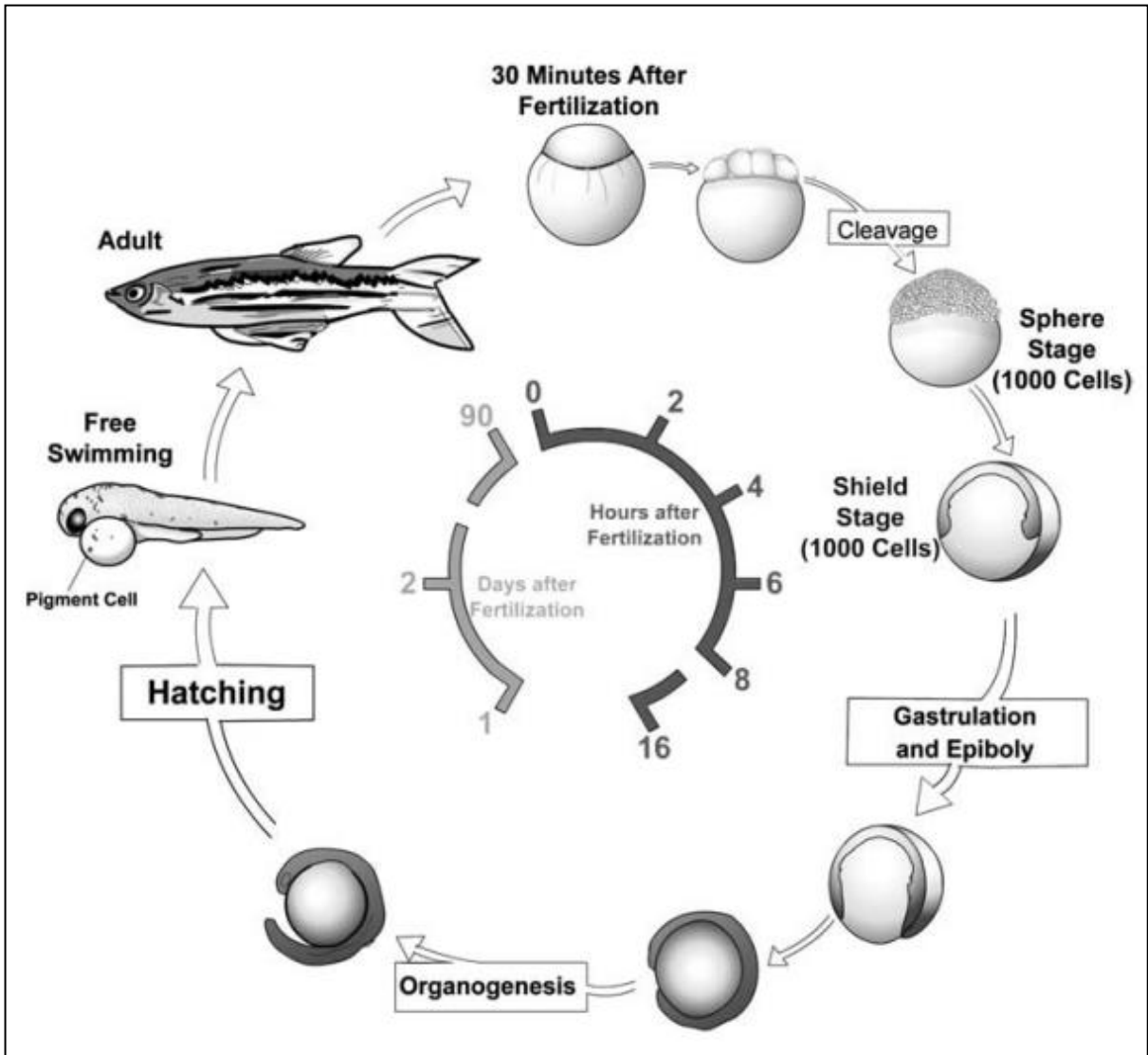


Figure 9. The life cycle of the zebrafish.

Zebrafish develop rapidly from a one-cell zygote that sits on top of a large yolk cell. Gastrulation begins approximately 6 h post fertilization, hatching at 2 days as free-swimming larvae. Zebrafish reach sexual maturity around 3 months of age and can live for up to 5 years. From (D’Costa & Shepherd, 2009).

1.9.2 Zebrafish Genetic Toolkit

To facilitate classical genetic analysis and the increasing need to develop experimental models to further our understanding of disease conditions, zebrafish model has received a lot of attention to close the gap between *in vitro* and *in vivo* assays. Forward genetic

approaches, which are used for the identification of mutated genes underpinning specific phenotypes of interest are complemented by reverse genetic approaches. While the expansion of the zebrafish genetic toolbox has increased the model's appeal, it is important to keep in mind the limits of the model and some experimental approaches.

1.9.3 Transient Genetic Approaches

Transient disruption of the gene can be achieved through the injection of either morpholino (MO) antisense oligonucleotides (gene suppression) or capped *in vitro* transcribed mRNA (ectopic expression) into zebrafish embryos (Summerton, 1999). Synthetic MOs are stable and can be easily injected into embryos at 1-2 cell stage, where they interfere with gene expression. MOs can bind and mask the translational start site of mRNAs or can interfere with splicing, creating loss-of-function phenotypes. This straightforward and simple approach became extremely popular among researchers looking for quick assays to test candidate genes from NGS and in numerous studies providing necessary proof to validate the identification of candidate genes listed (**Table 4**). MO technology was enthusiastically adopted by the zebrafish field and morphant phenotypes were often used in human genetic studies to provide independent proof for the involvement of particular genes in the observed pathologies. However, the approach has certain limitations. Some early studies of genome edited lines have raised serious questions about the veracity of many results that were based on MO-effects only (Kok et al., 2015). All these findings resulted in a reconsideration of the use of MOs in the zebrafish field and paved the way for stringent new guidelines (Stainier et al., 2017). A morphant phenotype should be considered specific only if it is able to phenocopy a mutation. However, recent research suggests that the unaltered phenotype in many zebrafish mutants could be the result of either genomic compensation triggered by non-sense mediated decay (Rossi et al., 2015) or altered mRNA processing (Balciunas, 2018). Overall, the current consensus in the field is to include the use of MOs, their careful titration and the demonstration that the gene of interest is successfully targeted either by Western blot if antibodies are available, or at least by RT-PCR to monitor altered splicing in the case of a splice blocking MO.

1.9.4 Stable Genetic Approaches

Independently of MOs, the molecular techniques to develop germline zebrafish mutants for a gene of interest have evolved substantially. With the application of transcription activator-like effector nucleases (TALEN) (Bedell et al., 2012) and, more recently, clustered regularly interspaced short palindromic repeats (CRISPR) based genome editing technologies in zebrafish (Hwang et al., 2013) can be designed easily using various online tools. The use of such stable transgenic approaches have reduced the use of MOs. These new methodological approaches have already revolutionized zebrafish genetics and provided independent means to test the accuracy of the MOs (**Table 4**). While most of the novel genome edited lines are loss-of-function alleles that arise due to the indel mutations resulting from non-homologous end joining (NHEJ) DNA repair mechanisms. Of the existing programmable nuclease techniques TALENs, albeit slower and more expensive to assembly, are usually considered superior, due to their higher specificity. As the problems with MOs became apparent, many people opted to complement or supplement MO studies with the description of “crispant” phenotypes. In crispants CRISPR/Cas9 technology was used to introduce mutations with gene-specific sgRNA. Due to the very nature of this method, most embryos will be highly mosaic for the mutations they carry, and only careful analysis can reveal if they indeed have bi-allelic mutations in most of their cells. Therefore, one should check carefully and only accept crispant phenotypes as specific if constitutive mutants show the same phenotype. Ideally, one should aim to conduct studies in F2 or F3 generations, where the possible confounding effects of off-target mutations can be minimized. In addition, transgenic lines have been instrumental in characterizing the effects of specific mutations (Peterson et al., 2004) highlighting the power of this approach. Further, Tol2 based transgenesis, based on the gateway technology has made the creation of transgenic lines an easy task (Kwan et al., 2007). Efficient transgenesis techniques have been also used for enhancer-trap and gene-trap screens (Kawakami, 2007), and a wide array of tissue-specific Gal4 and CreERT2 lines have been established, paving the way for genetic manipulations (Kawakami et al., 2010). Finally, the combination of transgenesis and genome editing techniques enabled researchers to create the conditional knock-out methodology (Ablain, Durand, Yang, Zhou, & Zon, 2015). Efforts have been made to create precise knock-in alleles exploiting the alternative, homologous recombination (HR) repair pathway (Hisano et al., 2015). While the excitement caused by these early results seemed justified,

later results suggested that the knock-in efficiency is highly locus dependent. It will be also important to compile databases of proven and effective single guide RNA (sgRNA) target sequences with low off-target effects, so that targeting of particular genes with CRISPR-based methods can become more standardized (Varshney et al., 2016). There can be off-target of CRISPR. However, considerably reduced with the right choice of sgRNAs and with the use of rationally engineered CRISPR (Kulcsár et al., 2017).

Table 4: List of existing zebrafish models of human neurological diseases.

Gene	Disease or Phenotype	Zebrafish Model Type	Reference
<i>MFN2</i> , <i>GDAP1</i> , <i>ABHD12</i> , <i>MED25</i> , <i>HSPB1</i> , <i>WNKI</i>	Charcot-Marie-Tooth syndrome	MO	(Gonzaga-Jauregui et al., 2015)
<i>SLC39A14</i>	Childhood-onset parkinsonism-dystonia	CRISPR	(Tuschl et al., 2016)
<i>SCN1A</i>	Dravet syndrome	Chemical mutagenesis	(Baraban, Dinday, & Hortopan, 2013)
<i>DMD</i>	Duchenne muscular dystrophy	MO	(Bassett et al., 2003)
<i>STX1B</i>	Generalized epilepsy with febrile seizures-plus	MO	(Schubert et al., 2014)
<i>SMN1</i>	Spinal muscular atrophy	MO, Chemical mutagenesis	(Boon et al., 2009; See et al., 2014)
<i>ABCD1</i>	X-linked adrenoleukodystrophy	TALENs	(Strachan et al., 2017)
<i>EXOSC3</i>	Pontocerebellar hypoplasia	MO	(Wan et al., 2012)
<i>ARMC9</i>	Joubert syndrome	CRISPR	(Van De Weghe et al., 2017)
<i>RORA</i>	Cerebellar ataxia	MO, CRISPR	(Guissart et al., 2018)
<i>GFAP</i>	Alexander disease	Transient	(S.-H. Lee et al., 2017)
<i>RNF216</i> , <i>OTUD4</i>	Hypogonadotropic Hypogonadism, ataxia, and dementia	MO	(Margolin et al., 2013)

(Continued on next page)

<i>BPTF</i>	Dysmorphic features	CRISPR	(Stankiewicz et al., 2017)
<i>BRF1</i>	Neurodevelopmental anomalies	MO	(Borck et al., 2015)
<i>CHP1</i>	Autosomal recessive cerebellar ataxias	MO	(Mendoza-Ferreira et al., 2018)
<i>KIAA1109</i>	Alkuraya-Kucinskas syndrome	MO	(Gueneau et al., 2018)
<i>LAT</i>	Neuroanatomical defects	CRISPR	(Loviglio et al., 2017)
<i>MAF</i>	Ayme-Gripp Syndrome	Transient	(Niceta et al., 2015)
<i>ABHD12</i>	PHARC syndrome,	MO	(Tingaud-Sequeira, Lavie, & Knoll-Gellida, 2017)
<i>PSMD12</i>	Neurodevelopmental disorder	CRISPR	(Küry et al., 2017)
<i>RAC1</i>	Brain malformations	Transient	(Reijnders et al., 2017)
<i>TAF1</i>	Developmental delay	MO	(O’Rawe et al., 2015)
<i>TMEM260</i>	Neurodevelopmental disorder	MO, CRISPR	Asaf Ta-Shma AJHG 2017
<i>EXOSC8</i>	Spinal muscular atrophy and cerebellar hypoplasia	MO	(Boczonadi et al., 2014)
<i>PYCR2</i>	Microcephaly and Hypomyelination	MO	(Nakayama et al., 2015)
<i>NPCI</i>	Niemann Pick disease	MO	(Louwette et al., 2013)
<i>FUS, TARDBP</i>	ALS	MO	(Kabashi, Bercier, et al., 2011)
<i>GALC</i>	Krabbe disease	MO	(Zizioli et al., 2014)
<i>MLC1</i>	Megalencephalic leukoencephalopathy	Chemical mutagenesis	(Sirisi et al., 2014)

1.9.5 Modelling Human Neurological Disorders Using Zebrafish

NGS techniques have so far identified hundreds of variants that are associated with neurological disorders. Before results from NGS can be translated into something that can be used in the clinic - for example into novel biomarkers or drugs - we need to identify and characterize the causal genes (**Fig. 10**). Recent developments in the zebrafish field, high-throughput imaging, and image-based analyses have highlighted the zebrafish importance in modeling the disease causative variants as listed (**Table 4**). When a mutation or a variant causing a human disease is identified, modeling of that disease in zebrafish is often used to provide additional evidence supporting the causative gene. In other cases, zebrafish models have been made as a tool to perform research into finding treatments, often for incurable fatal diseases. One prerequisite for the analysis of human neurological diseases in an animal model system is a comparable neuroanatomy as well as genetics/genomics capabilities. At the gross level morphology and major nuclei of the zebrafish brain are similar to human, even though the telencephalon does not develop into a layered cortex (Babin, Goizet, & Raldúa, 2014).

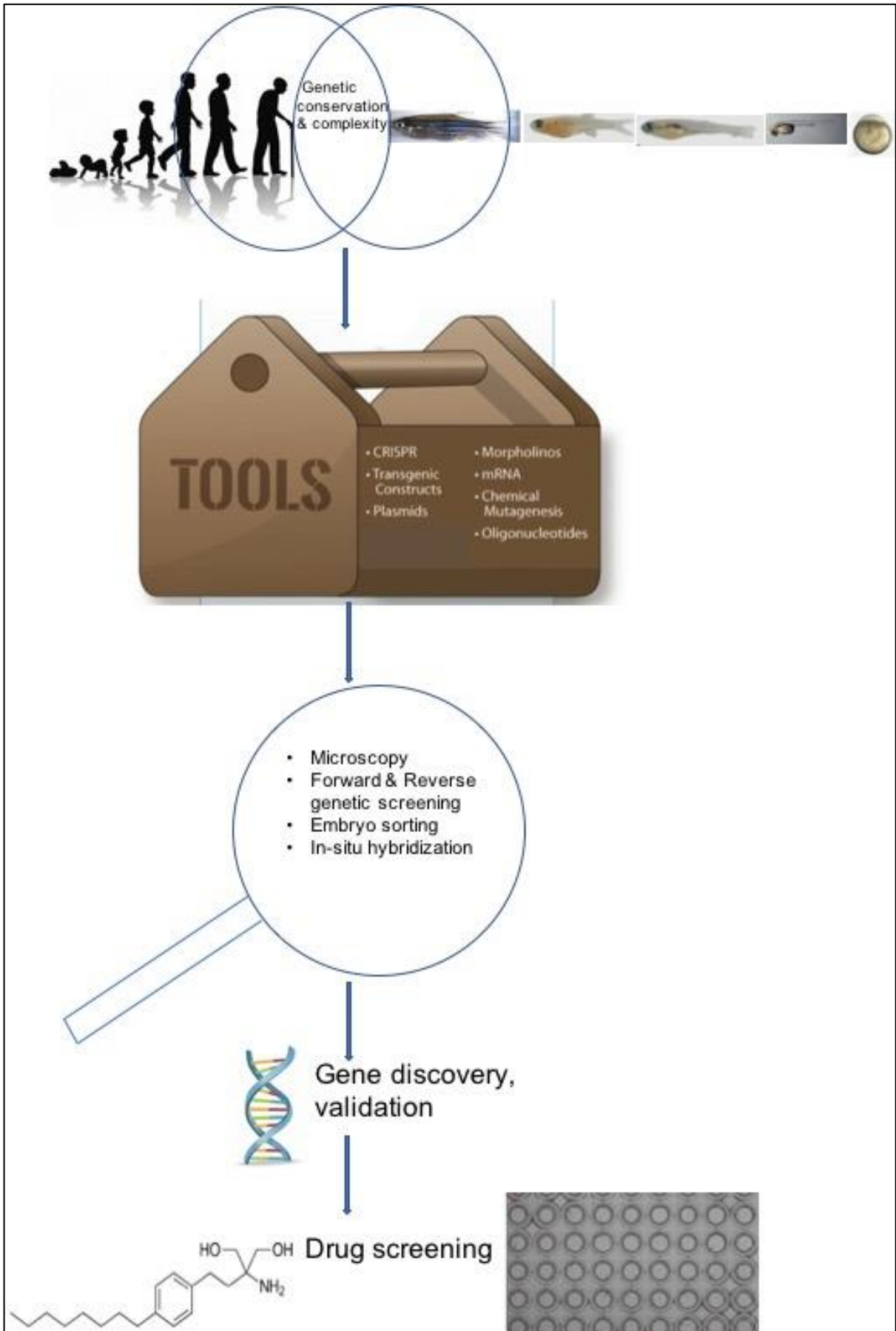


Figure 10. General illustration depicting zebrafish model in the study of human genetic diseases.

Zebrafish and humans share a high degree of genetic conservation. Zebrafish is amenable to a number of genetic tools, Genetically modified zebrafish can easily survey using light and fluorescent microscopy. Translational outputs include preclinical therapeutic studies using candidate drug can easily be studied using zebrafish embryos. Adapted from (Strynatka, Gurrola-Gal, Berman, & McMaster, 2018)

1.9.6 Zebrafish in Drug Discovery

An increasing number of human disease models has been generated in zebrafish. An extension of this paradigm is to use zebrafish models to identify novel therapeutic avenues. Due to its small size, it allows high-throughput screening and has made zebrafish a prominent model in drug screening over the past decade. In addition, high level of genetic conservation between zebrafish and humans, several drugs have similar targets in both species as reviewed (Kaufman, White, & Zon, 2009; Varga et al., 2018). Several models of pediatric disorders have been used in such screens, and these experiments confirm that both homologous and orthologous phenotypes can be successfully used in drug discovery experiments as summarised (**Table 5**). In addition to candidate treatment approaches, large-scale phenotypic screens have also shown promise in either uncovering repurposing opportunities for known drugs or discovering novel compound classes. For example, disruption of *ACVRI* activates the bone morphogenetic protein (BMP) type I receptor and causes fibrodysplasia ossificans progressiva (FOP), a congenital disorder of progressive postnatal ossification of soft tissues (Shore et al., 2006). By screening a diverse chemical library of 7500 compounds (P. B. Yu et al., 2008) identified a pyrazolopyrimidine called dorsomorphin as a BMP inhibitor that could compensate for the overactive signaling induced by *ACVRI* mutations; this compound, and its derivatives, are currently in mammalian trials for FOP (MacRae & Peterson, 2015). In addition, mutations in *RAP1A* have been implicated as a molecular cause of Kabuki syndrome. Knockdown of endogenous gene or CRISPR/Cas9 mutation of the zebrafish duplicated orthologs, *rap1a* and *rap1b*, reproduced the mandibular defects observed in patients and elucidated the involvement of known Kabuki syndrome genes in MEK/ERK signaling; administration of the MEK inhibitor PD184161 was shown to improve relevant phenotypes in zebrafish (Bögershausen et al., 2015).

In some instances, the known function of the human disease gene is sufficient to suggest a candidate therapeutic modulator in zebrafish; this was true for the recent identification of *NANS*, the causal gene underlying an infantile-onset severe developmental delay and

skeletal dysplasia disorder. *NANS* encode the synthase for N-acetylneuraminic acid (neunAc; sialic acid). MO-induced suppression of the zebrafish ortholog *nansa* recapitulated the abnormal skeletal development and, could be rescued with exogenous treatment with sialic acid (van Karnebeek et al., 2016). In a recent model of childhood-onset parkinsonism-dystonia, characterized by mutations in a manganese transporter, was successfully used to show that the symptoms of the disease can be ameliorated using Na_2CaEDTA as a chelator and this treatment also alleviates the patients' symptoms (Tuschl et al., 2016). An even more impressive story involves a zebrafish model of the Dravet syndrome: a high-throughput drug screen identified clemizole as potential drugs with anti-serotonin effects. It was possible to register them as a potential treatment. When applied directly to patients with the Dravet syndrome, these drugs outperformed conventional anticonvulsants (Griffin et al., 2017). While zebrafish studies will not always substitute pre-clinical tests in mammalian models, they can save time and money by pre-filtering the compounds that enter the more advanced phases of drug development (Ekins, 2017).

In summary, zebrafish phenotype screening has potential to contribute to novel therapeutic development for human genetic disorders. Further work is required to characterize compound exposure in zebrafish and to understand how timing and delivery in zebrafish is relevant to that of the human.

Table 5. Some examples for the use of drugs with human relevance in zebrafish neurological disease models.

Drug or Molecule used	Zebrafish disease model	Effect	Reference
Clemizole	Dravet syndrome	Reducing seizure behavior after acute treatment	(Baraban et al., 2013)
Ataluren	Duchenne muscular dystrophy	Improved contractile function and dystrophin expression	(M. Li, Andersson-Lendahl, Sejersen, & Arner, 2014)
Na₂CaEDTA	Childhood-onset parkinsonism dystonia	Improves Manganese homeostasis	(Tuschl et al., 2016)
Sialic acid	Spondyloepimetaphyseal dysplasia	Partially rescued the skeletal phenotype	(van Karnebeek et al., 2016)
6-OHDA	Parkinson disease	Restored locomotor deficit but not neuronal loss	(Cronin & Grealy, 2017)
L-DOPA	Parkinson disease	Exposure induced locomotor deficit and neuronal loss	(Cronin & Grealy, 2017)
Anti-epileptic drugs	Epilepsy	Reduced seizures	(Kundap, Kumari, Othman, & Shaikh, 2017)
FTY720	Multiple sclerosis	Improvement in % survival, body weight	(Kulkarni et al., 2017)
Vorinostat (Zolinza™)	Epilepsy	Blocks seizures and restored basal elevated respiration and total mitochondria respiration	(Ibhazehiebo et al., 2018)

AIMS & OBJECTIVES

2 AIMS & OBJECTIVES

The main aim of this thesis is to understand the cause of unknown neurological disorder as it is one of the greatest clinical challenges in the field of biomedical science. The diagnosis of a neurological disorder is a complex and difficult process due to high range of heterogeneity from both the clinical and genetic point of view. For this reason, in collaboration with different research centers, our laboratory is involved in a project aimed at study patients using NGS technologies. This aim was accomplished by implementing following objectives:

- 1) To improve the yield of definitive genetic diagnoses in a cohort of unsolved leukodystrophy cases. This required an accurate assessment of pathogenicity of candidate variants identified from WES data analysis.
- 2) Detailed functional characterization of the variants in a candidate gene *DEGSI* to discover fundamental new biology by the development of functional assays to test the deleterious effects of the variants identify by NGS. This objective was fulfilled by executing *in vitro* approach using the human skin derived fibroblasts from healthy subjects and patients.
- 3) *In vivo* modelling of the candidate gene was carried out by generating the zebrafish model using morpholino and characterized the functional importance of the candidate gene in CNS.
- 4) Using the combination of both *in vitro* and *in vivo* approaches, we evaluated the therapeutic potential of FTY720, a CerS inhibitor, to counteract the disease pathogenesis.

MATERIALS & METHODS

3 MATERIALS AND METHODS

3.1 MATERIALS

3.1.1 Reagents, Probes and Antibodies

The following chemicals were used: C18 Dihydroceramide (d18:0/18:0, Avanti Polar Lipids, Ref. 860627), Fingolimod, FTY720 (Selleckchem, Ref. S5002), Ethanol (Merck, Ref 100983), Dodecane (Sigma, Ref. 44010), TritonTM (Merck, Ref. 108643), Antimycin A (Sigma, Ref. A8674), DMEM: F12 (Dulbecco's Modified Eagle's Medium/Ham's Nutrient Mixture, Ref. 31330-038) from GIBCO, H₂DCFDA (2',7'-Dichlorodihydrofluorescein diacetate, Invitrogen, Ref. C2938), DHE (Dihydroethidium, Invitrogen, Ref. D23107), MitoTracker[®] (Molecular probes, Ref. M7512), DAPI (4',6-Diamidino-2-Phenylindole, Dihydrochloride) (Thermofisher Inc, Ref. D1306), MitoSOX (Red mitochondrial superoxide indicator, Invitrogen, Ref. M36008) from life technologies; FBS (Foetal bovine serum, Cultek, Ref. 91S1800). Taqman probes hDEGS1 (Hs00186447_m1), hDEGS2 (Hs01380343_m1), hRPLP0 (Hs9999902_m1), mDegs1 (Mm00492146_m1), mDegs2 (Mm00510313_m1), mRplp0 (Mm01974474_gH) and antibodies (ab) LC3 (Novus Biologicals, Ref. PD014), p62 (Abcam, Ref. ab56416), γ -tubulin (Sigma, Ref. T6557), GFP (Aves Lab, Ref. GFP1020), TOM20 (Santa Cruz, Ref. SC-11415). Anti-DIG-AP Fab fragments (alkalinephosphatase conjugated anti-DIG, Roche Cat#11093274910).

3.1.2 Human Samples

3.1.2.1 Clinical Recruitment

In this thesis, subjects displaying leukodystrophy features from various hospitals were included in the patient cohort of the Neurometabolic Diseases laboratory, IDIBELL (Spain). These patients remained genetically undiagnosed following biochemical or another molecular testing. The individuals characterized as Leukodystrophy patients (LNF), had abnormal white matter damage upon neuroimaging. Clinical records were reviewed by pediatricians and neurologists, and translated into Human Phenotype Ontology (HPO) terms (Köhler et al., 2017). Patients were mainly Spanish Caucasian, although a mixture of ethnicities was present including individuals with an African, Asian or Latin American origin. Other cohorts of patients include 17 consecutive probands with

leukodystrophy. The probands were included in the consortium for patients having mutations in *DEGSI* (coordinator: Dr. A Pujol). The use of all samples was approved by the local clinical research ethics committee of the Bellvitge University Hospital (no. PR076/14). Informed written consent was obtained prior to collecting blood samples for DNA extraction.

3.1.2.2 Post-Mortem CNS Samples

Human brain parts (frontal lobe BA9, putamen, entorhinal cortex, hippocampus, hypothalamus, pons, cerebellum, white matter frontal cortex) and spinal cord tissue samples from child and adult were obtained from the National Institutes of Health (NIH) NeuroBioBank. Frozen blocks of different parts of the human brain were dissected from frontal or parietal lobes from controls and stored in cryovials at -80 °C until further use.

3.1.2.3 Primary Human Fibroblasts

Control primary human fibroblasts were prepared from skin biopsies collected from healthy individuals (n=5) according to the IDIBELL guidelines for sampling, including informed consent from the persons involved or their representatives. Affected individuals (n=3) fibroblasts were provided by different collaborators. The fibroblasts were grown in DMEM containing 10% FBS and 100 µg/ml Penicillin-Streptomycin (Gibco, Ref. 15140-122) and maintained at 37 °C in humidified 95% air / 5% CO₂ incubator.

3.1.2.4 Treatments

The tested compounds or drugs were added with the following concentrations: 5 µM FTY720 (dissolved in DMSO), 20µM C18 Dihydroceramide (d18:0/18:0) (dissolved in ethanol/dodecane, 49:1 v/v). Cells were treated with the above compounds for 6 h and the experiments were performed. Experiments with fibroblasts were performed at passage 10 to 20 with 80–90% cell confluence. For analysis of autophagy flux, human control and patient fibroblasts were allowed to reach 80% confluency in medium containing FBS (10 %) and treated with 10 nM bafilomycin A1 (Baf A1) for 2h. Autophagic flux was assessed by measuring endogenous LC3-II levels and p62 relative to the γ-tubulin using specific antibodies.

3.1.2.5 Extraction of Genomic DNA

Human patient samples were received as whole blood, genomic DNA (gDNA), fibroblasts culture and frozen muscle tissue. When blood samples from affected individuals and available family members were obtained, gDNA was extracted from 3 ml of blood sample following the manufacturer instructions from Genra Puregene Blood Kit (Qiagen). Extraction of DNA from fibroblasts was carried out by harvesting cells (2×10^7 cells), detached by trypsinization and transferred to 15 ml centrifuge tube followed by centrifugation ($500 \times g$, 3 min) to pellet cells. The gDNA was extracted from the pellet as per manufacturer instructions (Qiagen). In case of human muscle tissue, 5 mg of frozen muscle tissue was homogenized in 300 μ l of cell lysis solution (Qiagen) using polytron benchtop homogenizer (POLYTRON[®] PT 1200 E) and was followed by (i) lysis (ii) removal of proteins and contaminants and (iii) recovery of DNA using Genra Puregene tissue kit (Qiagen). The quality and quantity of the extracted DNA were determined by spectrophotometric analysis (Nanodrop) and further confirmed by running on 0.8 % agarose gel electrophoresis. All samples of gDNA were stored at $-80 \text{ }^\circ\text{C}$.

3.1.3 Mouse Strain

We used male mice of a pure C57BL/6J background. All of the methods employed in this study were in accordance with the Guide for the Care and Use of Laboratory Animals (Guide, 8th edition, 2011, NIH) and European (2010/63/UE) and Spanish (RD 53/2013) legislation. Experimental protocol had been approved by IDIBELL, IACUC (Institutional Animal Care and Use Committee) and regional authority (3546 DMAH, Generalitat de Catalunya, Spain). IDIBELL animal facility has been accredited by The Association for Assessment and Accreditation of Laboratory Animal Care (AAALAC, Unit 1155). Animals were housed at $22 \text{ }^\circ\text{C}$ on specific-pathogen free conditions, in a 12- hour light/dark cycle, and ad libitum access to food and water. Cages contained 3 to 5 animals.

3.14 Zebrafish Strain

The zebrafish (strain AB) used in this thesis were maintained in the animal facility of the PRBB. The breeding and handling of the zebrafish were performed according to the guidelines of “The Zebrafish Book” (Westerfield 2000). Wild-type zebrafish strain was AB/Tu (RRID: ZIRC_ZL1/RRID: ZIRC_ZL57).

3.14.1 Production of Zebrafish Embryos

Zebrafish (*Danio rerio*) embryos were produced by paired mating of adult fish in the PRBB zebrafish facility. Zebrafish female and male pairs were placed in a mating chamber, separated by the chamber divider overnight in the evening before eggs were required. Eggs are usually laid and fertilized the following morning shortly after the lights are turned on (lights on occurs regularly at 8:00 am). The next day, zebrafish embryos were collected using a fine-mesh strainer and placed them in a Petri-dish containing fish water. Using a plastic transfer pipette to remove debris (solid waste). Next, we used a stereomicroscope to observe each clutch of embryos and remove any unfertilized eggs. Embryos were grown in 50 mm rounded Petri dishes (Sterlin, Cat#121V) in diluted methylene blue (2 ml of 0.1% methylene blue, to 1 liter of fish water) at 28.5 °C. Strains were maintained individually as inbred lines. All procedures used have been approved by the institutional animal care and use ethic committee (PRBB–IACUC), and implemented according to national rules and European regulations. Embryos were staged according to the morphological criteria provided in (Kimmel, Ballard, Kimmel, Ullmann, & Schilling, 1995). Zebrafish embryos collected for staining procedures were fixed at least overnight in 4% PFA in phosphate buffered saline (PBS: 137mM NaCl, 2.7mM KCl, 4.3mM Na₂HPO₄·7H₂O, 1.4mM KH₂PO₄) at 4 °C. Following fixation, embryos were dehydrated in increasing concentrations of methanol in PBS, 10 min each (25%, 50%, 75% then 100%). Dehydrated embryos were stored in 100% methanol at -20 °C until required.

3.14.2 Generation of *Tg(mbp:egfp)*

To visualize mature oligodendrocytes, transgenic *tg(mbp:egfp)* line was generated using Tol2 transposon vector (a gift from Dr. C H Kim, Korea). This construct consists of zebrafish mbp promoter that drives EGFP expression in mature oligodendrocytes. Fertilized eggs at one-cell stage were injected with 20 ng/μl of Tol2 mbp-EGFP plasmid DNA and 25 ng/μl of transposase mRNA. Injected embryos which have positive GFP fluorescence at 3dpf were raised to adult zebrafish and crossed with wild-type animals. F1 embryos were screened for GFP fluorescence at 3dpf under a fluorescent microscope (Leica) to generate a stable transgenic line.

3.14.3 PTU Treatment to Prevent Pigmentation

Embryos were treated with 1-phenyl 2-thiourea (PTU) to inhibit the melanization process and to improve optical transparency for imaging. PTU blocks all tyrosinase-dependent steps in the melanin pathway so that the embryos remain transparent. Embryos were treated with 0.003% PTU (1-phenyl 2-thiourea), an inhibitor of melanogenesis, to reveal internal structures in late stages of development after 24 hours post fertilization (hpf).

3.15 Synthesis of DIG Labelled Antisense RNA Probe

3.15.1 Cloning of *degs1*

The zebrafish *degs1* cDNA (ENSDART00000013007.5) was PCR amplified using the primers listed (**Table 6**) to obtain cDNA fragments between 1 bp and 743 bp to cover the open-reading frame (ORF). The PCR was performed using high fidelity *Pfu* DNA polymerase kit (Promega) according to the manufacturer's instructions. The correct size of the amplified PCR product was verified on 2 % agarose gel.

3.15.2 Ligation

The PCR product (200 ng) and a dual promoter pBSKS vector (2 µg) was digested with BamHI and EcoRI with appropriate buffer as per restriction enzyme data sheet (TaKaRa) in a final reaction volume of 50 µl at 37 °C overnight. After digestion, the digested products were purified using PCR purification kit (Qiagen) as per manufacturer instructions. The digested products were also run on a 2% agarose gel to confirm the digestion. The digested DNA fragments were ligated by using 1U of T4 ligase (Promega) for each reaction. The reactions were performed in a final volume of 10 µl for 3 h at 22°C, by using a 1:3 ratio of vector and insert. After that, ligation mixtures were directly used to transform chemically competent bacteria.

3.15.3 Heat Shock Transformation

After ligation, 50 µl of HB101 competent cells (Agilent) were thawed on ice, were mixed with 2 µl of ligation mixture and incubated on ice for 10 min. After that, the competent

cell/DNA mixture was placed into a 42 °C water bath for 45 sec, and then immediately incubated on ice for 2 min. 1 ml of autoclaved LB media was added to the competent cells, which were let to grow in 37 °C shaking incubator for 1 h. Finally, 100 µL of the transformation mix was plated onto LB agar plates containing ampicillin 100µg/mL (Sigma) and incubated at 37 °C overnight.

3.15.4 Screening

The correct insertion of the PCR fragment was verified *via* standard colony PCR. The product of colony PCR was run on 2 % agarose gel and the expected size on agarose gel was checked to know which colonies are positive. Three-five positive colonies were grown in overnight cultures (5 ml LB) and miniprep was performed to extract the plasmid using QIAprep Spin Miniprep kit (Qiagen). Afterward, the plasmid was tested by digestion with an appropriate restriction enzyme and further sequence confirmation was done by Sanger sequencing.

3.15.5 Riboprobe Synthesis

The dual promoter vector, used in the cloning process, carries T7 promoter on the one and a T3 promoter on the other side of the insert. Based on the orientation of the insert, the appropriate polymerase, which creates the required antisense and sense RNA was chosen. To obtain a better quality of the RNA probe, 5 µg of a plasmid containing the insert was linearized, purified prior to RNA probe synthesis using PCR purification Kit (Qiagen). Afterward, 1 µg of purified linearized plasmid was used for the RNA synthesis which was performed according to the protocol of the manufacturer (T7/T3 Polymerase, Roche). For the synthesis process, the DIG-RNA Labeling mix (Roche) and RNase inhibitor (TaKaRa) were used. The RNA synthesis was followed by purification using lithium chloride/ethanol precipitation as described in the SP6/T7 polymerase kit. The RNA was dissolved in 20 µl of RNase free water, the fragment size was verified on a 1 % agarose gel, and RNA probe was stored at -80 °C.

3.15.6 Cryosectioning

Cryosections provide a good system for visualizing fine details of the cell. Before cryosectioning, embryonic tissue needs to be cryoprotected. For this, embryos were dipped in 15% sucrose O/N 4°C. Embryos were then embedded in OCT (Tissue-Tek,

Cat#4583) to cryomold and orientate them for proper transverse sections. Blocks were at -80°C until sectioned. Before sectioning blocks were kept in the cryostat chamber for 15 min. Blocks were adhered to the cryostat sectioning support with OCT. 10 µm cryostat sections were made using Leica Cryostat (Leica CM3050) and were collected in superfrost slides, from this moment slides were maintained frost. Slides were rinsed in PBT and then they were processed for immunofluorescence studies.

3.16 FTY720 Treatment in *Danio rerio*

The zebrafish embryo is transparent and develops externally, enabling an easy and thorough assessment of drug effects on the internal organs in the live organism. For the drug treatment, a petri dish containing uninjected and MO-injected zebrafish embryos were taken. Using a transfer pipette, embryos were placed inside each well of a deep 96 well plate. Excess water from each well was removed carefully using a pipette. Using a multichannel pipette to add 150 µl of three different dosages (3.3, 1.0, 0.3 ng/ µl) of FTY720 to their respective wells in the deep 96 well plate containing arrayed zebrafish embryos until 5 dpf. DMSO was used as a vehicle (veh). Once the embryos are at 5 dpf, completely draw off and discard the remaining fish water. After treatment, lipidomics analysis, behaviour studies, and neuropathological studies were carried out.

3.2 METHODS

3.2 Whole Exome Sequencing (WES)

WES was carried out at Centro Nacional de Análisis Genómico (CNAG), Barcelona and was performed on exon targets isolated by capture using the SeqCap EZ Human Exome Kit v3.0 (Roche Nimblegen, USA) with 100-bp paired-end read sequences generated on a HiSeq2000 (Illumina, Inc. USA) in the CNAG. The sequencing methodology and variant interpretation protocol were performed at Neurometabolic Disease Lab identified through the Genome Analysis Tool Kit (GATK) pipeline. Sequence reads were aligned to the reference human genome (UCSC hg19 version) using the Burrows-Wheeler Aligner. Picard was used to mark duplicates. GATK was used for variant calling, and variants were annotated using the ANNOVAR (K. Wang et al., 2010) software (**Fig. 11**).

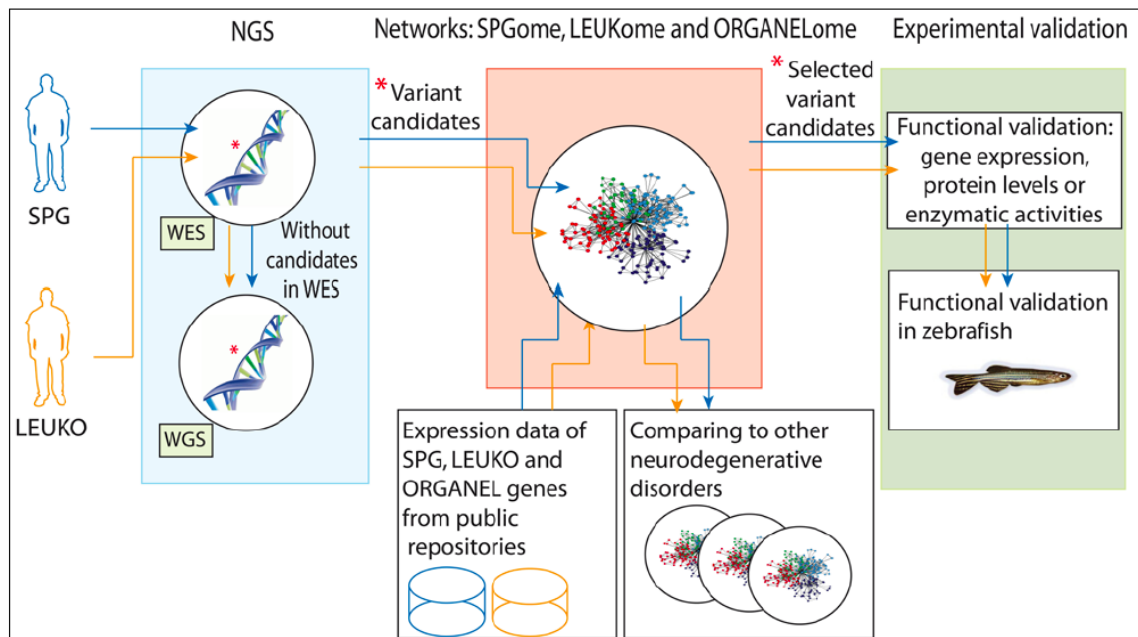


Figure 11. Flow diagram to depict the general work-flow for the methods used in this thesis. (Image courtesy: A Schluter)

3.3 Candidate Variant Filtering and Selection

Candidate variants were filtered out when present with a minor allele frequency (MAF) higher than 1% in population databases including; Exome Aggregation Consortium (ExAC) (Lek et al., 2016), 1000 Genomes project (Gibbs et al., 2015), and the National Heart, Lung, and Blood Institute - Exome Sequencing Project (NHLBI-ESP) Exome Variant Server (Mutarelli et al., 2014). Candidate variants were selected for co-segregation analysis based on factors including variant type, presence in patient databases, and pathogenicity predictors in the case of missense variants. Nonsynonymous variants were prioritized, as synonymous variants do not cause an amino acid change, they are considered non-pathogenic and therefore were filtered out. Variants that were previously described as pathogenic in patients were searched for in patient databases: ClinVar (NCBI) and Human Gene Mutation Database (HGMD) (Stenson et al., 2003). Deleteriousness of missense variants was assessed using 15 *in silico* tools including SIFT, Polyphen2, CADD, LRT, Mutation tester, Mutation assessor, FATHMM, PROVEAN, MetaSVM, MetaLR, M-CAP, VEST3, REVEL, GERP, ExacALL Polyphen2, SIFT, Meta-SVM, and PROVEAN among others. Multiple species alignment of candidate gene was generated using the Clustal Omega program. All the variants reported were confirmed with Sanger sequencing.

3.4 Sanger Confirmation

Sequencing data for the affected individuals and family members were used to conclude whether the segregation pattern of the candidate variants was compatible with the inheritance mode described for the gene of interest as described in the database, Online Mendelian Inheritance in Man (OMIM) (McKusick, 2007) or in literature. Primers to amplify the target locus were designed using online tool Primer3 (<http://bioinfo.ut.ee/primer3-0>) with an optimum annealing temperature in the range of 58-62 °C and, amplicon size of 400-700 bp including 200 bp upstream and downstream of the suspected variant. The specificity of the primers binding to the target site was confirmed by 'In-Silico PCR' (<http://genome-euro.ucsc.edu>). PCR conditions were set on control gDNA samples then performed on the corresponding samples from the patient and family members, if available, along with a high-quality DNA positive control and a negative control. The PCR reaction was assembled using: 10X PCR buffer containing MgCl₂ (Sigma), 2.5 mM dNTPs (Invitrogen), custom designed forward and reverse primers (10 µM each), 0.2 µl *Taq* DNA polymerase (5U/µl, Sigma) and template gDNA (50 ng). All reactions were prepared in 25 µl using the standard PCR conditions following the manufacturer's protocols that came with enzyme for PCR steps. These were 40 cycles of 30 sec at 94–98 °C, 30 sec at 58 °C, and 60 sec at 72 °C; with a final extension at 72 °C for 5 min. All cycling was performed on a Thermal Cycler (BioRad). All reactions, including blank controls, were checked for amplification success on a 1.5% agarose gel and visualized with SYBR[®] Safe (Invitrogen) dye. The PCR products were then purified by QIAquick PCR purification kit (Qiagen) and were bidirectionally sequenced using sequencing platform set up in STAB VIDA (Portugal). Sequence chromatograms were analysed using FinchTV v.1.4 (<http://www.geospiza.com>) to determine the presence or absence of the mutation and its zygosity in each family member.

3.6 Lipidomics

To quantify levels of saturated and unsaturated ceramides (C7 to C28), and their dihydro-counterparts (ceramides C7:0 to C28:0), samples were measured by MS/MS analytical methods (multiple reaction monitoring (MRM), precursor scans and neutral loss scans) for targeted the classes of metabolites. Afterward, mass chromatographs were interpreted using Biocrates software and a third party software (Biocrates Life Science AG). Briefly,

cells were harvested using trypsin, and cell pellets contained 3.5 million cells. 50 mg muscle biopsy was snap frozen and stored at -80 °C until extraction.

Lipid assay on zebrafish larvae was performed using AbsoluteIDQ p180 kit (Biocrates, Austria). Briefly, 5 zebrafish larvae at 5dpf were collected from the treated and untreated group with the fish water into a homogenizing tube. The tube was cooled in ice until the larvae sink to the bottom of the tube, and the water was removed. The tubes were frozen immediately and were sent to Biocrates for lipid and assay.

3.7 Evaluation of Reactive Oxygen Species

Intracellular radical oxygen species levels were measured by using ROS sensitive H₂DCFDA probe. Total superoxide and mitochondrial superoxide levels were measured by two specific probes DHE and MitoSox respectively. Primary fibroblasts cultures were seeded in 12-well tissue culture plates and were treated with interested compounds as indicated before. Treated cells were washed with pre-warmed PBS and incubated with the different probes with the following concentration: H₂DCFDA-10 μM, DHE-5 μM and MitoSox-5 μM for 15 min at 37 °C. The complex III inhibitor Antimycin (200 μM - 1 h) was used as a positive control for all the probes used. Cells were detached from the plate by using 1% TritonTM with mild agitation. Cells were collected in a 96-black well plate and the fluorescence was measured with a spectrofluorimeter (excitation wavelength 493 nm, emission wavelength 527 nm). Fluorescence values were corrected with protein content and results were expressed as fold change respect to controls or WT (untreated cells).

3.8 Inner Mitochondrial Membrane Potential Quantification

Inner mitochondrial membrane potential was measured by flow cytometry using the voltage-sensitive indicator, tetramethylrhodamine ethyl ester (TMRE) (Molecular Probes). This is a cell-permeant, cationic, red-orange fluorescent dye that is readily sequestered by active mitochondria. Disrupting or decreasing membrane potential results in a loss of dye from the mitochondria and a decrease in fluorescence intensity (Zhou et al., 2010). Primary fibroblasts cultures were plated in 12-well tissue culture plates and were treated with interested compounds as indicated before. Treated cells were washed with PBS and incubated with 50 nM of TMRE in pre-warmed PBS for 30 min at 37°C.

The uncoupler protonophore CCCP (200 μ M- 1h) was used as positive control of membrane depolarization (Kasianowicz et al., 1984). Cells were trypsinized, centrifuged at 1000 g for 5 min and resuspended in pre-warmed PBS. All samples were captured in FACS Canto TM recording 5000 cells for each condition and genotype tested. Percentage of depolarized cells was obtained after gating live cells. Data were analyzed with FlowJo Tree Star software.

3.9 Mitochondria Network

Cells were seeded on glass cover slips in 12-well tissue culture plates with semi confluence and treated accordingly. Then cells were fixed with 4 % paraformaldehyde for 15 min at RT and blocked with filtered blocking buffer (1 % bovine serum albumin (BSA), 0.2% powdered milk, 2% FBS, 0.1 M glycine, 0.1 % Triton-X-100) for half an hour. Following incubation with primary antibody for overnight, the cells were incubated with respective secondary antibody for 1 hour at RT in dark. Finally, cells were stained with DAPI and mounted with Fluoromount. Mitochondria were highlighted by immunofluorescence using an antibody anti-Tom20, as described above. Confocal images were processed using ImageJ. Images were transformed in 8-bit images, a moderate median filter was applied to extract the out-of-focus light and then cells were thresholded to select mitochondria. From the thresholded cells, binary (black and white) images were generated. For morphometric analysis we applied adapted methods recently described in literature (Losón, Song, Chen, & Chan, 2013; Merrill et al., 2011; Peng et al., 2011; Rosivatz & Woscholski, 2011). After inspection of the mitochondria morphology in different treatment conditions, we identified representative morphological subtypes that were classified according to parameters used in previous study (Ahmad et al., 2013; X. Liu & Hajnóczky, 2011; Peng et al., 2011). Mitochondria subtypes were scored manually introducing parameters of circularity and size (**Table 7**) and measured using the Analyze Particle function of ImageJ. To configure the particle analyzer a range of size (0.0 to infinity) and circularity (0.0 to 1.0) is introduced and particles outside the range specified are ignored. When the value of circularity is 1.0 indicates a perfect circle. As the value approaches 0.0, it indicates an increasingly elongated shape. Sometimes donut or blob, were selected and measured manually using the freeform drawing tools in order to avoid mismatch. For quantitative analysis, the number of mitochondria types was expressed as percentage respect to the total area per cell. The inverse of mitochondrial

circularity (1/circularity) was used as indicator of mitochondrial elongation (Dagda et al., 2009).

Table 7. Mitochondria subtypings.

Shape	Size	Circularity (0-1)
Small globule	0.1-1 μm^2	0.2-1
Bob-donuts	1-9 μm^2	0.2-1
Short tubule	1-9 μm^2	0-0.2
Long tubule	9 μm^2 -infinity	0-0.2

3.10 Quantitative Reverse Transcription Polymerase Chain Reaction (qRT-PCR)

Total RNA was extracted from human brains, human fibroblasts, mouse tissues and zebrafish embryos using RNeasy Kit (Qiagen, Hilden, Germany). 1 μg of RNA was transcribed into cDNA using 50 μM Oligo d(T)₂₀ custom synthesized primer (Invitrogen). The reverse transcription reaction was assembled using SuperScript™ IV Reverse Transcriptase kit (18090010, ThermoFisher Scientific Inc.) in a final volume of 25 μl . Dilutions ranging from 1/10 to 1/75 dilution of cDNA were used to measure mRNA levels. The expression of the genes of interest was analyzed by Q-PCR using TaqMan® Gene Expression Assays (Thermo Fisher Scientific Inc.), standardized Taqman® probes, SYBR Green Master Mix and standardized primers on a LightCycler® 480 Real-Time PCR System (Roche Diagnostics GmbH). Relative quantification was carried out using the ‘Delta-Delta Ct’ ($\Delta\Delta\text{Ct}$) method with *mRplp0/hPLP0* as endogenous control. Transcript quantification was performed in triplicates for each sample.

3.11 Western Blotting

Cells were directly collected in radioimmunoprecipitation assay (RIPA) buffer, then sonicated for 2 min with 10 sec intervals and centrifuged for 10 min at max speed. Samples were heated for 10 min at 70 °C with 4X NuPAGE® LDS Sample Buffer (Invitrogen, Thermo Fisher Scientific Inc.) before loading. Proteins at the concentration of 25 μg were loaded onto 12% Novex NuPAGE® SDS-PAGE gel system (Invitrogen, Thermo Fisher Scientific Inc.), and run for 60-90 min at 120 V in NuPAGE® MOPS SDS

Running Buffer (Invitrogen, Thermo 85 Fisher Scientific Inc.) supplemented with 5 mM sodium bisulfite (Ref. 243973, Sigma-Aldrich). SeeBlue® Plus2 Pre-stained (Invitrogen, Thermo Fisher Scientific Inc.) was used as a ladder. Resolved proteins were transferred onto nitrocellulose membranes using iBlot® 2 Gel Transfer Device (Invitrogen, Thermo Fisher Scientific Inc.). After blocking in 5 % bovine serum albumin (BSA, Sigma-Aldrich) in 0.05% TBS-Tween (TBS-T) for 1 hour at room temperature, membranes were incubated with corresponding diluted primary antibodies in 5% BSA in 0.05% TBS-T overnight (O/N) at 4 °C. Following incubation with diluted secondary antibody in 0.05% TBS-T for 1 hour at room temperature, proteins were detected with ECL western blotting analysis system.

3.12 Immunofluorescence

Cells were seeded on glass coverslips in 12-well tissue culture plates with semi confluence and treated accordingly. Then cells were fixed with 5 % sucrose in 4 % paraformaldehyde for 15 min at RT and blocked with filtered blocking buffer (1 % bovine serum albumin (BSA), 0.2 % powdered milk, 2 % FBS, 0.1 M glycine, 0.1 % Triton-X-100) for half an hour. Following incubation with primary antibody for O\N 4 °C, the cells were incubated with respective secondary antibody for 1 hour at RT in dark. Finally, cells were stained with DAPI and mounted with Fluoromount.

3.13 *In situ* Hybridization (ISH)

ISH is a technique for detection of specific nucleic acid sequences within tissues. RNA sequences are visualized by hybridization with labeled probes that are complementary to the sequence of interest. Depending on the method of colorization ISH can be chromogenic or fluorescent.

Permeabilization and Hybridization

For chromogenic ISH at the desired stage, permeabilization of embryos (n=10) was carried out using embryos stored after fixation at – 20 °C in 100 % methanol. Embryos were rehydrated through decrease methanol/PBT series (75 %, 50 %, 25 %; 5 min each). Embryos were incubated in 10 µg/µL proteinase K. The time of incubation is approximately according to the stage of the embryos (24hpf, 5 min; 48 hpf, 10 min; 72

hpf 15 min; 96 hpf, 20 min). After permeabilization, embryos were post-fix for 20 min in 4 % PFA in PBT. Hybridization of permeabilized embryos was carried out using 200 μ l hybridization buffer (**Appendix I**) in 2 ml Eppendorf tube for 1 hr. 1 μ l of riboprobe generated was added to hybridization buffer and let it hybridize O/N at 65°C. The probe dilution is derived empirically. Hybridization solution containing probe can be removed after use, stored at -20°C and reused many times without loss of signal.

Post-hybridization washes

Post-hybridization washes were carried out using 2 X SSC in MABT and embryos were washed in this solution for 5 min at 65 °C (**Appendix I**). Embryos were then washed in 0.2 X SSC for 5 min at 65°C. Prepare 0.2 X SSC containing 0.1% (v/v) Tween-20 and embryos were washed in this solution for 20 min at 65°C. The timing of this wash is critical. Tween 20 prevents embryos from sticking to tube sides during washes. Embryos were washed in PBT for 5 min at room temperature.

Anti-Digoxigenin Alkaline Phosphatase (AP) Labeling

Incubate washed embryos in blocking solution (10% goat serum + 10 % BBR) 1 hour at room temperature. The AP-conjugated anti-digoxigenin antibody was diluted 1:2000 in blocking solution and incubated 4°C O/N. Embryos were then washed in 0.5 ml of PBT five times, 15 min each.

Development of the staining

Wash the embryos in alkaline phosphatase buffer for 10 min. The colorization can be chromogenic (NBT/BCIP staining). 45 μ L of the NBT and 35 μ L of BCIP stock solution was mixed in 10 mL AP buffer. 500 μ L of the NBT/BCIP mix was added to the embryos. Embryos were incubated at room temperature on a slowly rotating platform, protected from light. The progress of the color reaction was checked every half hour until a blue reaction product is visible. The color should become visible within 0.5 - 4 h, depending on the probe. Color development can be hastened by incubating the samples at 37 °C, or slowed by incubation at 4 °C. Stop the coloration reaction by washing the embryos two to four times in PBT. After colorization, the embryos can be stored at 4 °C in PBS until mounted.

Flat-mounting in slides

Embryos were deyolk in a 10 mm-rounded Petri plate. Embryos were transferred one by one and lined up into a slide with 4 “posts” of high vacuum grease. And are oriented to have the dorsal part up and a coverslip (18x18 mm, Menzel-Glaser Cat#BB018018A1) is placed on top and gently press down until the embryo is flattened. Edges of the coverslip were filled with 50 % glycerol in PBT. The embryos were then visualized in the Nikon Eclipse 80i microscope.

3.14 Morpholinos

Morpholinos (MO) are antisense oligomers, designed to bind specific RNA by complementary sequence blocking either splicing or translation of the transcript. Morpholinos were obtained from Genetools, Virginia and were dissolved in RNase free water as per manufacturer instructions.

3.14.1 Microinjection

For the microinjection, embryos were collected immediately after being laid in a 150 mm petri dish and lined up against a microscope slide in a Petri dish using a clean Pasteur pipette.

The needles (glass filament outer diameter 1.0 mm, inner diameter 0.78 mm), needed for the injection, were fabricated using a micropipette puller (Narishige, Model#PC-10). Needles were loaded with 3 μ l of MO and inserted into the microinjector. The tip of the needle was broken by gently pushing it against the edge of a Petri plate. The injection volume was adjusted regulating the air pressure and tested in a mineral oil drop. Once the embryos were deposited in line to remain immobilized. The embryos were then injected with 1 nl of MO. Injection of MO was performed usually at one-cell stage. Injected embryos were transferred to Petri plate and let to develop at 28.5 °C until the desired stage was reached. In all the experiments MO-DEGS1 is used at 5-10 ng/nl and MO-control to avoid off-target expression caused by MO toxicity (Gerety & Wilkinson, 2011).

3.14.2 PCR Screening

After injection of MO, the efficiency of MO was checked by RT-PCR. RNA isolation and cDNA synthesis were performed from injected and un-injected animals (n=10). Using

the primers in the targeted region was PCR-amplified using primers complementary to sites in flanking exons located in exon 2 and exon 3 (**Table 7**) respectively using standard PCR conditions (95 °C - 5 min; 35 cycles of 95 °C - 2 min, 60 °C - 1 min, 72°C - 1 min; final extension step at 72 °C - 5 min), and migrated on a 1 % agarose gel; bands were excised, gel purified using QIAquick gel extraction kit (Qiagen) and resulting purified products were Sanger sequenced to confirm aberrant splicing events induced by the MO.

3.15 Locomotor Assay

By 5 dpf, zebrafish larvae perform spontaneous swimming and their visual system is fully developed (Colwill & Creton, 2011). Uninjected, MO control and MO-DEGS1 120 hpf (hours post fertilization) larvae were transferred to individual wells of 96-well plate with 150 µl fresh fish water and allowed to acclimate for a few hours. The zebrafish larvae behavior is tracked and analysed by the EthoVision XT 12 software and the DanioVision device from Noldus Information Technologies, Wageningen, The Netherlands. This closed system consists of a camera placed above a chamber with circulating water and a temperature sensor that is set at 28.5 °C. Individualized larvae in a 96-well plate are placed in the chamber, which can provide different stimuli (light/dark environment, tapping, sound) controlled by the software. Prior to each experiment, larvae were left for 10 minutes in dark for acclimation, then predetermined series of alternating dark and light environment is presented to the larvae. The natural locomotor behavior of zebrafish larvae is characterized by high activity in darkness and immobility in light environments. The final 25 min long experimental protocol is divided into 5 min period of darkness, and then two times repeated the cycle of 5 min of bright light followed by 5 min of darkness. During the behavioral trial, the total distance moved by every larva is measured. We obtained the distance moved and the mobility parameters from EthoVision tracking program analysis and baseline parameters were subtracted out before. All locomotor assays were performed at 1 pm onwards to ensure steady activity of zebrafish (Cornet et al., 2017). After observations, all subjects were euthanized with a lethal concentration of MS-222 Tricaine (ethyl-3-aminobenzoate methane-sulfonate salt; Sigma). Locomotor activity was analyzed as described previously (MacPhail et al., 2009). Behavior after drug treatment was performed by adding FTY720 to standard fish water to the final concentration of 3.3, 1.0, 0.3ng/µl. DMSO was used as a vehicle. MO control and MO-

DEGS1 embryos (0 hpf) were treated with FTY720 till 120 hpf and behavior assay was performed as described above.

3.16 Immunofluorescence Studies in Zebrafish Larvae

Larvae were fixed in 4% PFA in PBS at 4 °C overnight. Whole-mount immunofluorescence was carried out at 4 dpf larvae after rehydration as described in ISH method, embryos were treated with proteinase K for 30 min at room temperature. Embryos were immersed in blocking buffer (10% goat serum, 1% DMSO) for 2 h, and incubated in the primary antibody GFP at 4 °C overnight. Embryos were washed in PBS thrice for 15 min and then incubated with the corresponding secondary antibody (AlexFlour 488 anti-chicken) at 4 °C overnight. Embryos were then washed in PBS five times for 15 min. Immunofluorescence microscopy was carried out as described under imaging heading.

3.17 Imaging

Confocal laser scanning images were collected using Leica TCS SP5 confocal microscope (Leica Biosystems), images were acquired in the CMRB-IDIBELL Optical Microscopy Unit, located in the IDIBELL. Cryostat sections were imaged on a Nikon ECLIPSE 80i fluorescence microscope. ISH and fluorescent image processing were done with FIJI. Zebrafish embryos of the indicated stage were embedded in 1% low-melting-point agarose (LMA, Ecogen, Cat#AG-400), hindbrain was oriented close to the glass-bottom in a Petri dish in order to obtain a dorsal view in an inverted objective.

3.18 Statistical Analysis

All data are presented as the mean \pm standard deviation (SD). Statistical significance was assessed using Student's *t*-test when two groups were compared. When comparing multiple groups, significant differences were determined by one or two-way ANOVA followed by Tukey's posthoc test after verifying normality. All *p* values were two-tailed, and a *p*-value of less than 0.05 was considered statistically significant (**p* < 0.05; ***p* < 0.01; ****p* < 0.001). Statistical analyses were performed using GraphPad 7.0.

Table 6. List of oligonucleotides used as PCR primers. (L, forward; R, reverse; P, patient).

Name	Primer sequence (5'-3')	Remark
Zf_degs1_L	ATGGGGAACCGCGTGGCGCG	Cloning <i>degs1</i>
Zf_degs1_R	TCACTCCTGCTTGACGTCTC	
MO-control	CCTCTTACCTCAGTTACAATTTATA	Morpholinos zebrafish
MO-DEGS1	GCTGAATAACTGCTCTCACCATTGG	
Zf_degs1-exon 2_L	GGCTCTCTGAACCTGCTGAC	Screening morphants
Zf_degs1-exon 3_R	CTTGACGTCTCCGACCAGTT	
hDEGS1_603-L	AATCGCTGGTTTGGAAATGT	LNF 41 or P1 (Sanger)
hDEGS1_603-R	CAGGAATGTTGGGGAAATC	
hECSIT_553-L	AAAAGGAAGTGGAAAGGGAGTG	LNF 45 (Sanger)
hECSIT_553-R	GATTCTGGAGGGGTCTCG	
hECSIT_632-L	CTCCTCCCCCTCCATCTC	
hECSIT_632-R	CCAGGCATAGTGGTGTGTG	
hCSPP1_494-L	TGAGGTCCCTTCCACCTTA	LNF46 (Sanger)
hCSPP1_494-R	CATCCCAAATAACAACCCAAA	
hCSPP1_359-L	AAAATATAGATGTAGGCTGACTGAAGA	
hCSPP1_359-R	TCAATGGACAGAAAATACCAACA	
hATP1A2_328-L	TCAAGGCAGGACAGGAGAA	LNF 49 (Sanger)
hATP1A2_328-R	AAGGGATGGAGTAAGGTTTGG	
hSLC16A2_202-L	CAGACCAGGAACAGCAGGA	LNF 83 (Sanger)
hSLC16A2_202-R	TAAGGGGTAAGGGGAGGAGT	
RARS2_586-L	TTCCACCAGAAAACCTTGATC	LNF 63 (Sanger)
RARS2_586-R	AAGACTCCTGTGTCCCCGCG	
PTK2_384-L	ATGGCAGCTGCTTACCTTGA	LNF 87 (Sanger)
PTK2_384-R	GCTTTAAGTTCAGTAAACCT	
PSEN1_049-L	AGAGGCTTGGTGGGATTACC	LNF 85 (Sanger)
PSEN1_049-R	GCTACTTGGGAGGCTGAGG	
CPT1A_385-L	CCCCGGCTCCCGCTCGCCGCTC	LNF 64 (Sanger)
CPT1A_385-R	TGAATCTGATGAACTTCTT	
DSTYK_654-L	CACACGCTGGTTGCTCATC	LNF 84 (Sanger)
DSTYK_654-R	GGAGAGGCAGGAATGGGTAT	
SPTBN2_142-L	GGGTGGGCGAACTGACTC	LNF 64 (Sanger)
SPTBN2_142-R	TTTGCTCTTCCCTCCTGCTTG	
SON_075-L	TCCAGAACCACCACCAGAG	LNF 68 (Sanger)
SON_075-R	TCCAGAACAGGCACAGAAGG	

(Continued on next page)

GRID1_519-L	GAACCCCAGC CCCGATGGTG	LNF 87 (Sanger)
GRID1_519-R	TCCAGGTCCCCTGTGTCCTGC	
KCNA1_102--L	CAGTTCCCCAACACGCT	LNF 52 (Sanger)
KCNA1_102-R	CGGCGACTGAGGTCCTG	
hDEGS1_397-L	CCCAGTTGGGTGCATTTTAC	P6, P4 (Sanger)
hDEGS1_397-R	ACCTGTGCCACGGTATTGAT	
hDEGS1_752-L	GTGGCACAGGTCACTTTTGA	P6, P4 (Sanger)
hDEGS1_752-R	TGAGGCATGAGAATCGTTTG	
hDEGS1_341-L	CCCAGTTGGGTGCATTTTAC	P4 (Sanger)
hDEGS1_341-R	ACCTGTGCCACGGTATTGAT	
hDEGS1_764-L	GTGGCACAGGTCACTTTTGA	P7 (Sanger)
hDEGS1_764-R	TGAGGCATGAGAATCGTTTG	
hDEGS1_337-L	CCCAGTTGGGTGCATTTTAC	P9 (Sanger)
hDEGS1_337-R	ACCTGTGCCACGGTATTGAT	

RESULTS

4 RESULTS

4.1 Chapter 1

4.1.1 Identification of Novel Genetic Variants

In order to identify the causative gene in affected individuals with leukodystrophy of unknown origin, we performed Whole Exome Sequencing (WES) in the probands of a very large cohort. The WES experiments followed by bioinformatics pipeline and Sanger validation allowed us to identify variants. Variants were filtered against dbSNP build 137, 1000 Genomes (November 23, 2010 release version), Exome Variant Server (EVS, ESP6500SI-V2), Exome Aggregation Consortium (ExAC browser, v.0.3), NHLBI GO Exome Sequencing Project (ESP) and Genome Aggregation Database (gnomAD).

In this thesis, a small portion of this large cohort size was undertaken and 24 different variants were identified through WES data analysis and confirmed by Sanger sequencing (**Table 8**). Of these variants, 18 are in known disease-causing genes (according to OMIM, see **Table 8**) and 1 novel candidate gene (*DEGSI*) was identified. Altogether, candidate variants have been identified in 22 different genes. Among the variants verified by Sanger, 30 % of these genes behave in an autosomal recessive manner, another 70% have an autosomal dominant mode of inheritance (**Fig. 12**). Autosomal dominant inheritance was confirmed in these families: LNF45 (*ECSIT*), LNF46 (*CSPP1*), LNF49 (*ATPIA*), LNF93 (*MLC1*), LNF48 (*NDUFS2*), LNF48 (*NDUFAF6*), LNF87 (*PTK2*), LNF85 (*PSENI*), LNF64 (*CPTIA*), LNF72 (*PDGFRB*), LNF64 (*SPTBN2*), LNF68 (*SON*) and LNF87 (*GRID1*). Autosomal recessive inheritance of variants in *DEGSI*, *SLC16A2*, *RNASEH2B*, *GFPT1*, *MUT*, *DSTYK* and *KCNA1* were shown in the homozygous patients of the consanguineous families LNF41, LNF83, LNF93, LNF88, LNF84, and LNF87 respectively. A case of *de novo* mutation was confirmed in LNF 87 family and compound heterozygosity in family LNF63 in the gene *RARS2* carrying one intronic and splicing mutation.

Among the variants identified; 15 are missense, 2 are intronic variants neighboring splice sites, 1 is inframe deletion, 2 are frameshift deletions, and 1 creates a stop gain (**Table 8**). Of these variants, 8 are absent from control population databases and 16 are present in

control population databases gnomAD, NHLBI-ESP and 1000 Genomes with frequencies below 0.01%, indicating that they are not common variants in these cohorts.

In the last 3 years, the Neurometabolic Diseases Laboratory of the Bellvitge Biomedical Research Institute (IDIBELL) has implemented the molecular genetic diagnosis of leukodystrophies and spastic paraplegia. During this time, this research group has recruited more than 200 different families affected by these disorders from several Neurology units throughout Spain. In a recent study (under preparation) including more than 100 families, a high diagnosis rate (of 57 %) was obtained using WES on white matter disorder patients. However, many of these variants need an accurate assessment of co-segregation in relatives (and in some cases, functional validation by *ex vivo/in vitro* tests) to determine its pathogenicity.

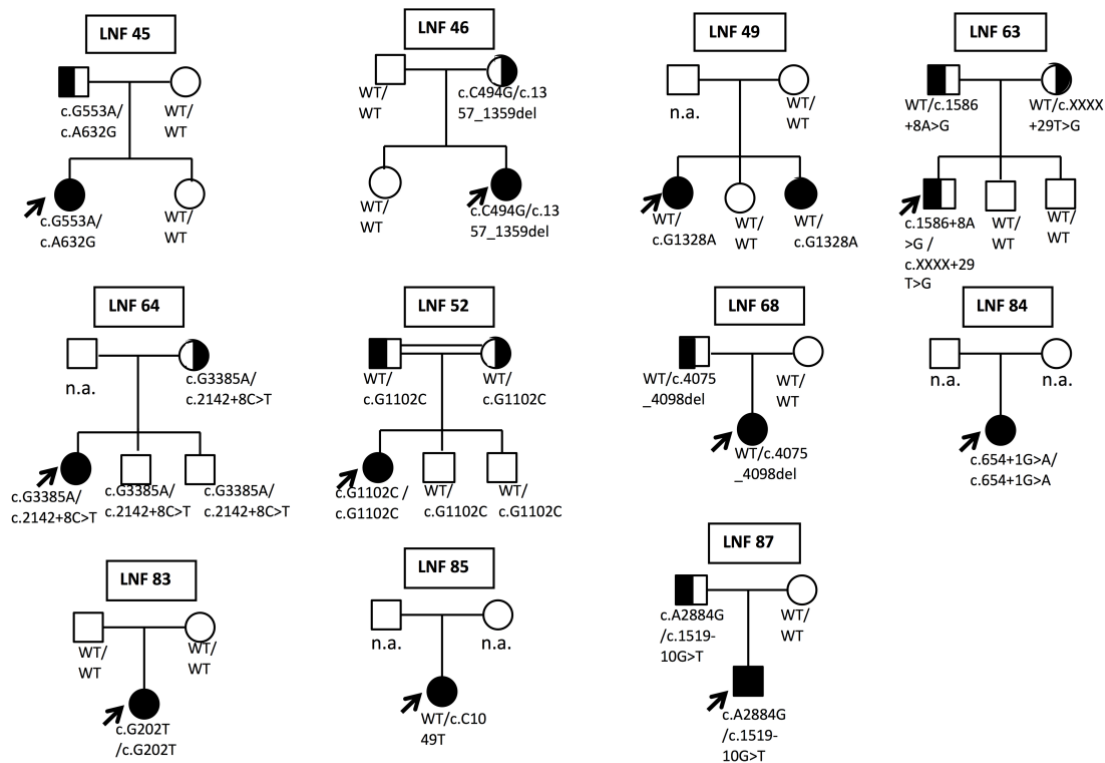


Figure 12: Pedigrees displaying compatible cosegregation of candidate variants.

Zygosity of the individuals is indicated as heterozygous or homozygous with the annotated cDNA change, arrow denotes proband. Abbreviations: LNF, leukodystrophy family patient; n.a. not available.

Table 8. Variants confirmed by Sanger sequencing in Leukodystrophy patients (LNF)

Family Code	Gene	Disease Association	Inheritance	Zygosity	Variant position (Ref: GRCh37/hg19)	cDNA Position	Amino Acid Change	Variant Type	Allele Frequency (gnomAD)	Patient Database (Clin Var)
LNF41	DEGS1	-	AR	HOM	chr1:22437779 9_T/-	c.604delT (NM_003676)	p.(Tyr202 Thrfs*8)	Frameshift deletion	Absent	Absent
LNF45	ECSIT	-	AD	HTZ	chr19:1161710 0_C/T	c.G553A (NM_001142465)	p.(Glu185 Lys)	Missense	0.000179	Absent
LNF45	ECSIT	-	AD	HTZ	chr19:1162397 7_T/C	c.A632G (NM_001142464)	p.(Asn21 ISet)	Missense	0.0003571	Absent
LNF46	CSPP1	Joubert syndrome 21	AD	HTZ	chr8:68028252 _C/G	c.C494G (NM_001291339)	p.(Ser165 Cys)	Missense	0.004182	Likely benign
LNF46	CSPP1	Joubert syndrome 21	AD	HTZ	chr8:68071241 _GAA/-	c.1357_1359del (NM_001291339)	p.(Glu799 del)	Deletion	4.92E-05	Absent
LNF49	ATP1A2	Alternating hemiplegia of childhood 1, Migraine, familial basilar, Migraine, familial hemiplegic 2	AD	HTZ	chr1:16009905 7_G/A	c.G1328A (NM_000702)	p.(Arg443 Gln)	Missense	2.84E-05	Absent
LNF83	SLC16A2	Allan-Herndon-Dudley syndrome	AR	HOM	chrX:7364167 4_G/T	c.G202T (NM_006517)	p.(Glu68*)	Stopgain	Absent	Absent

(Continued on next page)

LNF63	RARS2	Pontocerebellar hypoplasia, type 6	AD	Compound Heterozygous	chr6:88226516_A/C	c.XXXX+29T>G (NM_020320)	-	intronic	Absent	Absent
LNF63	RARS2	Pontocerebellar hypoplasia, type 6	AD	Compound Heterozygous	chr6:88255305_T/C	c.1586+8A>G (NM_020320)	-	splicing	Absent	Absent
LNF87	PTK2	-	AD	HTZ	chr8:141754876_C/A	c.1519-10G>T (NM_001199649)	-	splicing	0.000552	Absent
LNF85	PSEN1	Alzheimer disease, type 3	AD	HTZ	chr14:73678582_C/T	c.C1049TPSEN1 (NM_007318)	p.(Thr350Ile)	Missense	8.12E-06	Not provided
LNF64	CPT1A	CPT deficiency, hepatic, type IA	AD	HTZ	chr11:68527685_G/A	c.2142+8C>T (NM_001031847)	-	splicing	0.00077	Likely benign
LNF84	DSTYK	Congenital anomalies of kidney and urinary tract 1, Spastic paraplegia 23	AR	HOM	chr1:205156545_C/T	c.654+1G>A (NM_199462)	-	splicing	0.000278	Uncertain significance

(Continued on next page)

LNF64	SPTBN2	Spinocerebellar ataxia 5	AD	HTZ	chr11:66468185_C/T	c.G3385A (NM_006946)	p.(Glu1129Lys)	Missense	5.07E-05	Absent
LNF68	SON	ZTTK syndrome	AD	HTZ	chr21:34925612_GTCCTGGAGTCTTCCGGCTGTGACC/-	c.4075_4098del (NM_001291411)	-	Inframe deletion	0.005559	Absent
LNF87	GRID1	-	AD	HTZ	chr10:87614297_G/A	c.C1189T (NM_017551)	p.(Leu397Phe)	Missense	Absent	Absent
LNF52	KCNA1	Episodic ataxia/myokymia syndrome	AR	HO M	chr12:5021646_G/C	c.G1102C (NM_000217)	p.(Val368Leu)	Missense	Absent	Absent

Family code prefixes refer to probands clinically diagnosed leukodystrophy (LNF). Diseases associated are obtained from OMIM with the mode of inheritance (AR: autosomal recessive, AD: autosomal dominant, XLR: X-linked recessive). 'Zygosity' refers to the Sanger-validated zygosity of the index patient. 'gDNA position' refers to the Genome Browser release 19 map. 'cDNA position' refers to the variant position in the coding sequence in the corresponding transcript (reference sequences obtained from NCBI). The minor allele frequency is stated when variants are present in gnomAD, ExAC, 1000 Genomes (1000G) or NHLBI-ESP databases. The clinical significance of the variant is stated as pathogenic, likely pathogenic or uncertain significance when present in ClinVar.

4.1.2 Novel Variants in *DEGSI*

We found a novel variant in *DEGSI* (NM_003676.3) in our patient cohort as mentioned (**Table 8**) and we were mainly interested in this gene as it is an enzyme and encodes for a product. In general mutations in enzyme results in loss of enzyme activity (Impraim, Wang, & Yoshida, 1982; Oh, Choi, Goh, & Hahn, 2015). The first variant we identified in *DEGSI* (c.604delT) is a deletion (del) of thymine (T) which causes a frame shift (fs), p.(Tyr202Thrfs*8), affecting a conserved nucleotide (position 604) and amino acid (position 202), causing first amino acid Tyrosine (Tyr) changed to new amino acid Threonine (Thr), producing a new termination (*) site (8). The variant is not known to public databases (until June 2018). To validate if *DEGSI* is a disease-causing gene, it was needed to find additional patients with variants in this gene. For this reason, we contacted the leukodystrophy experts (Dr. Odile Boesplug-Tanguy, France; Dr. Ali Fatemi, USA). In collaboration with different research groups and with the help of GeneMatcher online tool, we identified 17 more patients belonging to 11 unrelated families harboring novel variants in *DEGSI* (**Table 9**). These variants were confirmed by Sanger sequencing where genetic material was available from different groups and appropriate segregation analysis was carried out (**Fig. 14**). *DEGSI* encodes an evolutionarily conserved fatty acid desaturase of 323 amino acids consisting of 6 transmembrane domains, 3 histidine motifs, a lipid desaturase domain and a fatty acid desaturase (FAD) domain. Notably, all the *DEGSI* deleterious variants identified in this study cluster in exon 2, 3 which encodes for the histidine motif domain, the fatty acid desaturase domain (FAD) and the transmembrane domain. Half of these variants are located in a transmembrane domain (**Fig. 13**). Therefore, we identified 12 different variants in 12 families (**Table 9**). For the nomenclature of variants we followed HGVS (Human Genome Variation Society) guidelines (den Dunnen et al., 2016). We expect additional patients to be identified soon.

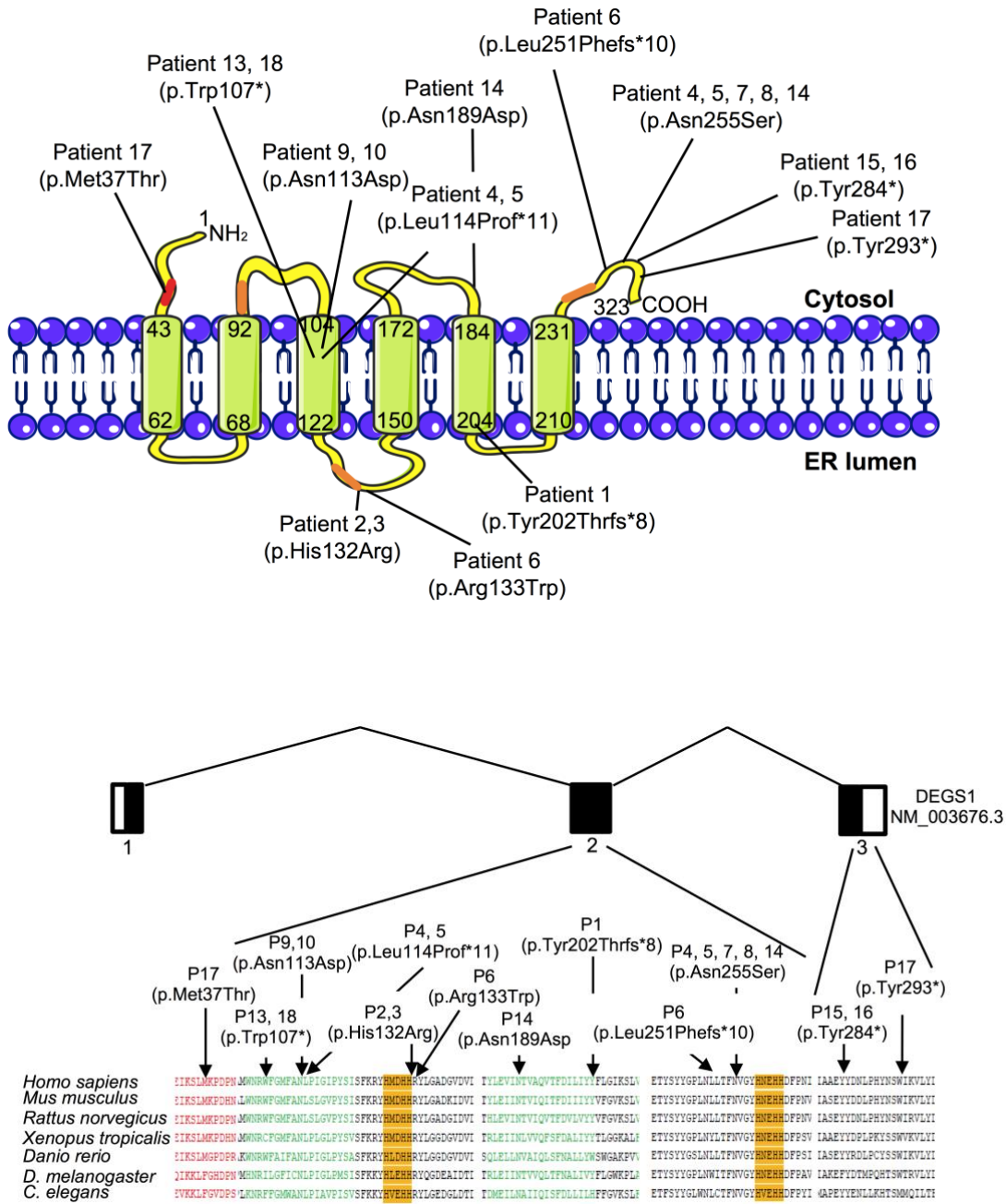


Figure 13. Schematic representation of human DEGS1 (NP_003667.1) and functional domain with variants identified in patients.

DEGS1 has 323 amino acids. Numbers under the protein line indicate boundaries of each domain. The Lipid DES domain (red) of DEGS1 comprises amino acids 6-42. The histidine domain (orange) of DEGS1 comprises amino acids 89-93, 128-132, 259-263. The transmembrane domain (green) of DEGS1 comprises amino acids 43-62, 68-92, 104-122, 150-172, 184-202, 210-231. The fatty acid desaturase (FAD) domain covers amino acids 64-293. Multiple protein sequence alignment of DEGS1 orthologs show conservation of missense mutations detected in cases (bottom). Schematic of the human *DEGS1* locus consisting of three exons. Protein sequence alignments from different species are shown (bottom). The lipid DES, transmembrane and histidine domain are indicated by red, green and orange shading respectively. Alignment was performed with ClustalW using the following RefSeq: NP_003667.1, *Homo sapiens*; NP_031879.1, *Mus musculus*; NP_445775.2, *Rattus norvegicus*; NP_001007485.1, *Xenopus tropicalis*; NP_997865.1, *Danio rerio*; NP_476594.1, *Drosophila melanogaster*; NP_493549.1, *Caenorhabditis elegans*.

Interestingly, the c.764A>G (p.Asn255Ser) was the most common variant present in patient 4, 5, 7, 8, 14. Although the three families (3, 5, 9) were not aware of a relationship, suggesting a possible founder effect for this mutation. The variants segregate with hypomyelinating leukodystrophy within the individual pedigrees where family members were available for families 4, 8, 11 (**Fig. 14**). In Family 8, in fact, c.320G>A was identified in the proband (patient 13) but DNA sample for patient 11, 12 was not available despite their clinical features were suggestive of hypomyelination, suggesting that the same variant was inherited in these two deceased individuals.

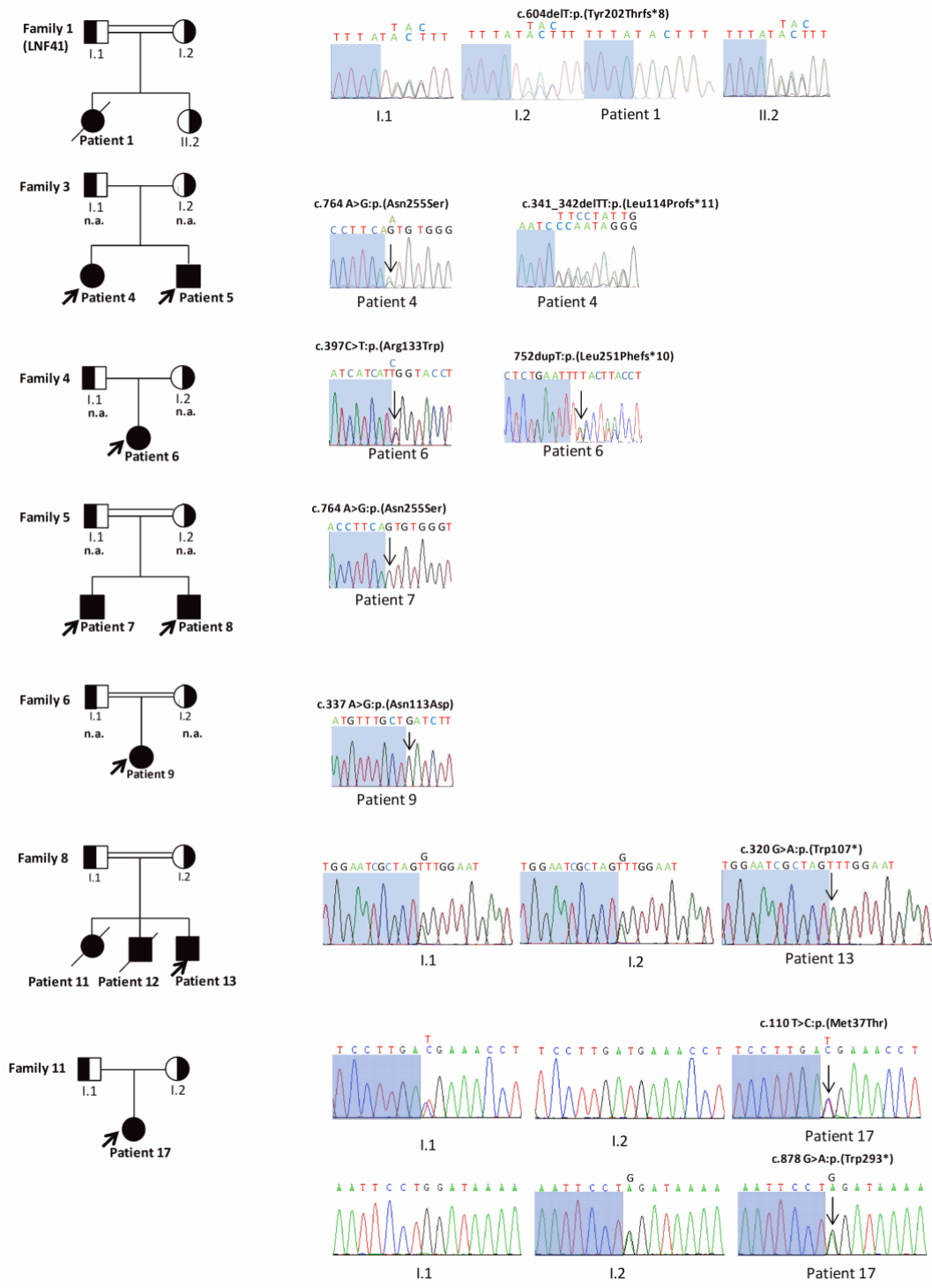


Figure 14. Pedigrees and sequencing chromatogram of families affected by *DEGS1* variants.

Variants in proband verified by Sanger sequencing indicated by an arrow. Sangers could not be performed for individuals where genetic material was not available (n.a.).

4.1.3 Evaluation of The Effect of *DEGS1* Variants

The multiple-sequence alignment indicated variants residues are highly conserved (**Fig. 13**). Furthermore, their potential effect on protein function was evaluated using 15 *in silico* predictors (SIFT, Polyphen2, CADD, LRT, Mutation tester, Mutation assessor, FATHMM, PROVEAN, MetaSVM, MetaLR, M-CAP, VEST3, REVEL, GERP, ExacALL). We identified 12 different single-nucleotide variations (SNV), in eighteen patients belonging to twelve unrelated families (**Table 9**). 7 out of 12 families are consanguineous and harbor a homozygous variant. 6 out of 12 variants are nonsynonymous SNV, 3 stop-gains, 2 frameshift deletions, 1 frameshift insertion. Most of the SNV variants are located in the exon 2 (10 variants), and only two are identified in the exon 3. 11 out of 12 SNV variants are located in the Fatty acid desaturase domain, and only one, p.(Met37Thr), in the Sphingolipid delta4-desaturase domain. The most prevalent *DEGS1* variants in our cohort are Asn255Ser and Asn113Asp identified in three and two independent families, respectively. 7 out of 12 variants have never been identified in control population and the rest of 5 variants have a minor allele frequency (MAF) lower than 0.0001 with none homozygous. The deleteriousness of the SNV variants is confirmed with 6 out of 12 nonsense variants and with the rest 6 nonsynonymous variants with damage prediction in most of the 15 *in silico* predictors tested (**Table 9**).

Table 9. Bioinformatics analysis for predicting the functional effect of the novel *DEGSI* variants

Variants	Chromosomal position of the variant ^a	HGVSc ^b (exon)	HGVSp ^b (amino acids)	Exonic variant function	SIFT (score) ^c	Polyphen2 HDIV (score) ^d
1	Chr1(GRCh37):g.224377306T>C	NM_003676.3:c.110T>C (exon 2/3)	p.(Met37Thr)	nonsynonymous SNV	D (0.012)	D (0.984)
2	Chr1(GRCh37):g.224377516G>A	NM_003676.3:c.320G>A (exon 2/3)	p.(Trp107*)	stopgain	.	.
3	Chr1(GRCh37):g.224377533A>G	NM_003676.3:c.337A>G (exon 2/3)	p.(Asn113AAsp)	nonsynonymous SNV	D (0.002)	D (1.0)
4	Chr1(GRCh37):g.224377538delTT	NM_003676.3:c.341_342delTT (exon 2/3)	p.(Leu114Profs*11)	frameshift deletion	.	.
5	Chr1(GRCh37):g.224377591A>G	NM_003676.3:c.395A>G (exon 2/3)	p.(His132Arg)	nonsynonymous SNV	D (0.0)	D (1.0)
6	Chr1(GRCh37):g.224377593C>T	NM_003676.3:c.397C>T (exon 2/3)	p.(Arg133Trp)	nonsynonymous SNV	D (0.0)	D (1.0)
7	Chr1(GRCh37):g.224377761A>G	NM_003676.3:c.565A>G (exon 2/3)	p.(Asn189Asp)	nonsynonymous SNV	D (0.002)	D (0.999)
8	Chr1(GRCh37):g.224377800delT	NM_003676.3:c.604delT (exon 2/3)	p.(Tyr202Thrfs*8)	frameshift deletion	.	.
9	Chr1(GRCh37):g.224377948dupT	NM_003676.3:c.752dupT (exon 2/3)	p.(Leu251Phefs*10)	frameshift insertion	.	.
10	Chr1(GRCh37):g.224377960A>G	NM_003676.3:c.764A>G (exon 2/3)	p.(Asn255Ser)	nonsynonymous SNV	D (0.032)	B (0.241)
11	Chr1(GRCh37):g.224380060_224380063delTGAC	NM_003676.3:c.852_855del (exon 3/3)	p.(Tyr284*)	stopgain	.	.
12	Chr1(GRCh37):g.224380086G>A	NM_003676.3:c.878G>A (exon 3/3)	p.(Trp293*)	stopgain	.	.

(Continued on next page)

^a The reference genome used for bioinformatic predictions is GRCh37/hg19.

^b HGVSc/HGVSp: coding DNA/protein variant described according to the nomenclature established by the Human Genome Variation Society.

^c SIFT (sift); D: Deleterious (sift<=0.05); T: tolerated (sift>0.05)

^d PolyPhen-2 HumDiv: PolyPhen-2 Human Diversity; D: Probably damaging (>=0.957), P: possibly damaging (0.453<=pp2_hdiv<=0.956); B: benign (pp2_hdiv<=0.452)

Polyphen2 HVAR (score) ^e	CADD (raw score) ^f	CADD (phred score) ^f	LRT (score) ^g	MutationTaster (score) ^h	MutationAssessor (score) ⁱ	FATHMM (score) ^j	PROVEAN (score) ^k	MetaSVM (score) ^l	MetaLR (score) ^m
D (0.917)	4.723	24.6	D (0.000)	D (1.00)	M (2.9)	T (0.85)	D (-4.49)	T (-0.637)	T (0.269)
.	10.813	36	D (0.000)	A (1.00)
D (0.999)	5.856	27.3	D (0.000)	D (1.00)	M (2.88)	T (2.33)	D (-4.53)	T (-0.873)	T (0.146)
.
D (1.0)	4.921	25.0	D (0.000)	D (1.00)	H (3.98)	D (-3.04)	D (-7.91)	D (1.076)	D (0.921)
D (0.995)	6.967	33	D (0.000)	D (1.00)	H (3.59)	T (2.14)	D (-7.67)	T (-0.438)	T (0.212)
D (0.998)	4.611	24.4	D (0.000)	D (1.00)	H (4.005)	T (2.31)	D (-4.62)	T (-0.399)	T (0.211)
.
.
P (0.571)	4.337	24.0	D (0.000)	D (1.00)	M (3.285)	T (1.9)	D (-4.62)	T (-0.701)	T (0.199)
.	13.658	43	D (0.000)	A (1.00)

(Continued on next page)

^e PolyPhen-2 HumVar: PolyPhen-2 Human Variation; D: Probably damaging (>=0.909), P: possibly damaging (0.447<=pp2_hdiv<=0.909); B: benign (pp2_hdiv<=0.446)

^f CADD: Combined Annotation Dependent Depletion; higher scores are more deleterious

^g LRT: likelihood ratio test; D: Deleterious; N: Neutral; U: Unknown

^h MutationTaster; A" ("disease_causing_automatic"); "D" ("disease_causing"); "N" ("polymorphism"); "P" ("polymorphism_automatic")

ⁱ MutationAssessor; H: high; M: medium; L: low; N: neutral. H/M means functional and L/N means non-functional

^j FATHMM: functional Analysis through Hidden Markov models; D: Deleterious; T: Tolerated

^k PROVEAN: Protein Variation Effect Analyzer; D: Deleterious; N: Neutral

^l MetaSVM: radial basis function kernel support vector machine; D: Deleterious; T: Tolerated

^m MetaLR: logistic regression; D: Deleterious; T: Tolerated

M-CAP (score) ⁿ	fathmm-MKL coding score ^o	VEST3 (score) ^p	REVEL ^q	GERP++ RS ^r	phyloP100way Vertebrate ^s	phyloP20way mammalian ^t	SiPhy_29way_logOdds ^u	Interpro domain ^v
D (0.041)	D (0.990)	0.861	0.512	5.45	8.010	1.051	15.823	Sphingolipid delta4-desaturase\X2c N-terminal
.	D (0.939)	.	.	5.72	3.145	1.038	20.242	Fatty acid desaturase domain
D (0.032)	D (0.991)	0.531	0.466	5.72	9.317	1.187	16.297	Fatty acid desaturase domain
.
D (0.244)	D (0.991)	0.993	0.957	6.02	9.317	1.187	16.543	Fatty acid desaturase domain
D (0.121)	D (0.974)	0.927	0.558	5.09	6.181	0.927	16.490	Fatty acid desaturase domain
D (0.035)	D (0.992)	0.639	0.550	6.02	9.317	1.187	16.543	Fatty acid desaturase domain
.
.
D (0.052)	D (0.990)	0.434	0.442	5.8	9.317	0.233	16.144	Fatty acid desaturase domain
.	D (0.993)	.	.	5.85	9.602	0.953	20.177	.

(Continued on next page)

^o fathmm-MKL: functional Analysis through Hidden Markov models; D: Deleterious; T: Tolerated

^p VEST3: Variant Effect Scoring Tool; higher scores are more deleterious.

^q REVEL: higher scores are more deleterious.

^r GERP: Genomic Evolutionary Rate Profiling, RS score: "rejected substitutions"³⁷ score; higher scores are more deleterious

^s PhyloP100way Vertebrate: PhyloP basewise conservation score derived from Multiz alignment of 100 vertebrate species; higher scores are more deleterious

^t PhyloP20way mammalian: PhyloP basewise conservation score derived from Multiz alignment of 20 mammals; PhyloP scores measure evolutionary conservation at individual alignment sites; higher scores are more deleterious

^u SiPhy_29way_logOdds: Site-specific PHYlogenetic analysis; based on a high-resolution map of evolutionary constraint in the human genome based on 29 eutherian mammals; higher scores are more deleterious

^v Interpro domain: interPro predicted domains.

1000G_ALL ^w	ExAC_ALL ^w	ESP6500siv2_ALL ^w	gnomAD_ALL ^w
•	•	•	•
•	•	•	4.061e-06
•	•	•	•
•	•	•	•
•	•	•	•
•	•	•	•
•	•	•	4.061e-06
•	8.237e-06	•	4.061e-06
•	•	•	•
•	•	•	9.877e-06
•	5.445e-05	•	5.859e-05
•	•	•	•
•	•	•	•

^w Frequency Databases queried: 1000 Genomes data (version 2015 Aug, from Annovar), the NHLBI GO Exome Sequencing Project (ESP) data (ESP6500SI-V2, from Annovar); the Exome Aggregation Consortium (ExAC) (Cambridge, MA (URL: <http://exac.broadinstitute.org>) [accessed on January 2018]), the Genome Aggregation Database (gnomAD) (URL: <http://gnomad.broadinstitute.org/>)

4.1.4 Clinical Manifestations of *DEGS1* Variants

Determination of the deleterious nature of variants identified through screening of mutation has allowed clinicians to define the clinical and laboratory features of this new form of hypomyelinating leukodystrophy. The first patient under investigation was a female who presented at the neonatal intensive care unit two weeks after birth with feeding difficulties, jitteriness, unexplained crying, extreme irritability, hypertonia with opisthotonus, nistagmus and fluttering eyelids. The symptoms were progressive with loss of ability to swallow and arrested development. The profound developmental delay with spasticity led to progressive respiratory complications over the second year of age, resulting in death at 18 months. Nerve conduction studies showed demyelinating neuropathy at 3 months of age. Her sequential cerebral MRI were profoundly abnormal with severe hypomyelination, and very thin corpus callosum (Patient 1, **Table 10**). Extensive investigations ruled out lysosomal enzyme deficiencies such as Krabbe. We carried out whole exome sequencing (WES) followed by appropriate filtering in proband-only, followed by Sanger validation and segregation analysis (**Fig. 14**). We identified a homozygous frameshift variant in *DEGS1* (GenBank ID: NM_003676.3, c.604delT; p.(Tyr202Thrfs*8)) which was not present in the genome aggregation database (gnomAD; >246,000 chromosomes), the NHLBI Exome Variant Server (EVS; >13,000 alleles) or ExAC (>150,000 alleles). No homozygous loss of function (LoF) variants were present for this gene in the mentioned databases. Personal communication and information exchange on the GeneMatcher19 platform facilitated the identification of additional 17 additional affected individuals with *DEGS1* variants who displayed overlapping phenotypes. These variants were present in homozygous or compound heterozygous manner in twelve independent families and segregated under a recessive paradigm (**Fig. 15**).

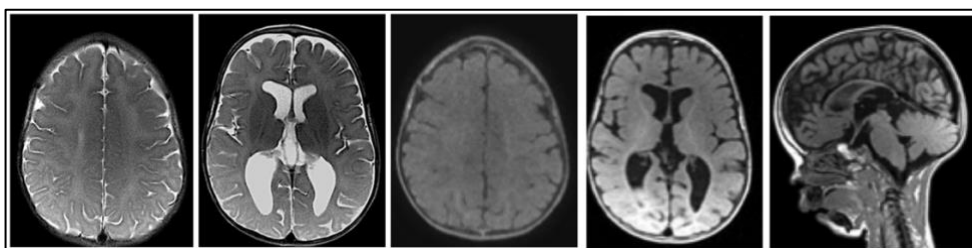


Figure 15. Neuroimaging findings in Patient 1: Presents delayed myelination at 13 months plus faint hyperintensity along the internal capsule and lateral thalamus.

Table 10. Clinical data from the 18 individuals with *DEGSI* variants.

Family	Family 1	Family2	
Patient number	Patient 1	Patient 2	Patient 3
Mutations	NM_003676.3: c.604delT:p.(Tyr202Thrfs*8)	NM_003676.3: c.395A>G: p.(His132Arg)	NM_003676.3: c.395A>G: p.(His132Arg)
Family	Healthy sister, dizygotic twin after IVF	2 consanguineous brothers	Sibling of patient 1
Ethnicity	Moroccan	Pakistani	Pakistani
DOB	Dec 2013 (deceased)	n.a.	Died at 7 years
Sex	F	M	M
MRI/MRS Neuroimaging	Poor myelination of internal capsule, and occipital area, tendency to colpocephaly	Cerebellar atrophy. Leukodystrophy. Brain scanner: diffuse calcifications	Cerebellar atrophy. Leukodystrophy. Brain scanner: diffuse calcifications
Ophthalmologic issues	Abnormal eye movements with fluttering eyelids (nystagmus, first horizontal, later rotating,	Optic atrophy. No cataract. Abnormal ocular movements (++)	No cataract. Abnormal ocular movements (++)
Developmental delay/ID	Yes	Severe	Severe
Age at sitting		Unable to sit	Unable to sit
Age at walking	Unable to walk	Unable to walk	Unable to walk
Age at talking		Unable to talk	Unable to talk
Current speech abilities	Limited language; 2 word phrases	Unable to talk	Unable to talk
Muscle tone	Hypotonia	Dystonia ++ Pyramidal signs ++	Dystonia ++ Pyramidal signs ++
Spasticity	Yes, tendency to opisthotonos	n.a.	n.a.
Full scale IQ	n.a	n.a	n.a
Seizure type/EEG results	Myoclonic movements	No seizures	No seizures

(Continued on next page)

Family 3		Family 4
Patient 4	Patient 5	Patient 6
NM_003676.3: c.341_342delTT:p.(Leu114Profs*11)/ c.764A>G:p.(Asn255Ser)	NM_003676.3: c.341_342delTT:p.(Leu114Profs *11)/c.764A>G:p.(Asn255Ser)	NM_003676.3: c.397C>T:p.(Arg133Trp)/c.752dup T:p.(Leu251Phefs*10)
Two siblings, non-consanguineous	Sibling of patient 4	non-consanguineous, 5 unaffected siblings
European Caucasian ancestry	European Caucasian ancestry	European Caucasian ancestry
2007, alive	2010, alive	n.a.
F	M	F
Delayed myelination/ dysmyelination; thalamic hyperintensities; thin splenium	Delayed myelination/ dysmyelination; thalamic hyperintensities; thin splenium	Normal
Nystagmus and abnormal saccades. Difficulty with lateral gaze and tracking. History of normal dilated exams, recently noted to have mild optic nerve pallor	Normal dilated exam	Anisocoria since 2 m
Yes	Yes	mild to moderate, regression age 9
Unable to sit without support	Unable to sit without support	Sits unassisted
Unable to walk	Unable to walk	Standing by 9 m, then regressed to 2 m level.; slow development since
First words by 1y	n.a.	Sound until 9 m, then regressed
Mostly nonverbal, uses gaze device and has some signed words. Has some work approximations and letter sounds.	Nonverbal, only babbles. Communicates with gaze device	Simple sentences
Severe truncal hypotonia, dystonia of all four limbs	Severe truncal hypotonia, dystonia of all four limbs	Dystonia ++ Pyramidal signs ++
Yes	Yes	Yes LE>UE
Intellectual disability. Unable to accurately measure IQ due to motor and language impairments.	Intellectual disability. No record of neuropsych testing	
Seizures started at 22months.	Seizures started at 2y.	Partial complex and clonic seizures, EEG with epileptiform discharges

(Continued on next page)

Family 5		Family 6	Family 7
Patient 7	Patient 8	Patient 9	Patient 10
NM_003676.3:c.764A>G:p.(Asn255Ser)	NM_003676.3:c.764A>G:p.(Asn255Ser)	NM_003676.3:c.337A>G:p.(Asn113Asp)	NM_003676.3:c.337A>G:p.(Asn113Asp)
2 consanguineous brothers	Sibling of patient 7	consanguineous (1 healthy sister)	consanguineous, 2 siblings with the similar disease died before the age of 14 years and 2 healthy siblings
Moroccan	Moroccan	Algerian	Algerian
18/12/03	28/05/08	04/24/2008	12/23/1996
M	M	F	M
n.a.	n.a.	*MRI at 8 months : Diffuse hypomyelination *MRI at 2,5 years : hypomyelination but myelination of MCP, internal capsule and corpus callosum ; SRM increased choline & decreased NAA in WM. *MRI at 6 years : global atrophy with cerebellar predominance and thin corpus callosum; progress in myelination, thalamic hyperintensities on FLAIR and T2 and decreased volume of the thalamus *CT at 7 years : no calcifications	*MRI at age 2 : delayed myelination (however the superior limb of the internal capsule and the middle cerebellar peduncles appeared myelinated), mild T1 hypointensity of some areas of the deep hemispheric WM, thin corpus callosum and small vermis. * CT at age 2 : no calcifications, hypointensity of WM. * MRI age 12 : global cerebral atrophy with cerebellar predominance and very thin corpus callosum, thalamic hyperintensities on FLAIR and decreased volume of the thalamus , WM on FLAIR : increased signal of the hemispheric WM with posterior predominance.
n.a.	n.a.	nystagmus (since first weeks of life), fundus	nystagmus (since first weeks of life), ERG nl
n.a.	n.a.	nl at age 2 years	Normal
yes moderate: able to speak, to read simple sentences	yes more severe than his brother: able to say words but no sentences, unable to read nor to count	severe (head oscillations noticed between	severe (head oscillations between birth to 3 months)
unable to sit	unable to sit	Unable to sit without support	Unable to sit without support
Unable to walk	Unable to walk	Unable to walk	Unable to walk
4-5 years		unable to talk	unable to talk
simple sentences	only words	Nonverbal, only babbles. Communicates with gaze device	Nonverbal, only babbles. Communicates with gaze device
truncal hypotony, limbs hypertony	truncal hypotony, limbs hypertony	truncal hypotonia, limb spasticity and dystonia	truncal hypotonia, limb spasticity and dystonia
Yes+++	Yes+++	yes, since the first months of age, tend to	yes
no problem	no problem	feeding difficulties	feeding difficulties, gastrostomy at age 18 years
not performed (moderate ID)	not performed (moderate to severe ID)	severe to profound intellectual disability. Unable to accurately measure IQ due to motor and language impairments. Bedridden	profound intellectual disability. Unable to accurately measure IQ due to motor and language impairments. Bedridden
no	TCG seizures, with diphasic spikes and waves in left centro-temporal areas	seizures and status epilepticus since the	seizures since the age of 2 years, myoclonic seizures, EEG slow background

(Continued on next page)

Family 8			Family 9
Patient 11	Patient 12	Patient 13	Patient14
Presumed same as Patient 13- patient deceased	Presumed same as Patient 13- patient deceased	NM_003676.3:c.320G>A: p.(Trp107*)	N M_003676.3: c.565A>G : p.(Asn189Asp)/ c.764A>G p.(Asn255Ser)
Sibling of patient 13	Sibling of patient 13	consanguineous, 2 siblings with similar symptoms died before the age of six. No healthy siblings	Distantly consanguineous (4th cousins). One older sister with no symptoms.
Egyptian 25/1/2009 F	Egyptian 03/10/12 M	Egyptian 27/11/2013 M	Indian sub-continent 01/25/1999 M
MRI at the age of 2ys: mild cortical atrophy, deep sylvian fissures, deep white matter changes with	MRI at the age of 1y: mild cortica atrophy, bilateral deep sylvian fissures more in left side, bilateral high signal of white mater at	MRI at the age of 10 months: mild deep sylvian fissures, diffuse hypomyelination more prominent in correlation with the patient's age.	MRI (age 17): corpus callosum atrophy (body and genu), ventricle dilatation (moderate of 3rd, 4th, and lateral), inferior cerebellar atrophy, high T2
Nystagmus, could follow objects, normal fundus, delayed latency in VEP and normal ERG	Nystagmus, could follow objects, normal fundus, delayed latency in VEP and normal ERG	Nystagmus, can follow objects, normal fundus, delayed latency in VEP and normal ERG	Nystagmus.
Severe delay, never aquired milestones, only followed objects	Severe delay, never aquired milestones, only followed objects	Severe delay, never aquired milestones, only followed objects	Yes, Regression at 6 months of age after viral illness.
Unable to sit	Unable to sit	Unable to sit	Sit at 5 months - lost it at 8 months
Unable to walk	Unable to walk	Unable to walk	Unable to walk
Unable to talk	Unable to talk	Unable to talk	Single words at age 2 - no speech since age 16y.
Non verbal, only communicate	Non verbal, only communicate	Non verbal, only communicate	Currently non-verbal
truncal hypotonia, limb spasticity and dystonia	truncal hypotonia, limb spasticity and dystonia	truncal hypotonia, limb spasticity and dystonia	Severe spasticity - some non-purposeful movements of arms and legs. Bedridden/Motorozed wheelchair
Yes	Yes	Yes	spasticity
Profound, bed ridden	Profound, bed ridden	Profound, bed ridden	Profound ID with inability to assess IQ due to no language.
Seizures at the age of 3ys, focal , myoclonic, staring look	Seizures at the age of 8 months, tonic with cyanosis, atonic	Seizures at 2 6/ 12y (only once as tonic with cyanosis)	Seizures starting age 5 y with one status GTC admission and cardiac arrest; currently onn 2 AED medications but still has some GTC seizures.

(Continued on next page)

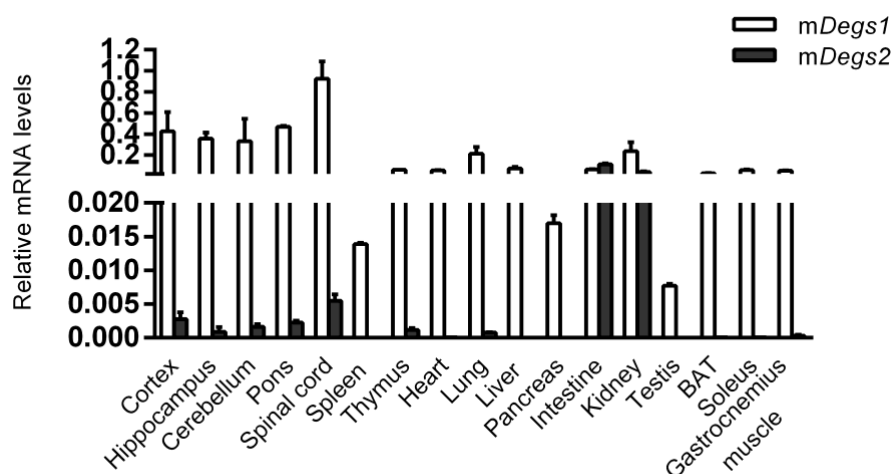
Family 10		Family 11	Family 12
Patient 15	Patient 16	Patient17	Patient18
NM_003676.3 :c.852_855del:p.(Tyr284*)	NM_003676.3 :c.852_855del:p.(Tyr284*)	NM_003676.3: c.T110C;p.(Met37Thr)/c.G878A:p.(Trp293*)	NM_003676.3:c.320G>A:p.(Trp107*)
Two siblings, non-consanguineous	Two siblings, non-consanguineous	nonconsanguineous, one younger sister with no symptoms.	consanguineous, only child
European Caucasian ancestry	European Caucasian ancestry	Chinese	Egyptian
Feb 2, 2015 - alive	Jan 15, 2012 - alive	19/12/11	01/01/08
M	M	F	F
Delayed myelination/Hypomyelination; thin corpus callosum	Delayed myelination/Hypomyelination; thin corpus callosum	Brain CT (8months);(-). Twice MRIs (8m and 16m): diffuse hypomyelination.	Cerebellar atrophy, Central atrophy, white matter changes.
Asymmetric horizontal nystagmus more pronounced on the right than the left	There is minimal nystagmus, particularly apparent on funduscopic examination. This tends to be horizontal and jerky in character.	None	Nystagmus
Yes	Yes	severe delay	severe delay, no acquired milestones
Unable to sit without support	Unable to sit without support	Unable to sit	Unable to sit
Unable to walk	Unable to walk	Unable to walk	Unable to walk
Unable to talk	Unable to talk	Unable to talk	Unable to talk
A number of vocalizations but no recognizable words	A number of vocalizations but no recognizable words	Non verbal	Non verbal, only communicate
Axial hypotonia with limb spasticity, most pronounced in the lower extremities. Clonus	Axial hypotonia with limb spasticity, most pronounced in the lower extremities. Clonus	truncal hypotonia, limb spasticity	truncal hypotonia, limb spasticity, hyperreflexia, severe wasting
Yes	Yes	spasticity	Yes
Not performed	Not performed	Gesell (8months): DQ in adaptive ability, gross motor, fine motor, language and personal social area were 54.6, 70.4, 68.7, 80.1, 70.1,	Profound, bed ridden
No seizures	Three seizures in life. His EEG was normal as a baby, but subsequently has disclosed the presence of epileptiform activity. He is being treated with levetiracetam which appears to be well tolerated.	No seizure	Febrile seizures at age 4.

4.2 Chapter 2

4.2.1 *Degs1* is Highly Expressed in Mice Central Nervous System (CNS)

We tested different commercial antibodies available against DEGS1 by western blots, but none of the antibodies tested gave a specific signal. We then investigated the pattern of expression of *Degs1* mRNA levels in different tissues of 4-month-old wild-type mice (n=3) and we obtained high expression of this gene in CNS, particularly in spinal cord, brain cortex, pons, cerebellum, and hippocampus, compared to other organs such as liver, soleus muscle, brown adipose tissue, thymus, intestine, pancreas or spleen (**Fig. 16a**). Moreover, we also found that the levels of *Degs2*, the closest homologue of *Degs1* in mice different tissues were comparatively lowered in central nervous system (**Fig. 16a**). Among different tissues, they were found to be highly expressed in kidney and intestine. To gain a better understanding of the neuropathology, we sought to conduct mRNA profile examinations of *DEGSI* in control human child and adult post-mortem CNS tissues (n=2) and because of the fact that the patients were in the early stage of the disease. We performed qPCR in different child and adult control human CNS tissues (Frontal lobe BA9, Putamen, Entorhinal cortex, Hippocampus, Hypothalamus, Pons, Cerebellum, White matter Frontal cortex, Spinal Cord) obtained from NeuroBioBank, NIH and we found expression of this gene across all parts of the CNS with no major differences between child and adult CNS tissues (**Fig. 16b**). Altogether, these results suggest that *DEGSI* is predominantly expressed in the CNS.

a)



b)

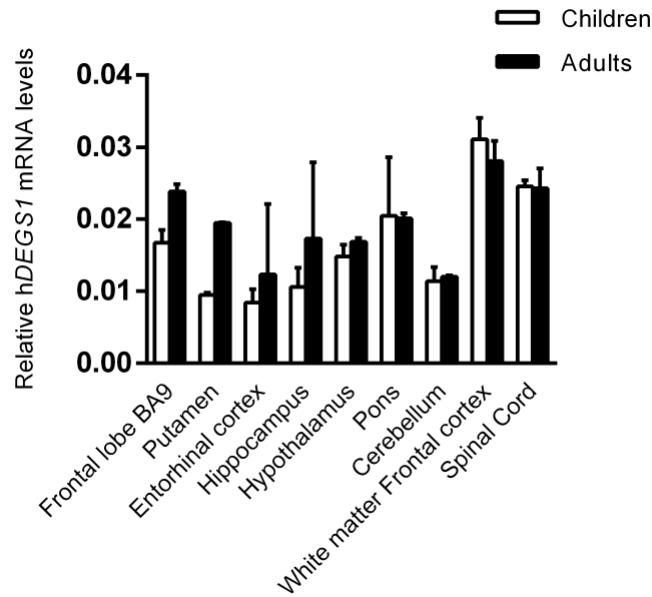


Figure 16. *DeGS1* transcript level is predominantly expressed in the CNS.

(a) *DeGS1* and *DeGS2* expression were measured by quantitative RT-PCR in mice different tissues (n=3). *DeGS2* expression was not detected in spleen, liver and pancreas with the concentration of RNA we used. (b) *DEGS1* expression measured by quantitative RT-PCR in human control (n=5). Gene expression normalized relative to *RPLP0*. Experiments have been performed in triplicate. Data shown as mean \pm SD.

4.2.2 *DEGS1* Transcript Level is Altered in Patient Fibroblasts

To determine whether the variants identified in our cohort triggered nonsense-mediated mRNA decay, we performed qPCR to assess the *DEGS1* mRNA expression in fibroblasts from individuals (Patients 4, 7 and 9) and healthy age-matched control individuals (n=5). qPCR analyses showed low *DEGS1* mRNA expression in patient 4,7. (**Fig. 17a**). However, we observed an increase in mRNA expression in patient 9 fibroblast. Thus, to further speculate the reason for these differences among different patients in *DEGS1* mRNA levels we analyzed the expression of *DEGS2*, the closest paralog to *DEGS1*, with a similar function regarding desaturase activity (Ternes et al., 2002). qPCR analysis showed high *DEGS2* mRNA levels in patient 4,7 (**Fig. 17a**) and no significant difference was found in case of patient 9. In conclusion, very low expression of *DEGS1* in patient 4 could be due to the mRNA decay in the allele bearing the stop variant. There was approximately 7 cycles difference between *DEGS1* and *DEGS2* (more than 100-fold in favor of *DEGS1*). However, no differences in *DEGS2* mRNA levels was seen in patient 9, indicating that such endogenous responses were absent in spite of high *DEGS1* level.

We, therefore, hypothesized that the alterations in transcription levels identified in these patient cohorts are likely to be relevant to the disease process.

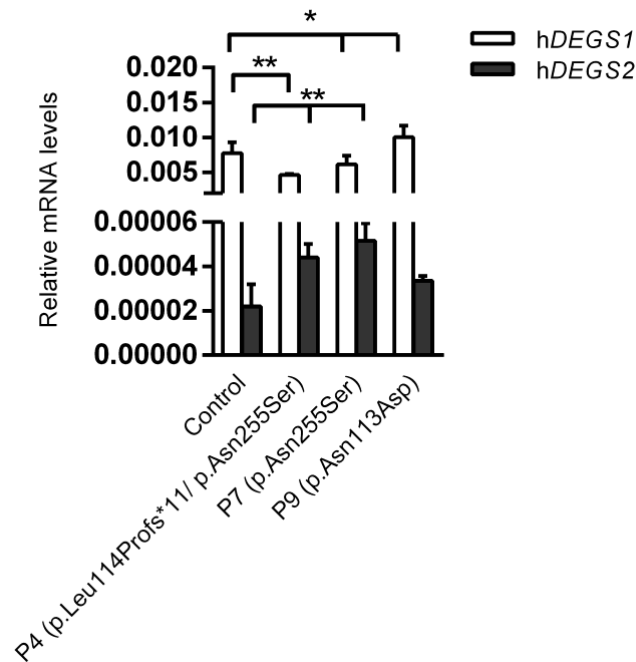


Figure 17. *DEGS1*, *DEGS2* expression measured by qPCR in patients from Families 3, 5, 6

(a) *DEGS1*, *DEGS2* expression measured by quantitative RT-PCR in human control (n=5) and affected individuals fibroblasts (P4, P7, P9; n=1 each). Gene expression normalized relative to *RPLP0*. Experiments with fibroblasts are from three independent experiments and have been performed in triplicate. Data are shown as mean \pm SD * p<0.05; ** p<0.01; *** p<0.001 after one-way ANOVA test followed by Tukey's posthoc test.

4.2.3 *DEGS1* Activity is Inhibited in Patients

To investigate the functional effects of the identified *DEGS1* variants and to functionally validate the impact of the variants on *DEGS1* protein function, we used targeted lipidomics to quantify 2-hydroxyacyl-ceramides, saturated and monounsaturated ceramides, the products of *DEGS1* as well as its substrates and their dihydro counterparts in cultured skin fibroblasts of affected individuals (Patient 4, 7, 9) and muscle tissue (Patient 6). The results indicated a reduction of ceramides concomitant with an accumulation of dihydroceramides in all these affected individuals (**Fig. 18a, b**). By mass-spectrometry analysis, we could identify different species of ceramide and dihydroceramide in control and patient's (fibroblasts and muscle). The major species detected in fibroblasts and muscle are listed (**Table 11, 12**). The levels of short chain and long chain ceramide species were found to be reduced in patient's fibroblasts. However, their dihydro-counterparts were found to be increased as compared to controls, indicating

impaired activity of DEGS1 enzyme in affected individual fibroblasts (P3, P4, P7, P9). In addition, the ratio dihydroceramide/ceramide, DhCer/Cer and unsaturated UNSAT-DhCer/UNSAT-Cer which represents the activity of the DEGS1 enzyme, is altered consistent with the notion that the variants identified cause reduction or loss of function of the DEGS1 enzyme. Together, these data suggest that impairment in desaturase activity of an enzyme involved in *de novo* ceramide pathway might contribute to the hypomyelination observed in the four subjects.

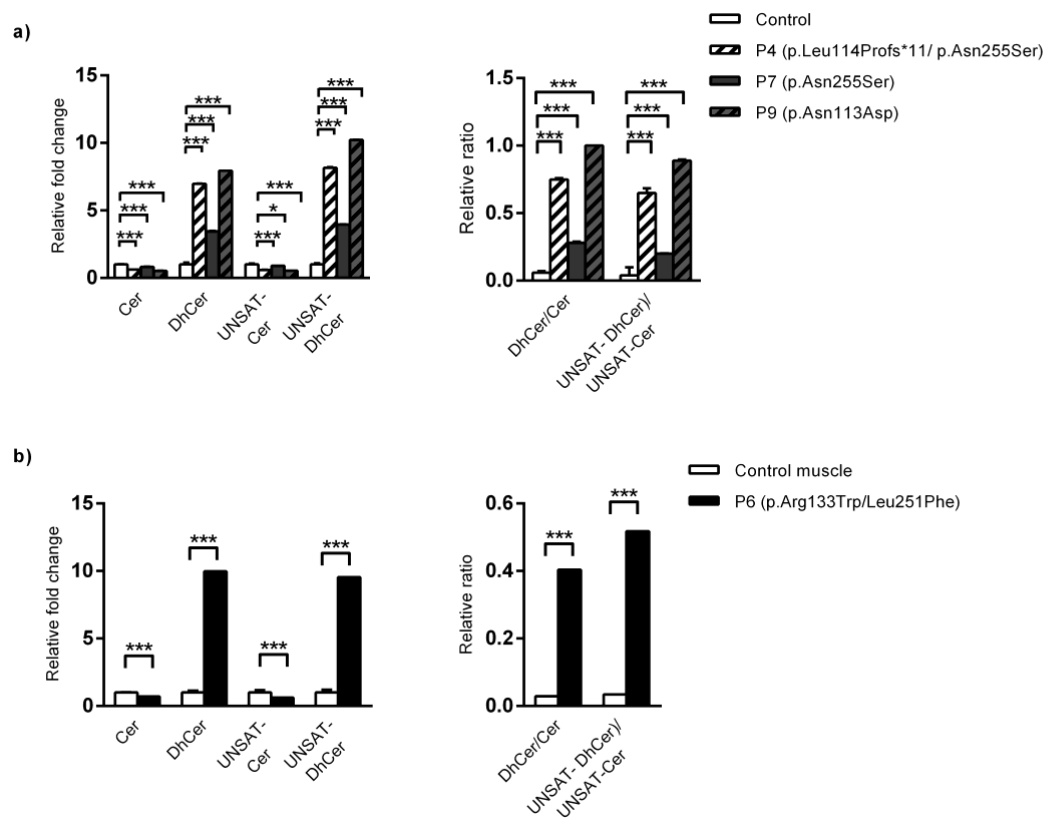


Figure 18. Ceramides and Dihydroceramides imbalance in patient's fibroblasts (P4, P7, P9) and muscle (P6).

(a) Cer (Saturated ceramides (C7:0 to C28:0)), DhCer (Saturated dihydroceramides (C7:0 to C28:0)), UNSAT-Cer (Monounsaturated ceramides (C7:1 to C28:1)), UNSAT-DhCer (Monounsaturated dihydroceramides (C7:1 to C28:1)) levels, the ratios DhCer/Cer and UNSAT-DhCer/UNSAT-Cer in human controls (n=9) and patient fibroblasts⁺⁺ (P4, P7, P9) and (b) in human controls (n=5) and patient muscle⁺ (P6). Experiments with fibroblasts are from two independent experiments and have been performed in triplicate. Data are shown as mean \pm SD * p<0.05; ** p<0.01; *** p<0.001 after one-way ANOVA⁺⁺ test followed by Tukey's posthoc test or Student t test⁺.

Table 11: Lipid profiling of ceramide (Cer) and dihydroceramide (DhCer) species in control and patient's fibroblasts.

Species	Control fibroblasts			P4			P7			P9		
C16:0-Cer	30.735	±	1.050	18.771	±	0.177**	25.610	±	0.748*	12.613	±	0.258**
C18:0-Cer	2.515	±	0.211	3.093	±	0.476	4.413	±	0.222**	1.973	±	0.092
C22:0-Cer	4.647	±	0.090	3.936	±	0.314	5.756	±	0.012**	3.566	±	0.055***
C23:0-Cer	2.179	±	0.089	1.407	±	0.024*	1.967	±	0.213	1.344	±	0.004**
C24:0-Cer	22.914	±	1.673	11.931	±	1.067*	13.772	±	0.099*	14.214	±	0.320*
C25:0-Cer	0.783	±	0.075	0.395	±	0.052	0.397	±	0.007*	0.411	±	0.053
C26:0-Cer	0.585	±	0.070	0.288	±	0.022*	0.288	±	0.021*	0.277	±	0.011*
C16:0-DhCer	2.801	±	0.313	15.815	±	0.024***	9.306	±	0.196**	13.418	±	0.136**
C18:0-DhCer	0.256	±	0.051	0.965	±	0.086*	0.665	±	0.014**	1.015	±	0.015**
C22:0-DhCer	0.393	±	0.069	2.501	±	0.061**	1.228	±	0.026**	2.990	±	0.078***
C23:0-DhCer	0.094	±	0.010	0.799	±	0.023***	0.311	±	0.032*	1.099	±	0.006***
C24:0-DhCer	0.598	±	0.041	9.459	±	0.223***	2.876	±	0.035***	15.658	±	0.126***
C25:0-DhCer	0.059	±	0.004	0.178	±	0.006**	0.079	±	0.002*	0.243	±	0.016**
C26:0-DhCer	0.016	±	0.004	0.145	±	0.031*	0.043	±	0.007	0.165	±	0.008**
C16:1-Cer	0.183	±	0.013	0.081	±	0.002*	0.126	±	0.010*	0.077	±	0.008**
C18:1-Cer	0.106	±	0.013	0.079	±	0.002	0.134	±	0.016	0.054	±	0.010
C20:1-Cer	0.045	±	0.008	0.051	±	0.008	0.087	±	0.023	0.022	±	0.003
C22:1-Cer	0.831	±	0.089	0.680	±	0.073	1.069	±	0.006	0.469	±	0.007*
C23:1-Cer	0.891	±	0.040	0.647	±	0.025*	0.979	±	0.051	0.492	±	0.038*
C24:1-Cer	20.694	±	0.264	11.963	±	0.268***	18.538	±	0.141*	11.329	±	0.073***
C25:1-Cer	1.021	±	0.039	0.569	±	0.041*	0.743	±	0.024***	0.526	±	0.020***
C26:1-Cer	0.896	±	0.147	0.495	±	0.053	0.689	±	0.033	0.394	±	0.008*
C28:1-Cer	0.096	±	0.027	0.064	±	0.012	0.044	±	0.006	0.029	±	0.002
C16:1-DhCer	0.182	±	0.011	0.177	±	0.005	0.196	±	0.023	0.147	±	0.006
C18:1-DhCer	0.036	±	0.009	0.062	±	0.006*	0.074	±	0.003*	0.067	±	0.001
C20:1-DhCer	0.013	±	0.007	0.046	±	0.008**	0.064	±	0.033	0.045	±	0.014
C22:1-DhCer	0.105	±	0.006	0.470	±	0.039**	0.351	±	0.029*	0.414	±	0.009**
C23:1-DhCer	0.068	±	0.018	0.598	±	0.025**	0.322	±	0.028*	0.743	±	0.023***
C24:1-DhCer	0.691	±	0.026	7.505	±	0.236***	3.349	±	0.093**	9.835	±	0.083***
C25:1-DhCer	0.022	±	0.008	0.341	±	0.009**	0.121	±	0.005*	0.419	±	0.022**
C26:1-DhCer	0.024	±	0.009	0.413	±	0.093*	0.157	±	0.019**	0.392	±	0.030**

Values are mean ± SD (% of total lipids analysed; n = 3) * p<0.05; ** p<0.01; *** p<0.001 after one-way ANOVA test followed by Tukey's posthoc test.

Table 12: Lipid profiling of ceramide (Cer) and dihydroceramide (DhCer) species in control and patient muscle.

Species	Control muscle		P6
C16:0-Cer	6.119	± 4.164	5.636
C18:0-Cer	23.242	± 5.115	12.699
C20:0-Cer	1.188	± 0.728	1.061
C22:0-Cer	6.558	± 1.267	4.748
C23:0-Cer	6.025	± 2.373	3.742
C24:0-Cer	20.171	± 7.244	13.907
C16:0-DhCer	0.335	± 0.201	3.477
C18:0-DhCer	0.321	± 0.112	3.586
C20:0-DhCer	0.088	± 0.059	0.604
C22:0-DhCer	0.181	± 0.066	3.156
C23:0-DhCer	0.094	± 0.060	1.290
C24:0-DhCer	0.446	± 0.141	7.649
C18:1-Cer	0.508	± 0.109	0.531
C24:1-Cer	17.004	± 4.035	10.933
C18:1-DhCer	0.108	± 0.043	0.165
C24:1-DhCer	0.294	± 0.092	5.618

Values are mean ± SD (% of total lipids analysed; controls n = 5)

4.2.4 Impaired Function of DEGS1 Induces Intracellular ROS Production

Excess of dihydroceramides has been recently reported to generate reactive oxygen species (ROS) in *Drosophila* KO photoreceptors (Jung et al., 2017). As fibroblasts represent the main resource material obtainable from affected individuals, we next quantified intracellular ROS levels using the probe H₂DCFDA in patients 4, 7 and 9 and control fibroblasts at baseline as described (Jone López-Erauskin, Ferrer, Galea, & Pujol, 2013). We observed that ROS production was increased in all patients' fibroblasts compared to controls (**Fig.19a**). However, the origin of this ROS was unknown. This led us to investigate its role in mitochondrial function as mitochondria constitute the main source of ROS under many neuropathological conditions. We sought to investigate whether mitochondria from these patient fibroblasts represent the main source of ROS. We used two fluorescent probes DHE (dihydroethidium) and MitoSOX (DHE covalently bonded to hexyl triphenylphosphonium cation), which measure intracellular and intra-mitochondrial superoxide levels respectively (J López-Erauskin et al., 2013). We observed that the levels of superoxide (O₂^{•-}) measured by either DHE or MitoSOX were similar in patient 4, which indicates mitochondria as the major source of ROS (**Fig.19b**). However, no changes were seen in patient 7 and a significant decrease was found in the case of patient 9 which also suggests that impaired mitochondria drove pathogenesis in this patient (**Fig.19b**). Overall, these results suggest accumulation of DhCers results in increased ROS.

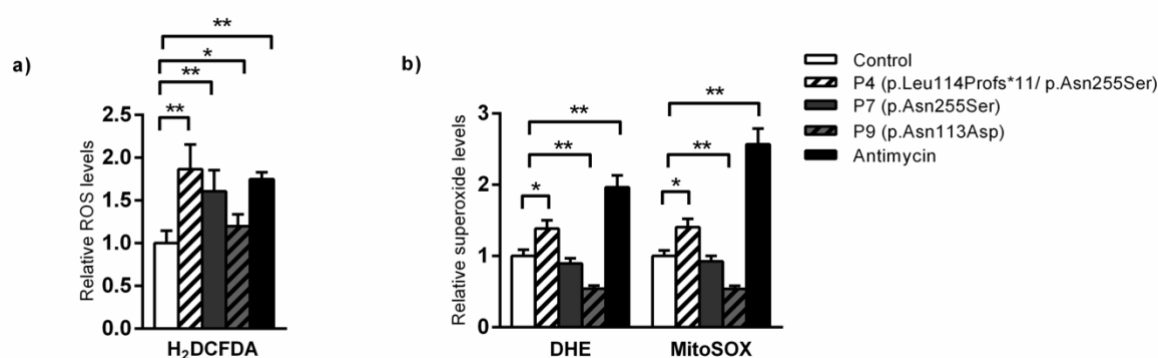


Figure 19. ROS production in patient's fibroblasts

Intracellular ROS has been quantified using H₂DCFDA probe in patient's fibroblasts (Patients 4, 7, 9) and controls (n=5) at basal level. Data are from three independent experiments performed in triplicate, shown

as mean \pm SD * $p < 0.05$; ** $p < 0.01$; *** $p < 0.001$ after one-way ANOVA test followed by Tukey's posthoc test.

4.2.5 Exogenous Long Chain DhCer Increases ROS Levels in Control Fibroblasts

Relatively little is known regarding specific roles for individual DhCer in neurological disorders, although our data suggest that DhCer accumulation induces ROS production. We sought to determine whether commercially available DhCer directly impact cell survival. We treated control and patient's fibroblast cultures (patient 4, 7, 9) with exogenous C18:0-DhCer to check the toxicity. We found exogenous DhCer dramatically increases cell death in both fibroblasts at three different doses (30 μ M, 60 μ M, 90 μ M) after 6 h. However, some morphological alterations were observed at a low dose i.e. 20 μ M, 6 h and no cell death were found until 48 h. This led us to check the ROS levels at this dosage and time period. Interestingly, this dose increased ROS production in control fibroblasts (n=5), although we could not find an increase in ROS levels in patient fibroblasts (**Fig. 20**). Collectively, these data indicate that DhCer excess is able to generate ROS in human fibroblasts, whereas the blunted response in patient's fibroblasts may obey to saturation effects, due to the steady-state accumulation.

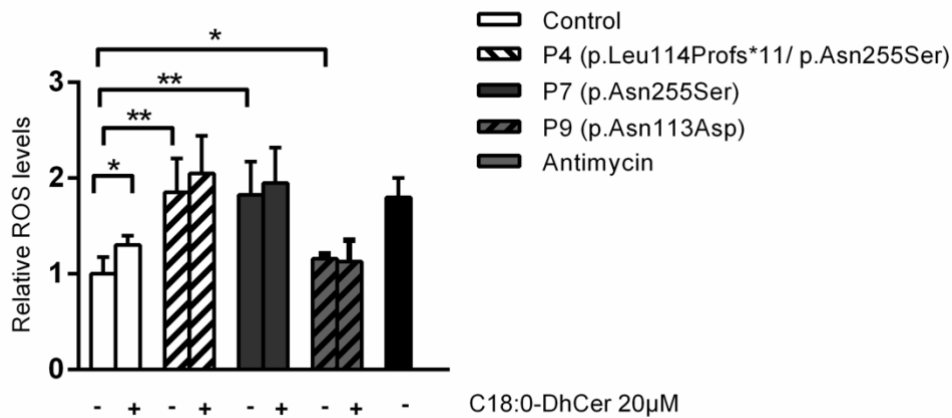


Figure 20. Exogenous long chain C18:0-DhCer increases ROS levels in control fibroblasts

Exogenous DhCer (C18:0) treatment (20 μ M, 6 h) to control and DEGS1 patient's fibroblasts. Antimycin has been used as positive control. Experiments with fibroblasts have been performed in triplicate. Data are shown as mean \pm SD * $p < 0.05$; ** $p < 0.01$; *** $p < 0.001$ after two-way ANOVA test followed by Tukey's posthoc test.

4.2.6 Lack of DEGS1 Activity Results in Low MMP and Mitochondrial Fragmentation in Patient 9

We then investigated the impact of the loss of DEGS1 function on mitochondrial transmembrane potential, reported to be affected in mouse *Degs1* model. We then measured inner mitochondrial membrane potential (MMP) with TMRE and analyzed the results by flow cytometry. TMRE is a voltage-sensitive red-orange fluorescent indicator for mitochondrial transmembrane potential. Mitochondrial depolarization (disrupting or decreasing membrane potential) results in a loss of dye from the mitochondria and a decrease in fluorescence intensity. In addition, inner mitochondrial membrane potential was quantified in patient fibroblasts (Patient 4,7,9) and control fibroblasts at baseline. We found a significant decrease in $\Delta\Psi_m$ in fibroblasts from patient 9 but not in patient 4,7 (**Fig. 21**). Moreover, clinical mitochondria studies for patient 9 exploring the mitochondrial respiratory chain have also highlighted that there was low global mitochondrial activity in muscle, complex I deficiency in fibroblast, and complex III deficiency in lymphocytes (data not shown). we evaluated mitochondria integrity in fibroblasts derived from patients. We carried out mitochondrial immunostaining with Mitotracker Red to determine possible changes in mitochondrial shape in patients' cells compared to control. We observed that mitochondrial network was disrupted in patient 9, with accumulation of donut or blob-shaped mitochondria, suggesting an alteration of mitochondrial integrity but not in patient 4, 7 fibroblasts (**Fig. 22**). Collectively, these data suggest mitochondrial dysfunction in Patient 9.

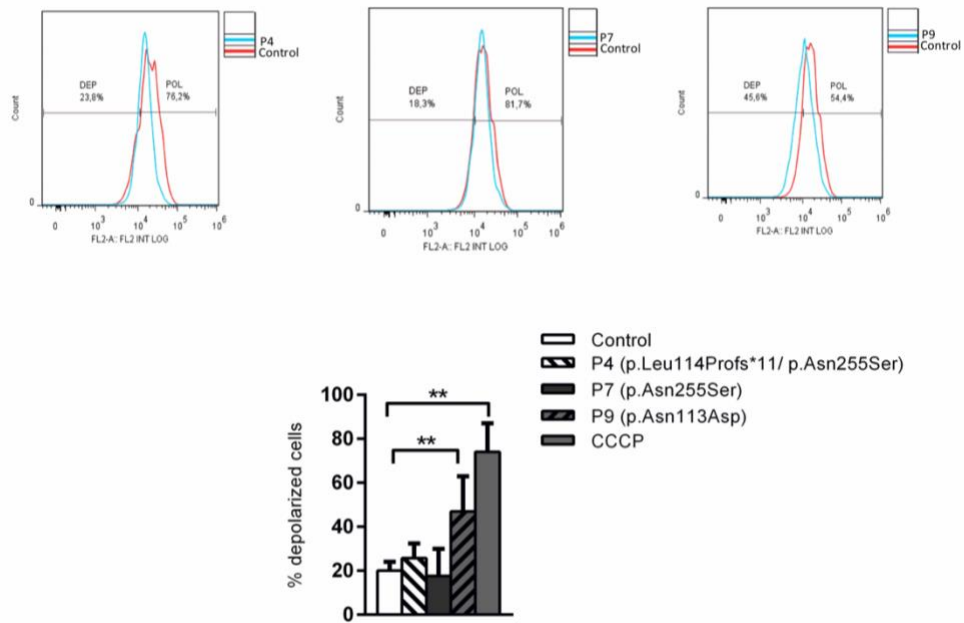


Figure 21. Lack of DEGS1 activity causes low MMP in Patient 9 fibroblasts

MMP was measured by comparing control and patient fibroblasts (P4, P7, P9). CCCP has been used as positive control. Experiments with fibroblasts have been performed in triplicate. Data are shown as mean \pm SD * $p < 0.05$; ** $p < 0.01$; *** $p < 0.001$ after one-way ANOVA test followed by Tukey's posthoc test.

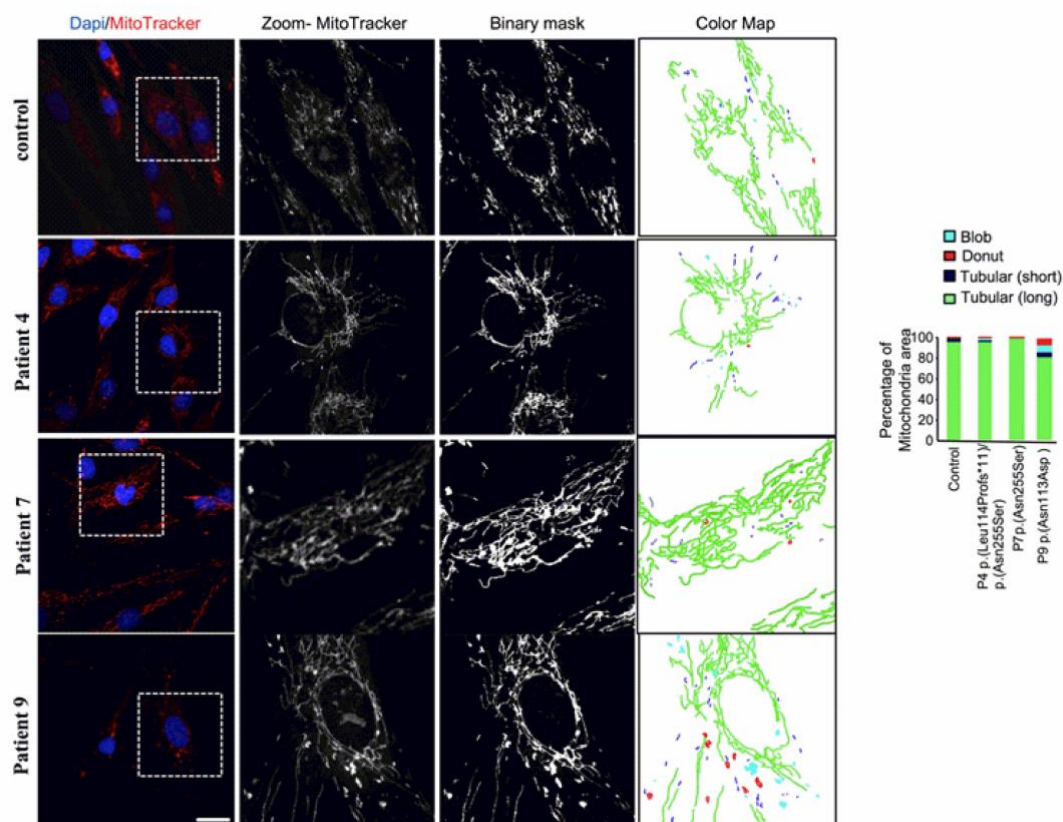


Figure 22. Mitochondrial fragmentation in Patient 9

Representative confocal images of immunofluorescence MitoTracker (red), DAPI (blue). Fluorescence intensity over the mitochondria area were quantified in controls (n=3) and patient's fibroblasts. Scale bar 10 μ m.

4.2.7 Lack of DEGS1 Activity Results in Impaired Autophagy Patient 4,9

Autophagy, like the ubiquitin-proteasome system, is considered to play an important role in preventing the accumulation of abnormal proteins. Microtubule-associated protein 1 light chain 3 (LC3) is important for autophagy, and the conversion from LC3-I into LC3-II is accepted as a simple method for monitoring autophagy. In our study, we analyzed LC3 and P62/SQSTM1, an adaptor protein that interacts with lipidated LC3, by immunoblotting. To monitor autophagy and autophagic flux in control and patient's fibroblasts, cells were cultured in a complete medium to assess basal autophagy together with the presence and absence of lysosomal inhibitor bafilomycin A1 (Baf A1). We found that in the presence of Baf A1 (10 nM, 2 h) treatment Patient 9 (**Fig.23b**) exhibited higher LC3-II levels compared with the controls indicating that autophagy is stimulated in

patient 9. In contrast, we observed low levels of LC3-II in patient 4 (**Fig. 23b**) indicating that autophagy machinery is impaired in this patient. There was no difference observed in patient 7. Of note, we detected no differences in p62 levels in patients after Baf A1 compared to control fibroblasts by Western blot (**Fig. 23c**). Thus, these observations indicated that autophagy flux is stimulated in patient 9 and impaired in patient 4.

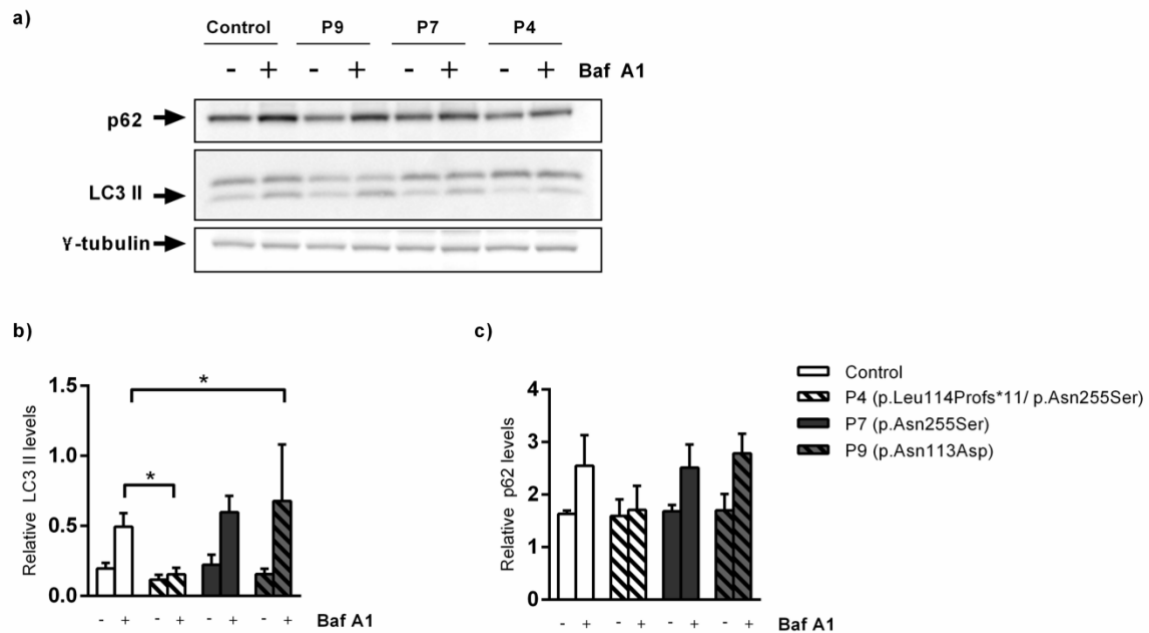


Figure 23. Impaired autophagic flux in Patient 4, 9 fibroblasts

Controls fibroblasts (n=5) and patient fibroblast (P4, P7, P9) were treated with the autophagic inhibitor Baf A1 (100 nM, 2 h). Representative immunoblots for p62 and LC3-II from control, patient (4, 7, 9) fibroblasts. Protein levels are normalized respected to γ -tubulin. The Histograms show the LC3 II and the p62 levels relative to control. Data are from three independent experiments and are shown as mean \pm SD * p<0.05; ** p<0.01; *** p<0.001 after two-way ANOVA test followed by Tukey's posthoc test.

4.2.8 FTY720 Attenuates ROS Levels in Patient's Fibroblasts

To get insight into the underlying causes of FTY720 protective effect and to corroborate these findings in *in vitro*, we treated the control (n=5) and patient fibroblasts (Patient 4, 7, 9) with FTY720 at a sub-lethal dose of 5 μ M for 6 h and ROS levels were measured using H₂DCFDA probe (Chen, Zhong, Xu, Chen, & Wang, 2010). FTY720 treatment prevented the elevated ROS levels in patient fibroblasts (**Fig. 24**). No effect of FTY720 was seen in control fibroblasts. These results might support the concept that FTY720 might restrain DhCer levels and result in diminished ROS levels in affected individuals.

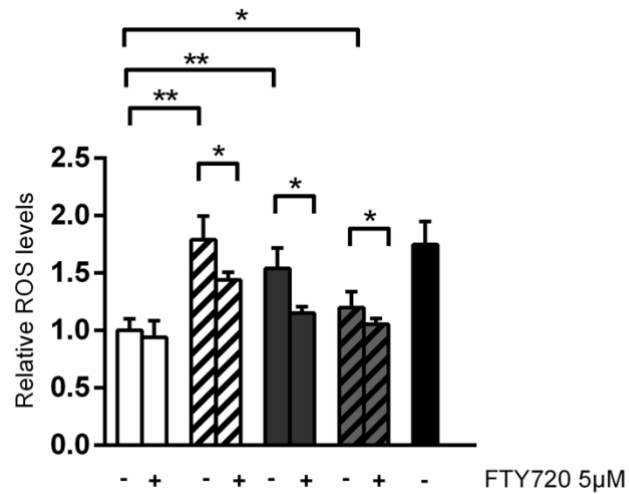


Figure 24. High intracellular ROS levels in patient’s fibroblast are prevented by FTY720 treatment

Intracellular ROS levels are partially normalized by Fingolimod (FTY720) treatment at 5 μ M, 6 h in patient fibroblasts (P4, P7, P9). Antimycin has been used as positive control. Results are from three independent experiments. Data are shown as mean \pm SD * $p < 0.05$; ** $p < 0.01$; *** $p < 0.001$ after two-way ANOVA test followed by Tukey’s posthoc test.

4.3 Chapter 3

4.3.1 Localization of *degs1* in Oligodendrocytes

The genome sequence of zebrafish contained one *DEGS1* ortholog with high conservation of coding exons with those encoding human *DEGS1* and high amino acid identity. Given both the amino acid conservation and also the spatiotemporal expression of *degs1*, we explored the expression profile of *degs1* within the primordium of the CNS of zebrafish larvae in order to know whether *degs1* expression would be compatible with the clinical phenotype of our patients, and hence, make more plausible the hypothesis of zebrafish as a suitable animal model. ISH was performed at 24 hpf, the latest timing of somitogenesis, during organogenesis at 48 and 72 hpf and during early larval development, soon before zebrafish become free feeding larvae, and at 5 dpf and do not solely rely on yolk reserves anymore using wild-type zebrafish embryos (**Fig. 25**). At 24 hpf, the body was mostly stain-free. By 48 hpf, the stain was present in the forebrain, around the eye, and underneath the otic vesicle. At 72 hpf, the stain had increased in these regions. Expression continued to increase in these developing organs at all later time points. No signal was detected using the sense probe. In situ hybridization on transverse histological sections at 5 dpf, reveals expression in the dorsal part of the brain, being more prominent in the dorsal thalamus, the posterior tuberculum, the tectum opticum, the hindbrain and as well in the spinal cord (**Fig. 26**). Moreover, an overlap between *degs1* mRNA and Mbp immunofluorescence signals was detected in oligodendrocytes, suggesting that oligodendrocytes do express *degs1* (**Fig. 26c-d**). The expression pattern of *degs1* is thus consistent with the roles of *DEGS1* in humans and the phenotype of the patients identified, pointing to the possibility of using the advantages of *Danio rerio* to model this disease.

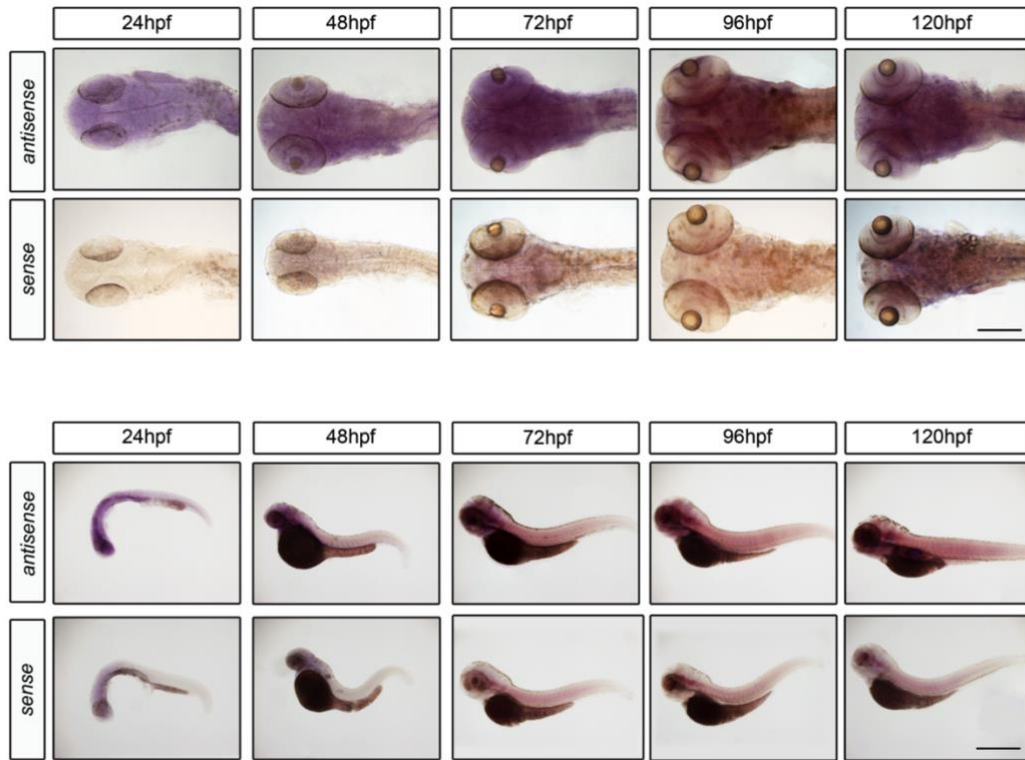


Figure 25. Whole mount *in situ* hybridization of *degs1* in wild type *Danio rerio*

Expression of *degs1* throughout embryogenesis. Bright field images from 24 to 120 hpf. Dorsal view (top), lateral view (bottom).

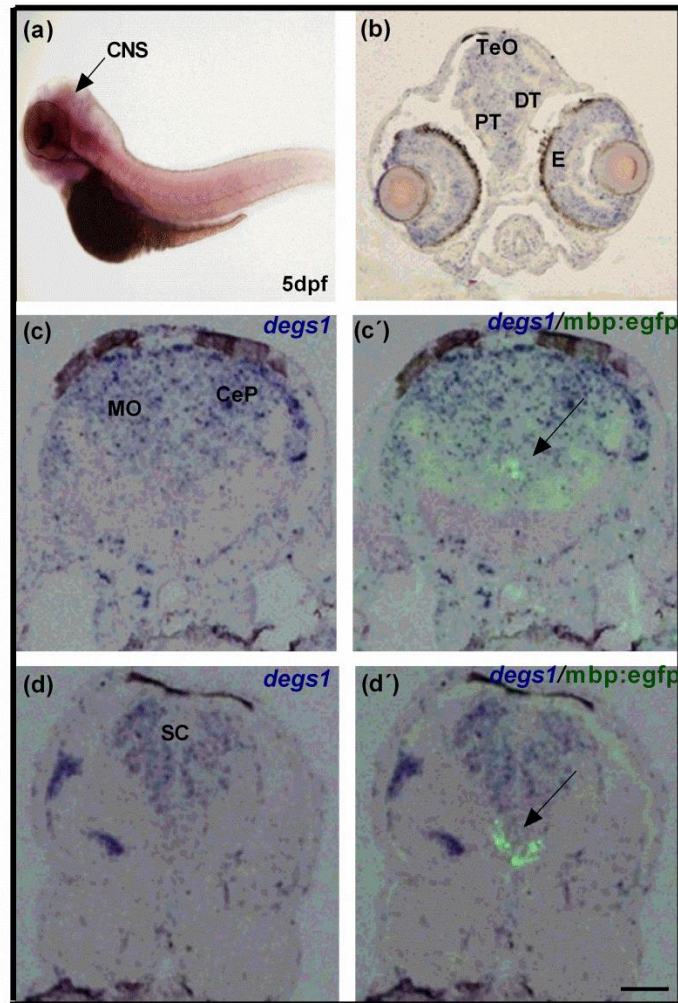


Figure 26. Localization of *degs1* in *Danio rerio*

In situ hybridization for *degs1* either in whole mount (a), or on sections (b-d) of 5dpf larvae. (a) Lateral view of whole-mount embryo in situ hybridization presented in lateral view (b-d) Transverse histological sections at different levels along the antero-posterior axis (head (b), hindbrain (c) and spinal cord (d)). Note that the hybridization signal is reinforced in the blablbla. (c', d') Immunofluorescence localization of GFP on histological sections of zebrafish larvae *Tg[mbp:egfp]* of (c,d) respectively. Note that *degs1* expression overlaps with GFP in the hindbrain and spinal cord. CNS, central nervous system; B, brain; DT, dorsal thalamus; E, eye; PT, posterior tuberculum; TeO, tectum opticum; MO, medulla oblongata; CeP, cerebellar plate; HB, hindbrain; SC, spinal cord. Scale bar: 50 μ m.

4.3.2 Morphogenetic and Functional Defects Induced by Downregulation of Zebrafish *degs1* During Early Development

To determine the relevance of *DEGS1* disruption to patient phenotype, we designed splice blocker antisense MO aimed to knockdown *degs1* in zebrafish, affecting the splicing of intron 2. MO was injected into the cell of one-cell stage zebrafish embryos, and we detected efficient disruption of the *degs1* locus through the introduction of small insertion.

MO-DEGS1 compared to either control MO or compared to larval batches uninjected. MO efficiently interfered with splicing at the targeted intron-exon boundary and reduced the levels of wild-type transcripts, as assessed by RT-qPCR resulted in inclusion of intron 2 (+97 bp) which was confirmed by sanger sequencing (**Fig. 27a-c**). The MO-DEGS1 morphant phenotypes induced were graded into two categories, mild and moderate, according to their morphology (**Fig. 27d-e**). In order to understand the effects of the knockdown in the biochemical function of DEGS1, we used targeted lipidomics of the ceramide species. The results obtained in larvae at 5 dpf indicate an impaired function of DEGS1, with an increase of saturated DhCer and unsaturated DhCer, as well as an increased of the ratios DhCer/Cer and UNSAT-DhCer/UNSAT-Cer (**Fig. 27f; Table 13**). This increase in the ratio was more important in the saturated species, in contrast to the profile obtained in the fibroblasts, for which saturated and unsaturated levels and ratios of DhCer were similarly altered.

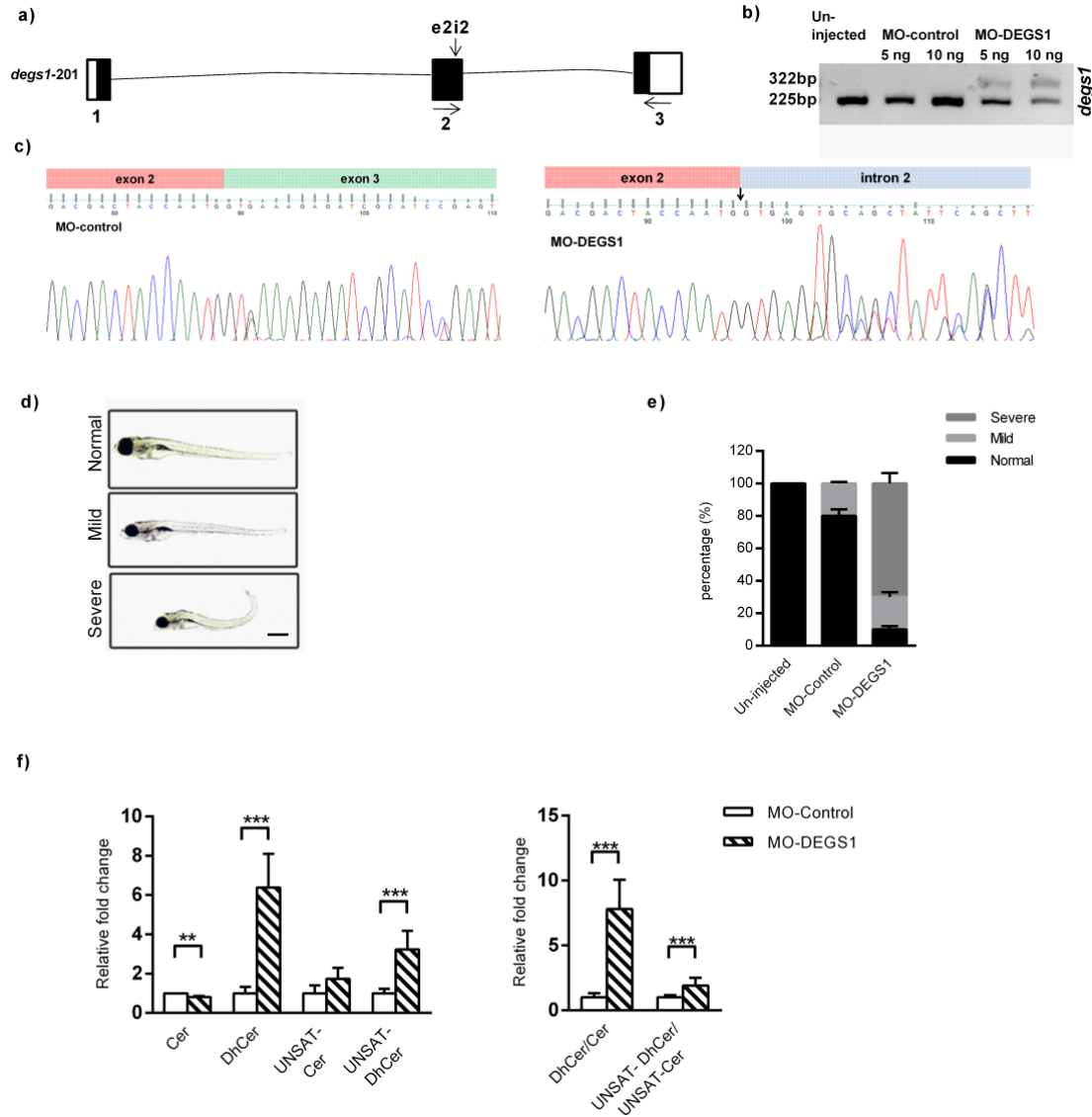


Figure 27. Morphogenetic and functional defects due to loss of function of *degs1* in zebrafish

(a) Representation of the zebrafish *degs1* transcript, *degs1*-201 (genome assembly Zv10); coding regions, black boxes; untranslated regions, white boxes. Zebrafish *degs1* -201 encodes GenBank ID: NP_997865. The vertical arrow indicates splice-blocking (sb) morpholino (MO) target sites of exon 2, intron 2 (e2i2) boundary, horizontal arrows indicate RT-PCR primers used to generate amplicons. Agarose gel showing the aberrant splicing products induced by the morpholinos, as detected by RT-PCRs (right). (b) The gels show the morphants' aberrant transcripts with the inclusion of Intron 2 (+97 bp) and (c) chromatograms of PCR product (bottom) demonstrate that the e2i2 sb MO induces inclusion of intron. (d) Representative images of the normal, mild, and severe phenotypes observed in control and MO-DEGS1 injected groups. (e) Quantification at 5 dpf of the percentage of normal (black bar), mild (gray bar), and severe (hatched bar) phenotype groups obtained. Values are mean \pm SD of three independent experiments with n = 30 to 50 animals per group. (f) Cer (Saturated ceramides (C7:0 to C28:0)), DhCer (Saturated dihydroceramides (C7:0 to C28:0)), UNSAT-Cer (Monounsaturated ceramides (C7:1 to C28:1)), UNSAT-DhCer (Monounsaturated dihydroceramides (C7:1 to C28:1)) levels, the ratios of DhCer/Cer and UNSAT-DhCer/UNSAT-Cer in zebrafish MO-control and MO-DEGS1 n=3 (5 larvae per tube/condition) at 5 dpf. Data are shown as mean \pm SD * p<0.05; ** p<0.01; *** p<0.001 after Student t test.

4.3.3 Loss of *degs1* in Zebrafish Causes Locomotor Impairment and Reduced Number of Mature oligodendrocytes

Thus, to determine if functional changes were associated with behavioral deficits in MO-DEGS1 zebrafish larvae, locomotor activity was analyzed by measuring the total movement distance. There were three groups in the trial: i) uninjected, ii) MO-control, iii) MO-DEGS1. We performed the locomotor assay in larvae at 5dpf, and we found that the total movement distance (mm) of MO-DEGS1 was significantly reduced compared with uninjected and MO-control larvae (uninjected larvae: 1564.43 ± 321.65 , MO-control: 1146.62 ± 255.19 , vs. MO-DEGS1: 28.27 ± 24.55) (**Fig. 28a-b**). In all cases, average of $n = 20-30$ larvae/condition were used. To test the effect of suppression of endogenous DEGS1 in zebrafish on myelination, we measured the number of oligodendrocytes in the dorsal spinal cord at 4.5 dpf using the transgenic line *tg(mbp:EGFP)*. Myelination was strongly impaired after the *degs1* knockdown, as revealed by immunodetection of Mbp at the trunk levels of 4.5 dpf. In morphants (**Fig. 28c-d**), a very faint signal was detected. A lower Mbp signal was found by comparison to controls around the spinal cord. Interestingly, we found that the number of oligodendrocytes was reduced by 30% in MO-DEGS1 compared to control larvae (**Fig. 28e**). Altogether, these results indicate that *degs1*-deficient exhibited locomotor deficits and weak myelination.

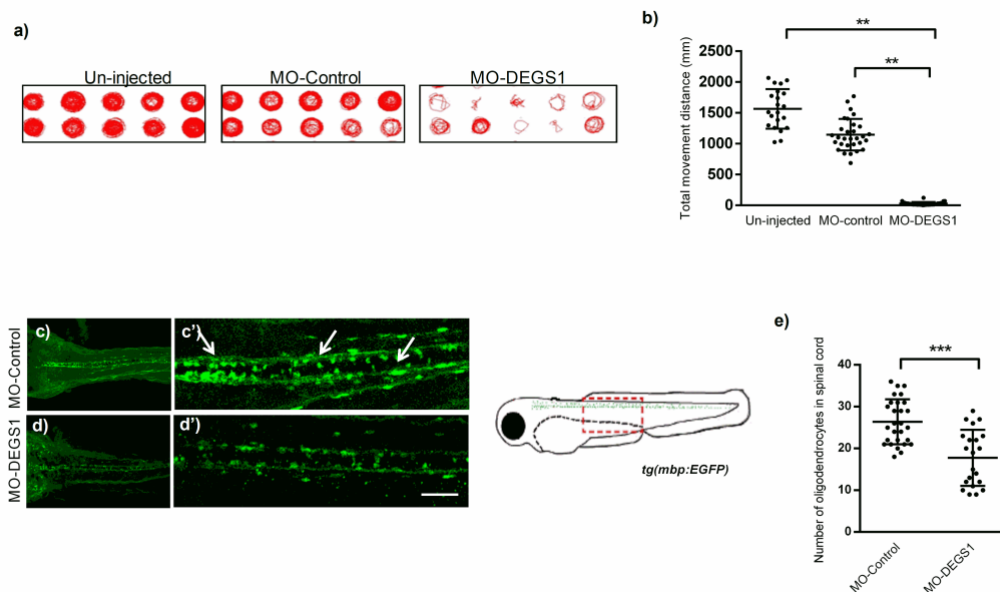


Figure 28. Locomotor impairment and reduced oligodendrocytes following *degs1* knockdown during zebrafish development

(a) Digital tracks of 10 single larvae of each condition shown in red. (b) Scatter plot displaying the total movement distance⁺⁺ (mm) carried by different larvae. Behavior test was carried out using Ethovision XT software (Noldus Information Technology, Wageningen, Netherlands). (c-d) Dorsal view of larvae injected with control and MO-DEGS1 (left), zoomed views of boxed areas are shown (right) at 4.5 dpf. White arrows indicate oligodendrocytes. Illustration of the *tg(mbp:EGFP)* larvae. Distribution of oligodendrocyte is marked with green spots. Dashed box represents the imaged area in the spinal cord. (e) Scatter plot showing the number of oligodendrocytes counted in the dorsal SC of 4.5 dpf larvae⁺ (MO control: n=30, MO-DEGS1: n=28). Data are shown as mean \pm SD * p<0.05; ** p<0.01; *** p<0.001 after one way ANOVA⁺⁺ or Student t test⁺.

4.3.5 FTY720 Ameliorates Locomotor Deficits in MO-DEGS1 larvae

In an attempt to provide a therapeutic option for our cohort, we chose an FDA-approved drug targeting the *de novo* ceramide biosynthesis pathway. FTY720 is an inhibitor of ceramide synthase, the enzyme that synthesizes DhCer from dihydrosphingosine. We treated *degs1*-deficient zebrafish larvae in an attempt to compensate for the effects of *degs1* knockdown. We used concentrations of 3.3, 1, 0.3 ng/ μ l, from birth to 120 hpf, when locomotor tests ensued after verifying no deleterious effects of FTY720 on survival. Results indicate that the locomotor deficit was remarkably ameliorated after treatment in all parameters; total movement distance (mm) traveled by MO control (veh, 1268.18 \pm 402.9), (FTY720, 1230 \pm 365.20); MO-DEGS1 (veh 44.60 \pm 39.2) (FTY720 3.3ng/ μ l, 542.35 \pm 238.77, FTY720 1ng/ μ l, 615.26 \pm 330.80, FTY720 0.3ng/ μ l, 670.32 \pm 476.63) larvae (**Fig. 29a-b**). All measures were averaged across larvae within each condition (n = 20 larvae/condition) and reported as population means \pm SD. These results indicate that FTY720 improved the locomotor deficits in MO-DEGS1 larvae.

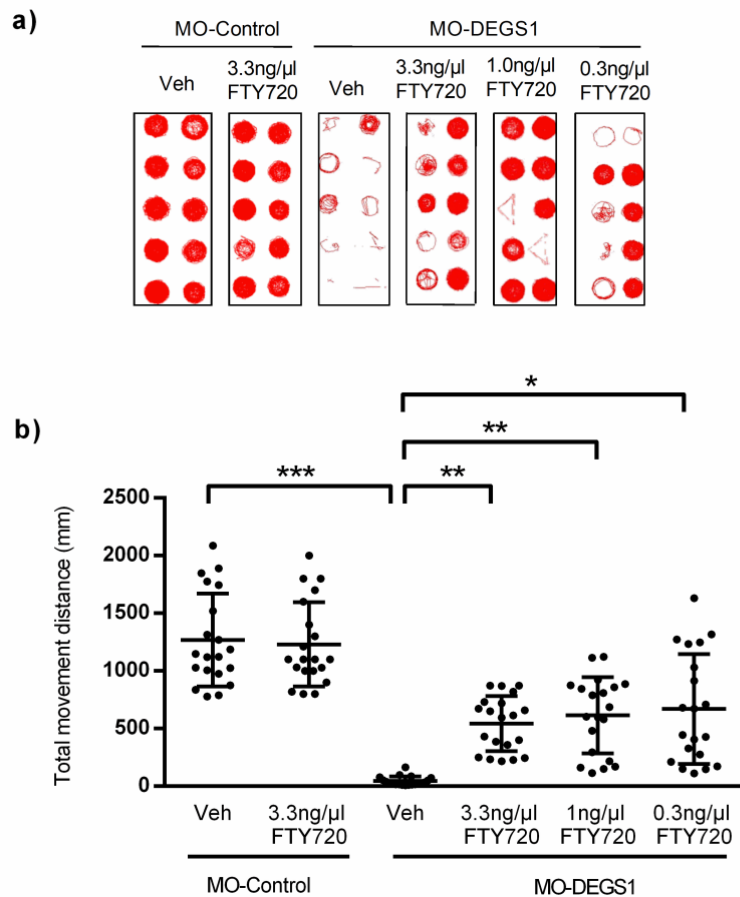


Figure 29. FTY720 prevents locomotor deficits caused due to loss of *degs1* in zebrafish larvae

MO-DEGS1 larvae were treated for 120 h with fingolimod (FTY720) at 0.3, 1 and 3.3 ng/ μ l. **(a)** Digital tracks of larvae shown in red. **(b)** Total movement distance (mm) upon FTY720 treatment in MO-control and MO-DEGS1 larvae represented by scatter plot. Results are from three independent experiments. Data are shown as mean \pm SD * $p < 0.05$; ** $p < 0.01$; *** $p < 0.001$ after two-way ANOVA test followed by Tukey's posthoc test.

4.3.6 FTY720 Prevents the Imbalance of Dihydroceramide and Ceramide Imbalance in *degs1* Knockdown Zebrafish Larvae

Previously, we have shown that suppression of endogenous DEGS1 in zebrafish larvae causes an imbalance in DhCer/Cer levels. Therefore, we wanted to study the effect of FTY720 in sphingolipids imbalances and we treated the larvae injected with control MO and MO-DEGS1 at a moderate dose (1.0 ng/ μ l) until 5 days. Lipidomics analysis showed that both increased saturated and unsaturated DhCer levels in MO-DEGS1 were reduced after FTY720 treatment whereas saturated Cer levels were found to be normalized to control levels. FTY720 treatment appears to have reduced the levels of dihydroceramide

species of saturated (C20 - C26) or unsaturated (C24, C26) (**Table 13**). Moreover, the ratios of these sphingolipids were partially corrected after FTY720 treatment in MO-DEGS1 larvae. There was no effect of FTY720 in control MO larvae (**Fig. 30; Table 13**). Thus, FTY720 partially rescue the DhCer/Cer imbalance in *degs1* knockdown zebrafish larvae. Taken together, these data suggest FTY720 has a protective effect in the present model.

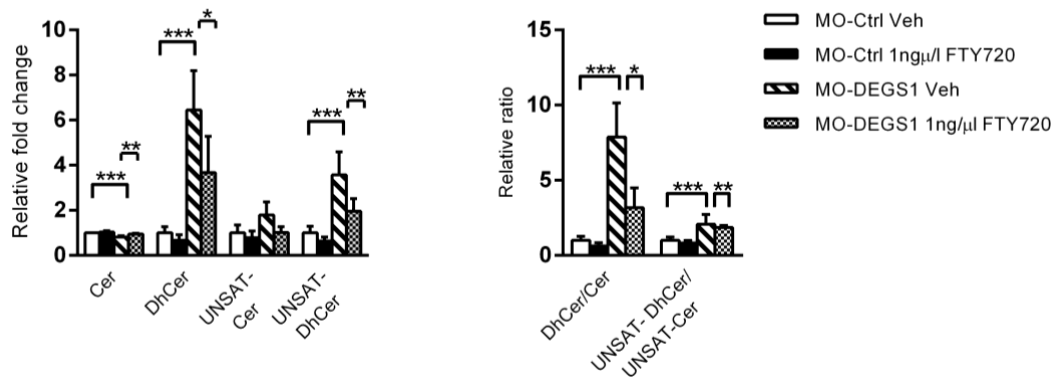


Figure 30. Fingolimod lowers DhCer, Cer levels and DhCer/Cer ratio in *degs1* knockdown zebrafish larvae

Cer (Saturated ceramides (C7:0 to C28:0)), DhCer (Saturated dihydroceramides (C7:0 to C28:0)), UNSAT-Cer (Monounsaturated ceramides (C7:1 to C28:1)), UNSAT-DhCer (Monounsaturated dihydroceramides (C7:1 to C28:1)) levels, the ratios DhCer/Cer and UNSAT-DhCer/UNSAT-Cer in zebrafish MO-control and MO-control and MO-DEGS1 treated with 1 ng/μl of FTY720 n=4 (5 larvae per tube/condition) larvae at 5dpf⁺⁺. Results are from three independent experiments. Data are shown as mean ± SD * p<0.05; ** p<0.01; *** p<0.001 after two-way ANOVA test followed by Tukey's posthoc test.

Table 13. Lipid profiling of ceramide (Cer) and dihydroceramide (DhCer) species in MO-Control and MO-DEGS1 zebrafish larvae at 5dpf after FTY720 (1 ng/ul) treatment.

Species	MO-Control				MO-DEGS1			
	Veh		FTY720		Veh		FTY720	
C7:0-Cer	0.083	± 0.03	0.09	± 0.017	0.029	± 0.005*	0.088	± 0.009 ^{b**}
C10:0-Cer	35.929	± 12.5	44.244	± 10.89	3.560	± 2.954 ^{***}	28.761	± 12.199*
C11:0-Cer	0.051	± 0.02	0.017	± 0.007	0.023	± 0.014*	0.009	± 0.004
C12:0-Cer	13.817	± 5.52	3.601	± 5.101	15.866	± 1.003*	11.482	± 4.358
C15:0-Cer	0.086	± 0.068	0.069	± 0.051	0.092	± 0.052 ^{a**}	0.075	± 0.025
C16:0-Cer	11.701	± 2.232	10.125	± 3.644	25.188	± 4.494	21.774	± 2.883
C17:0-Cer	0.229	± 0.122	0.173	± 0.069	0.317	± 0.201	0.212	± 0.064
C18:0-Cer	4.339	± 2.000	3.512	± 0.879	2.315	± 1.232	4.402	± 1.004
C20:0-Cer	1.896	± 0.601	1.826	± 0.800	2.192	± 1.158	2.276	± 0.513
C22:0-Cer	2.430	± 0.427	2.228	± 0.836	4.176	± 2.133 ^{a**}	2.817	± 0.731 ^{b**}
C23:0-Cer	0.773	± 0.160	0.507	± 0.201	1.599	± 0.866 ^{a***}	0.678	± 0.130 ^{b***}
C24:0-Cer	3.554	± 0.658	2.529	± 0.880	8.256	± 1.500 ^{a***}	3.202	± 0.798 ^{b***}
C15:0-DhCer	0.050	± 0.028	0.035	± 0.023	0.072	± 0.034	0.084	± 0.061
C16:0-DhCer	1.316	± 0.311	0.947	± 0.485	10.174	± 2.685 ^{a**}	6.706	± 2.052
C17:0-DhCer	0.036	± 0.013	0.020	± 0.013	0.101	± 0.075 ^{a*}	0.080	± 0.037
C18:0-DhCer	0.110	± 0.109	0.107	± 0.043	0.672	± 0.269 ^{a***}	0.746	± 0.267
C20:0-DhCer	0.100	± 0.035	0.058	± 0.032	1.012	± 0.543 ^{a***}	0.491	± 0.227 ^{b**}
C22:0-DhCer	0.161	± 0.036	0.081	± 0.018	1.483	± 0.733 ^{a***}	0.733	± 0.297 ^{b***}
C23:0-DhCer	0.034	± 0.011	0.025	± 0.013	0.223	± 0.120 ^{a***}	0.109	± 0.033 ^{b***}
C24:0-DhCer	0.217	± 0.062	0.125	± 0.016	1.246	± 0.653 ^{a***}	0.577	± 0.195 ^{b***}
C16:1-Cer	0.057	± 0.053	0.033	± 0.015	0.048	± 0.020	0.035	± 0.015
C18:1-Cer	0.037	± 0.035	0.021	± 0.014	0.051	± 0.012	0.024	± 0.012
C22:1-Cer	0.249	± 0.180	0.205	± 0.130	0.343	± 0.161	0.280	± 0.078
C24:1-Cer	3.295	± 1.184	2.686	± 1.200	5.821	± 2.181	3.505	± 0.848
C26:1-Cer	0.543	± 0.057	0.451	± 0.166	1.309	± 0.680	0.554	± 0.127
C16:1-DhCer	0.075	± 0.054	0.079	± 0.064	0.122	± 0.068	0.111	± 0.035
C18:1-DhCer	0.012	± 0.002	0.017	± 0.005	0.026	± 0.014	0.037	± 0.022
C22:1-DhCer	0.040	± 0.023	0.016	± 0.007	0.122	± 0.062	0.058	± 0.027
C24:1-DhCer	0.082	± 0.019	0.055	± 0.016	0.819	± 0.269 ^{a***}	0.485	± 0.189 ^{b***}
C26:1-DhCer	0.027	± 0.023	0.008	± 0.004	0.179	± 0.073 ^{a***}	0.087	± 0.040 ^{b***}

Values are mean ± SD (% of total lipids analysed; n = 4) * p<0.05; ** p<0.01; *** p<0.001 after two-way ANOVA test followed by Tukey's posthoc test. a, indicates significant change in MO-DEGS1 from MO-control; b, indicates significant change in MO-DEGS1 after FTY720 treatment.

4.3.7 Knockdown of *degs1* Mediated Loss of Oligodendrocytes is Normalised by FTY720

In search of protective effects to MO-DEGS1 larvae by FTY720 treatment, we evaluated the efficacy of FTY720 on reduced number of mature oligodendrocytes in MO-DEGS1

larvae. To quantify the cell number, adult *tg(mbp:EGFP)* zebrafish line was in-crossed and MO-control and MO-DEGS1 were microinjected (as described previously) into the cell of one-cell stage embryo. FTY720 treatment (1ng/μl) was given to MO-control and MO-DEGS1 larvae after microinjection of respective MOs. We counted the number of mature oligodendrocytes in the dorsal spinal cord of MO-control, MO-DEGS1, MO-DEGS1 + FTY720 larvae. Image analysis showed that the number of EGFP-positive signals was normalized in MO-DEGS1 and was similar to the number of mature oligodendrocytes along the spinal cord in MO-control larvae at 4.5 dpf (**Fig. 31a-c**). This amelioration correlated with a correction of saturated and unsaturated N-Cer (2H) levels determined as previously, upon treatment during 5 days with FTY720 at 1.0 ng/μl (**Fig. 30**). Taken together, therefore, these results demonstrate that FTY720 reverses the MO-DEGS1 induced reduced number of oligodendrocytes in dorsal spinal cord.

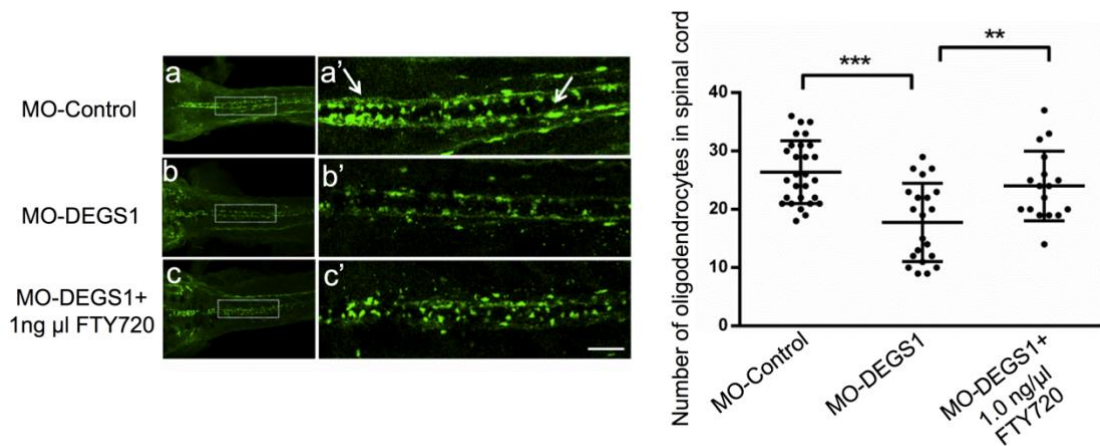


Figure 31. FTY720 protective effects on reduced number of mature oligodendrocytes in *degs1* knockdown zebrafish.

(a-c) Dorsal views of larvae injected with control and MO-DEGS1 and inserts of boxed areas at 4.5 dpf. White arrows indicate oligodendrocytes. Scatter plot displaying the number of oligodendrocytes in the dorsal spinal cord of 4.5 dpf larvae (MO control: n=30, MO-DEGS1: n=28, MO-DEGS1+ 1ng/μl FTY720: n=19). Data are shown as mean ± SD * p<0.05; ** p<0.01; *** p<0.001 after one-way ANOVA test followed by Tukey's posthoc test.

DISCUSSION

5 DISCUSSION

Many recent studies have demonstrated the use of NGS in the identification of candidate genes in small families and even in single individuals (Chelban et al., 2017; Cheng et al., 2018). In the last years, rare and ultra rare diseases have attracted worldwide more and more attention. However, there is no universal definition of a rare disease: In Japan the term “orphan disease” describes a condition with a prevalence of 2.5 cases per 10,000 population; in the US 7 cases per 10,000 population. In Europe, an orphan disease is defined as a disorder that affects 5 or less per 10,000 populations (Beck, 2012; Gahl et al., 2012; Irvine & Irvine, 2013; Richter et al., 2015). There are many different causes of rare diseases and are thought to be genetic, directly caused by changes in genes or chromosomes. In some cases, genetic changes that cause disease are passed from one generation to the next. In other cases, they occur randomly in a person who is the first in a family to be diagnosed. Studies of rare genetic disorders are not just important for the families involved, but also provide important new information about function and dysfunction of genes and associated proteins, especially when the gene is novel and has not been explored. Discovery of these novel genes is necessary to gain information on how these particular genetic variants lead to disease. One of the major challenges within the next decade in human genetics lies in understanding and model the impact of the novel variants identified in a particular gene. A prior requirement in this process is to gather and share accurate extensive clinical information for the patient. It is currently one of the major obstacles the community is facing with the development of large public databases overflowing with variants detected by high-throughput sequencing studies. This could preclude accurate interpretation of the impact of the particular variant on an individual’s phenotype. Assuming we overcome these challenges leading to a comprehensive understanding of genetic variants and their implications in disease. Some common global initiatives like Rare Disease Day is a great example of how progress continues to be made, with events being held worldwide each year to increase awareness (<https://www.rarediseaseday.org>), the International Network for Undiagnosed Diseases (UDNI) was established in 2014 across several countries to address rare and undiagnosed diseases (<http://www.udninternational.org>). The Centre for Biomedical Network Research on Rare Diseases (CIBERER) was created in 2006 in order to act as a reference, coordinate and foster research on rare diseases in Spain. The National Institutes of Health

(NIH) supports research to improve the health of people with rare diseases. Many of centers at the NIH fund medical research for rare diseases. One of these centers, the National Center for Advancing Translational Sciences (NCATS), focuses on getting new cures and treatments to all patients more quickly. NIH coordinate wide activities involving research for rare diseases. Some of these programs for rare diseases include: Undiagnosed Diseases Network (UDN), Rare Diseases Clinical Research Network (RDCRN); Therapeutics for Rare and Neglected Diseases (TRND); Rare Diseases Registry Program (RaDaR); Genetic and Rare Diseases Information Center (GARD). One of the best ways in which societies can be benefited from these is preconception screening. We believe in the near future stringent methods will be developed which will increase our knowledge and understanding of the impact of each genetic variants.

In this thesis, we identified one variant in *DEGS1* and data aggregation of WES from multiple laboratories allowed 11 more variants in *DEGS1* with anomalies in cohorts of undetermined leukodystrophy. This study links for the first-time loss of function of the dihydroceramide desaturase gene *DEGS1*, also called membrane lipid desaturase, to a novel, distinct hypomyelinating leukodystrophy. Shared features among the patients are delayed myelination, thin splenium of corpus callosum, and hyperintensities of thalamic regions. Patients present with early childhood developmental delay, intellectual disability, spasticity, speech abnormalities and early death in most severe cases.

5.1 Expression of DEGS1 in CNS

Gene expression studies of the CNS are particularly challenging due to the extreme cellular heterogeneity. There are probably over 7,000 statistically distinct cell types with unique mRNA and protein expression profiles in the brain (Pandey & Williams, 2014). The identification of variants in *DEGS1* in affected individuals with hypomyelination, cerebellar atrophy suggests that this gene could play a vital role in CNS. Further, the identification of variants in siblings with hypomyelination strengthen the importance of this gene in the cause of the neurological disorder. We postulate that the DEGS1 protein is important in the normal development of the brain, and especially the cerebellum since the affected individuals have cerebellar defects.

Here, we first analyzed the expression of endogenous DEGS1 level in various mice tissues at mRNA level. We limited the expression studies by qPCR due to the non-

specificity of the available commercial antibodies tested. The expression of this gene in different tissue of a 4 months old wild-type mice was carried out and the results indicate the expression was highest in CNS tissues and among the CNS tissues spinal cord has the highest expression of this gene (**Fig. 16a**). To correlate these findings, we also checked the expression of *DEGS1* in different CNS tissues of control human adult and child. We observed that among the human CNS tissues this gene was highly expressed in white matter frontal cortex and spinal cord in both child and adult (**Fig. 16b**). The data from mice and human provides the importance of *DEGS1* in the brain and spinal cord and these results were in correlation with different human (GTEx portal) and mice (Allen brain atlas) gene expression databases.

Moreover, the functional importance of *DEGS1* over other desaturase enzymes i.e. *DEGS2* in CNS can be highlighted by the high expression of mouse *Degs1* mRNA levels in different parts of mice CNS. By contrast, mouse *Degs2* mRNA expression showed tissue specificity and was found to be abundant in small-intestinal epithelial cells, intermediate in the small intestine and kidney, and quite sparse in testis, brain, liver, uterus, heart, and lung (Omae et al., 2004). These results were in agreement with our findings showing that human and mouse *Degs1* mRNA levels were found to be higher when compared with *Degs2* in different human and mice CNS tissues (**Fig. 16a**).

5.2 Dihydroceramides/Ceramides as Regulators of Lipid Homeostasis

Most of the insights governing the role of sphingolipids mainly DhCer and ceramide species on global lipid homeostasis comes from pioneering work by Merrill group using pharmacological inhibitor i.e. fenretinide, an inhibitor of *DEGS1* the last enzyme of the *de novo* ceramide synthesis pathway (Zheng et al., 2006) showed imbalances in DhCer and ceramide levels characterized by increase DhCer and low ceramide levels. Similar observations associated to severe alterations at different levels such as transcription, cell migration, cytoskeleton modification, cellular response to insulin, lipid profiling and impaired endomembrane trafficking were seen by using siRNA against *deg1* in a model of human hepatocarcinoma cells (Huh7) to unravel the role of *DEGS1* in global cellular energetics (Ruangsiriluk et al., 2012). The action of ceramide, DhCer in cholesterol metabolism comes from multiple studies showing that short chain analogues of ceramide, DhCer can inhibit the acyl-CoA: cholesterol acyltransferase (ACAT) and stimulates

ABCA1-mediated cholesterol efflux to apolipoprotein A1 in Chinese hamster ovary (CHO) cells (Ghering & Davidson, 2006; Lagace, Byers, Cook, & Ridgway, 1999). An elegant study was performed by Scott Summers group in 2007 by generating a knockout *Degs1*^{-/-} mice model, showing an imbalance in the levels of DhCer and ceramide due to impaired Degs1 activity. The *Degs1*^{-/-} mice displayed an incomplete penetrant lethality, complex phenotype, tremors and animals ultimately failed to thrive, died within 8 to 10 weeks of birth (Holland et al., 2007). Recently, the group of Chan did a knockout of *degsl* orthologue *ifc* in *Drosophila* using CRISPR which have provided further support and results in larvae lethality, increased levels of DhCer and low levels of ceramide (Jung et al., 2017). Altogether these data support that DhCers are not inert lipids, and that similarly to ceramides might play an active role in the regulation of global lipid homeostasis by diverse mechanisms. Nevertheless, an unsolved question in the field is whether those effects are directly mediated by the accumulation of DhCer, or the decreased levels of ceramide, or both.

To validate the impact of the rare *DEGS1* variants at the functional level, we took advantage of resources: biopsy tissue, primary fibroblast from affected individuals. Here, we demonstrated that patient-derived fibroblasts and muscle tissue exhibited high DhCer and low ceramide levels, indicating impaired DEGS1 activity in these affected individuals. These results were in agreement with biochemical abnormalities detected in the derived *degsl*^{-/-} mice embryonic fibroblasts (MEFs) were more pronounced than the ones we obtained in three patient's fibroblasts, with over hundred-fold increase in the ratio DhCer/Cer (Rodriguez-Cuenca et al., 2015; Monowarul Mobin Siddique et al., 2015), which may suggest that the function of DEGS1 in the fibroblastic lines is not completely abolished. Of note, the mutations found in these fibroblasts lines are missense in one of the alleles at least. These data argue against a loss of function and for an adverse effect on protein stability of the identified *DEGS1* variants.

In terms of clinical and biochemical phenotype, affected individuals in our study exhibited consistent findings without any additional biochemical or clinical hallmarks. It is unclear why the loss of DEGS1 activity causes only a neurological phenotype in the cohort. The specific neurological manifestations of DEGS1-deficient individuals might be attributed to high levels of DEGS1 in the brain. Importantly, there are examples of proteins that are expressed in multiple tissues but where a gain or loss of function

mutation causes a phenotype only in a subset of organs in which the gene is expressed. Mutations in the *SMN1* gene cause spinal muscular atrophy (Monani, 2005). Although the protein is ubiquitously expressed and mutations in the gene cause motor neuron loss and skeletal muscle atrophy specifically in motor neurons (A. J.-H. Lee, Awano, Park, & Monani, 2012). Differences in the impact of genetic mutations in specific tissues can be due to increased sensitivity of particular organs to changes in protein expression or due to tissue-specific interacting proteins or regulators. Further assessment of the function of DhCer/Cer lipid homeostasis in neuronal cells is necessary in order to understand the requirements of DEGS1 in neuronal and non-neuronal tissues.

5.3 Role of DhCer and Oxidative Stress

Oxidative stress refers to the imbalance of enhanced production of ROS or impaired function of the antioxidant system. ROS include superoxide anions ($O_2^{\cdot-}$), hydroxyl radicals, and hydrogen peroxide (H_2O_2). The generation of ROS usually starts with the production of $O_2^{\cdot-}$, which rapidly dismutates into H_2O_2 at low pH or *via* catalysis by superoxide dismutase (SOD). H_2O_2 can be further converted into highly reactive hydroxyl radicals *via* iron-catalyzed Fenton reactions under pathological conditions. $O_2^{\cdot-}$, also rapidly reacts with nitric oxide (NO) to form a more stable free radical, peroxynitrite ($OONO^{\cdot-}$), which is a potent cytotoxic oxidant ROS including oxygen ions and peroxides are chemically reactive intermediates produced by the normal aerobic metabolism of oxygen. The role of ceramide in ROS signaling has been extensively reviewed by two different groups (Dumitru, Zhang, Li, & Gulbins, 2007; Won & Singh, 2006). The importance of ceramide in ROS generation has been elucidated by several research groups mainly using cancer cell lines by using different ceramide analogs. The studies were carried out using the human neuroblastoma cell line (SH-SY5Y) and demonstrated that C2-ceramide induced production of ROS in a concentration-dependent manner (Czubowicz & Strosznajder, 2014). Ceramide effects on the respiratory chain were demonstrated by direct addition of short-chain ceramide on isolated mitochondria (Degli Esposti & McLennan, 1998; Guduz, Tserng, & Hoppel, 1997). Disorders of ceramide metabolism can lead to pathogenesis of various neurological disorders such as Alzheimer's disease (Cutler et al., 2004), Parkinson's disease (Xing et al., 2016), Schizophrenia (Prabakaran et al., 2004; E. Schwarz et al., 2008) and Depression (Gracia-Garcia et al., 2011). However, these studies lack the information on the precursors of ceramide i.e. DhCer.

The causative link between DhCer and ROS production has been less studied. The effect of C2-DhCer on the production of H₂O₂ was first demonstrated using mitochondria suspension isolated from rat liver (García-Ruiz, Colell, Marí, Morales, & Fernández-Checa, 1997). In 2011, the group of Hannun showed that DhCer production is also a consequence of ROS generation, as the oxidative stressors (H₂O₂, *tert*-butylhydroperoxide, and menadione) increases DhCer levels in HEK293 (human embryonic kidney) and SMS-KCNR (human neuroblastoma) cell lines (Idkowiak-Baldys et al., 2010). In contrast, Apraiz *et al* demonstrated in a leukemia cell model by using Fenretinide, *DEGS1* inhibitor, resulting in DhCer accumulation which is independent of the increased in cellular ROS (Apraiz et al., 2012). Tserng and Griffin reported DhCer (C16:0) accumulation prior to cell death in human leukemia cells (Tserng & Griffin, 2004). The role of DhCer accumulation on oxidative stress was reviewed by Scott Summers group where they mentioned an unpublished observation that knockdown of *Degs1* increases ROS several-fold (Monowarul Mobin Siddique et al., 2015). Similarly, in *Drosophila* model, constant light stimulation increased the levels of ROS in *ifc*-KO photoreceptors as measured by H₂DCFDA probe, and the expression of ROS responsive genes cap'n'collar (*cnc*) and glutathione S-transferase D1 (*gstD1*) was found to be upregulated in *ifc*-KO larvae (Jung et al., 2017).

In our study, we found an accumulation of DhCer associated with increased ROS generation in all three patient fibroblast cultures showing an interaction between ROS and DhCer. These results were consistent with previous reports showing that ROS production is increased when *DEGS1* is absent or pharmacologically inhibited (Rodriguez-Cuenca et al., 2015; Monowarul Mobin Siddique et al., 2015), although the precise mechanism of DhCer on ROS production remains unclear. To find a mechanistic link between ROS and DhCer, we selected a long chain DhCer (C18:0) and challenge the control and patient's fibroblasts cultures. We found that exogenous DhCer was able to generate ROS in control fibroblasts. Nevertheless, the ROS levels in patients' fibroblasts did not increase, perhaps due to a blunted effect and the high levels of this metabolite in these cells. Of note, we found no clear correlation between the amount of ROS and the levels of DhCer, ceramide or the DhCer/Cer ratios in the patient's fibroblasts. Furthermore, the mRNA levels of *DEGS1* in patient 4, 7 was associated with biochemical imbalance which was not in the case of patient 9 (**Fig. 17**).

As mitochondria constitute the main source of ROS under many neuropathological conditions (Fernandez-Checa et al., 2010). We sought to investigate whether mitochondria from these patients' fibroblasts represent the main source of ROS. We used two different fluorescent probes DHE (dihydroethidium) and MitoSOX (DHE covalently bonded to hexyl triphenylphosphonium cation), which measure intracellular and intramitochondrial superoxide levels, respectively. We observed that the levels of superoxide ($O_2^{\cdot-}$) measured by either DHE or MitoSOX were similar in patient 4, which indicates mitochondria as the major source of ROS. No changes were seen in patient 7 and a significant decrease was found in the case of patient 9. However, no correlation between the total free radicals and total superoxide production in Patient 7, 9 were found indicating the presence of other sources of ROS productions such as NADPH oxidases. Previous studies have reported Des1 knockout cells (MEF) shown to have higher mitochondrial membrane potential (M. M. Siddique et al., 2013). These results were in contrast to our findings, as a significant decrease in $\Delta\Psi_m$ in fibroblasts from patient 9 but not in patient 4,7 were found (**Fig. 21**). Mitochondrial quality control is essential for cells to maintain mitochondrial integrity and normal function. Even under basal conditions, continuous cycles of mitochondrial fusion and fission and of biogenesis and degradation serve to produce daughter mitochondria and remove dysfunctional mitochondria. Mitochondrial dynamics is believed to play a key role in neurodegenerative diseases and the aging process itself. In most mammalian cells, mitochondria are tubular in shape under normal conditions but may attain various forms during various cellular perturbations. During apoptosis mitochondria are extensively fragmented and form small punctuate or round structures, while during necrosis mitochondria usually swell and become distended. During autophagy, mitochondria become elongated and are spared from degradation. Besides being tubular, swollen or elongated, mitochondria have also been shown to be 'donut' shaped, which is a recently discovered form of mitochondria with biochemical and pathophysiological significance. This diversification in shape of mitochondria makes this organelle a highly versatile in its function for maintaining cell survival and tissue homeostasis (Bertholet et al., 2016; Lionaki, Markaki, Palikaras, & Tavernarakis, 2015). In the current study, we thus evaluated the mitochondrial network in affected individual's fibroblasts. We found mitochondrial network to be disrupted in patient 9, results in formation of 'donut' shaped mitochondria (**Fig. 22**). Moreover, clinical mitochondria

studies for patient 9 exploring the mitochondrial respiratory chain have also highlighted that there was low global mitochondrial activity in muscle, complex I deficiency in fibroblast, and complex III deficiency in lymphocytes (data not shown) which suggests that impaired mitochondria drove pathogenesis in this patient. Results concerning mitochondria membrane potential are inconclusive so far and needs to be further validated in fibroblasts from other probands. Current results require further research into DhCer metabolism as potential new targets for the prevention or treatment of neurological disorders. In conclusion, many of the relationships between oxidative stress and DhCer signaling remain obscure, and research efforts are needed to fill this gap.

5.4 DhCer Accumulation and Autophagy Impairment

Autophagy is an evolutionary conserved cellular catabolic mechanism involving the lysosomal degradation and recycling of proteins and organelles. Under physiological conditions, cells undergo autophagy to eliminate aberrant, damaged biomolecules or structures to maintain tissue homeostasis (Mizushima, Levine, Cuervo, & Klionsky, 2008). Problems in the execution of autophagy are linked to different pathological conditions, such as neurodegeneration, aging, and cancer (Papáčková & Cahová, 2014) also in one of the most common leukodystrophy – XALD (Launay et al., 2015).

The role of sphingolipids in autophagy is reviewed in detail by several groups (Tommasino, Marconi, Ciarlo, Matarrese, & Malorni, 2015). Moreover, *degs1^{-/-}* MEF exhibited an elevated level of basal autophagy that was potentiated by serum withdrawal. Similarly, lack of *ifc* in *Drosophila* larvae photoreceptors results in lipid droplets accumulation which further leads to lipophagy activation, a specialized form of autophagy for the degradation of lipid droplets. The role of DhCer in autophagy arises from studies with pharmacological tools mainly DEGS1 inhibitors indicating a role for DhCer in the induction of autophagy. Intracellular accumulation of DhCer was shown to mediate autophagy and survival in HGC-27 cells (Signorelli et al., 2009). Similar observations were also seen in HEK293 cell lines upon treatment with fenretinide (Zheng et al., 2006). Recently, the group of Gemma Fabrias showed that induction of autophagy can occur by DhCer independent and dependent mechanism by using T98G and U87MG glioblastoma cell lines and different DEGS1 inhibitors (CCX, celecoxib; PXD, phenoxodiol; RV, resveratrol; γ TE, γ -tocotrienol, and XM462) at sub-lethal dosages and showed that autophagy induction occurs with DhCer accumulation. However, autophagy

was also induced in the absence of DhCer accumulation (Casasampere, Ordoñez, Pou, & Casas, 2016). This method negates concerns related to nonspecific pharmacological effects or incomplete inhibition of the enzyme.

Herein, we tested the role of DEGS1 in autophagy in patients' derived fibroblasts. We didn't observe any change in autophagy at basal level in these patient's fibroblasts. Moreover, using protease inhibitor (BaF A1), autophagy flux was stimulated in patient 9, impaired in patient 4 and no change in patient 7, as determined by a number of different molecular readouts (i.e., detection of the active form of LC3). No clear correlation was deduced between the accumulation of DhCer and autophagy flux. Therefore, more mechanistic studies need to be performed in these fibroblasts and also using other probands. DEGS1 may interact with other proteins, these interactions need to be further validated.

5.5 Knockdown Of *degs1* in Zebrafish Larvae Reproduces Patient's Main Phenotypes

The strategy to determine the functional importance of a gene in an organism is to decrease or abolish expression of the gene and to study the effects of reduction or loss of the gene product. Zebrafish have recently been used to successfully study variants in a human gene as listed (**Table 4**) First, we wanted to study the expression of *degs1* in zebrafish by ISH and we found the expression of *degs1* to be predominant in CNS at larval stages. Since the zebrafish genome shows conservation of many of the genetic pathways for myelin development and maintenance (Czopka, 2016). Combining ISH and IF studies further revealed the expression of *degs1* in mature oligodendrocytes (**Fig. 26**). This was an interesting finding as it provides an insight into the involvement of this gene in the formation of oligodendrocytes.

To find a rapid *in vivo* phenotypic readout, we wanted to model the findings of our cohorts in zebrafish larvae through endogenous DEGS1 ablation, followed by relevant phenotyping. In our study, knockdown of *degs1* using a splice blocker MO in zebrafish causes inclusion of intron 2 leads to nonsense-mediated decay of the RNA transcript, which is demonstrated by knockdown on RT-PCR (**Fig. 27a-c**). Loss of function of *degs1* in zebrafish can be seen from DhCer and ceramide imbalances and abnormal motor

behavior. Employing our zebrafish model, we could show that suppression of endogenous DEGS1 in zebrafish larvae recapitulates the high DhCer and low ceramide levels as shown in mice (*degs1^{-/-}*) and *Drosophila* (*ifc*) knockout models. Additionally, examination of the hindbrain, and specifically mature oligodendrocytes using *tg[mbp:EGFP]* line revealed reduced staining with GFP antibody at 4.5 dpf, suggesting that the knockdown of *degs1* causes weak myelination in the zebrafish larvae. Indeed, the zebrafish MO-DEGS1 model recapitulates key elements of affected individuals. In addition to observed findings in mice and *Drosophila*, our data further suggest conservation of *degs1* that play a functional role in fish, human and mice, in spite of different morphology and primary cellular functions. The stringent *in vivo* conditions that allow *degs1* dysfunction in fish larvae underline the importance of zebrafish as a model organism to decipher pathogenic mechanisms underlying these complex human rare disorders.

5.6 FTY720: A Potential Therapeutic Target Against Neurological Disorders

The neuroprotective effect of FTY720 is classically seen in case of MS disease despite FTY720 having been tested in a number of other diseases in which autoimmune mechanisms play important role, the pathology of MS is generally believed to be the activation of autoimmune lymphocytes in the periphery. These cells proliferate and mature within lymphoid tissues and then egress into the blood, cross the BBB entering the CNS, where their auto aggressive nature produces inflammation, demyelination, axonal damage, gliosis and, ultimately, neurodegeneration (Compston & Coles, 2008; Frohman, Racke, & Raine, 2006). A key action of FTY720 is the inhibition of lymphocyte egress from the thymus and lymph nodes, thereby sequestering them in these tissues and reducing their numbers in peripheral blood and the CNS (Chun & Hartung, 2010; Mehling, Johnson, Antel, Kappos, & Bar-Or, 2011). This alters both the numbers and relative distribution of various lymphocyte subtypes in blood and cerebrospinal fluid (CSF).

The first use of FTY720 to counteract the toxic effects caused due to increased DhCer levels was shown in *ifc*-KO *Drosophila* model (Jung et al., 2017). FTY720 partially normalized the morphology and function of photoreceptors in *ifc*-KO flies by inhibiting

the upstream enzyme schlang (orthologue of CerS). However, the study lacks the information on the elevated levels of DhCer and reduced ceramide levels upon FTY720 treatment. Moreover, the efficacy of FTY720 was also validated in a zebrafish experimental autoimmune encephalomyelitis (EAE) model that can be used to test candidate drugs for multiple sclerosis (MS) and related disorders (Kulkarni et al., 2017).

Zebrafish are currently being used in various studies for drug screening against many neurological disorders including bipolar disorder and epilepsy (AMSTERDAM & HOPKINS, 2006; Becker & Rinkwitz, 2012; Kabashi, Brustein, Champagne, & Drapeau, 2011). Drug screening in zebrafish has been successfully used to identify target pathways as well as therapeutic compounds for human diseases (Baraban et al., 2013). Since development and behavior can be easily visualized and manipulated in zebrafish larvae they represent a versatile model for studying the effects of loss of *degs1* and for high throughput screening of therapeutic compounds to treat this rare genetic disorder. The increased DhCer, low ceramide levels, motor phenotypes, weak myelination observed in our zebrafish *degs1* KD model are apparent in larvae, providing a good system for screening of therapeutic compounds, and our own work demonstrates conservation of *degs1* expression and function, mechanisms of action for compounds identified in zebrafish may be of relevance for humans. Considering this, we tested the efficacy of FTY720 in zebrafish larvae soon after the embryos were laid or injected. Interestingly, FTY720 was able to rescue motor deficits, partially normalized elevated DhCer levels, reduced ceramide levels and also increases the number of mature oligodendrocytes in the spinal cord of *degs1* zebrafish model. A bulk of evidence suggests that FTY720 is relevant in this context, as it can promote neuronal and oligodendrocyte survival (Dev et al., 2008; Miron et al., 2008). We hypothesized that FTY720 may rescue the toxic effects induced by DhCer by having multimodal effects on both glial and neuronal cells.

It was tempting to speculate that effect of FTY720 on observed elevated ROS levels in human patient fibroblasts. We found FTY720 was able to partially normalized the total intracellular ROS levels observed in the patients' fibroblasts (**Fig. 24**). Thus, our study supports that inhibiting the synthesis of DhCer in a zebrafish model of *degs1* deficiency, improving the locomotor deficits, increasing the number of mature oligodendrocytes and reducing the elevated ROS levels in human patient's fibroblasts, is a plausible therapeutic strategy aimed at providing a personalized medicine to the patients.

5.7 Global Discussion

In this thesis, the importance of DEGS1 in maintaining DhCer/Cer ratio and to the *de novo* synthesis of sphingosine for the nervous system can be inferred from the paramount importance of the ceramides and sphingolipids in CNS. Sphingolipid imbalance has been associated with a wide variety of neurological diseases affecting the white matter as outlined (**Fig. 7**). In many lipid storage disorders, deficiency or malfunctioning of one of the enzymes involved in sphingolipid metabolism results in accumulation and diminution of the corresponding lipid substrate leading to cellular dysfunction and death. Galactosylceramides and sulfatides with very long-chain fatty acid moieties, in particular, 24:0 and 24:1 fatty acids, are the most abundant myelin lipids (Schmitt et al., 2015). The biosynthesis of ceramide is followed by the transfer of sugar moieties to generate glucosylceramide and galactosylceramide, which can be further transformed into gangliosides and sulfatides, respectively. Galactosylceramides/ sulfatides with 2-hydroxylated and saturated long-chain fatty acids appear to act as myelin stabilizers. Gangliosides are brain-enriched glycosphingolipids that contain an oligosaccharide head structure with one or more sialic acids (e.g., N-acetyl-neuraminic acid). Gangliosides constitute a large family of lipids with more than 100 different species, of which GM1, GD1a, GD1b and GT1b account for 96% of the gangliosides in the human brain (Schmitt et al., 2015). Thus, mutations in enzymes involved in sphingomyelin biosynthesis cause alteration of ceramides, ceramide derivatives and precursors levels which is associated with several neurodegenerative disorders such as Krabbe's disease, Gaucher's disease or Niemann Pick's disease (Mencarelli et al., 2013; Schmitt et al., 2015). Patients with mutations in the ceramidase *ACER3* (alkaline ceramidase 3), which leads to accumulation of various sphingolipids (ceramide, DhCer, Lactosylceramides) just one step after DEGS1, account for a new form of childhood leukodystrophy (Edvardson et al., 2016). Ceramides are central elements in the metabolic pathways of sphingolipids and play a crucial role in neuronal development, depending upon neuronal developmental stage, stimulus type, and ceramide species and concentration. In the first stage of neuronal development, ceramide enhances the formation of minor processes from lamellipodia (a Schwarz & Futerman, 1997). Decreasing ceramide content by ISP-1, a specific inhibitor of serine palmitoyltransferase decreased cell survival and provoked aberrant Purkinje cell dendritic differentiation (Furuya, Mitoma, Makino, & Hirabayashi, 1998). Recently, secondary disturbances on ceramides and sphingolipids have been shown in the *Hsp27*

KO mouse model of Charcot-Marie-Tooth (CMT) disease. Decreased ceramide levels in sciatic nerve and brain tissue are described, suggesting that sphingolipid metabolism may be altered when peripheral neuropathy is present (Schwartz et al., 2018). A similar scenario applies to Huntington’s disease, where the *de novo* biosynthesis pathway of sphingolipids is defective, with a decrease in contents of dihydroceramide, dihydrosphingosine, and dihydroSphingosine-1-phosphate (Pardo et al., 2017).

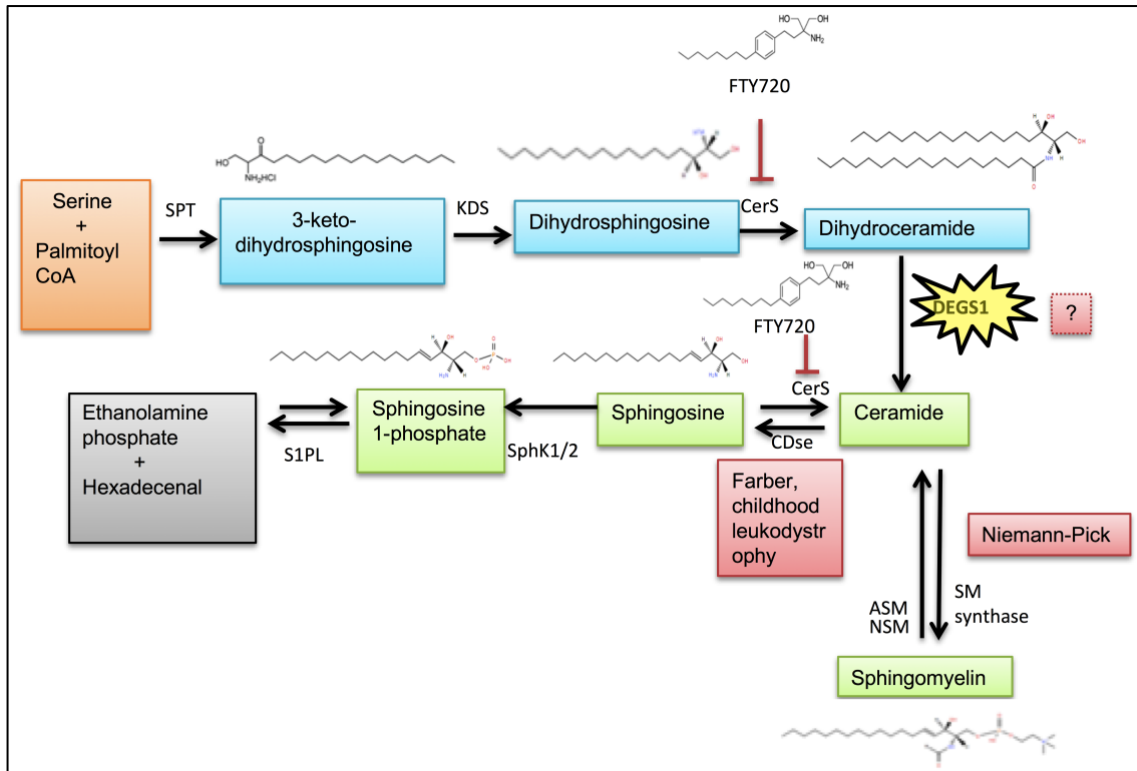


Figure 32: *De novo* Sphingosine biosynthesis pathway and Fingolimod (FTY720) effects.

Serine palmitoyltransferase (SPT) catalyzes the initial reaction of the *de novo* sphingolipid pathway. Dihydrosphingosine is produced after an intermediate step regulated by 3-keto-dihydrosphingosine reductase (KDS), which is then followed by acylation by the ceramide synthase (CerS) to produce dihydroceramide. The final reaction is the addition of a double bond by dihydroceramide desaturase to form ceramide. Ceramide is metabolized by Ceramidase (CDse) to generate Sphingosine, which in turn produces Sphingosine 1-phosphate through phosphorylation by Sphingosine Kinase-1 and Sphingosine Kinase-2 (SphK1/2). Sphingosine 1-phosphate can be catabolized into hexadecenal and ethanolamine phosphate by Sphingosine 1-Phosphate Lyase (S1PL). Ceramide can be generated by the breakdown of sphingomyelin (SM) by the acid (ASM) or neutral sphingomyelinases (NSM). Fingolimod (FTY720) has inhibitory effects on CerS.

The thesis also provides evidences that confirm the role of sphingolipids imbalance, especially ceramide and DhCer species, in the pathogenesis of neurological disorders. It has been reported that sphingomyelinase deficiency reduces ceramide levels and enhances myelin repair in acute and chronic demyelination models (Chami et al., 2017).

Like ceramide, accumulation of DhCer has been shown to be involved in many stress signals like ROS, apoptosis. It has been recently demonstrated that in *Drosophila (ifc)* knockout photoreceptor degeneration was caused by increased DhCer, not reduced levels of Cer (Jung et al., 2017). Here, we report that *degs1* deficient larvae causes accumulation of DhCer, impaired locomotor and weak myelination. However, no studies have been carried out showing the correlation between DhCer and myelin. Further analysis is necessary to determine whether accumulated DhCer is selectively targeted for myelin problems in many neurological disorders. New therapeutic strategies targeting sphingolipid imbalances can be applied to overcome these hypomyelinating disorders. In conjunction, a recent study shows protective effect of FTY720 in white matter tracts of human MS patients (Gurevich, Waknin, Stone, & Achiron, 2018). In addition, a recent study in rats after neonatal hyperoxia-mediated brain injury associated with hypomyelination and impaired neuro-cognitive outcome, concluded with a neuroprotective effect of FTY720 counterbalancing the loss of oligodendrocytes, inflammation and oxidative stress (Serdar et al., 2016). Indeed, we showed that FTY720 prevents the locomotor deficits and weak myelination in *degs1* deficient larvae. These observed positive effects were due to reduced levels of DhCers as FTY720 is a target inhibitor of ceramide synthase. Furthermore, FTY720 regulates the synthesis of different bioactive sphingolipids and can potentially affect sphingolipid metabolism globally by inhibiting enzymes involved in this pathway (**Fig. 32**) (Brunkhorst, Vutukuri, & Pfeilschifter, 2014b; W. Li, Xu, & Testai, 2016), thereby can be used as a potential therapeutic drug to attenuate disease severity in patients. There is growing evidence supporting the protective effect of FTY720 in sphingolipid metabolism-related disorders. First, neuroprotective effects of FTY720 are derived from Globoid cell leukodystrophy (Krabbe disease), caused due to mutation in galactosylceramidase (GALC) enzyme involved in sphingolipid pathway resulting in accumulation of toxic metabolite galactosylsphingosine (psychosine) in the brain. The disease is characterized by demyelination and loss of oligodendrocytes. FTY720 treatment attenuated the psychosine induced demyelination in mice organotypic cerebellar slice cultures (O'Sullivan & Dev, 2015). Second, mutations in *NPC1* gene causes Niemann-Pick type C (NPC) disease which is characterized by cholesterol and glycosphingolipid (GSL) accumulation. It has been demonstrated that FTY720 treatment reduces cholesterol and total GSL levels in NPC mutant cells (Newton et al., 2017). Finally, mutations in *HEXB* gene causes Sandhoff disease (SD), mouse model (*Hexb*^{-/-}) of SD shows accumulation of GM2

ganglioside and causes microglial activation, astrogliosis and impaired motor coordination, a common feature seen in SD patients. The anomalies observed in *Hexb*^{-/-} mice were ameliorated by treating with FTY720 which act as an immunosuppressant (Ogawa et al., 2017). Taken together these findings, may contribute to FTY720 ability to correct aberrant sphingolipid trafficking associated with several other diseases such as, mutations in human acid ceramidase (*ASAH1*) gene causes Farber Disease (FD) which results in accumulation of ceramides (F. P. S. Yu, Dworski, & Medin, 2018). Sphingolipid accumulation is also seen in case of Fabry disease patients caused due to mutations in the enzyme alpha-galactosidase A (*GLA*) causes accumulation of glycosphingolipids (Germain, 2010). Likewise, glucosylceramide (GlcCer) accumulation, ROS production in Gaucher disease (GD) patients, resulting from glucocerebrosidase deficiency (B. H. Young, Eun, & Jung, 2006). Overall, the *in vitro* and *in vivo* studies described above suggests that FTY720 could counteract elevated ceramide, glycosphingolipids and GlcCer levels toxic effects in FD, Fabry disease and GD patients, respectively. With this in mind, FTY720 may be a potential new therapeutic option for the treatment of white matter disorders, in particular in those linked to sphingolipid metabolism. Hence, our study could provide insights on the importance of DEGS1 in neurological disorder and offer new therapeutic possibilities for patients with similar sphingolipid imbalances disorders.

CONCLUSIONS

6 CONCLUSIONS

1. We uncovered a possible candidate gene for leukodystrophy using whole exome analysis and in-house bioinformatics pipeline on an index case, identifying a novel frameshift variant p.(Tyr202Thrfs*8) in homozygosis in the sphingolipid desaturase *DEGS1* gene.
2. With the help of a collaborative network and data aggregation of whole exome sequencing (WES) from multiple laboratories through the platform GeneMatcher we disclosed 17 additional patients with variants in the same gene. These individuals shared overlapping phenotypes that include severe hypomyelination, cerebellar atrophy, and thinning of the corpus callosum on MRI, accompanied by speech abnormalities, developmental delay and intellectual disability.
3. Initial characterization of *Degs1* in mice tissues and human brain necropsies demonstrated the tissue-specific distribution of this gene and was highly expressed in CNS.
4. Lipidomics analysis in three affected individual's fibroblasts and muscle biopsy of a fourth case showed high dihydroceramides (DhCer) and low ceramides (Cer) levels suggesting an impaired DEGS1 enzyme activity.
5. Accumulation of DhCers results in increased intracellular ROS production in affected individuals. In addition, exogenous DhCer C18:0 was able to induce intracellular ROS levels in control fibroblasts indicating the toxic role of DhCers.
6. Patient 4 p.(Leu114Profs*11/Asn255Ser) showed high levels of mitochondrial ROS and low autophagy flux. In contrast, patient 9 p.(Asn255Ser) showed low levels of mitochondrial ROS and high autophagy flux suggesting an evidence of mitochondrial dysfunction and impaired autophagy flux in both the cases.

7. Combining *in situ* hybridization and immunofluorescence approaches revealed expression of zebrafish *degs1* in mature oligodendrocytes at 4.5 days post fertilization (dpf), indicating the importance of *degs1* in myelin development.
8. Morpholino (MO) mediated knockdown of *degs1* in zebrafish showed high DhCer and low ceramide levels, locomotor impairment and weak myelination. These phenotypes are compatible with the clinical symptoms observed in patients, suggesting MO-DEGS1 as a good model to study this rare leukodystrophy.
9. FTY720 treatment normalized the increased DhCer and low ceramide levels, prevents locomotor deficits and increases the number of mature oligodendrocytes in MO-DEGS1 larvae and reduced the ROS levels in patient's fibroblast, unveiling a plausible therapeutic hope to treat patients.
10. In summary, this work is an example of the power of clinical genomics of molecular diagnosis, novel gene identification and identification of plausible treatments in record time. Thus, democratizing clinical care even for the ultrarare disorders.

APPENDIX I

List of solutions

5X MAB

Maleic acid	29.02 g
NaCl	21.91 g
Sterile H ₂ O	350 ml

Adjust pH to 7.5 and bring final volume to 500 ml

20X SSC

NaCl	87.65 g
Sodium citrate	44.1 g
Sterile H ₂ O	350 ml

Adjust pH 4.5 and bring final volume to 500 ml

1M Tris

Tris	12.11 g
Sterile H ₂ O	80 ml

Adjust pH to 9.5 and bring final volume to 100 ml

0.1M MgCl₂

MgCl ₂	2.033 g
Sterile H ₂ O	70 ml

Stir to dissolve and bring final volume to 100 ml

5M NaCl

NaCl	14.6 g
Sterile H ₂ O	30 ml

Adjust the final volume to 50ml

10X Blocking Reagent

5gm blocking powder (Roche, 11096176001) in 50mL MABT. Dissolved by keeping at 65 C for 1-2 hours with shaking in between to dissolve.

25mg/mL tRNA

tRNA (Sigma)	250 mg
100% Formamide (FAD)	5 ml
20X SSC	2.5 ml
Sterile H ₂ O	2.5 ml

Hybridisation Buffer (HB) 50mL

100 % FAD (Ambion)	25 ml
20X SSC	12.5 ml
10mg/ml Heparin	0.25 ml
25mg/ml tRNA	1 ml
10% Tween 20 (Sigma)	0.5 ml
Sterile H ₂ O	10.75 ml

REFERENCES

7 REFERENCES

- Ablain, J., Durand, E. M., Yang, S., Zhou, Y., & Zon, L. I. (2015). A CRISPR/Cas9 vector system for tissue-specific gene disruption in zebrafish. *Developmental Cell*, 32(6), 756–764. <https://doi.org/10.1016/j.devcel.2015.01.032>
- Ahmad, T., Aggarwal, K., Pattnaik, B., Mukherjee, S., Sethi, T., Tiwari, B. K., ... Agrawal, A. (2013). Computational classification of mitochondrial shapes reflects stress and redox state. *Cell Death & Disease*, 4(1), e461–e461. <https://doi.org/10.1038/cddis.2012.213>
- AMSTERDAM, A., & HOPKINS, N. (2006). Mutagenesis strategies in zebrafish for identifying genes involved in development and disease. *Trends in Genetics*, 22(9), 473–478. <https://doi.org/10.1016/j.tig.2006.06.011>
- Apraiz, A., Idkowiak-Baldys, J., Nieto-Rementería, N., Boyano, M. D., Hannun, Y. A., & Asumendi, A. (2012). Dihydroceramide accumulation and reactive oxygen species are distinct and nonessential events in 4-HPR-mediated leukemia cell death. *Biochemistry and Cell Biology = Biochimie et Biologie Cellulaire*, 90(2), 209–223. <https://doi.org/10.1139/o2012-001>
- Arunachalam, M., Raja, M., Vijayakumar, C., Malaiammal, P., & Mayden, R. L. (2013). Natural History of Zebrafish (*Danio rerio*) in India. *Zebrafish*, 10(1), 1–14. <https://doi.org/10.1089/zeb.2012.0803>
- Babin, P. J., Goizet, C., & Raldúa, D. (2014). Zebrafish models of human motor neuron diseases: Advantages and limitations. *Progress in Neurobiology*, 118, 36–58. <https://doi.org/10.1016/j.pneurobio.2014.03.001>
- Balciunas, D. (2018). Fish mutant, where is thy phenotype? *PLOS Genetics*, 14(2), e1007197. <https://doi.org/10.1371/journal.pgen.1007197>
- Bamshad, M. J., Ng, S. B., Bigham, A. W., Tabor, H. K., Emond, M. J., Nickerson, D. A., & Shendure, J. (2011). Exome sequencing as a tool for Mendelian disease gene discovery. *Nature Reviews Genetics*, 12(11), 745–755. <https://doi.org/10.1038/nrg3031>
- Bandhuvula, P., Tam, Y. Y., Oskouian, B., & Saba, J. D. (2005). The immune modulator FTY720 inhibits sphingosine-1-phosphate lyase activity. *The Journal of Biological Chemistry*, 280(40), 33697–33700. <https://doi.org/10.1074/jbc.C500294200>
- Baraban, S. C., Dinday, M. T., & Hortopan, G. A. (2013). Drug screening in Scn1a zebrafish mutant identifies clemizole as a potential Dravet syndrome treatment. *Nature Communications*, 4(1), 2410. <https://doi.org/10.1038/ncomms3410>
- Barkovich, A. J. (2000). Concepts of myelin and myelination in neuroradiology. *AJNR. American Journal of Neuroradiology*, 21(6), 1099–1109. Retrieved from <http://www.ncbi.nlm.nih.gov/pubmed/10871022>
- Barkovich, A. J., Kjos, B. O., Jackson, D. E., & Norman, D. (1988). Normal maturation of the neonatal and infant brain: MR imaging at 1.5 T. *Radiology*, 166(1), 173–180. <https://doi.org/10.1148/radiology.166.1.3336675>
- Bassett, D. I., Bryson-Richardson, R. J., Daggett, D. F., Gautier, P., Keenan, D. G., & Currie, P. D. (2003). Dystrophin is required for the formation of stable muscle attachments in the zebrafish embryo. *Development*, 130(23), 5851–5860. <https://doi.org/10.1242/dev.00799>
- Beck, M. (2009). Therapy for lysosomal storage disorders. *IUBMB Life*, 62(1), n/a-n/a. <https://doi.org/10.1002/iub.284>
- Beck, M. (2012). Rare and Ultra Rare Diseases• . *Journal of Developing Drugs*, 01(06).

- <https://doi.org/10.4172/2329-6631.1000e107>
- Becker, T. S., & Rinkwitz, S. (2012). Zebrafish as a genomics model for human neurological and polygenic disorders. *Developmental Neurobiology*, 72(3), 415–428. <https://doi.org/10.1002/dneu.20888>
- Bedell, V. M., Wang, Y., Campbell, J. M., Poshusta, T. L., Starker, C. G., Krug II, R. G., ... Ekker, S. C. (2012). In vivo genome editing using a high-efficiency TALEN system. *Nature*, 491(7422), 114–118. <https://doi.org/10.1038/nature11537>
- Bejaoui, K., Wu, C., Scheffler, M. D., Haan, G., Ashby, P., Wu, L., ... Brown, R. H. (2001). SPTLC1 is mutated in hereditary sensory neuropathy, type 1. *Nature Genetics*, 27(3), 261–262. <https://doi.org/10.1038/85817>
- Ben-David, O., Pewzner-Jung, Y., Brenner, O., Laviad, E. L., Kogot-Levin, A., Weissberg, I., ... Futerman, A. H. (2011). Encephalopathy caused by ablation of very long acyl chain ceramide synthesis may be largely due to reduced galactosylceramide levels. *The Journal of Biological Chemistry*, 286(34), 30022–30033. <https://doi.org/10.1074/jbc.M111.261206>
- Bendikov-Bar, I., & Horowitz, M. (2012). Gaucher disease paradigm: from ERAD to comorbidity. *Human Mutation*, 33(10), 1398–1407. <https://doi.org/10.1002/humu.22124>
- Bernard, G., Chouery, E., Putorti, M. L., Tétreault, M., Takanohashi, A., Carosso, G., ... Brais, B. (2011). Mutations of POLR3A Encoding a Catalytic Subunit of RNA Polymerase Pol III Cause a Recessive Hypomyelinating Leukodystrophy. *The American Journal of Human Genetics*, 89(3), 415–423. <https://doi.org/10.1016/j.ajhg.2011.07.014>
- Bertholet, A. M., Delerue, T., Millet, A. M., Moulis, M. F., David, C., Daloyau, M., ... Belenguier, P. (2016). Mitochondrial fusion/fission dynamics in neurodegeneration and neuronal plasticity. *Neurobiology of Disease*, 90, 3–19. <https://doi.org/10.1016/j.nbd.2015.10.011>
- Bielawska, A., Crane, H. M., Liotta, D., Obeid, L. M., & Hannun, Y. A. (1993). Selectivity of ceramide-mediated biology: Lack of activity of erythro-dihydroceramide. *Journal of Biological Chemistry*.
- Billich, A., Bornancin, F., Dévay, P., Mechtcheriakova, D., Urtz, N., & Baumruker, T. (2003). Phosphorylation of the immunomodulatory drug FTY720 by sphingosine kinases. *The Journal of Biological Chemistry*, 278(48), 47408–47415. <https://doi.org/10.1074/jbc.M307687200>
- Binks, X., & Wattenberg, W. (2018). The long and the short of ceramides. <https://doi.org/10.1074/jbc.H118.003522>
- Boccuto, L., Aoki, K., Flanagan-Steet, H., Chen, C.-F., Fan, X., Bartel, F., ... Schwartz, C. E. (2014). A mutation in a ganglioside biosynthetic enzyme, ST3GAL5, results in salt & pepper syndrome, a neurocutaneous disorder with altered glycolipid and glycoprotein glycosylation. *Human Molecular Genetics*, 23(2), 418–433. <https://doi.org/10.1093/hmg/ddt434>
- Boczonadi, V., Müller, J. S., Pyle, A., Munkley, J., Dor, T., Quartararo, J., ... Horvath, R. (2014). EXOSC8 mutations alter mRNA metabolism and cause hypomyelination with spinal muscular atrophy and cerebellar hypoplasia. *Nature Communications*, 5(1), 4287. <https://doi.org/10.1038/ncomms5287>
- Bögershausen, N., Tsai, I.-C., Pohl, E., Kiper, P. Ö. S., Beleggia, F., Percin, E. F., ... Wollnik, B. (2015). RAP1-mediated MEK/ERK pathway defects in Kabuki syndrome. *The Journal of Clinical Investigation*, 125(9), 3585–3599. <https://doi.org/10.1172/JCI80102>
- Bonkowsky, J. L., Nelson, C., Kingston, J. L., Filloux, F. M., Mundorff, M. B., &

- Srivastava, R. (2010). The burden of inherited leukodystrophies in children. *Neurology*. <https://doi.org/10.1212/WNL.0b013e3181eee46b>
- Boon, K.-L., Xiao, S., McWhorter, M. L., Donn, T., Wolf-Saxon, E., Bohnsack, M. T., ... Beattie, C. E. (2009). Zebrafish survival motor neuron mutants exhibit presynaptic neuromuscular junction defects. *Human Molecular Genetics*, *18*(19), 3615–3625. <https://doi.org/10.1093/hmg/ddp310>
- Borck, G., Hög, F., Dentici, M. L., Tan, P. L., Sowada, N., Medeira, A., ... Kubisch, C. (2015). BRF1 mutations alter RNA polymerase III-dependent transcription and cause neurodevelopmental anomalies. *Genome Research*, *25*(2), 155–166. <https://doi.org/10.1101/gr.176925.114>
- Botstein, D., & Risch, N. (2003). Discovering genotypes underlying human phenotypes: past successes for mendelian disease, future approaches for complex disease. *Nature Genetics*, *33*(3s), 228–237. <https://doi.org/10.1038/ng1090>
- Boukhris, A., Schule, R., Loureiro, J. L., Lourenço, C. M., Mundwiler, E., Gonzalez, M. A., ... Stevanin, G. (2013). Alteration of Ganglioside Biosynthesis Responsible for Complex Hereditary Spastic Paraplegia. *The American Journal of Human Genetics*, *93*(1), 118–123. <https://doi.org/10.1016/j.ajhg.2013.05.006>
- Boycott, K. M., Vanstone, M. R., Bulman, D. E., & MacKenzie, A. E. (2013). Rare-disease genetics in the era of next-generation sequencing: discovery to translation. *Nature Reviews Genetics*, *14*(10), 681–691. <https://doi.org/10.1038/nrg3555>
- Brady, R. O. (2006). Enzyme Replacement for Lysosomal Diseases. *Annual Review of Medicine*, *57*(1), 283–296. <https://doi.org/10.1146/annurev.med.57.110104.115650>
- Brinkmann, V. (2007). Sphingosine 1-phosphate receptors in health and disease: Mechanistic insights from gene deletion studies and reverse pharmacology. *Pharmacology & Therapeutics*, *115*(1), 84–105. <https://doi.org/10.1016/j.pharmthera.2007.04.006>
- Brockman, H. L., Momsen, M. M., Brown, R. E., He, L., Chun, J., Byun, H.-S., & Bittman, R. (2004). The 4,5-double bond of ceramide regulates its dipole potential, elastic properties, and packing behavior. *Biophysical Journal*, *87*(3), 1722–1731. <https://doi.org/10.1529/biophysj.104.044529>
- Brunkhorst, R., Vutukuri, R., & Pfeilschifter, W. (2014a). Fingolimod for the treatment of neurological diseases-state of play and future perspectives. *Frontiers in Cellular Neuroscience*, *8*, 283. <https://doi.org/10.3389/fncel.2014.00283>
- Brunkhorst, R., Vutukuri, R., & Pfeilschifter, W. (2014b). Fingolimod for the treatment of neurological diseases — state of play and future perspectives. *Frontiers in Cellular Neuroscience*, *8*(September), 1–20. <https://doi.org/10.3389/fncel.2014.00283>
- Cadena, D. L., Kurten, R. C., & Gill, G. N. (1997). The product of the MLD gene is a member of the membrane fatty acid desaturase family: Overexpression of MLD inhibits EGF receptor biosynthesis. *Biochemistry*, *36*(23), 6960–6967. <https://doi.org/10.1021/bi9700911>
- Casasampere, M., Ordoñez, Y. F., Pou, A., & Casas, J. (2016). Inhibitors of dihydroceramide desaturase 1: Therapeutic agents and pharmacological tools to decipher the role of dihydroceramides in cell biology. *Chemistry and Physics of Lipids*, *197*, 33–44. <https://doi.org/10.1016/j.chemphyslip.2015.07.025>
- Chami, M., Halmer, R., Schnoeder, L., Becker, K. A., Meier, C., Fassbender, K., ... Walter, S. (2017). Acid sphingomyelinase deficiency enhances myelin repair after acute and chronic demyelination. *PLoS ONE*, *12*(6), e0178622. <https://doi.org/10.1371/journal.pone.0178622>
- Chelban, V., Patel, N., Vandrovцова, J., Zanetti, M. N., Lynch, D. S., Ryten, M., ...

- Houlden, H. (2017). Mutations in NKX6-2 Cause Progressive Spastic Ataxia and Hypomyelination. *The American Journal of Human Genetics*, *100*(6), 969–977. <https://doi.org/10.1016/j.ajhg.2017.05.009>
- Chen, X., Zhong, Z., Xu, Z., Chen, L., & Wang, Y. (2010). 2',7'-Dichlorodihydrofluorescein as a fluorescent probe for reactive oxygen species measurement: Forty years of application and controversy. *Free Radical Research*, *44*(6), 587–604. <https://doi.org/10.3109/10715761003709802>
- Cheng, H., Dharmadhikari, A. V, Varland, S., Ma, N., Domingo, D., Kleyner, R., ... Lyon, G. J. (2018). Truncating Variants in NAA15 Are Associated with Variable Levels of Intellectual Disability, Autism Spectrum Disorder, and Congenital Anomalies. *American Journal of Human Genetics*, *102*(5), 985–994. <https://doi.org/10.1016/j.ajhg.2018.03.004>
- Chiavegatto, S., Sun, J., Nelson, R. J., & Schnaar, R. L. (2000). A functional role for complex gangliosides: motor deficits in GM2/GD2 synthase knockout mice. *Experimental Neurology*, *166*(2), 227–234. <https://doi.org/10.1006/exnr.2000.7504>
- Chiba, K., Kataoka, H., Seki, N., Maeda, Y., & Sugahara, K. (2011). Special Issue "Lipid mediator and Inflammation " Fingolimod (FTY720), the Sphingosine 1-Phosphate Receptor Modulator, as a New Therapeutic Drug in Multiple Sclerosis Introduction: Discovery of FTY720. *Inflammation and Regeneration*, *31*(2). Retrieved from http://jsir.gr.jp/journal/Vol31No2/pdf/06_S3_167.pdf
- Chun, J., & Hartung, H.-P. (2010). Mechanism of action of oral fingolimod (FTY720) in multiple sclerosis. *Clinical Neuropharmacology*, *33*(2), 91–101. <https://doi.org/10.1097/WNF.0b013e3181cbf825>
- Chun J. (2011). Discovery Medicine. *Discovery Medicine*, *12*(1264). Retrieved from <https://www.scripps.edu/chun/PDFs/Chun Discov Med 2011.pdf>
- Clarke, C. J., & Hannun, Y. A. (2006). Neutral sphingomyelinases and nSMase2: Bridging the gaps. *Biochimica et Biophysica Acta (BBA) - Biomembranes*, *1758*(12), 1893–1901. <https://doi.org/10.1016/j.bbamem.2006.06.025>
- Cohen, J. A., Barkhof, F., Comi, G., Hartung, H.-P., Khatri, B. O., Montalban, X., ... Kappos, L. (2010). Oral Fingolimod or Intramuscular Interferon for Relapsing Multiple Sclerosis. *New England Journal of Medicine*, *362*(5), 402–415. <https://doi.org/10.1056/NEJMoa0907839>
- Colwill, R. M., & Creton, R. (2011). Locomotor behaviors in zebrafish (*Danio rerio*) larvae. *Behavioural Processes*, *86*(2), 222–229. <https://doi.org/10.1016/j.beproc.2010.12.003>
- Compston, A., & Coles, A. (2008). Multiple sclerosis. *Lancet (London, England)*, *372*(9648), 1502–1517. [https://doi.org/10.1016/S0140-6736\(08\)61620-7](https://doi.org/10.1016/S0140-6736(08)61620-7)
- Contreras, F.-X., Sot, J., Alonso, A., & Goñi, F. M. (2006). Sphingosine increases the permeability of model and cell membranes. *Biophysical Journal*, *90*(11), 4085–4092. <https://doi.org/10.1529/biophysj.105.076471>
- Cornet, C., Calzolari, S., Minana-Prieto, R., Dyballa, S., van Doornmalen, E., Rutjes, H., ... Terriente, J. (2017). ZeGlobalTox: An Innovative Approach to Address Organ Drug Toxicity Using Zebrafish. *Int J Mol Sci*, *18*(4). <https://doi.org/10.3390/ijms18040864>
- Cox, T. M., Drelichman, G., Cravo, R., Balwani, M., Burrow, T. A., Martins, A. M., ... Puga, A. C. (2015). Eliglustat compared with imiglucerase in patients with Gaucher's disease type 1 stabilised on enzyme replacement therapy: a phase 3, randomised, open-label, non-inferiority trial. *The Lancet*, *385*(9985), 2355–2362. [https://doi.org/10.1016/S0140-6736\(14\)61841-9](https://doi.org/10.1016/S0140-6736(14)61841-9)

- Cronin, A., & Greal, M. (2017). Neuroprotective and Neuro-restorative Effects of Minocycline and Rasagiline in a Zebrafish 6-Hydroxydopamine Model of Parkinson's Disease. *Neuroscience*, *367*, 34–46. <https://doi.org/10.1016/J.NEUROSCIENCE.2017.10.018>
- Cutler, R. G., Kelly, J., Storie, K., Pedersen, W. A., Tammara, A., Hatanpaa, K., ... Mattson, M. P. (2004). Involvement of oxidative stress-induced abnormalities in ceramide and cholesterol metabolism in brain aging and Alzheimer's disease. *Proceedings of the National Academy of Sciences of the United States of America*, *101*(7), 2070–2075. <https://doi.org/10.1073/pnas.0305799101>
- Czopka, T. (2016). Insights into mechanisms of central nervous system myelination using zebrafish. *GLIA*, *64*(3), 333–349. <https://doi.org/10.1002/glia.22897>
- Czubowicz, K., & Strosznajder, R. (2014). Ceramide in the molecular mechanisms of neuronal cell death. The role of sphingosine-1-phosphate. *Molecular Neurobiology*, *50*(1), 26–37. <https://doi.org/10.1007/s12035-013-8606-4>
- D'Costa, A., & Shepherd, I. T. (2009). Zebrafish Development and Genetics: Introducing Undergraduates to Developmental Biology and Genetics in a Large Introductory Laboratory Class. *Zebrafish*, *6*(2), 169–177. <https://doi.org/10.1089/zeb.2008.0562>
- da Veiga Pereira, L., Desnick, R. J., Adler, D. A., Distèche, C. M., & Schuchman, E. H. (1991). Regional assignment of the human acid sphingomyelinase gene (SMPD1) by PCR analysis of somatic cell hybrids and in situ hybridization to 11p15.1----p15.4. *Genomics*, *9*(2), 229–234. Retrieved from <http://www.ncbi.nlm.nih.gov/pubmed/2004772>
- Dagda, R. K., Cherra, S. J., Kulich, S. M., Tandon, A., Park, D., & Chu, C. T. (2009). Loss of PINK1 Function Promotes Mitophagy through Effects on Oxidative Stress and Mitochondrial Fission. *Journal of Biological Chemistry*, *284*(20), 13843–13855. <https://doi.org/10.1074/jbc.M808515200>
- Dawkins, J. L., Hulme, D. J., Brahmabhatt, S. B., Auer-Grumbach, M., & Nicholson, G. A. (2001). Mutations in SPTLC1, encoding serine palmitoyltransferase, long chain base subunit-1, cause hereditary sensory neuropathy type I. *Nature Genetics*, *27*(3), 309–312. <https://doi.org/10.1038/85879>
- Dawson, G., & Qin, J. (2011). Gilenya (FTY720) inhibits acid sphingomyelinase by a mechanism similar to tricyclic antidepressants. *Biochemical and Biophysical Research Communications*, *404*(1), 321–323. <https://doi.org/10.1016/j.bbrc.2010.11.115>
- DeBruin, L. S., Haines, J. D., Wellhauser, L. A., Radeva, G., Schonmann, V., Bienzle, D., & Harauz, G. (2005). Developmental partitioning of myelin basic protein into membrane microdomains. *Journal of Neuroscience Research*, *80*(2), 211–225. <https://doi.org/10.1002/jnr.20452>
- Degli Esposti, M., & McLennan, H. (1998). Mitochondria and cells produce reactive oxygen species in virtual anaerobiosis: relevance to ceramide-induced apoptosis. *FEBS Letters*, *430*(3), 338–342. [https://doi.org/10.1016/S0014-5793\(98\)00688-7](https://doi.org/10.1016/S0014-5793(98)00688-7)
- den Dunnen, J. T., Dalgleish, R., Maglott, D. R., Hart, R. K., Greenblatt, M. S., McGowan-Jordan, J., ... Taschner, P. E. M. (2016). HGVS Recommendations for the Description of Sequence Variants: 2016 Update. *Human Mutation*, *37*(6), 564–569. <https://doi.org/10.1002/humu.22981>
- Dev, K. K., Mullershausen, F., Mattes, H., Kuhn, R. R., Bilbe, G., Hoyer, D., & Mir, A. (2008). Brain sphingosine-1-phosphate receptors: Implication for FTY720 in the treatment of multiple sclerosis. *Pharmacology and Therapeutics*. <https://doi.org/10.1016/j.pharmthera.2007.08.005>

- Dumitru, C. A., Zhang, Y., Li, X., & Gulbins, E. (2007). Ceramide: A Novel Player in Reactive Oxygen Species-Induced Signaling? *Antioxidants & Redox Signaling*, 9(9), 1535–1540. <https://doi.org/10.1089/ars.2007.1692>
- Dupree, J. L., Coetzee, T., Blight, A., Suzuki, K., & Popko, B. (1998). Myelin galactolipids are essential for proper node of Ranvier formation in the CNS. *The Journal of Neuroscience : The Official Journal of the Society for Neuroscience*, 18(5), 1642–1649. Retrieved from <http://www.ncbi.nlm.nih.gov/pubmed/9464989>
- Edvardson, S., Hama, H., Shaag, A., Gomori, J. M., Berger, I., Soffer, D., ... Elpeleg, O. (2008). Mutations in the Fatty Acid 2-Hydroxylase Gene Are Associated with Leukodystrophy with Spastic Paraparesis and Dystonia. *The American Journal of Human Genetics*, 83(5), 643–648. <https://doi.org/10.1016/j.ajhg.2008.10.010>
- Edvardson, S., Yi, J. K., Jalas, C., Xu, R., Webb, B. D., Snider, J., ... Elpeleg, O. (2016). Deficiency of the alkaline ceramidase ACER3 manifests in early childhood by progressive leukodystrophy. *Journal of Medical Genetics*, 53(6), 389–396. <https://doi.org/10.1136/jmedgenet-2015-103457>
- Ekins, S. (2017). Industrializing rare disease therapy discovery and development. *Nature Biotechnology*, 35(2), 117–118. <https://doi.org/10.1038/nbt.3787>
- Endo, K., Akiyama, T., Kobayashi, S., & Okada, M. (1996). Degenerative spermatocyte, a novel gene encoding a transmembrane protein required for the initiation of meiosis in Drosophila spermatogenesis. *Molecular and General Genetics*, 253(1–2), 157–165. <https://doi.org/10.1007/s004380050308>
- Fahy, E., Subramaniam, S., Murphy, R. C., Nishijima, M., Raetz, C. R. H., Shimizu, T., ... Dennis, E. A. (2009). Update of the LIPID MAPS comprehensive classification system for lipids. *Journal of Lipid Research*, 50(Supplement), S9–S14. <https://doi.org/10.1194/jlr.R800095-JLR200>
- Farfel-Becker, T., Vitner, E. B., Kelly, S. L., Bame, J. R., Duan, J., Shinder, V., ... Futerman, A. H. (2014). Neuronal accumulation of glucosylceramide in a mouse model of neuronopathic Gaucher disease leads to neurodegeneration. *Human Molecular Genetics*, 23(4), 843–854. <https://doi.org/10.1093/hmg/ddt468>
- Fernandez-Checa, J. C., Fernandez, A., Morales, A., Mari, M., Garcia-Ruiz, C., & Colell, A. (2010). Oxidative Stress and Altered Mitochondrial Function in Neurodegenerative Diseases: Lessons From Mouse Models. *CNS & Neurological Disorders - Drug Targets*, 9(4), 439–454. <https://doi.org/10.2174/187152710791556113>
- Fragaki, K., Ait-El-Mkadem, S., Chaussenot, A., Gire, C., Mengual, R., Bonesso, L., ... Paquis-Flucklinger, V. (2013). Refractory epilepsy and mitochondrial dysfunction due to GM3 synthase deficiency. *European Journal of Human Genetics*, 21(5), 528–534. <https://doi.org/10.1038/ejhg.2012.202>
- Frohman, E. M., Racke, M. K., & Raine, C. S. (2006). Multiple Sclerosis — The Plaque and Its Pathogenesis. *New England Journal of Medicine*, 354(9), 942–955. <https://doi.org/10.1056/NEJMra052130>
- Fujita, T., Inoue, K., Yamamoto, S., Ikumoto, T., Sasaki, S., Toyama, R., ... Okumoto, T. (1994). Fungal metabolites. Part 11. A potent immunosuppressive activity found in *Isaria sinclairii* metabolite. *The Journal of Antibiotics*, 47(2), 208–215. Retrieved from <http://www.ncbi.nlm.nih.gov/pubmed/8150717>
- Furuya, S., Mitoma, J., Makino, a, & Hirabayashi, Y. (1998). Ceramide and its interconvertible metabolite sphingosine function as indispensable lipid factors involved in survival and dendritic differentiation of cerebellar Purkinje cells. *Journal of Neurochemistry*, 71(1), 366–377.
- Futerman, A. H., & van Meer, G. (2004). The cell biology of lysosomal storage

- disorders. *Nature Reviews Molecular Cell Biology*, 5(7), 554–565.
<https://doi.org/10.1038/nrm1423>
- Gahl, W. A., Markello, T. C., Toro, C., Fajardo, K. F., Sincan, M., Gill, F., ... Adams, D. (2012). The NIH Undiagnosed Diseases Program: Insights into Rare Diseases. *Genet Med*. <https://doi.org/10.1038/gim.0b013e318232a005>
- García-Ruiz, C., Colell, A., Marí, M., Morales, A., & Fernández-Checa, J. C. (1997). Direct effect of ceramide on the mitochondrial electron transport chain leads to generation of reactive oxygen species. Role of mitochondrial glutathione. *The Journal of Biological Chemistry*, 272(17), 11369–11377.
<https://doi.org/10.1074/JBC.272.17.11369>
- Gerety, S. S., & Wilkinson, D. G. (2011). Morpholino artifacts provide pitfalls and reveal a novel role for pro-apoptotic genes in hindbrain boundary development. *Developmental Biology*, 350(2), 279–289.
<https://doi.org/10.1016/j.ydbio.2010.11.030>
- Germain, D. P. (2010). Fabry disease. *Orphanet Journal of Rare Diseases*.
<https://doi.org/10.1186/1750-1172-5-30>
- Ghering, A. B., & Davidson, W. S. (2006). Ceramide structural features required to stimulate ABCA1-mediated cholesterol efflux to apolipoprotein A-I. *Journal of Lipid Research*, 47(12), 2781–2788. <https://doi.org/10.1194/jlr.M600380-JLR200>
- Gibbs, R. A., Boerwinkle, E., Doddapaneni, H., Han, Y., Korchina, V., Kovar, C., ... Rasheed, A. (2015). A global reference for human genetic variation. *Nature*, 526(7571), 68–74. <https://doi.org/10.1038/nature15393>
- Gielen, E., Baron, W., Vandeven, M., Steels, P., Hoekstra, D., & Ameloot, M. (2006). Rafts in oligodendrocytes: Evidence and structure–function relationship. *Glia*, 54(6), 499–512. <https://doi.org/10.1002/glia.20406>
- Gilissen, C., Hoischen, A., Brunner, H. G., & Veltman, J. A. (2012). Disease gene identification strategies for exome sequencing. *European Journal of Human Genetics*, 20(5), 490–497. <https://doi.org/10.1038/ejhg.2011.258>
- Gonzaga-Jauregui, C., Harel, T., Gambin, T., Kousi, M., Griffin, L. B., Francescato, L., ... Lupski, J. R. (2015). Exome Sequence Analysis Suggests that Genetic Burden Contributes to Phenotypic Variability and Complex Neuropathy. *Cell Reports*, 12(7), 1169–1183. <https://doi.org/10.1016/j.celrep.2015.07.023>
- Gracia-Garcia, P., Rao, V., Haughey, N. J., Ratnam Banduru, V. V., Smith, G., Rosenberg, P. B., ... Mielke, M. M. (2011). Elevated Plasma Ceramides in Depression. *Journal of Neuropsychiatry*, 23(2), 215–218.
<https://doi.org/10.1176/appi.neuropsych.23.2.215>
- Grassi, S., Chiricozzi, E., Mauri, L., Sonnino, S., & Prinetti, A. (2018). Sphingolipids and neuronal degeneration in lysosomal storage disorders. *Journal of Neurochemistry*. <https://doi.org/10.1111/jnc.14540>
- Greenfield, J. G. (Joseph G., Love, S., Louis, D. N., & Ellison, D. (David W. (2008). *Greenfield's neuropathology*. Hodder Arnold. Retrieved from [https://books.google.es/books?id=nrEWkAc7W7IC&pg=PA588&lpg=PA588&dq=Gravel+,+R+2001,+McGraw-Hill,+New+York+sphingolipid&source=bl&ots=CgJH3YrbTn&sig=70lhpTLusMiX0pxMYtvaCnZPBP8&hl=en&sa=X&ved=0ahUKEwilko3gkerbAhWKJ8AKHVjoDwgQ6AEIODAD#v=onepage&q=Gravel %2C R 2001%2C McGraw-Hill%2C New York sphingolipid&f=false](https://books.google.es/books?id=nrEWkAc7W7IC&pg=PA588&lpg=PA588&dq=Gravel+,+R+2001,+McGraw-Hill,+New+York+sphingolipid&source=bl&ots=CgJH3YrbTn&sig=70lhpTLusMiX0pxMYtvaCnZPBP8&hl=en&sa=X&ved=0ahUKEwilko3gkerbAhWKJ8AKHVjoDwgQ6AEIODAD#v=onepage&q=Gravel%20R%202001%20McGraw-Hill%20New%20York%20sphingolipid&f=false)
- Griffin, A., Hamling, K. R., Knupp, K., Hong, S., Lee, L. P., & Baraban, S. C. (2017). Clemizole and modulators of serotonin signalling suppress seizures in Dravet syndrome. *Brain*, 140(3), aww342. <https://doi.org/10.1093/brain/aww342>

- Grunwald, D. J., & Eisen, J. S. (2002). Headwaters of the zebrafish — emergence of a new model vertebrate. *Nature Reviews Genetics*, 3(9), 717–724. <https://doi.org/10.1038/nrg892>
- Grunwald, D. J., Kimmel, C. B., Westerfield, M., Walker, C., & Streisinger, G. (1988). A neural degeneration mutation that spares primary neurons in the zebrafish. *Developmental Biology*, 126(1), 115–128. [https://doi.org/10.1016/0012-1606\(88\)90245-X](https://doi.org/10.1016/0012-1606(88)90245-X)
- Gudz, T. I., Tserng, K. Y., & Hoppel, C. L. (1997). Direct inhibition of mitochondrial respiratory chain complex III by cell-permeable ceramide. *The Journal of Biological Chemistry*, 272(39), 24154–24158. <https://doi.org/10.1074/JBC.272.39.24154>
- Gueneau, L., Fish, R. J., Shamseldin, H. E., Voisin, N., Tran Mau-Them, F., Preiksaitiene, E., ... Reymond, A. (2018). KIAA1109 Variants Are Associated with a Severe Disorder of Brain Development and Arthrogyrosis. *American Journal of Human Genetics*, 102(1), 116–132. <https://doi.org/10.1016/j.ajhg.2017.12.002>
- Guissart, C., Latypova, X., Rollier, P., Khan, T. N., Stamberger, H., McWalter, K., ... Küry, S. (2018). Dual Molecular Effects of Dominant RORA Mutations Cause Two Variants of Syndromic Intellectual Disability with Either Autism or Cerebellar Ataxia. *The American Journal of Human Genetics*, 102(5), 744–759. <https://doi.org/10.1016/j.ajhg.2018.02.021>
- Gurevich, M., Waknin, R., Stone, E., & Achiron, A. (2018). Fingolimod-improved axonal and myelin integrity of white matter tracts associated with multiple sclerosis-related functional impairments. *CNS Neuroscience and Therapeutics*. <https://doi.org/10.1111/cns.12796>
- Hahn, C. N., del Pilar Martin, M., Schröder, M., Vanier, M. T., Hara, Y., Suzuki, K., ... d'Azzo, A. (1997). Generalized CNS disease and massive GM1-ganglioside accumulation in mice defective in lysosomal acid beta-galactosidase. *Human Molecular Genetics*, 6(2), 205–211. Retrieved from <http://www.ncbi.nlm.nih.gov/pubmed/9063740>
- Hama, H. (2010). Fatty acid 2-Hydroxylation in mammalian sphingolipid biology. *Biochimica et Biophysica Acta (BBA) - Molecular and Cell Biology of Lipids*, 1801(4), 405–414. <https://doi.org/10.1016/j.bbalip.2009.12.004>
- Hammer, M. B., Eleuch-Fayache, G., Schottlaender, L. V., Nehdi, H., Gibbs, J. R., Arepalli, S. K., ... Singleton, A. B. (2013). Mutations in GBA2 Cause Autosomal-Recessive Cerebellar Ataxia with Spasticity. *The American Journal of Human Genetics*, 92(2), 245–251. <https://doi.org/10.1016/j.ajhg.2012.12.012>
- Hanada, K. (2003). Serine palmitoyltransferase, a key enzyme of sphingolipid metabolism. *Biochimica et Biophysica Acta*, 1632(1–3), 16–30. Retrieved from <http://www.ncbi.nlm.nih.gov/pubmed/12782147>
- Hannun, Y. A., & Luberto, C. (2004). Lipid Metabolism: Ceramide Transfer Protein Adds a New Dimension. *Current Biology*, 14(4), R163–R165. <https://doi.org/10.1016/j.cub.2004.01.049>
- Hannun, Y. A., & Obeid, L. M. (2018). Sphingolipids and their metabolism in physiology and disease. *Nature Reviews Molecular Cell Biology*. <https://doi.org/10.1038/nrm.2017.107>
- Harlalka, G. V., Lehman, A., Chioza, B., Baple, E. L., Maroofian, R., Cross, H., ... Crosby, A. H. (2013). Mutations in B4GALNT1 (GM2 synthase) underlie a new disorder of ganglioside biosynthesis. *Brain : A Journal of Neurology*, 136(Pt 12), 3618–3624. <https://doi.org/10.1093/brain/awt270>

- Hendriksz, C. J., Corry, P. C., Wraith, J. E., Besley, G. T. N., Cooper, A., & Ferrie, C. D. (2004). Juvenile Sandhoff disease—Nine new cases and a review of the literature. *Journal of Inherited Metabolic Disease*, 27(2), 241–249. <https://doi.org/10.1023/B:BOLI.0000028777.38551.5a>
- Hisano, Y., Sakuma, T., Nakade, S., Ohga, R., Ota, S., Okamoto, H., ... Kawahara, A. (2015). Precise in-frame integration of exogenous DNA mediated by CRISPR/Cas9 system in zebrafish. *Scientific Reports*, 5(1), 8841. <https://doi.org/10.1038/srep08841>
- Hofmeister, R., Wiegmann, K., Korherr, C., Bernardo, K., Krönke, M., & Falk, W. (1997). Activation of acid sphingomyelinase by interleukin-1 (IL-1) requires the IL-1 receptor accessory protein. *The Journal of Biological Chemistry*, 272(44), 27730–27736. <https://doi.org/10.1074/JBC.272.44.27730>
- Holland, W. L., Brozinick, J. T., Wang, L. P., Hawkins, E. D., Sargent, K. M., Liu, Y., ... Summers, S. A. (2007). Inhibition of Ceramide Synthesis Ameliorates Glucocorticoid-, Saturated-Fat-, and Obesity-Induced Insulin Resistance. *Cell Metabolism*, 5(3), 167–179. <https://doi.org/10.1016/j.cmet.2007.01.002>
- Howe, K., Clark, M. D., Torroja, C. F., Torrance, J., Berthelot, C., Muffato, M., ... Stemple, D. L. (2013). The zebrafish reference genome sequence and its relationship to the human genome. *Nature*, 496(7446), 498–503. <https://doi.org/10.1038/nature12111>
- Hwang, W. Y., Fu, Y., Reyon, D., Maeder, M. L., Tsai, S. Q., Sander, J. D., ... Joung, J. K. (2013). Efficient genome editing in zebrafish using a CRISPR-Cas system. *Nature Biotechnology*, 31(3), 227–229. <https://doi.org/10.1038/nbt.2501>
- Ibhazehiebo, K., Gavrilovici, C., de la Hoz, C. L., Ma, S.-C., Rehak, R., Kaushik, G., ... Kurrasch, D. M. (2018). A novel metabolism-based phenotypic drug discovery platform in zebrafish uncovers HDACs 1 and 3 as a potential combined anti-seizure drug target. *Brain*, 141(3), 744–761. <https://doi.org/10.1093/brain/awx364>
- Idkowiak-Baldys, J., Apraiz, A., Li, L., Rahmaniyan, M., Clarke, C. J., Kravetka, J. M., ... Hannun, Y. A. (2010). Dihydroceramide desaturase activity is modulated by oxidative stress. *The Biochemical Journal*, 427(2), 265–274. <https://doi.org/10.1042/BJ20091589>
- Impraim, C., Wang, G., & Yoshida, A. (1982). Structural mutation in a major human aldehyde dehydrogenase gene results in loss of enzyme activity. *American Journal of Human Genetics*, 34(6), 837–841. Retrieved from <http://www.ncbi.nlm.nih.gov/pubmed/7180842>
- Irvine, G., & Irvine, G. (2013). An Ultra-rare Disease? Where Do We Go from Here? *Tremor and Other Hyperkinetic Movements (New York, N.Y.)*, 3. <https://doi.org/10.7916/D8GB22R8>
- Ishibashi, T., Dupree, J. L., Ikenaka, K., Hirahara, Y., Honke, K., Peles, E., ... Baba, H. (2002). A myelin galactolipid, sulfatide, is essential for maintenance of ion channels on myelinated axon but not essential for initial cluster formation. *The Journal of Neuroscience : The Official Journal of the Society for Neuroscience*, 22(15), 6507–6514. <https://doi.org/20026705>
- Jeyakumar, M., Norflus, F., Tiffit, C. J., Cortina-Borja, M., Butters, T. D., Proia, R. L., ... Platt, F. M. (2001). Enhanced survival in Sandhoff disease mice receiving a combination of substrate deprivation therapy and bone marrow transplantation. *Blood*, 97(1), 327–329. <https://doi.org/10.1182/BLOOD.V97.1.327>
- Jiang, J. C., Kirchman, P. A., Zagulski, M., Hunt, J., & Jazwinski, S. M. (1998). Homologs of the yeast longevity gene LAG1 in *Caenorhabditis elegans* and human. *Genome Research*, 8(12), 1259–1272.

- <https://doi.org/10.1101/GR.8.12.1259>
- Jung, W., Liu, C., Yu, Y., Chang, Y., Lien, W., Chao, H., ... Chan, C. (2017). Lipophagy prevents activity-dependent neurodegeneration due to dihydroceramide accumulation *in vivo*. *EMBO Reports*, *18*(7), 1150–1165. <https://doi.org/10.15252/embr.201643480>
- Kabashi, E., Bercier, V., Lissouba, A., Liao, M., Brustein, E., Rouleau, G. A., & Drapeau, P. (2011). FUS and TARDBP but Not SOD1 Interact in Genetic Models of Amyotrophic Lateral Sclerosis. *PLoS Genetics*, *7*(8), e1002214. <https://doi.org/10.1371/journal.pgen.1002214>
- Kabashi, E., Brustein, E., Champagne, N., & Drapeau, P. (2011). Zebrafish models for the functional genomics of neurogenetic disorders. *Biochimica et Biophysica Acta (BBA) - Molecular Basis of Disease*, *1812*(3), 335–345. <https://doi.org/10.1016/j.bbadis.2010.09.011>
- Kappos, L., Cohen, J., Collins, W., de Vera, A., Zhang-Auberson, L., Ritter, S., ... Francis, G. (2014). Fingolimod in relapsing multiple sclerosis: An integrated analysis of safety findings. *Multiple Sclerosis and Related Disorders*, *3*(4), 494–504. <https://doi.org/10.1016/j.msard.2014.03.002>
- Kaufman, C. K., White, R. M., & Zon, L. (2009). Chemical genetic screening in the zebrafish embryo. *Nature Protocols*, *4*(10), 1422–1432. <https://doi.org/10.1038/nprot.2009.144>
- Kawakami, K. (2007). Tol2: a versatile gene transfer vector in vertebrates. *Genome Biology*, *8*(Suppl 1), S7. <https://doi.org/10.1186/gb-2007-8-s1-s7>
- Kawakami, K., Abe, G., Asada, T., Asakawa, K., Fukuda, R., Ito, A., ... Yoshida, M. (2010). zTrap: zebrafish gene trap and enhancer trap database. *BMC Developmental Biology*, *10*(1), 105. <https://doi.org/10.1186/1471-213X-10-105>
- Keshelava, N., Seeger, R. C., Groshen, S., & Reynolds, C. P. (1998). Drug resistance patterns of human neuroblastoma cell lines derived from patients at different phases of therapy. *Cancer Research*, *58*(23), 5396–5405. Retrieved from <http://www.ncbi.nlm.nih.gov/pubmed/9850071>
- Kimmel, C. B., Ballard, W. W., Kimmel, S. R., Ullmann, B., & Schilling, T. F. (1995). Stages of embryonic development of the zebrafish. *Developmental Dynamics*, *203*(3), 253–310. <https://doi.org/10.1002/aja.1002030302>
- Köhler, S., Vasilevsky, N. A., Engelstad, M., Foster, E., McMurry, J., Aymé, S., ... Robinson, P. N. (2017). The Human Phenotype Ontology in 2017. *Nucleic Acids Research*, *45*(D1), D865–D876. <https://doi.org/10.1093/nar/gkw1039>
- Kok, F. O., Shin, M., Ni, C.-W., Gupta, A., Grosse, A. S., van Impel, A., ... Lawson, N. D. (2015). Reverse genetic screening reveals poor correlation between morpholino-induced and mutant phenotypes in zebrafish. *Developmental Cell*, *32*(1), 97–108. <https://doi.org/10.1016/j.devcel.2014.11.018>
- Kulcsár, P. I., Tálás, A., Huszár, K., Ligeti, Z., Tóth, E., Weinhardt, N., ... Welker, E. (2017). Crossing enhanced and high fidelity SpCas9 nucleases to optimize specificity and cleavage. *Genome Biology*, *18*(1), 190. <https://doi.org/10.1186/s13059-017-1318-8>
- Kulkarni, P., Yellanki, S., Medishetti, R., Sriram, D., Saxena, U., & Yogeewari, P. (2017). Novel Zebrafish EAE model: A quick *in vivo* screen for multiple sclerosis. *Multiple Sclerosis and Related Disorders*, *11*, 32–39. <https://doi.org/10.1016/j.msard.2016.11.010>
- Kundap, U. P., Kumari, Y., Othman, I., & Shaikh, M. F. (2017). Zebrafish as a Model for Epilepsy-Induced Cognitive Dysfunction: A Pharmacological, Biochemical and Behavioral Approach. *Frontiers in Pharmacology*, *8*.

- <https://doi.org/10.3389/fphar.2017.00515>
- Küry, S., Besnard, T., Ebstein, F., Khan, T. N., Gambin, T., Douglas, J., ... Isidor, B. (2017). De Novo Disruption of the Proteasome Regulatory Subunit PSMD12 Causes a Syndromic Neurodevelopmental Disorder. *The American Journal of Human Genetics*, *100*(2), 352–363. <https://doi.org/10.1016/j.ajhg.2017.01.003>
- Kwan, K. M., Fujimoto, E., Grabher, C., Mangum, B. D., Hardy, M. E., Campbell, D. S., ... Chien, C.-B. (2007). The Tol2kit: A multisite gateway-based construction kit for Tol2 transposon transgenesis constructs. *Developmental Dynamics*, *236*(11), 3088–3099. <https://doi.org/10.1002/dvdy.21343>
- Lachmann, R. H. (2006). Miglustat: Substrate reduction therapy for glycosphingolipid lysosomal storage disorders. *Drugs of Today*, *42*(1), 29. <https://doi.org/10.1358/dot.2006.42.1.937457>
- Lagace, T. A., Byers, D. M., Cook, H. W., & Ridgway, N. D. (1999). Chinese hamster ovary cells overexpressing the oxysterol binding protein (OSBP) display enhanced synthesis of sphingomyelin in response to 25-hydroxycholesterol. *Journal of Lipid Research*, *40*(1), 109–116. Retrieved from <http://www.ncbi.nlm.nih.gov/pubmed/9869656>
- Lahiri, S., Park, H., Laviad, E. L., Lu, X., Bittman, R., & Futerman, A. H. (2009). Ceramide Synthesis Is Modulated by the Sphingosine Analog FTY720 via a Mixture of Uncompetitive and Noncompetitive Inhibition in an Acyl-CoA Chain Length-dependent Manner. *Journal of Biological Chemistry*, *284*(24), 16090–16098. <https://doi.org/10.1074/jbc.M807438200>
- Lang, P. A., Schenck, M., Nicolay, J. P., Becker, J. U., Kempe, D. S., Lupescu, A., ... Lang, F. (2007). Liver cell death and anemia in Wilson disease involve acid sphingomyelinase and ceramide. *Nature Medicine*, *13*(2), 164–170. <https://doi.org/10.1038/nm1539>
- Laroni, A., Brogi, D., Morra, V. B., Guidi, L., Pozzilli, C., Comi, G., ... EAP Investigators. (2014). Safety of the first dose of fingolimod for multiple sclerosis: results of an open-label clinical trial. *BMC Neurology*, *14*(1), 65. <https://doi.org/10.1186/1471-2377-14-65>
- Launay, N., Aguado, C., Fourcade, S., Ruiz, M., Grau, L., Riera, J., ... Pujol, A. (2015). Autophagy induction halts axonal degeneration in a mouse model of X-adrenoleukodystrophy. *Acta Neuropathologica*, *129*(3), 399–415. <https://doi.org/10.1007/s00401-014-1378-8>
- Lee, A. J.-H., Awano, T., Park, G.-H., & Monani, U. R. (2012). Limited Phenotypic Effects of Selectively Augmenting the SMN Protein in the Neurons of a Mouse Model of Severe Spinal Muscular Atrophy. *PLoS ONE*, *7*(9), e46353. <https://doi.org/10.1371/journal.pone.0046353>
- Lee, S.-H., Nam, T.-S., Kim, K.-H., Kim, J. H., Yoon, W., Heo, S.-H., ... Choi, S.-Y. (2017). Aggregation-prone GFAP mutation in Alexander disease validated using a zebrafish model. *BMC Neurology*, *17*(1), 175. <https://doi.org/10.1186/s12883-017-0938-7>
- Leegwater, P. A. J., Vermeulen, G., Könst, A. A. M., Naidu, S., Mulders, J., Visser, A., ... van der Knaap, M. S. (2001). Subunits of the translation initiation factor eIF2B are mutant in leukoencephalopathy with vanishing white matter. *Nature Genetics*, *29*(4), 383–388. <https://doi.org/10.1038/ng764>
- Leegwater, P. A., Yuan, B. Q., van der Steen, J., Mulders, J., Könst, A. A., Boor, P. K., ... van der Knaap, M. S. (2001). Mutations of MLC1 (KIAA0027), encoding a putative membrane protein, cause megalencephalic leukoencephalopathy with subcortical cysts. *American Journal of Human Genetics*, *68*(4), 831–838.

- <https://doi.org/10.1086/319519>
- Lek, M., Karczewski, K. J., Minikel, E. V., Samocha, K. E., Banks, E., Fennell, T., ... Consortium, E. A. (2016). Analysis of protein-coding genetic variation in 60,706 humans. *Nature*, 536(7616), 285–291. <https://doi.org/10.1038/nature19057>
- Li, C. M., Park, J. H., He, X., Levy, B., Chen, F., Arai, K., ... Schuchman, E. H. (1999). The human acid ceramidase gene (ASAH): structure, chromosomal location, mutation analysis, and expression. *Genomics*, 62(2), 223–231. <https://doi.org/10.1006/geno.1999.5940>
- Li, H., & Durbin, R. (2009). Fast and accurate short read alignment with Burrows-Wheeler transform. *Bioinformatics*, 25(14), 1754–1760. <https://doi.org/10.1093/bioinformatics/btp324>
- Li, M., Andersson-Lendahl, M., Sejersen, T., & Arner, A. (2014). Muscle dysfunction and structural defects of dystrophin-null *sapje* mutant zebrafish larvae are rescued by ataluren treatment. *The FASEB Journal*, 28(4), 1593–1599. <https://doi.org/10.1096/fj.13-240044>
- Li, W., Xu, H., & Testai, F. D. (2016). Mechanism of action and clinical potential of fingolimod for the treatment of stroke. *Frontiers in Neurology*, 7(AUG). <https://doi.org/10.3389/fneur.2016.00139>
- Lim, K. G., Tonelli, F., Li, Z., Lu, X., Bittman, R., Pyne, S., & Pyne, N. J. (2011). FTY720 analogues as sphingosine kinase 1 inhibitors: enzyme inhibition kinetics, allosterism, proteasomal degradation, and actin rearrangement in MCF-7 breast cancer cells. *The Journal of Biological Chemistry*, 286(21), 18633–18640. <https://doi.org/10.1074/jbc.M111.220756>
- Lionaki, E., Markaki, M., Palikaras, K., & Tavernarakis, N. (2015). Mitochondria, autophagy and age-associated neurodegenerative diseases: New insights into a complex interplay. *Biochimica et Biophysica Acta (BBA) - Bioenergetics*, 1847(11), 1412–1423. <https://doi.org/10.1016/j.bbabi.2015.04.010>
- Lissens, W., Arena, A., Seneca, S., Rafi, M., Sorge, G., Liebaers, I., ... Fiumara, A. (2007). A single mutation in the GALC gene is responsible for the majority of late onset Krabbe disease patients in the Catania (Sicily, Italy) region. *Human Mutation*, 28(7), 742–742. <https://doi.org/10.1002/humu.9500>
- Liu, L., Li, Y., Li, S., Hu, N., He, Y., Pong, R., ... Law, M. (2012). Comparison of Next-Generation Sequencing Systems. *Journal of Biomedicine and Biotechnology*, 2012, 1–11. <https://doi.org/10.1155/2012/251364>
- Liu, X., & Hajnóczky, G. (2011). Altered fusion dynamics underlie unique morphological changes in mitochondria during hypoxia–reoxygenation stress. *Cell Death & Differentiation*, 18(10), 1561–1572. <https://doi.org/10.1038/cdd.2011.13>
- López-Erauskin, J., Ferrer, I., Galea, E., & Pujol, A. (2013). Cyclophilin D as a potential target for antioxidants in neurodegeneration: The X-ALD case. In *Biological Chemistry* (Vol. 394, pp. 621–629). <https://doi.org/10.1515/hsz-2012-0323>
- López-Erauskin, J., Galino, J., Ruiz, M., Cuezva, J. M., Fabregat, I., Cacabelos, D., ... Pujol, A. (2013). Impaired mitochondrial oxidative phosphorylation in the peroxisomal disease X-linked adrenoleukodystrophy. *Human Molecular Genetics*, 22(16), 3296–3305. <https://doi.org/10.1093/hmg/ddt186>
- Losón, O. C., Song, Z., Chen, H., & Chan, D. C. (2013). Fis1, Mff, MiD49, and MiD51 mediate Drp1 recruitment in mitochondrial fission. *Molecular Biology of the Cell*, 24(5), 659–667. <https://doi.org/10.1091/mbc.E12-10-0721>
- Louwette, S., Régál, L., Wittevrongel, C., Thys, C., Vandeweeghde, G., Decuyper, E., ... Freson, K. (2013). NPC1 defect results in abnormal platelet formation and

- function: studies in Niemann–Pick disease type C1 patients and zebrafish. *Human Molecular Genetics*, 22(1), 61–73. <https://doi.org/10.1093/hmg/dds401>
- Loviglio, M. N., Arbogast, T., Jønch, A. E., Collins, S. C., Popadin, K., Bonnet, C. S., ... Reymond, A. (2017). The Immune Signaling Adaptor LAT Contributes to the Neuroanatomical Phenotype of 16p11.2 BP2-BP3 CNVs. *American Journal of Human Genetics*, 101(4), 564–577. <https://doi.org/10.1016/j.ajhg.2017.08.016>
- Lukina, E., Watman, N., Arreguin, E. A., Dragosky, M., Iastrebner, M., Rosenbaum, H., ... Peterschmitt, M. J. (2010). Improvement in hematological, visceral, and skeletal manifestations of Gaucher disease type 1 with oral eliglustat tartrate (Genz-112638) treatment: 2-year results of a phase 2 study. *Blood*, 116(20), 4095–4098. <https://doi.org/10.1182/blood-2010-06-293902>
- Lupski, J. R., Reid, J. G., Gonzaga-Jauregui, C., Rio Deiros, D., Chen, D. C. Y., Nazareth, L., ... Gibbs, R. A. (2010). Whole-Genome Sequencing in a Patient with Charcot–Marie–Tooth Neuropathy. *New England Journal of Medicine*, 362(13), 1181–1191. <https://doi.org/10.1056/NEJMoa0908094>
- Lyon, G., Fattal-Valevski, A., & Kolodny, E. H. (2006). Leukodystrophies. *Topics in Magnetic Resonance Imaging*, 17(4), 219–242. <https://doi.org/10.1097/RMR.0b013e31804c99d4>
- MacPhail, R. C., Brooks, J., Hunter, D. L., Padnos, B., Irons, T. D., & Padilla, S. (2009). Locomotion in larval zebrafish: Influence of time of day, lighting and ethanol. *NeuroToxicology*, 30(1), 52–58. <https://doi.org/10.1016/j.neuro.2008.09.011>
- MacRae, C. A., & Peterson, R. T. (2015). Zebrafish as tools for drug discovery. *Nature Reviews Drug Discovery*, 14(10), 721–731. <https://doi.org/10.1038/nrd4627>
- Majewski, J., Schwartzenuber, J., Lalonde, E., Montpetit, A., & Jabado, N. (2011). What can exome sequencing do for you? *Journal of Medical Genetics*, 48(9), 580–589. <https://doi.org/10.1136/jmedgenet-2011-100223>
- Mamanova, L., Coffey, A. J., Scott, C. E., Kozarewa, I., Turner, E. H., Kumar, A., ... Turner, D. J. (2010). Target-enrichment strategies for next-generation sequencing. *Nature Methods*, 7(2), 111–118. <https://doi.org/10.1038/nmeth.1419>
- Margolin, D. H., Kousi, M., Chan, Y.-M., Lim, E. T., Schmahmann, J. D., Hadjivassiliou, M., ... Seminara, S. B. (2013). Ataxia, Dementia, and Hypogonadotropism Caused by Disordered Ubiquitination. *From the Department of Neurology N Engl J Med*, 21368(23), 1992–2003. <https://doi.org/10.1056/NEJMoa1215993>
- Margulies, M., Egholm, M., Altman, W. E., Attiya, S., Bader, J. S., Bemben, L. A., ... Rothberg, J. M. (2005). Genome sequencing in microfabricated high-density picolitre reactors. *Nature*, 437(7057), 376–380. <https://doi.org/10.1038/nature03959>
- Martin, E., Schüle, R., Smets, K., Rastetter, A., Boukhris, A., Loureiro, J. L., ... Stevanin, G. (2013). Loss of Function of Glucocerebrosidase GBA2 Is Responsible for Motor Neuron Defects in Hereditary Spastic Paraplegia. *The American Journal of Human Genetics*, 92(2), 238–244. <https://doi.org/10.1016/j.ajhg.2012.11.021>
- McKenna, A., Hanna, M., Banks, E., Sivachenko, A., Cibulskis, K., Kernytzky, A., ... DePristo, M. A. (2010). The genome analysis toolkit: A MapReduce framework for analyzing next-generation DNA sequencing data. *Genome Research*, 20(9), 1297–1303. <https://doi.org/10.1101/gr.107524.110>
- McKusick, V. A. (2007). Mendelian Inheritance in Man and Its Online Version, OMIM. *The American Journal of Human Genetics*, 80(4), 588–604. <https://doi.org/10.1086/514346>

- Mehling, M., Johnson, T. A., Antel, J., Kappos, L., & Bar-Or, A. (2011). Clinical immunology of the sphingosine 1-phosphate receptor modulator fingolimod (FTY720) in multiple sclerosis. *Neurology*, *76*(Issue 8, Supplement 3), S20–S27. <https://doi.org/10.1212/WNL.0b013e31820db341>
- Mencarelli, C., Martinez–Martinez, P., & Martinez-Martinez, P. Ceramide function in the brain: When a slight tilt is enough, *70 Cellular and Molecular Life Sciences §* (2013). <https://doi.org/10.1007/s00018-012-1038-x>
- Mendoza-Ferreira, N., Coutelier, M., Janzen, E., Hosseinibarkooie, S., Löhr, H., Schneider, S., ... Wirth, B. (2018). Biallelic CHP1 mutation causes human autosomal recessive ataxia by impairing NHE1 function. *Neurology Genetics*, *4*(1), e209. <https://doi.org/10.1212/NXG.0000000000000209>
- Menke, A. L., Spitsbergen, J. M., Wolterbeek, A. P. M., & Woutersen, R. A. (2011). Normal Anatomy and Histology of the Adult Zebrafish. *Toxicologic Pathology*, *39*(5), 759–775. <https://doi.org/10.1177/0192623311409597>
- Merrill, R. A., Dagda, R. K., Dickey, A. S., Cribbs, J. T., Green, S. H., Usachev, Y. M., & Strack, S. (2011). Mechanism of Neuroprotective Mitochondrial Remodeling by PKA/AKAP1. *PLoS Biology*, *9*(4), e1000612. <https://doi.org/10.1371/journal.pbio.1000612>
- Micu, I., Plemel, J. R., Caprariello, A. V., Nave, K.-A., & Stys, P. K. (2017). Axo-myelinic neurotransmission: a novel mode of cell signalling in the central nervous system. *Nature Reviews Neuroscience*, *19*(1), 58–58. <https://doi.org/10.1038/nrn.2017.166>
- Miller, D. H., Robb, S. A., Ormerod, I. E., Pohl, K. R., MacManus, D. G., Kendall, B. E., ... McDonald, W. I. (1990). Magnetic resonance imaging of inflammatory and demyelinating white-matter diseases of childhood. *Developmental Medicine and Child Neurology*, *32*(2), 97–107. Retrieved from <http://www.ncbi.nlm.nih.gov/pubmed/2338183>
- Miron, V. E., Jung, C. G., Kim, H. J., Kennedy, T. E., Soliven, B., & Antel, J. P. (2008). FTY720 modulates human oligodendrocyte progenitor process extension and survival. *Annals of Neurology*, *63*(1), 61–71. <https://doi.org/10.1002/ana.21227>
- Mizushima, N., Levine, B., Cuervo, A. M., & Klionsky, D. J. (2008). Autophagy fights disease through cellular self-digestion. *Nature*, *451*(7182), 1069–1075. <https://doi.org/10.1038/nature06639>
- Mizutani, Y., Kihara, A., & Igarashi, Y. (2004). Identification of the human sphingolipid C4-hydroxylase, hDES2, and its up-regulation during keratinocyte differentiation. *FEBS Letters*, *563*(1–3), 93–97. [https://doi.org/10.1016/S0014-5793\(04\)00274-1](https://doi.org/10.1016/S0014-5793(04)00274-1)
- Monani, U. R. (2005). Spinal Muscular Atrophy: A Deficiency in a Ubiquitous Protein; a Motor Neuron-Specific Disease. *Neuron*, *48*(6), 885–895. <https://doi.org/10.1016/j.neuron.2005.12.001>
- Morell, P. (1984). A correlative synopsis of the leukodystrophies. *Neuropediatrics*. <https://doi.org/10.1055/s-2008-1052383>
- Morell, P., & Quarles, R. H. (1999). Myelin Formation, Structure and Biochemistry. Retrieved from <https://www.ncbi.nlm.nih.gov/books/NBK20402/>
- Mosbech, M.-B., Olsen, A. S. B., Neess, D., Ben-David, O., Klitten, L. L., Larsen, J., ... Færgeman, N. J. (2014). Reduced ceramide synthase 2 activity causes progressive myoclonic epilepsy. *Annals of Clinical and Translational Neurology*, *1*(2), 88–98. <https://doi.org/10.1002/acn3.28>
- Moser, H. W. (1997). Adrenoleukodystrophy: Phenotype, genetics, pathogenesis and therapy. *Brain*. <https://doi.org/10.1093/brain/120.8.1485>

- Murphy, S. M., Laura, M., Fawcett, K., Pandraud, A., Liu, Y.-T., Davidson, G. L., ... Reilly, M. M. (2012). Charcot–Marie–Tooth disease: frequency of genetic subtypes and guidelines for genetic testing. *Journal of Neurology, Neurosurgery & Psychiatry*, *83*(7), 706–710. <https://doi.org/10.1136/jnnp-2012-302451>
- Mutarelli, M., Marwah, V. S., Rispoli, R., Carrella, D., Dharmalingam, G., Oliva, G., & di Bernardo, D. (2014). A community-based resource for automatic exome variant-calling and annotation in Mendelian disorders. *BMC Genomics*. <https://doi.org/10.1186/1471-2164-15-S3-S5>
- Nakayama, T., Al-Maawali, A., El-Quessny, M., Rajab, A., Khalil, S., Stoler, J. M., ... Mochida, G. H. (2015). Mutations in PYCR2, Encoding Pyrroline-5-Carboxylate Reductase 2, Cause Microcephaly and Hypomyelination. *American Journal of Human Genetics*, *96*(5), 709–719. <https://doi.org/10.1016/j.ajhg.2015.03.003>
- Neufeld, E. F. (1991). Lysosomal Storage Diseases. *Annual Review of Biochemistry*, *60*(1), 257–280. <https://doi.org/10.1146/annurev.bi.60.070191.001353>
- Newton, J., Hait, N. C., Maceyka, M., Colaco, A., Maczys, M., Wassif, C. A., ... Spiegel, S. (2017). FTY720/fingolimod increases NPC1 and NPC2 expression and reduces cholesterol and sphingolipid accumulation in Niemann-Pick type C mutant fibroblasts. *FASEB Journal*, *31*(4), 1719–1730. <https://doi.org/10.1096/fj.201601041R>
- Ng, S. B., Buckingham, K. J., Lee, C., Bigham, A. W., Tabor, H. K., Dent, K. M., ... Bamshad, M. J. (2010). Exome sequencing identifies the cause of a mendelian disorder. *Nature Genetics*, *42*(1), 30–35. <https://doi.org/10.1038/ng.499>
- Ng, S. B., Turner, E. H., Robertson, P. D., Flygare, S. D., Bigham, A. W., Lee, C., ... Shendure, J. (2009). Targeted capture and massively parallel sequencing of 12 human exomes. *Nature*, *461*(7261), 272–276. <https://doi.org/10.1038/nature08250>
- Niceta, M., Stellacci, E., Gripp, K. W., Zampino, G., Kousi, M., Anselmi, M., ... Tartaglia, M. (2015). Mutations Impairing GSK3-Mediated MAF Phosphorylation Cause Cataract, Deafness, Intellectual Disability, Seizures, and a Down Syndrome-like Facies. *American Journal of Human Genetics*, *96*(5), 816–825. <https://doi.org/10.1016/j.ajhg.2015.03.001>
- Nilsson, O., & Svennerholm, L. (1982). Accumulation of glucosylceramide and glucosylsphingosine (psychosine) in cerebrum and cerebellum in infantile and juvenile Gaucher disease. *Journal of Neurochemistry*, *39*(3), 709–718. Retrieved from <http://www.ncbi.nlm.nih.gov/pubmed/7097276>
- Norton, N., Li, D., Rieder, M. J., Siegfried, J. D., Rampersaud, E., Züchner, S., ... Hershberger, R. E. (2011). Genome-wide Studies of Copy Number Variation and Exome Sequencing Identify Rare Variants in BAG3 as a Cause of Dilated Cardiomyopathy. *The American Journal of Human Genetics*, *88*(3), 273–282. <https://doi.org/10.1016/j.ajhg.2011.01.016>
- O'BRIEN, J. S. (1965). STABILITY OF THE MYELIN MEMBRANE. *Science (New York, N.Y.)*, *147*(3662), 1099–1107. Retrieved from <http://www.ncbi.nlm.nih.gov/pubmed/14242030>
- O'Rawe, J. A., Wu, Y., Dörfel, M. J., Rope, A. F., Au, P. Y. B., Parboosingh, J. S., ... Lyon, G. J. (2015). TAF1 Variants Are Associated with Dysmorphic Features, Intellectual Disability, and Neurological Manifestations. *American Journal of Human Genetics*, *97*(6), 922–932. <https://doi.org/10.1016/j.ajhg.2015.11.005>
- O'Sullivan, C., & Dev, K. K. (2015). Galactosylsphingosine (psychosine)-induced demyelination is attenuated by sphingosine 1-phosphate signalling. *Journal of Cell Science*, *128*(21), 3878–3887. <https://doi.org/10.1242/jcs.169342>
- Ogawa, Y., Sano, T., Irisa, M., Kodama, T., Saito, T., Furusawa, E., ... Oishi, K.

- (2017). FcR γ -dependent immune activation initiates astrogliosis during the asymptomatic phase of Sandhoff disease model mice. *Scientific Reports*, 7. <https://doi.org/10.1038/srep40518>
- Oh, H. J., Choi, D., Goh, C. J., & Hahn, Y. (2015). Loss of gene function and evolution of human phenotypes. *BMB Reports*, 48(7), 373–379. <https://doi.org/10.5483/BMBREP.2015.48.7.073>
- Okada, S., & O'Brien, J. S. (1969). Tay-Sachs disease: generalized absence of a beta-D-N-acetylhexosaminidase component. *Science (New York, N.Y.)*, 165(3894), 698–700. Retrieved from <http://www.ncbi.nlm.nih.gov/pubmed/5793973>
- Omae, F., Miyazaki, M., Enomoto, A., & Suzuki, A. (2004). Identification of an essential sequence for dihydroceramide C-4 hydroxylase activity of mouse DES2. *FEBS Letters*, 576(1–2), 63–67. <https://doi.org/10.1016/j.febslet.2004.08.060>
- Pan, B., Fromholt, S. E., Hess, E. J., Crawford, T. O., Griffin, J. W., Sheikh, K. A., & Schnaar, R. L. (2005). Myelin-associated glycoprotein and complementary axonal ligands, gangliosides, mediate axon stability in the CNS and PNS: neuropathology and behavioral deficits in single- and double-null mice. *Experimental Neurology*, 195(1), 208–217. <https://doi.org/10.1016/j.expneurol.2005.04.017>
- Pandey, A. K., & Williams, R. W. (2014). Genetics of gene expression in CNS. *International Review of Neurobiology*, 116, 195–231. <https://doi.org/10.1016/B978-0-12-801105-8.00008-4>
- Papáčková, Z., & Cahová, M. (2014). Important Role of Autophagy in Regulation of Metabolic Processes in Health, Disease and Aging. *Physiol. Res*, 63, 409–420. Retrieved from www.biomed.cas.cz/physiolres
- Pardo, A. Di, Basit, A., Armirotti, A., Amico, E., Castaldo, S., Pepe, G., ... Maglione, V. (2017). De novo synthesis of sphingolipids is defective in experimental models of Huntington's disease. *Frontiers in Neuroscience*, 11(DEC). <https://doi.org/10.3389/fnins.2017.00698>
- Pathak, D., Mehendale, N., Singh, S., Mallik, R., & Kamat, S. S. (2018). Lipidomics suggests a new role for ceramide synthase in phagocytosis. *ACS Chemical Biology*, acschembio.8b00438. <https://doi.org/10.1021/acschembio.8b00438>
- Peng, J.-Y., Lin, C.-C., Chen, Y.-J., Kao, L.-S., Liu, Y.-C., Chou, C.-C., ... Hsu, C.-N. (2011). Automatic Morphological Subtyping Reveals New Roles of Caspases in Mitochondrial Dynamics. *PLoS Computational Biology*, 7(10), e1002212. <https://doi.org/10.1371/journal.pcbi.1002212>
- Penno, A., Reilly, M. M., Houlden, H., Laurá, M., Rentsch, K., Niederkofler, V., ... Hornemann, T. (2010). Hereditary sensory neuropathy type 1 is caused by the accumulation of two neurotoxic sphingolipids. *The Journal of Biological Chemistry*, 285(15), 11178–11187. <https://doi.org/10.1074/jbc.M109.092973>
- Peterson, R. T., Shaw, S. Y., Peterson, T. A., Milan, D. J., Zhong, T. P., Schreiber, S. L., ... Fishman, M. C. (2004). Chemical suppression of a genetic mutation in a zebrafish model of aortic coarctation. *Nature Biotechnology*, 22(5), 595–599. <https://doi.org/10.1038/nbt963>
- Pewzner-Jung, Y., Ben-Dor, S., & Futerman, A. H. (2006). When do Lasses (longevity assurance genes) become CerS (ceramide synthases)? Insights into the regulation of ceramide synthesis. *The Journal of Biological Chemistry*, 281(35), 25001–25005. <https://doi.org/10.1074/jbc.R600010200>
- Prabakaran, S., Swatton, J. E., Ryan, M. M., Huffaker, S. J., Huang, J.-J., Griffin, J. L., ... Bahn, S. (2004). Mitochondrial dysfunction in schizophrenia: evidence for compromised brain metabolism and oxidative stress. *Molecular Psychiatry*, 9(7), 684–697. <https://doi.org/10.1038/sj.mp.4001511>

- Pujol, A., Hindelang, C., Callizot, N., Bartsch, U., Schachner, M., & Mandel, J. L. (2002). Late onset neurological phenotype of the X-ALD gene inactivation in mice: a mouse model for adrenomyeloneuropathy. *Human Molecular Genetics*, *11*(5), 499–505. <https://doi.org/10.1093/hmg/11.5.499>
- Puranam, K., Qian, W.-H., Nikbakht, K., Venable, M., Obeid, L., Hannun, Y., & Boustany, R.-M. (1997). Upregulation of Bcl-2 and Elevation of Ceramide in Batten Disease. *Neuropediatrics*, *28*(01), 37–41. <https://doi.org/10.1055/s-2007-973664>
- Rademakers, R., Baker, M., Nicholson, A. M., Rutherford, N. J., Finch, N., Soto-Ortolaza, A., ... Wszolek, Z. K. (2012). Mutations in the colony stimulating factor 1 receptor (CSF1R) gene cause hereditary diffuse leukoencephalopathy with spheroids. *Nature Genetics*, *44*(2), 200–205. <https://doi.org/10.1038/ng.1027>
- Rapola, J. (1994). Lysosomal Storage Diseases in Adults. *Pathology - Research and Practice*, *190*(8), 759–766. [https://doi.org/10.1016/S0344-0338\(11\)80422-X](https://doi.org/10.1016/S0344-0338(11)80422-X)
- Realini, N., Solorzano, C., Pagliuca, C., Pizzirani, D., Armirotti, A., Luciani, R., ... Piomelli, D. (2013). Discovery of highly potent acid ceramidase inhibitors with in vitro tumor chemosensitizing activity. *Scientific Reports*, *3*(1), 1035. <https://doi.org/10.1038/srep01035>
- Reijnders, M. R. F., Anson, N. M., Kousi, M., Yue, W. W., Tan, P. L., Clarkson, K., ... Banka, S. (2017). RAC1 Missense Mutations in Developmental Disorders with Diverse Phenotypes. *American Journal of Human Genetics*, *101*(3), 466–477. <https://doi.org/10.1016/j.ajhg.2017.08.007>
- Richards, S., Aziz, N., Bale, S., Bick, D., Das, S., Gastier-Foster, J., ... ACMG Laboratory Quality Assurance Committee. (2015). Standards and guidelines for the interpretation of sequence variants: a joint consensus recommendation of the American College of Medical Genetics and Genomics and the Association for Molecular Pathology. *Genetics in Medicine*, *17*(5), 405–423. <https://doi.org/10.1038/gim.2015.30>
- Richter, T., Nestler-Parr, S., Babela, R., Khan, Z. M., Tesoro, T., Molsen, E., ... International Society for Pharmacoeconomics and Outcomes Research Rare Disease Special Interest Group. (2015). Rare Disease Terminology and Definitions—A Systematic Global Review: Report of the ISPOR Rare Disease Special Interest Group. *Value in Health*, *18*(6), 906–914. <https://doi.org/10.1016/j.jval.2015.05.008>
- Riebeling, C., Allegood, J. C., Wang, E., Merrill, A. H., & Futerman, A. H. (2003). Two mammalian longevity assurance gene (LAG1) family members, trh1 and trh4, regulate dihydroceramide synthesis using different fatty acyl-CoA donors. *The Journal of Biological Chemistry*, *278*(44), 43452–43459. <https://doi.org/10.1074/jbc.M307104200>
- Rodriguez-Cuenca, S., Barbarroja, N., & Vidal-Puig, A. (2015). Dihydroceramide desaturase 1, the gatekeeper of ceramide induced lipotoxicity. *Biochimica et Biophysica Acta - Molecular and Cell Biology of Lipids*. <https://doi.org/10.1016/j.bbalip.2014.09.021>
- Rosivatz, E., & Woscholski, R. (2011). Removal or masking of phosphatidylinositol(4,5)bisphosphate from the outer mitochondrial membrane causes mitochondrial fragmentation. *Cellular Signalling*, *23*(2), 478–486. <https://doi.org/10.1016/j.cellsig.2010.10.025>
- Rossi, A., Kontarakis, Z., Gerri, C., Nolte, H., Hölper, S., Krüger, M., & Stainier, D. Y. R. (2015). Genetic compensation induced by deleterious mutations but not gene knockdowns. *Nature*, *524*(7564), 230–233. <https://doi.org/10.1038/nature14580>

- Rotthier, A., Baets, J., Timmerman, V., & Janssens, K. (2012). Mechanisms of disease in hereditary sensory and autonomic neuropathies. *Nature Reviews Neurology*, 8(2), 73–85. <https://doi.org/10.1038/nrneuro.2011.227>
- Ruangsiluk, W., Grosskurth, S. E., Ziemek, D., Kuhn, M., des Etages, S. G., & Francone, O. L. (2012). Silencing of enzymes involved in ceramide biosynthesis causes distinct global alterations of lipid homeostasis and gene expression. *Journal of Lipid Research*, 53(8), 1459–1471. <https://doi.org/10.1194/jlr.M020941>
- Rubinstein, A. L. (2003). Zebrafish: from disease modeling to drug discovery. *Current Opinion in Drug Discovery & Development*, 6(2), 218–223. Retrieved from <http://www.ncbi.nlm.nih.gov/pubmed/12669457>
- Saiki, R. K., Scharf, S., Faloona, F., Mullis, K. B., Horn, G. T., Erlich, H. A., & Arnheim, N. (1985). Enzymatic amplification of beta-globin genomic sequences and restriction site analysis for diagnosis of sickle cell anemia. *Science (New York, N.Y.)*, 230(4732), 1350–1354. Retrieved from <http://www.ncbi.nlm.nih.gov/pubmed/2999980>
- Sanger, F., Nicklen, S., & Coulson, A. R. (1977). DNA sequencing with chain-terminating inhibitors. *Proceedings of the National Academy of Sciences of the United States of America*, 74(12), 5463–5467. <https://doi.org/10.1073/PNAS.74.12.5463>
- Sango, K., Yamanaka, S., Hoffmann, A., Okuda, Y., Grinberg, A., Westphal, H., ... Proia, R. L. (1995). Mouse models of Tay–Sachs and Sandhoff diseases differ in neurologic phenotype and ganglioside metabolism. *Nature Genetics*, 11(2), 170–176. <https://doi.org/10.1038/ng1095-170>
- Sanvicens, N., & Cotter, T. G. (2006). Ceramide is the key mediator of oxidative stress-induced apoptosis in retinal photoreceptor cells, 98(5), 1432–1444. <https://doi.org/10.1111/j.1471-4159.2006.03977.x>
- Sawkar, A. R., Cheng, W.-C., Beutler, E., Wong, C.-H., Balch, W. E., & Kelly, J. W. (2002). Chemical chaperones increase the cellular activity of N370S beta -glucosidase: a therapeutic strategy for Gaucher disease. *Proceedings of the National Academy of Sciences of the United States of America*, 99(24), 15428–15433. <https://doi.org/10.1073/pnas.192582899>
- Scandroglio, F., Venkata, J. K., Loberto, N., Prioni, S., Schuchman, E. H., Chigorno, V., ... Sonnino, S. (2008). Lipid content of brain, brain membrane lipid domains, and neurons from acid sphingomyelinase deficient mice. *Journal of Neurochemistry*, 107(2), 329–338. <https://doi.org/10.1111/j.1471-4159.2008.05591.x>
- Schenck, M., Carpinteiro, A., Grassmé, H., Lang, F., & Gulbins, E. (2007). Ceramide: Physiological and pathophysiological aspects. *Archives of Biochemistry and Biophysics*, 462(2), 171–175. <https://doi.org/10.1016/j.abb.2007.03.031>
- Scheper, G. C., van der Kloek, T., van Anandel, R. J., van Berkel, C. G. M., Sissler, M., Smet, J., ... van der Knaap, M. S. (2007). Mitochondrial aspartyl-tRNA synthetase deficiency causes leukoencephalopathy with brain stem and spinal cord involvement and lactate elevation. *Nature Genetics*, 39(4), 534–539. <https://doi.org/10.1038/ng2013>
- Schiffmann, R., & Van Der Knaap, M. S. (2009). Invited Article: An MRI-based approach to the diagnosis of white matter disorders. *Neurology*. <https://doi.org/10.1212/01.wnl.0000343049.00540.c8>
- Schloss, J. A. (2008). How to get genomes at one ten-thousandth the cost. *Nature Biotechnology*, 26(10), 1113–1115. <https://doi.org/10.1038/nbt1008-1113>
- Schmitt, S., Cantuti Castelvetti, L., & Simons, M. (2015). Metabolism and functions of

- lipids in myelin. *Biochimica et Biophysica Acta - Molecular and Cell Biology of Lipids*, 1851(8), 999–1005. <https://doi.org/10.1016/j.bbalip.2014.12.016>
- Schnaar, R. L., & Lopez, P. H. H. (2009). Myelin-associated glycoprotein and its axonal receptors. *Journal of Neuroscience Research*, 87(15), 3267–3276. <https://doi.org/10.1002/jnr.21992>
- Schubert, J., Siekierska, A., Langlois, M., May, P., Huneau, C., Becker, F., ... Lerche, H. (2014). Mutations in STX1B, encoding a presynaptic protein, cause fever-associated epilepsy syndromes. *Nature Genetics*, 46(12), 1327–1332. <https://doi.org/10.1038/ng.3130>
- Schuchman, E. H. (2010). Acid sphingomyelinase, cell membranes and human disease: Lessons from Niemann-Pick disease. *FEBS Letters*, 584(9), 1895–1900. <https://doi.org/10.1016/j.febslet.2009.11.083>
- Schütze, S., Potthoff, K., Machleidt, T., Berkovic, D., Wiegmann, K., & Krönke, M. (1992). TNF activates NF-kappa B by phosphatidylcholine-specific phospholipase C-induced "acidic" sphingomyelin breakdown. *Cell*, 71(5), 765–776. Retrieved from <http://www.ncbi.nlm.nih.gov/pubmed/1330325>
- Schwartz, N. U., Linzer, R. W., Truman, J. P., Gurevich, M., Hannun, Y. A., Senkal, C. E., & Obeid, L. M. (2018). Decreased ceramide underlies mitochondrial dysfunction in Charcot-Marie-Tooth 2F. *FASEB Journal*, 32(3), 1716–1728. <https://doi.org/10.1096/fj.201701067R>
- Schwarz, a., & Futerman, a H. (1997). Distinct roles for ceramide and glucosylceramide at different stages of neuronal growth. *The Journal of Neuroscience : The Official Journal of the Society for Neuroscience*, 17(9), 2929–2938.
- Schwarz, E., Prabakaran, S., Whitfield, P., Major, H., Leweke, F. M., Koethe, D., ... Bahn, S. (2008). High Throughput Lipidomic Profiling of Schizophrenia and Bipolar Disorder Brain Tissue Reveals Alterations of Free Fatty Acids, Phosphatidylcholines, and Ceramides. *Journal of Proteome Research*, 7(10), 4266–4277. <https://doi.org/10.1021/pr800188y>
- Sedel, F. (2007). Les maladies de Niemann-Pick de l'adulte. *La Revue de Médecine Interne*, 28, S292–S293. <https://doi.org/10.1016/j.revmed.2007.09.017>
- See, K., Yadav, P., Giegerich, M., Cheong, P. S., Graf, M., Vyas, H., ... Winkler, C. (2014). SMN deficiency alters Nrnx2 expression and splicing in zebrafish and mouse models of spinal muscular atrophy. *Human Molecular Genetics*, 23(7), 1754–1770. <https://doi.org/10.1093/hmg/ddt567>
- Serdar, M., Herz, J., Kempe, K., Lumpe, K., Reinboth, B. S., Sizonenko, S. V., ... Bendix, I. (2016). Fingolimod protects against neonatal white matter damage and long-term cognitive deficits caused by hyperoxia. *Brain, Behavior, and Immunity*, 52, 106–119. <https://doi.org/10.1016/j.bbi.2015.10.004>
- Sheikh, K. A., Sun, J., Liu, Y., Kawai, H., Crawford, T. O., Proia, R. L., ... Schnaar, R. L. (1999). Mice lacking complex gangliosides develop Wallerian degeneration and myelination defects. *Proceedings of the National Academy of Sciences of the United States of America*, 96(13), 7532–7537. Retrieved from <http://www.ncbi.nlm.nih.gov/pubmed/10377449>
- Shendure, J., & Ji, H. (2008). Next-generation DNA sequencing. *Nature Biotechnology*, 26(10), 1135–1145. <https://doi.org/10.1038/nbt1486>
- Shore, E. M., Xu, M., Feldman, G. J., Fenstermacher, D. A., Cho, T.-J., Choi, I. H., ... Kaplan, F. S. (2006). A recurrent mutation in the BMP type I receptor ACVR1 causes inherited and sporadic fibrodysplasia ossificans progressiva. *Nature Genetics*, 38(5), 525–527. <https://doi.org/10.1038/ng1783>

- Siddique, M. M., Li, Y., Chaurasia, B., Kaddai, V. A., & Summers, S. A. (2015). Dihydroceramides: From bit players to lead actors. *Journal of Biological Chemistry*, 290(25), 15371–15379. <https://doi.org/10.1074/jbc.R115.653204>
- Siddique, M. M., Li, Y., Wang, L., Ching, J., Mal, M., Ilkayeva, O., ... Summers, S. A. (2013). Ablation of Dihydroceramide Desaturase 1, a Therapeutic Target for the Treatment of Metabolic Diseases, Simultaneously Stimulates Anabolic and Catabolic Signaling. *Molecular and Cellular Biology*, 33(11), 2353–2369. <https://doi.org/10.1128/MCB.00226-13>
- Signorelli, P., Munoz-Olaya, J. M., Gagliostro, V., Casas, J., Ghidoni, R., & Fabriàs, G. (2009). Dihydroceramide intracellular increase in response to resveratrol treatment mediates autophagy in gastric cancer cells. *Cancer Letters*, 282(2), 238–243. <https://doi.org/10.1016/j.canlet.2009.03.020>
- Simpson, M. A., Cross, H., Proukakis, C., Priestman, D. A., Neville, D. C. A., Reinkensmeier, G., ... Crosby, A. H. (2004). Infantile-onset symptomatic epilepsy syndrome caused by a homozygous loss-of-function mutation of GM3 synthase. *Nature Genetics*, 36(11), 1225–1229. <https://doi.org/10.1038/ng1460>
- Sirisi, S., Folgueira, M., López-Hernández, T., Minieri, L., Pérez-Rius, C., Gaitán-Peñas, H., ... Barrallo-Gimeno, A. (2014). Megalencephalic leukoencephalopathy with subcortical cysts protein 1 regulates glial surface localization of GLIALCAM from fish to humans. *Human Molecular Genetics*, 23(19), 5069–5086. <https://doi.org/10.1093/hmg/ddu231>
- Smith, D., Wallom, K.-L., Williams, I. M., Jeyakumar, M., & Platt, F. M. (2009). Beneficial effects of anti-inflammatory therapy in a mouse model of Niemann-Pick disease type C1. *Neurobiology of Disease*, 36(2), 242–251. <https://doi.org/10.1016/j.nbd.2009.07.010>
- Sobreira, N., Schiettecatte, F., Valle, D., & Hamosh, A. (2015). GeneMatcher: a matching tool for connecting investigators with an interest in the same gene. *Human Mutation*, 36(10), 928–930. <https://doi.org/10.1002/humu.22844>
- SRIVASTAVA, S. K., & BEUTLER, E. (1973). Hexosaminidase-A and Hexosaminidase-B: Studies in Tay-Sachs' and Sandhoff's Disease. *Nature*, 241(5390), 463–463. <https://doi.org/10.1038/241463a0>
- Stainier, D. Y. R., Raz, E., Lawson, N. D., Ekker, S. C., Burdine, R. D., Eisen, J. S., ... Moens, C. B. (2017). Guidelines for morpholino use in zebrafish. *PLOS Genetics*, 13(10), e1007000. <https://doi.org/10.1371/journal.pgen.1007000>
- Stankiewicz, P., Khan, T. N., Szafranski, P., Slattery, L., Streff, H., Vetrini, F., ... Yang, Y. (2017). Haploinsufficiency of the Chromatin Remodeler BPTF Causes Syndromic Developmental and Speech Delay, Postnatal Microcephaly, and Dysmorphic Features. *The American Journal of Human Genetics*, 101(4), 503–515. <https://doi.org/10.1016/j.ajhg.2017.08.014>
- Steenweg, M. E., Ghezzi, D., Haack, T., Abbink, T. E. M., Martinelli, D., van Berkel, C. G. M., ... Zeviani, M. (2012). Leukoencephalopathy with thalamus and brainstem involvement and high lactate 'LTBL' caused by EARS2 mutations. *Brain*, 135(5), 1387–1394. <https://doi.org/10.1093/brain/aws070>
- Steenweg, M. E., Vanderver, A., Blaser, S., Bizzi, A., de Koning, T. J., Mancini, G. M. S., ... van der Knaap, M. S. (2010). Magnetic resonance imaging pattern recognition in hypomyelinating disorders. *Brain*, 133(10), 2971–2982. <https://doi.org/10.1093/brain/awq257>
- Steenweg, M. E., Vanderver, A., Ceulemans, B., Prabhakar, P., Régál, L., Fattal-Valevski, A., ... van der Knaap, M. S. (2012). Novel Infantile-Onset Leukoencephalopathy With High Lactate Level and Slow Improvement. *Archives*

- of Neurology*, 69(6), 718–722. <https://doi.org/10.1001/archneuro.2011.1048>
- Stenson, P. D., Ball, E. V., Mort, M., Phillips, A. D., Shiel, J. A., Thomas, N. S. T., ... Cooper, D. N. (2003). Human Gene Mutation Database (HGMD[®]): 2003 update. *Human Mutation*, 21(6), 577–581. <https://doi.org/10.1002/humu.10212>
- Stiban, J., Fistere, D., & Colombini, M. (2006). Dihydroceramide hinders ceramide channel formation: Implications on apoptosis. *Apoptosis*, 11(5), 773–780. <https://doi.org/10.1007/s10495-006-5882-8>
- Stirnemann, J., Belmatoug, N., Camou, F., Serratrice, C., Froissart, R., Caillaud, C., ... Berger, M. (2017). A Review of Gaucher Disease Pathophysiology, Clinical Presentation and Treatments. *International Journal of Molecular Sciences*, 18(2), 441. <https://doi.org/10.3390/ijms18020441>
- Strachan, L. R., Stevenson, T. J., Freshner, B., Keefe, M. D., Miranda Bowles, D., & Bonkowsky, J. L. (2017). A zebrafish model of X-linked adrenoleukodystrophy recapitulates key disease features and demonstrates a developmental requirement for *abcd1* in oligodendrocyte patterning and myelination. *Human Molecular Genetics*, 26(18), 3600–3614. <https://doi.org/10.1093/hmg/ddx249>
- Streisinger, G., Walker, C., Dower, N., Knauber, D., & Singer, F. (1981). Production of clones of homozygous diploid zebra fish (*Brachydanio rerio*). *Nature*, 291(5813), 293–296. Retrieved from <http://www.ncbi.nlm.nih.gov/pubmed/7248006>
- Strynatska, K. A., Gurrola-Gal, M. C., Berman, J. N., & McMaster, C. R. (2018). How Surrogate and Chemical Genetics in Model Organisms Can Suggest Therapies for Human Genetic Diseases. *Genetics*, 208(3), 833–851. <https://doi.org/10.1534/genetics.117.300124>
- Summerton, J. (1999). Morpholino antisense oligomers: the case for an RNase H-independent structural type. *Biochimica et Biophysica Acta*, 1489(1), 141–158. Retrieved from <http://www.ncbi.nlm.nih.gov/pubmed/10807004>
- Suzuki, S., Li, X. K., Enosawa, S., & Shinomiya, T. (1996). A new immunosuppressant, FTY720, induces bcl-2-associated apoptotic cell death in human lymphocytes. *Immunology*, 89(4), 518–523. Retrieved from <http://www.ncbi.nlm.nih.gov/pubmed/9014815>
- Ternes, P., Franke, S., Zähringer, U., Sperling, P., & Heinz, E. (2002). Identification and characterization of a sphingolipid delta 4-desaturase family. *The Journal of Biological Chemistry*, 277(28), 25512–25518. <https://doi.org/10.1074/jbc.M202947200>
- Thudichum, J. (1962). *A treatise on the chemical constitution of the brain*. Hamden Conn.: Archon Books. Retrieved from <http://www.worldcat.org/title/treatise-on-the-chemical-constitution-of-the-brain/oclc/14612433>
- Tidhar, R., & Futerman, A. H. (2013). The complexity of sphingolipid biosynthesis in the endoplasmic reticulum. *Biochimica et Biophysica Acta (BBA) - Molecular Cell Research*, 1833(11), 2511–2518. <https://doi.org/10.1016/J.BBAMCR.2013.04.010>
- Tingaud-Sequeira, A., Lavie, J., & Knoll-Gellida, A. (2017). Functional validation of ABHD12 mutations in the neurodegenerative disease PHARC " A Mechanistic Approach to Fight against Chemical Warfare Agents " Project NATO-SFP-984777 View project NeuroAquaTox: Development of medium-and high-throughput methodologies for chemical risk assessment in aquatic ecosystems: neurobehavioural effects and pathophysiological mechanisms in zebrafish and *Daphnia magna* View project. <https://doi.org/10.1016/j.nbd.2016.11.008>
- Tommasino, C., Marconi, M., Ciarlo, L., Matarrese, P., & Malorni, W. (2015). Autophagic flux and autophagosome morphogenesis require the participation of

- sphingolipids. *Apoptosis*, 20(5), 645–657. <https://doi.org/10.1007/s10495-015-1102-8>
- Trilck, M., Peter, F., Zheng, C., Frank, M., Dobrenis, K., Mascher, H., ... Frech, M. J. (2017). Diversity of glycosphingolipid GM2 and cholesterol accumulation in NPC1 patient-specific iPSC-derived neurons. *Brain Research*, 1657, 52–61. <https://doi.org/10.1016/j.brainres.2016.11.031>
- Tserng, K.-Y., & Griffin, R. L. (2004). Ceramide metabolite, not intact ceramide molecule, may be responsible for cellular toxicity. *The Biochemical Journal*, 380(Pt 3), 715–722. <https://doi.org/10.1042/BJ20031733>
- Tuschl, K., Meyer, E., Valdivia, L. E., Zhao, N., Dadswell, C., Abdul-Sada, A., ... Wilson, S. W. (2016). Mutations in SLC39A14 disrupt manganese homeostasis and cause childhood-onset parkinsonism–dystonia. *Nature Communications*, 7, 11601. <https://doi.org/10.1038/ncomms11601>
- Ullmann, J. F. P., Cowin, G., Kurniawan, N. D., & Collin, S. P. (2010). A three-dimensional digital atlas of the zebrafish brain. *NeuroImage*, 51(1), 76–82. <https://doi.org/10.1016/j.neuroimage.2010.01.086>
- Valouev, A., Ichikawa, J., Tonthat, T., Stuart, J., Ranade, S., Peckham, H., ... Johnson, S. M. (2008). A high-resolution, nucleosome position map of *C. elegans* reveals a lack of universal sequence-dictated positioning. *Genome Research*, 18(7), 1051–1063. <https://doi.org/10.1101/gr.076463.108>
- Van De Weghe, J. C., Rusterholz, T. D. S., Latour, B., Grout, M. E., Aldinger, K. A., Shaheen, R., ... Doherty, D. (2017). Mutations in ARMC9, which Encodes a Basal Body Protein, Cause Joubert Syndrome in Humans and Ciliopathy Phenotypes in Zebrafish. *American Journal of Human Genetics*, 101(1), 23–36. <https://doi.org/10.1016/j.ajhg.2017.05.010>
- van der Knaap, M. S., & Bugiani, M. (2017). Leukodystrophies: a proposed classification system based on pathological changes and pathogenetic mechanisms. *Acta Neuropathologica*. <https://doi.org/10.1007/s00401-017-1739-1>
- van der Knaap, M. S., Naidu, S., Pouwels, P. J. W., Bonavita, S., van Coster, R., Lagae, L., ... Valk, J. (2002). New syndrome characterized by hypomyelination with atrophy of the basal ganglia and cerebellum. *AJNR. American Journal of Neuroradiology*, 23(9), 1466–1474. Retrieved from <http://www.ncbi.nlm.nih.gov/pubmed/12372733>
- van der Knaap, M. S., & Valk, J. (2006). *Magnetic resonance of myelination and myelin disorders*. *Journal of Neuroradiology*. <https://doi.org/10.1007/s00415-006-0105-3>
- van der Knaap, M. S., Valk, J., de Neeling, N., & Nauta, J. J. P. (1991). Pattern recognition in magnetic resonance imaging of white matter disorders in children and young adults. *Neuroradiology*, 33(6), 478–493. <https://doi.org/10.1007/BF00588038>
- van Dijk, E. L., Auger, H., Jaszczyszyn, Y., & Thermes, C. (2014). Ten years of next-generation sequencing technology. *Trends in Genetics*, 30(9), 418–426. <https://doi.org/10.1016/j.tig.2014.07.001>
- van Doorn, R., Nijland, P. G., Dekker, N., Witte, M. E., Lopes-Pinheiro, M. A., van het Hof, B., ... de Vries, H. E. (2012). Fingolimod attenuates ceramide-induced blood–brain barrier dysfunction in multiple sclerosis by targeting reactive astrocytes. *Acta Neuropathologica*, 124(3), 397–410. <https://doi.org/10.1007/s00401-012-1014-4>
- van Karnebeek, C. D. M., Bonafé, L., Wen, X.-Y., Tarailo-Graovac, M., Balzano, S., Royer-Bertrand, B., ... Superti-Furga, A. (2016). NANS-mediated synthesis of sialic acid is required for brain and skeletal development. *Nature Genetics*, 48(7), 777–784. <https://doi.org/10.1038/ng.3578>

- Vanderver, A., Prust, M., Tonduti, D., Mochel, F., Hussey, H. M., Helman, G., ... van der Knaap, M. S. (2015). Case definition and classification of leukodystrophies and leukoencephalopathies. *Molecular Genetics and Metabolism*.
<https://doi.org/10.1016/j.ymgme.2015.01.006>
- Vanni, N., Fruscione, F., Ferlazzo, E., Striano, P., Robbiano, A., Traverso, M., ... Zara, F. (2014). Impairment of ceramide synthesis causes a novel progressive myoclonus epilepsy. *Annals of Neurology*, *76*(2), 206–212. <https://doi.org/10.1002/ana.24170>
- Varga, M., Ralbovski, D., Balogh, E., Hamar, R., Keszthelyi, M., & Tory, K. (2018). Zebrafish Models of Rare Hereditary Pediatric Diseases. *Diseases*, *6*(2), 43.
<https://doi.org/10.3390/diseases6020043>
- Varshney, G. K., Zhang, S., Pei, W., Adomako-Ankomah, A., Fohtung, J., Schaffer, K., ... Burgess, S. M. (2016). CRISPRz: a database of zebrafish validated sgRNAs. *Nucleic Acids Research*, *44*(D1), D822–D826. <https://doi.org/10.1093/nar/gkv998>
- Velić, E. H. (2015). Molecular biology of myelin. *Gyrus*, *144*.
<https://doi.org/10.17486/gyr.3.1030>
- Walker, C., & Streisinger, G. (1983). Induction of Mutations by gamma-Rays in Pregonial Germ Cells of Zebrafish Embryos. *Genetics*, *103*(1), 125–136. Retrieved from <http://www.ncbi.nlm.nih.gov/pubmed/17246099>
- Wan, J., Yourshaw, M., Mamsa, H., Rudnik-Schöneborn, S., Menezes, M. P., Hong, J. E., ... Jen, J. C. (2012). Mutations in the RNA exosome component gene EXOSC3 cause pontocerebellar hypoplasia and spinal motor neuron degeneration. *Nature Genetics*, *44*(6), 704–708. <https://doi.org/10.1038/ng.2254>
- Wang, H., Charles, A. G., Frankel, A. J., & Cabot, M. C. (2003). Increasing intracellular ceramide: an approach that enhances the cytotoxic response in prostate cancer cells. *Urology*, *61*(5), 1047–1052. Retrieved from <http://www.ncbi.nlm.nih.gov/pubmed/12736045>
- Wang, J. L., Yang, X., Xia, K., Hu, Z. M., Weng, L., Jin, X., ... Tang, B. S. (2010). TGM6 identified as a novel causative gene of spinocerebellar ataxias using exome sequencing. *Brain*, *133*(12), 3510–3518. <https://doi.org/10.1093/brain/awq323>
- Wang, K., Li, M., & Hakonarson, H. (2010). ANNOVAR: functional annotation of genetic variants from high-throughput sequencing data. *Nucleic Acids Research*, *38*(16), e164–e164. <https://doi.org/10.1093/nar/gkq603>
- Wang, R., Qi, B., Dong, Y. W., Cai, Q. Q., Deng, N. H., Chen, Q., ... Wu, X. Z. (2016). Sulfatide interacts with and activates integrin $\alpha 5 \beta 1$ and $\alpha 5 \beta 2$ in human hepatocellular carcinoma cells. *Oncotarget*, *7*(24), 36563–36576.
<https://doi.org/10.18632/oncotarget.9095>
- Weiss, M. M., Van der Zwaag, B., Jongbloed, J. D. H., Vogel, M. J., Brüggewirth, H. T., Lekanne Deprez, R. H., ... van der Stoep, N. (2013). Best Practice Guidelines for the Use of Next-Generation Sequencing Applications in Genome Diagnostics: A National Collaborative Study of Dutch Genome Diagnostic Laboratories. *Human Mutation*, *34*(10), 1313–1321. <https://doi.org/10.1002/humu.22368>
- White, C., Alshaker, H., Cooper, C., Winkler, M., & Pchejetski, D. (2016). The emerging role of FTY720 (Fingolimod) in cancer treatment. *Oncotarget*, *7*(17), 23106–23127. <https://doi.org/10.18632/oncotarget.7145>
- Won, J.-S., Singh, A. K., & Singh, I. (2016). Biochemical, cell biological, pathological, and therapeutic aspects of Krabbe's disease. *Journal of Neuroscience Research*, *94*(11), 990–1006. <https://doi.org/10.1002/jnr.23873>
- Won, J.-S., & Singh, I. (2006). Sphingolipid signaling and redox regulation. *Free Radical Biology and Medicine*, *40*(11), 1875–1888.
<https://doi.org/10.1016/j.freeradbiomed.2006.01.035>

- Xing, Y., Tang, Y., Zhao, L., Wang, Q., Qin, W., Ji, X., ... Jia, J. (2016). Associations between plasma ceramides and cognitive and neuropsychiatric manifestations in Parkinson's disease dementia. *Journal of the Neurological Sciences*, 370, 82–87. <https://doi.org/10.1016/j.jns.2016.09.028>
- Young, B. H., Eun, Y. K., & Jung, S. C. (2006). Upregulation of proinflammatory cytokines in the fetal brain of the Gaucher mouse. *Journal of Korean Medical Science*, 21(4), 733–738. <https://doi.org/10.3346/jkms.2006.21.4.733>
- Young, I. R., Hall, A. S., Pallis, C. A., Legg, N. J., Bydder, G. M., & Steiner, R. E. (1981). Nuclear magnetic resonance imaging of the brain in multiple sclerosis. *Lancet (London, England)*, 2(8255), 1063–1066. Retrieved from <http://www.ncbi.nlm.nih.gov/pubmed/6118521>
- Yu, F. P. S., Dworski, S., & Medin, J. A. (2018). Deletion of MCP-1 impedes pathogenesis of acid ceramidase deficiency. *Scientific Reports*, 8(1). <https://doi.org/10.1038/s41598-018-20052-6>
- Yu, P. B., Hong, C. C., Sachidanandan, C., Babitt, J. L., Deng, D. Y., Hoyng, S. A., ... Peterson, R. T. (2008). Dorsomorphin inhibits BMP signals required for embryogenesis and iron metabolism. *Nature Chemical Biology*, 4(1), 33–41. <https://doi.org/10.1038/nchembio.2007.54>
- Zara, F., Biancheri, R., Bruno, C., Bordo, L., Assereto, S., Gazzero, E., ... Minetti, C. (2006). Deficiency of hyccin, a newly identified membrane protein, causes hypomyelination and congenital cataract. *Nature Genetics*, 38(10), 1111–1113. <https://doi.org/10.1038/ng1870>
- Zheng, W., Kollmeyer, J., Symolon, H., Momin, A., Munter, E., Wang, E., ... Merrill, A. H. Ceramides and other bioactive sphingolipid backbones in health and disease: Lipidomic analysis, metabolism and roles in membrane structure, dynamics, signaling and autophagy, 1758 *Biochimica et Biophysica Acta - Biomembranes* § (2006). <https://doi.org/10.1016/j.bbamem.2006.08.009>
- Zizioli, D., Guarienti, M., Tobia, C., Gariano, G., Borsani, G., Bresciani, R., ... Presta, M. (2014). Molecular cloning and knockdown of galactocerebrosidase in zebrafish: New insights into the pathogenesis of Krabbe's disease. *Biochimica et Biophysica Acta (BBA) - Molecular Basis of Disease*, 1842(4), 665–675. <https://doi.org/10.1016/J.BBADIS.2014.01.008>